

**TRIBOLOGICAL CHARACTERISTICS OF COATINGS
ON ALUMINIUM AND ITS ALLOYS**

**A thesis submitted for the degree
of**

DOCTOR OF PHILOSOPHY

By

Fadhil S. Abdul-Mahdi (M.Phil)

**Department of Materials Technology
Brunel, The University of West London**

November, 1987

ABSTRACT

Hard anodising on aluminium and its alloys has been widely practised for many years in order to improve the resistance of the otherwise poor wear characteristics of aluminium. In recent years there has been an increasing interest in other treatments and coatings, on both aluminium and other base metals.

The aim of this investigation is to explain the tribological performance and wear mechanism(s) of an uncoated aluminium alloy, four anodic coated alloys, and also an electroless nickel alloy. All of the coatings are produced on three different aluminium alloys. The thickness of the anodic films is 30-35 micron, as this thickness falls within the range commonly used by industry. In an endeavour to explain the role of coating thickness on wear life, electroless nickel alloy has been produced in a range of thicknesses of 10, 20 and 30 micron.

To evaluate abrasive and adhesive wear, the samples were rubbed against a single point diamond and steel ball, respectively, in a reciprocating movement at room temperature and 65-75% relative humidity, under a wide range of load and sliding distance. Some tests continued to run until a breakdown of the coatings occurred, whilst other tests were interrupted at intermediate stages. This enabled the initiation and propagation of failure mechanisms to be studied.

Abrasive wear was performed under dry conditions, whereas, adhesive wear was evaluated under both dry and lubricated conditions. Wear of these coatings was proportional to the applied load and sliding distance, but there was no direct relationship between wear and hardness. The tribological performance of these coatings appears to be dictated by a) the composition of the substrate, b) the chemical and physical nature of the coatings and c) the test conditions.

Under boundary lubricated conditions there was a considerable increase in the wear life of the coatings. A three dimensional surface texture is superior to a machined surface, in controlling contact conditions. There is an approximate linear relationship between coating thickness and wear life for electroless nickel alloys.

These coatings predominantly fail by adhesion, plastic deformation and brittle fracture. A microscopic model for fracture of brittle materials, under both static and dynamic conditions for abrasive and adhesive wear correlates very well with the behaviour of these coatings. Analytical interpretation of adhesive wear was made by separately calculating the coefficient of wear "K" of the counterbodies. This information enables an improved understanding of the wear test itself to be added to the model of the wear mechanisms involved.

IN LOVING MEMORY
OF MY
FATHER

ACKNOWLEDGEMENT

I would like to thank all my colleagues in the department of Materials Technology for their help and assistance which was invaluable in carrying out this work. In particular I would like to thank Professor M.J. Bevis for providing the facilities, Dr. T. Eyre for his guidance, encouragement, and valuable discussion throughout the work. I would also like to express my gratitude to my family for their endless support, in particular, Mr. K.M. Al-Hakak, to whom I am indebted for his inexhaustive moral and financial support. Many thanks also to Acorn Anodising Company for supplying the materials.

C O N T E N T S

CHAPTER 1	INTRODUCTION	1
CHAPTER 2	LITERATURE REVIEW	6
2.1	The Concept of Coating	6
2.2	The Anodising Process	8
2.3	Types of Anodising Process	9
	2.3.1 Sulphuric Acid	9
	2.3.2 Chromic Acid	11
	2.3.3 Oxalic Acid	12
2.4	Mechanism of Anodic Film Formation	12
2.5	Composition of Anodic Oxide	14
2.6	Anodised Aluminium for Wear Applications	15
2.7	Factors Affecting Wear Properties of Anodic Films	16
2.8	Electroless Nickel Coating	20
2.9	Wear Testing of Anodised Aluminium	23
2.10	Wear Mechanisms	28
	2.10.1 Abrasive Wear	29
	2.10.2 Erosion Wear	31
	2.10.3 Adhesive Wear	32
2.11	Archard Theory of Wear	34
2.12	Delamination Theory of Wear	36
2.13	Some Factors Affecting the Wear Process	39
	2.13.1 The Role of Hardness	39
	2.13.2 The Role of Fracture Toughness	40
2.14	Summary	41
CHAPTER 3	EXPERIMENTAL DETAILS	44
3.1	Introduction	44
3.2	Materials Investigated	47
3.3	Surface Morphology of the Coating Investigated	49
	3.3.1 Composition of the Anodic Films	50
	3.3.2 Coating Thickness Measurement	50
	3.3.3 Microhardness Measurement	50
3.4	Wear Procedure	50
	3.4.1 Wear Rig	50
	3.4.2 Abrasive Wear Test	52
	3.4.3 Adhesive Wear Test	53
3.5	Evaluation of the Role of Coating Thickness	54
3.6	The Major Analytical Techniques Used	54
	3.6.1 Talysurf	55
	3.6.2 Scanning Electron Microscopy	55
	3.6.3 Electron Spectroscopy for Chemical Analysis 'ESCA'	55
	3.6.4 Taper Sectioning	56

CHAPTER 4	RESULTS	57
4.1	Wear Results	57
	4.1.1 Abrasive Wear Results	57
4.2	Adhesive Wear Results	61
	4.2.1 Under Dry Conditions	61
	4.2.2 Results of Lubricated Tests	67
	4.2.3 Adhesive Wear of Electroless Nickel	68
4.3	Microscopic Examination of Worn Surfaces	69
	4.3.1 Under Abrasive Wear	69
	4.3.2 Under Adhesive Wear	72
	4.3.3 Microscopic Examination of the Worn Balls	75
4.4	Examination of Wear Debris	76
	4.4.1 Abrasive Wear Debris	76
	4.4.2 Adhesive Wear Debris	77
CHAPTER 5	DISCUSSION	79
5.1	Abrasive Wear	80
	5.1.1 <i>Fracture Concept of Hard Anodised</i> <i>Alloy 9H under Abrasive Wear</i>	85
5.2	Evaluation of Adhesive Wear Data	89
5.3	The Role of the Substrate	98
5.4	The Effect of Coating Thickness	99
5.5	Friction Properties	100
CHAPTER 6	CONCLUSIONS	107
	REFERENCES	109
	TABLES	113

CHAPTER ONE

INTRODUCTION

In recent years there has been an increasing industrial awareness of the importance of good tribological design. It has frequently been shown that significant economic savings are possible through currently available technology transfer techniques (1). Materials technology can make a considerable contribution to both fuel and lubricant efficiency through the use of light weight materials and the use of treatments and coatings to reduce friction and increase wear life. Aluminium and its alloys are continuously under scrutiny particularly in the automotive industry where there is considerable political, technical and economic pressure to reduce fuel consumption.

Design engineers are actively seeking ways to extend the use of aluminium alloys, without the necessity for separate cast iron liners in engine blocks or other bearing inserts to support rotating parts. Their use at higher ambient temperatures, through the use of suitable surface insulation coatings or the use of composite reinforcement to retain hot strength, are both areas where ceramics are potential materials for the future.

In aiming to provide improved tribological alloys and coatings there are a number of different problems which must be addressed if success is to be achieved in their application:-

1. There is no unified theory of the wear of materials which allows design engineers to select and apply these successfully without extensive field trials. However, as aluminium alloys are most likely to be used under lubricated sliding conditions or under low load non-lubricated conditions, adhesive and abrasive wear conditions need to be considered in further detail. Current knowledge of these is sufficiently well developed to stimulate industrial improvements.
2. Tribological behaviour of materials cannot be derived directly from their physical, chemical or mechanical characteristics. Friction and wear are not intrinsic materials properties but are a reflection of the systems characteristics and although this has been appreciated for quite some time, the work of Czichos has established this on a more rational basis (2). It must be appreciated therefore, that the counterface surface as well as many environmental variables have a very important effect on the tribological behaviour of the material under discussion. This systems approach must be appreciated if success is to be achieved in the more widespread use of aluminium alloys for wear applications.
3. At the present time there is no single unified view of the way materials should be tested for use in wear applications. Although various national test specifications exist they have not been widely adopted on an international basis. A.S.T.M. specifications are however widely used in the area of lubrication and abrasive wear. As a result of the **Versailles Agreement on Advanced Materials and Standards (VAMAS)**, an international working group has been set up, consisting of representatives of the **U.S.A., Japan, France, Canada, Federal**

Republic of Germany, Italy and the U.K. Work has already commenced, based upon a pin on disc technique to evaluate the tribological behaviour of advanced materials, these being defined as ceramics and surface coatings. Both of these groups of materials are of considerable interest in the automotive industry where new projects are developing rapidly, particularly in Japan and the U.S.A. It is very important to establish a suitable standard, so that materials development can be orientated specifically for wear applications.

As far as aluminium alloys are concerned, there are three main areas which require further development to ensure their successful exploitation and thus wider industrial use for tribological components.

1. To optimise the bulk properties of these alloys in terms of composition, manufacture route and microstructure so that they may be successfully used in plain bearings and as the cylinder bore in reciprocating engines. The alloys of most significant interest are those based upon Al-Sn, Al-Si and Al-Graphite.
2. To improve the strength of aluminium alloys so that they can be used at higher temperatures, particularly on the piston crown and in the vicinity of the top piston ring groove which would eliminate the need for a special ring groove insert or coating. If the strength of these alloys can be improved to compete with steel then they will also replace steel conrods and other steel actuators. The main interest in this area therefore lies in the use of fibre reinforcement, particularly with SiC and Al₂O₃.
3. To improve the surface characteristics of currently available

aluminium alloys to enable them to generate low friction, an extended wear life and to achieve a satisfactory lubrication regime, in terms of both hydrodynamic and boundary conditions. They are required to be equal or superior to materials like grey cast iron which is currently the most widely used cylinder bore material. In this area therefore, there are two procedures that can be adopted. Firstly to treat the surface by a chemical process, for example, etching of Al/Si alloys to selectively remove the soft aluminium matrix to prevent adhesion (3). The second approach is to coat the alloy to provide a different surface with the required tribological characteristics. These consist essentially of electrolytic and electroless coating, and also the well established anodising process and these are summarised in Table 1.

Coatings, their thickness, mechanical properties, surface morphology, as well as the nature of the substrate, have all been shown to influence the tribological performance of coatings. A range of anodised aluminium alloys was therefore selected for this investigation in response to a request made by Acorn Anodised Company. Electroless nickel on aluminium alloy was also included in this study as one of the most important new coatings. This enabled a broad based investigation to be undertaken which covers materials currently used in service.

Having outlined the technical considerations of surface treatment and coating for tribological applications, an understanding of the wear mechanism seems an indispensable criterion in materials selection and design. Although many tests on the wear behaviour of anodised coatings on aluminium and its alloys and, to a lesser extent, on electroless nickel,

are reported in the literature, there is little information on the wear mechanism involved. This is because the appropriate surface analysis of the wear damage has not always been carried out. Some of the tests do not allow a fundamental approach to be adopted early. The wear tests described later were chosen so that the applied load and the number of passes could be varied in order that the different stages of initiation and propagation of wear damage could be easily followed. This investigation has therefore oriented to offer information on the following aspects:

- 1) The tribological characteristics of anodised aluminium alloys and electroless nickel on aluminium alloy, under both dry and lubricated conditions.
- 2) The mechanism of wear on surface coatings.
- 3) The role of the substrate on the tribological behaviour of the coatings investigated.
- 4) The role of coating thickness on the wear life of electroless nickel on aluminium alloys.
- 5) The role of surface texture in oil retention and its subsequent effect on the coating life.

With these tasks in mind, the author has used two test methods:

- 1) To evaluate abrasive wear, a single point diamond applied over a wide range of load and number of passes.
- 2) Adhesive wear has been investigated by using a steel ball as a rider against the flat samples under both dry and lubricated conditions.

The use of these test methods is discussed in Chapter 3.

CHAPTER TWO

LITERATURE REVIEW

2.1 THE CONCEPT OF COATING

'In all engineering applications it is the surface of the component which has to coexist with the external environment which consists of the contacting surface and process atmosphere. It follows therefore, that the designers should choose a bulk material from the standpoint of structural and economic criteria, and surface material to deal with the external conditions. The required surface properties can be achieved either by the application of specialised coatings or by modification of the bulk material.' (4)

Coating technology is now being applied on a wide range of materials such as steel, cast iron, nimonic alloys, and aluminium alloys. Aluminium and its alloys have attracted a great deal of attention as a base material for many engineering and decorative applications. This attraction resides in its light weight, high thermal conductivity, availability, and machinability. It has been predicted that aluminium may replace some heavier engineering materials due to the introduction of aluminium silicon alloy containing 17% Si, 4.5% Cu. These alloys are now widely accepted as having excellent tribological properties when both the composition and microstructure are correctly optimised (3). Surface treatments and coatings are of considerable interest in meeting an increasing industrial awareness of good tribological design.

The understanding of both strengthening mechanisms and the development of coating technology has led to the expansion in use of aluminium and its alloys.

The world consumption of aluminium has vastly accelerated from 66,200 tonnes in the early years of this century (1913) to 165,000 tonnes in 1918 to nearly 2,000,000 tonnes in 1946 (5). Figure 1 illustrates the trend in world production and consumption of aluminium since 1960.

According to studies carried out by the United Nations (6,7), the total world production is growing further to cover a wider range of applications (Table 2).

The ultimate choice of the bulk alloy and type of surface must be based on a number of considerations (5,8) i.e.:

1. The service environment, for example, indoor, outdoor, marine, etc.
2. The base metal, i.e. suitable finish for particular type of alloy chosen.
3. The decorative effect aimed at, for example, colour, reflectivity.
4. Industrial purpose where additional features such as wear or corrosion are encountered.

Aluminium and its alloys have an inherent ability to develop a film of oxide immediately they are exposed to an oxidising atmosphere. The thickness of this oxide is about 0.25 to 1.0×10^{-2} microns, (8). Such oxide offers negligible protection against external forces often encountered in many engineering applications. The thickness of the film is therefore, artificially increased by anodising.

The first anodic film produced in sulphuric acid was first reported in 1857 (8). Since then it has been used as a dielectric material. The earliest use of the process for protection was in 1923 when 3% chromic acid was used. During the past 35 years anodising as well as all other aluminium finishing has grown from an art to scientifically controlled operations

providing aesthetic appeal and customer acceptance (9).

2.2 THE ANODISING PROCESS

Anodising is an electrochemical process by which a layer of metal oxide is produced at the surface of a component usually made of aluminium and its alloys. The process can only be achieved when a current of sufficient voltage passes through a suitable electrolytic solution in which aluminium acts as an anode and another suitable material, usually lead as a cathode.

When a direct current passes through an electrolytic solution, the negatively charged oxygen anion migrates to the anode where it reacts chemically with aluminium to form an aluminium oxide. Depending on a number of factors, particularly the nature of the electrolyte, the treatment conditions such as the current density, formation voltage, temperature, time of treatment, various reactions may occur resulting in one of the following possibilities (5):

1. The anode reaction products may be completely soluble in the solution, in which case no anodic film is produced.
2. The reaction products are almost insoluble, in which case only a thin film of oxide is formed.
3. The reaction products may be sparingly soluble in the electrolyte, in which case a porous oxide is produced. The thickness of this coating continues until the growth rate becomes equal to the dissolution rate.

2.3 TYPES OF ANODISING PROCESS

Depending on the properties required, different electrolytes have been developed. These are mainly:

2.3.1 Sulphuric acid

This type was first commercially used in Russia and the U.K. (10). By far the largest amount of anodising is being carried out in 15% sulphuric acid in purified water at a temperature of about 0°C at 20-25 amp/sq.ft. and an initial voltage of 5-30 later increased to 60 volts.

This process is suitable to produce a hard thick oxide which may reach 250 microns (9). For normal industrial application, a 25-35 microns coating is frequently used. In addition to the treatment conditions, anodic film characteristics are influenced by the presence of impurities in the solution and alloying elements (9,10,11).

According to Jack (9), anodising in sulphuric acid can be applied to every kind of product made of aluminium. Jenny (12), on the other hand, has reported considerable difficulties in anodising aluminium alloys containing over 3% Cu and 7.5% Si because of the high forming voltage required to maintain a continuous flow of current. Processing difficulties cause staining of the coating surface and impair coating integrity, leading to exfoliation of the coating. An addition of 15-20% glycol to the solution has been suggested to inhibit the production of a film of high hardness (10). Chromates increase the coating uniformity and oxalic acid has often been added to enhance coating thickness. The presence of chloride in an excessive amount may cause pitting of the coating (13). Kneeshaw (14),

however, has introduced ferric chloride solution as a modifier by which a desirable coating thickness could be achieved in a relatively shorter treatment time. Hardness is markedly reduced, hence wear resistance, according to Kneeshaw, would be impaired.

Anodic films designed to operate in areas where wear is involved are usually hard with a coating thickness of up to 35 microns, produced in sulphuric acid. A superimposed a.c. and d.c. current is also commercially used. A mixture of substances may be used for anodising different aluminium alloys. This mixture consists of the following:

Sulphuric acid	7%
Plant extract	3%
Nonyl alcohol	0.02%
Polyethylene glycol	0.02%
Methyl alcohol	7%

This solution is used at 10°C and 50 microns is claimed to be obtainable in 53 minutes at 10-20 amp/sq.ft. The voltage is raised in steps from 15 to 60 volts (10). Anodic coatings of 25-50 micron and a hardness of 1400 H_v can also be achieved in a solution of:

Oxalic acid	50 g/l
Calcium fluoride	0.1 g/l
Sulphuric acid	0.5 g/l
Chromic sulphate	1 g/l

However, in view of the evidence available, the hardness value of anodised aluminium is in the range of 300-450 H_v. Considerable doubt must be placed on a hardness value as high as 1400 H_v (10) because of the porous nature of anodic film. For bulk alumina, values of greater than 2000H_v

have been reported. The microhardness value of anodic film varies across the thickness. The layer adjacent to the metal being the harder with a progressive decrease from the metal oxide interface to the outer layer. Anodic coating of a hardness value higher than 450H_v can be achieved by using a mixed electrolyte solution thereby the current density will be increased. Provided the growth rate is higher than the dissolution rate, hardness up to 650H_v and a thick coating up to 50 micron can be obtained. Brace (11) has shown that the hardness of anodised alloys is both dependent upon the base alloy and also on the load used in the test procedure. It is also widely recognised that the hardness also depends upon the process conditions. For example, hardness values in the range of 300Hv to 650 Hv do not fully represent the hardness of Al₂O₃ in its bulk. The recorded values of 300-650Hv therefore represent composition, process and structural variations, and both natural and hard coatings fall into this range. These hardness values cannot easily be compared with those of the bulk hardness of more homogenous material and can not be used to indicate wear resistance. For example, Campbell (15) reports that an anodic coating of 450Hv is superior to a steel of 950Hv in its abrasion resistance for a specific condition under lightly loaded conditions.

2.3.2 Chromic Acid

This system was extensively used during World War II on military hardware (9). It was first developed in the United Kingdom by Bengouh and Stuart. The solution consists of 30-100gm of chromic acid per litre of high purity water. A limited coating thickness in the range of 2-5 microns is usually

achieved by using this system. However, a thickness of 10 microns has been reported by using 10% CrO₃ concentration (16).

Chromic acid type is still being used in the aircraft industry for such applications as propellers and high strength wing skin (5,10,12). Its main advantage is that it does not leave corrosive residues in riveted joints. The coating produced in chromic acid is reported to have poor resistance to wear.

2.3.3 Oxalic Acid

This type did not receive much attention in the U.S.A. although it has been used for many years in Europe and Japan where it was developed (5). The sulphuric acid system is now replacing the oxalic acid type (9). The solution consists of 3-5% oxalic acid, and up to 10% has also been employed (16). It does not leave a corrosive residue in rivets and joints and thick coatings of up to 60 microns can readily be obtained.

2.4 MECHANISM OF ANODIC FILM FORMATION

The first theory of the mechanism of anodic oxidation was put forward by Setoh and Miyata (17) who explained the formation of oxide by allowing the passage of oxygen evolved from the decomposition of the solution which acts continuously on the aluminium to produce an oxide film. The mechanism of the process has been a rather controversial issue for many years. Wernick (10) suggested the formation of hydroxide at the anode was due to a hydrolysis process in the form of a net-like sponge over the metal

Baumann (18) postulated the existence of a vapour film layer at the bottom of the pores which are rich in oxygen ions, formed at the gas-electrolyte interface, where heat is also generated due to the electric current to facilitate the reactions. Gunterschulze (19) regards the oxide film as a dense, non-porous layer of aluminium oxide with ions of aluminium and oxygen occupying the corners of the crystal lattice. When an anodic potential is applied to the metal, the oxygen moves towards the surface of the metal and oxidizes it. The aluminium ions move towards the surface of the film where they will be oxidized by the oxygen. Growth of this film will thus take place simultaneously in both directions. However, this hypothesis can no longer be accepted after the calculations of the dimensional changes which occur during ionizing of aluminium and oxygen carried out by Scherk (20). He suggested a reduction of the aluminium atom by 1/23rd of its original size when ionized to Al^{3+} and an enlargement of the oxygen atom by almost the same amount when ionized to O^{-2} . This will make it highly unlikely for oxygen ions to pass through the coating during growth. It is the aluminium ions which migrate through the coating behind this film growth. Fischer (21) believes that the anodising of aluminium starts with the dissolution of the natural oxide film. When a sufficiently high current reaches the area adjoining the electrolyte, a thin film saturated with ions of a basic salt of aluminium is formed on the surface of the anode. This according to Fisher, will bring about an increase in voltage, causing a rapid increase in temperature at the oxide film resulting in cracking as the pore allows further growth (22). Barkman (23) attributes the nucleation of anodic oxide to the low resistance to the current passing at certain points and growth commences with the

formation of a hexagonal structure.

2.5 COMPOSITION OF ANODIC OXIDE

It has been known for some time that in an electrolyte, where dissolution of oxide formation is achieved, the oxide film consists of two layers:

- a) A barrier layer which is dense and compact having a thickness which does not exceed 0.01 - 0.1 microns. This thickness however, is determined by the formation voltage (5,24).
- b) The outer layer which is porous and has a columnar microstructure, accounts for the major properties of the anodised finish (8).

In all commonly used electrolyte solutions, the film consists of Al_2O_3 partially hydrated and containing some constituents derived from the electrolyte and the material being treated (20). Depending on the anodising conditions, different anodic structures may be obtained.

Franklin (25) however, has identified three forms of alumina in the anodic film:

- a) Anhydrous amorphous alumina, constituting the bulk of the film.
- b) Hydrated amorphous occurring as a layer at the oxide electrolyte interface.
- c) Crystalline γ - Al_2O_3 of small size occurring in agglomerates as islands in the amorphous matrix.

The structure of the anodic layer is a close packed cell of oxide (26), hexagonal in shape, each of which contains a single pore (Fig.4) (16). Pore volume is largely governed by the formation voltage (Fig.5) (10).

Increasing the forming voltage may significantly increase not only the coating thickness but also its hardness by increasing the individual cell size which decreases the porosity per unit area. A thicker barrier is produced, hence the abrasion resistance may well be improved. A schematic representation of the cell size is shown in Figure 6.

The final composition, structure and properties of the anodic oxide appeared to be affected by a number of factors (27) such as:

- a) Alloy composition, i.e.
 - (i) constituent
 - (ii) grain structure
- b) Pretreatment before anodising, i.e.
 - (i) mechanical
 - (ii) chemical
 - (iii) electro-chemical
- c) Anodising conditions, i.e.
 - (i) electrolyte composition
 - (ii) electrolyte temperature
 - (iii) anodising current density

2.6 ANODISED ALUMINIUM FOR WEAR APPLICATIONS

Anodised aluminium is now being used in applications where wear

resistance is of prime interest, particularly in the aircraft industry where weight saving is a major issue. Many parts previously made of steel are being replaced by anodised aluminium.

Some examples are reported by Wernick (10).

1. Screw threads of hydraulic jacks.
2. Gears for ticket machines.
3. Pumps for water containing a substantial amount of sand.
4. Clutch and brake discs.

2.7 FACTORS AFFECTING WEAR PROPERTIES OF ANODIC FILMS

The performance of the anodic films is affected by the anodising conditions; temperature, current density, voltage, acid concentration, and treatment time. However, the most important factors are considered to be as follows:

a) Alloy structure

Alloys containing more than 3% copper or 7.5 silicon were reported (10) to be impossible to coat by the conventional anodising process. Copper for example, appears in the anodic film and impairs its continuity. According to Wernick (10), for the best resistance to wear and abrasion, it is preferable to use pure aluminium or alloys with a low percentage of alloying elements. On the other hand, good wear properties of hard anodised heterogeneous alloys have been attributed to the existence of intermetallic compounds in the coating (28). AlMgSi, and AlZnMg alloys

are preferred for hard, wear resistant applications (10). Alloys containing excess of ZnMg produce a coating of low adhesion, thereby causing early exfoliation.

b) Anodising parameters

Machlin (29) showed that there were slight variations in coating thickness on three different aluminium alloys even though they were coated in the same bath for the same period of time. Indentation hardness was also different from one coating to another. He attributed the difference in hardness to the discontinuity of the coating rather than variation in the coating thickness.

Abrasive wear behaviour of an anodic film is influenced by the anodising temperature. At high temperatures the dissolution rate is greater than the growth rate and the anodic film does not increase in thickness.

The effect of current density on abrasion resistance has not been established. However, in the case of a constant conductivity of the electrolyte, a rise in the current density demands the application of a higher voltage. This brings about an increase of the cell diameter and consequently, an improvement in the abrasive wear behaviour (10,29).

c) Surface Topography

Surface topography of anodic films has also been elevated to a high level of importance with regard to the wear of this coating. In some cases, the requirement of the surface finish may take priority over hardness and a range of semi-hard coatings may offer an adequate wear performance

compared to hard coatings (10). Coatings with high porosity may give rise to poor abrasion resistance because of their poor mechanical strength. Smooth anodic surfaces will provide a lower coefficient of friction which is also likely to reduce wear.

The performance of a hard anodised aluminium alloy as a bearing material may be further improved by impregnating the coating with lubricants such as molybdenum disulphide, nylon and teflon (10).

d) Sealing Process

Wear resistance of anodic films is very much influenced by the sealing process (5) in which aluminium oxide, 'the coating', is converted into one of its hydrated states. During this process a porous structure is closed up to give the coating a better resistance to most corrosive environments (5,11), but its potential protection against abrasives deteriorates. The reduction in abrasion resistance of a sealed anodic film has been attributed to the deterioration in hardness as a result of the formation of boehmite $\text{Al}_2\text{O}_3 \cdot \text{H}_2\text{O}$.

The amorphous structure of the anodic film before sealing becomes partially crystalline after sealing. Spooner (30) has given the following composition of the coating before and after sealing:

Composition	Unsealed	Water Sealed
Al_2O_3	78.9%	61.7%
$\text{Al}_2\text{O}_3 \cdot \text{H}_2\text{O}$	0.5%	17.6%
$\text{Al}_2(\text{SO}_4)_3$	20.2%	17.9%
H_2O	0.4%	2.8%

The sealing process can be carried out in different ways. Perfect (8) suggested chemical and mechanical sealing. Much of the published information recommended sealing in water and a solution of nickel acetate, potassium dichromate and sodium silicate at 80-100°C for about 30 minutes. For bearing applications, impregnation of the coating with molybdenum disulphide or graphite, nylon and teflon is recommended (10). The mechanism of sealing has been dealt with by many investigators (8,10,30).

A thick, hard and unsealed coating has been recognised as a wear resistant coating (5,9,10,15), and is comparable to a number of other engineering materials (10) (Fig.7).

The effect of coating thickness on wear behaviour is somewhat confused. Deal (31) reports that there is a direct linear relationship between thickness and wear resistance, i.e. thicker coatings are better than thinner coatings. As far as wear life is concerned, it is easy to see that the wear life will be increased in direct proportion to thickness. However, it is not easy to argue that the wear rate itself, i.e. the slope of wear graphs, will be dependent upon thickness. In fact the available evidence points to the opposite effect because thicker coatings do not adhere readily to the subsurface and the less flexible and crack resistant it becomes. The fatigue strength of anodised alloys may also be impaired as the thickness of the anodic film increases (Fig.8). The decrease in fatigue strength may be attributed to the pre-existence of micro cracks in the coating which increase in proportion to the thickness. Table 3 shows the mechanical properties of anodised alloys as a function of the anodic film thickness.

2.8 ELECTROLESS NICKEL COATING

An attempt has been made to compare the tribological characteristics of anodised aluminium with other coatings such as chromium plated aluminium. However, due to technical difficulties with the chromium plating of aluminium and its alloys, involving the presence of the naturally formed aluminium oxide, formation of this oxide impairs coating integrity and a lack of adhesion subsequently occurs. Chromium plated aluminium is therefore not commercially available. This has led instead to the investigation of the now well established electroless nickel coating as an alternative material. This coating is formed on a catalytic surface in a solution of nickel salts and a reducing agent such as a sodium hypophosphate (3 2). Electroless nickel is a chemically formed compound of nickel and phosphorus or boron, and is metallurgically different from electroplated nickel phosphorus alloys. Electroplated nickel is chemically crystalline in nature. The electroless coating varies from a poorly defined crystalline solid to completely non crystalline, depending on the phosphorus content. Deposits with less than 5% weight of phosphorus result in beta phase, 5% to 8.5% phosphorus of mixed beta and alpha, more than 8.5% phosphorus produces alpha+ beta+ a non crystalline form of phosphorus (3 2).

Aluminium and its alloys must be treated with care when they are coated by this process. This is because of the presence of the naturally formed film of aluminium oxide. This oxide impairs the adhesion of the coating to the substrate which deteriorates its mechanical properties. A zincating process is therefore required in which aluminium oxide is

replaced by a thin metallic film of zinc which must be resistant to oxidation. The zincating process may also be a source of adhesion failure if the zinc concentration has not been carefully controlled (33). The use of electroless nickel as a substitute coating for hard chromium has proved successful for the treatment of sliding parts of a medium sized plastic moulding machine and an automobile rocker-shaft. However, in other cases, electroless nickel was less satisfactory and failed to give adequate surface protection when applied to a large machine where conditions of high pressure and temperature existed (33). Wear behaviour of electroless coatings have been evaluated with a wide range of apparatus. Ma and Gawne (34) have used the Falex, reciprocating steel pin, Taber abrader, and diamond scratch tests. They concluded that the relative wear performance of an electroless nickel coating depends upon the specific test used. Gould et al (35) investigated fretting wear by using a sphere on a flat configuration and showed that heat treating the coating at 400° raised the coating hardness to 1000Hv, and reduced the fretting wear rate at all thicknesses. Justice (36) has shown a similar effect of heat treatment on abrasive wear resistance.

Ruff et al (37) evaluated dry sliding wear of electroless nickel in an argon atmosphere. A heat treated coating at 400°C for 30 minutes showed superior wear behaviour to that of the plated coating. The improvement of the wear characteristics of the heat treated coating is due to the crystallization of the coating and precipitation of nickel phosphide " Ni_3P_2 " from the solid solution. This eventually increases the hardness of the coating. However, this mechanism of precipitation is usually combined with some shrinkage which produces cracks in the coating, thus

reducing its protective value to the substrate (38). Heat treatment at high temperatures for a long time softens the coating because the nickel phosphide redissolves and leaves a low stress condition due to the coarsening effect of the undissolved precipitates. Electroless nickel is like hard chromium in the sense that it may easily suffer from seizure when it is used in applications where lubricants fail to reach the surface. Incorporation of polymeric materials like Polytetrafluoroethylene (PTFE) particles was found to reduce friction and stop seizure by producing "non-stick" non galling surfaces (39). The scope of electroless nickel has further been expanded by co-depositing materials such as silicon carbide, ceramics, and diamond. A hardness of 1155Hv was reported (40) to have been achieved when chromium carbide was introduced to an electroless nickel matrix and wear behaviour was also improved.

The attraction of using electroless nickel coating can be summarised as follows:

1. The process does not require an external source of current.
2. The coating can be applied to almost any substrate including non-metallic materials.
3. A uniform coating is obtainable.
4. It confers resistance to aqueous corrosion and oxidation. In general corrosion resistance is enhanced with increasing phosphorus content.
5. A hardness value of 950Hv can be obtained by suitable heat treatment.
6. Improved tribological properties can be achieved.

2.9 WEAR TESTING OF ANODISED ALUMINIUM

There are no ASTM standard tests for evaluating the wear resistance of coatings (41). Some non-standard methods have been evaluated (15,41,42,43,44) based on the following principles:

1. Tests simulating actual surface conditions.
2. Industrial tests on the surface or cross sections including single or repeated scratch hardness tests.
3. Abrasive jet with sand, alumina, silicon carbide and, or freely falling sand.
4. Abrasive wear tests using abrasive papers or wheels.

Wernick (10) however, reported a method developed by Siens and Halske in which the workpiece is moved to and fro under a hard metal point which presses on it with a constant load. When the film is penetrated, the device is then automatically stopped. Wear resistance is expressed in terms of specific abrasion resistance $(h) = H/t$. Where H is a number of the double movements for the rider to penetrate through the film, and t is the coating thickness. Campbell (15) used a diamond stylus with 25 micron radius, traversing a small area of about 6.5mm^2 until it raised debris at the end of the area. The shadow of the debris as shown by a lamp set at a low angle is interpreted as a measure of wear resistance. This method is not reliable because of the way it assesses wear; since any change in the angle of the lamp will alter the results. The debris may easily be disturbed by an air current.

The Taber abrader is also widely used. This consists of a pair of rotating abrasive discs which rub against a disc of the material under test. The total abraded area being 280 cm^2 . Wear is interpreted as the wear index in which weight loss in mg per 1000 cycles is measured. This method is a comparative wear test, its main drawbacks are:

1. The variability of the abrasive discs.
2. The abrasive discs wear and generate debris as the test is being carried out.
3. The sequence of events by which coating breakdown occurs cannot be investigated.

The Erichsen abrasive meter apparatus has been marketed in Germany (45), in which an abrasive medium on a fine grade paper abrades the surface in such a manner that each area of the paper is used only once. Abrasive papers are fastened to the periphery of a metallic wheel. After each double movement the wheel indexes forward by a small amount to bring a completely fresh abrasive paper into action. The abrasive wear resistance is determined by fixing the number of double movements of the wheel and finding either the weight in mg removed or the volume in mm^3 .

An abrasive jet method has been recognized by many national standards (42,46). Abrasive particles are blown towards the workpiece in a controlled chamber. Abrasive wear resistance is evaluated in terms of the time required for a controlled jet stream to break through the coating, or as the weight of abrasive particles required to penetrate through the anodic film. Deal (31) found that the most consistent results with this abrasive jet were obtained if a single spot is abraded for only 4 seconds,

after which the jet is switched off for a short time before resuming the test on the same spot. He used an abrasive jet in which abrasion resistance was measured in terms of the time required for a stream of abrasive particles to break through the coating.

The advantages of the abrasive jet method are:

1. A very small area can be tested.
2. There is no sample shape limitation, since it can be applied on a flat or curved surface.

The disconcerting features of the abrasive jet lies in a number of points observed by some workers (47) as follows:

1. Different jet assemblies seldom give the same results in absolute terms.
2. Abrasive powder is found to vary from batch to batch.
3. Wear of the jet assembly is the most serious problem encountered. This is due to the delivery of abrasive particles, the nozzle of the assembly becomes tapered by the action of the abrasive and forms a cone shaped end with consequent variations in the apparant flow rate of the abrasive.
4. It is vitally important to control the air flow at 40 litres/min. Variations of 1% may cause variations in the abrasion value of about 3.5%.

5. The humidity of the air is a very important feature affecting abrasive wear results. Wernick (10) has reported a 30% reduction in abrasion resistance when tested in humid air. The reduction of abrasive wear may be caused by the absorption of water in the pores, transforming $\alpha\text{-Al}_2\text{O}_3$ into $\gamma\text{-Al}_2\text{O}_3\cdot\text{H}_2\text{O}$ which is regarded as inferior.

However, if it is accepted that abrasive wear is a process in which a hard sharp indenter is pressed against the surface of the workpiece and forms grooves in the direction of sliding, the abrasive jet results have been overconfidently utilised to express abrasive wear properties (10,12). The more serious limitations of the abrasive jet method are given below:

1. Abrasive jet method does not develop tangential forces, thus frictional properties can not be investigated.
2. Abrasive jet test is often referred to as an impact or erosion wear test in which the scale of damage is largely dependent on a number of parameters, which are:
 - a) The physical nature of the impinging particles.
 - b) Their mass.
 - c) Particle velocity.
 - d) Impingement angle.
 - e) Shape and size of the particle.
 - f) The nature of the material being impacted.

According to the classic theory of impact between frictionless bodies, the contact is merely quasi-static, in the sense that the damage

is assumed to be confined to the vicinity of the contact area. It usually results from the acquired energy which is equivalent to the kinetic energy of the abrasive particles. Hertzian stresses are generated and the maximum compressive stresses are set up beneath the impacted zone. If the pressure is reflected, the surface will be left in a vibration state, in which case surface fatigue may result. In most cases where the impact is causing elastic/plastic contact, Hertzian stresses may lead to subsurface shearing that could exceed the shear strength of the bond between the coating and substrate, resulting in extensive damage of the coating. Furthermore, during impact loading, a heat source arises at the contact region, and due to internal energy dissipation, this may result in crazing of the anodic film due to the large difference of the coefficient of linear thermal expansion between the anodic film and substrate aluminium. The coefficient of thermal expansion for an anodic coating is $5 \times 10^{-6} \text{K}$ and aluminium is $23 \times 10^{-6} \text{K}$.

This may explain the limitations of the coatings where impact loading is encountered. Coatings are most likely being subjected to metal-to-metal sliding or abrasive wear conditions. The type of damage produced in the latter condition is largely governed by the development and interaction of different kinds of stresses manifested in the formation of median/radial and lateral cracks in the case of abrasion, ring and Hertzian cracks in the case of metal-to-metal sliding.

2.10 WEAR MECHANISMS

It has always been accepted as somewhat inevitable that wear will lead to some expenditure in the maintenance and replacement of industrial plant and equipment (48). In the present and foreseeable future economic situation, materials and energy conservation are becoming increasingly important. Wear is a principal cause of material wastage, and friction is a serious cause of energy dissipation (49). According to Eyre (50), the estimated cost of abrasive wear to an industrial nation, accounts for between 1-4% of the gross national product. He also acknowledges the U.K. estimate of an 80% saving possible in maintenance and replacement costs, losses due to breakdown, and an increase in the life of machinery, by exploitation of existing knowledge (50). Wear is one of the three most commonly encountered industrial problems leading to the replacement of components and assemblies, the others being fatigue and corrosion (51). Wear is rarely catastrophic but it reduces operating efficiency by increasing the power losses, oil consumption and the rate of component replacement (50). It has been suggested that wear can only occur as a direct result of friction arising between one surface and another, where the surfaces are either solid, liquid, under both load and motion (52). Kragelskii (53) defined wear as 'the destruction of material as a result of repeated disturbance of the frictional bonds'. However, it is noted that wear is usually defined as the removal of material by mechanical action. These definitions were criticised by Peterson (54) who stated, 'These definitions tend to de-emphasize the importance of corrosion in wear'. In addition, there

are some processes that have similar results as wear but are not specified as wear, for example, plastic deformation and creep. Friction and wear result from a rather complex engineering system in which surface degradation of material is not only governed by the material properties, but also by design and the environment. Each of these play a key factor in the friction and wear properties of the system (55).

Eyre (51) described the possible variables which contribute to friction and wear in engineering systems (Fig.9) and how it may be possible to achieve a better solution to a particular wear problem by optimizing the tribo-system parameters.

Wear encountered in industry has been specified in the following way (51):

Abrasive	50%
Adhesive	15%
Erosion	8%
Fretting	8%
Chemical	5%

It is unusual if one type operates individually, since more than one mechanism is often encountered simultaneously. It is well known for example, that corrosion, by selectively attacking the microstructural constituents, can produce hard particles which accelerate abrasive wear.

2.10.1 Abrasive Wear

This type of wear occurs when hard particles penetrate a surface and

displace material in the form of elongated chips or slivers (50). In the U.S.A. mining industry, three terms are used to describe the various types of industrial abrasion (48), viz. scoring, grinding and gouging. These are used to describe qualitatively the severity of the damage since all of them are caused by the same mechanism. A recent definition has been reported by Peters (56) in which abrasive wear is described as a dynamic process in which strain energy induced by abrasive particles bring about elastic and plastic changes in the structure of the material. Abrasive wear usually takes place under two or three body conditions (51). They are termed as low stress abrasion and high stress abrasion respectively (Fig. 10).

Modelling of Abrasive Wear

During the last thirty years, a number of attempts have been made to theorize mathematically the abrasive wear process. The usual model was proposed by Rabinowicz (57) in which a conical shaped asperity was assumed to have been loaded normally on a flat surface (Fig.11). If the cone penetrates to a depth of X through the flat surface, the projected area in the vertical plane is rx , when the cone moves horizontally a distance of S , it will sweep out a volume V given by:

$$V = r.x.S = \frac{L.\tan \theta.S}{H} \quad (2.1)$$

Where H is the hardness of the abraded material, L is the applied load.

However, this suggests that the harder the material, the less loose

particles will eventually be generated. From equation (2.1) wear volume displaced during abrasion is:

- a) Proportional to the applied load
- b) Proportional to the sliding distance
- c) Inversely proportional to the hardness of the abraded material.

This simple abrasive wear theory tends to:

- 1) Ignore the importance of other properties of materials, for example, fracture toughness is now thought to play a major role in determining the wear properties of materials. Hence, the use of hard and brittle materials may lead to the formation of wear fragments by a chipping process from areas away from the wear track. Thus the total volume of wear may then be greater than the volume swept through by the abrasive particles predicted by this model.
- 2) Suggest a direct relationship between hardness and wear resistance whilst many experimental results reflect a considerable degree of inconsistency of such a relationship (58,59).

2.10.2 Erosion Wear

Erosion wear has been classified in many ways. Suh (60) suggests two types of erosion wear, these are:

- 1) Impingement erosion - this occurs when solid particles are impacting on the surface.
- 2) Cavitation erosion - this occurs when fluid particles impact on a

surface. According to Rabinowiz (57), cavitation erosion occurs when a liquid under tensile stress boils. The bubble collapses producing a mechanical shock wave. Solid surfaces may be damaged by this shock wave leading to material being removed by a surface fatigue mechanism.

Bitter (61), however, suggests two types of wear occur simultaneously during erosion, these are:

- 1) Deformation wear
- 2) Cutting wear

Material removal during erosion depends on the magnitude of stresses generated due to the collision between the particles and the surface. The maximum stress concentration occurs in the centre of the contact and at a depth largely dependent on the kinetic energy of the particles. If the elastic limit is exceeded, deformation wear occurs. Cutting wear occurs if the particles strike the material at an acute angle, removing some material from the surface. If the penetration force does not exceed the bond strength of the material, the collision is said to be purely elastic and no damage occurs.

2.10.3 Adhesive Wear

The terms cohesion and adhesion refer respectively to the ability of atomic structures to hold themselves together and form surface bonds with other atoms or surfaces with which they are in intimate contact (57).

In the case of adhesive wear, the mating surfaces come close enough to form strong bonds or junctions at the real area of contact, and for sliding to occur, these junctions must be subjected to a force higher than the strength of either the junctions or the softer bodies. This force is called the friction force. All engineering surfaces are microscopically rough and are made up of asperities. The interaction of these asperities with adjoining surfaces govern the friction and adhesion behaviour of the solids. The asperities are typically 10 to 300 micron high and 1,000 to 10,000 micron in width at their bases (60). When the asperities of the surface are brought into a sliding process, work is done at the interface and consumed in different modes:

- a) Causing elastic and plastic deformation.
- b) Generation of thermal energy which raises the temperature of the interface.
- c) Creation of new surfaces.
- d) Stored in the form of residual elastic strain energy.
- e) Energy released as frictional noise.

When the applied pressure is high, the thermal energy generated may be sufficient to melt the asperities at their apexes and welded junctions may result. Applying a tangential force leads to the following possibilities (62):

- a) If the shearing stress of the junction is greater than that of the softest body, fracture occurs inside the softest body and metallic transfer occurs. The friction of A on B will become friction of B on B (Fig.1 2).
- b) When the welded interface is weaker than the softer material, it then becomes a location for shearing. In this case there is neither

transfer nor tearing and the coefficient of friction is lower than in the preceding case and this is called shearing friction. Adhesive wear is very much influenced by mechanical, as well as the chemical and physical properties of material, such as hardness, plasticity and surface energy, all of which play an important role in determining the real area of contact. The harder the material, the greater the resistance to adhesive wear, which is expressed to some extent by Archard's model. When hard debris is trapped between the surface during sliding, further wear will be promoted by abrasion. Eyre (63) has shown that certain surface treatments such as carbo-nitriding of steel, reduce the wear rate by diminishing the material's tendency to welding and the susceptibility to metal transfer will be substantially reduced.

2.11 ARCHARD'S THEORY OF WEAR

This theory is widely referred to in the literature (64) on Wear, and regarded as the most plausible quantitative theory. It states that Wear volume $W_{(v)}$ is directly proportional to the applied load, L , and sliding distance, S , and inversely proportional to hardness, H , i.e.

$$W_{(v)} = \frac{K.L.S}{3H}$$

where K is the coefficient of wear and 3 is being regarded as a junction shape factor. It is similar in its physical concept to friction and adhesion theory. It is postulated that when asperities come into contact adhesion may occur between these asperities to form junctions. The subsequent shearing in the weaker asperity occurs

provided sufficient tangential force is applied. This leads to the transfer of material from the weak body to the stronger one. When the transferred material becomes free, loose particles are formed. According to this theory, the number and size of junctions is governed by the applied load and hardness of the weaker asperities. The higher the load, the larger the junctions size, and the greater the number of asperities involved. Using a hard material reduces the number of asperities in the contact area. The size of the particles produced is proportional to the size of the junctions. This theory assumes the debris to be hemispherical in shape.

Despite the wide recognition of the validity of this theory, it is weak in that:

- 1) It emphasises the role of hardness in a way which suggests that greater hardness of a specific material should increase its wear resistance. Whilst experimental evidence shows that this is not always the case.
- 2) It ignores the role of fracture toughness. If wear is recognised as a fracture process, attention should be given to incorporate the fracture toughness parameter in wear equations.
- 3) It does not take into consideration the behaviour of the subsurface. This suggests that wear is a surface process similar to friction. Once again, experimental evidence illustrates that no direct relationship between friction and wear is observed.
- 4) It is assumed that the particles generated are hemispherical in shape with a size proportional to the asperity size, whereas, many experimental observations suggest a production of thin plate-like debris with a length exceeding the base of the original asperities.

The essential point of this theory is that wear expressed as volume of material removed per unit sliding distance is proportional to the applied load and inversely proportional to the hardness of the weaker body. To make use of the relationship between these parameters, a 'K' factor was introduced which is basically a constant of proportionality. However, its physical meaning goes significantly beyond that. Archard (65) defines 'K' as the probability of production of wear debris, since bringing two asperities into contact under normal and tangential forces does not guarantee the formation of loose particles. The coefficient of wear 'K' is therefore, meant to embrace all of those characteristics of materials that are loosely embraced by the term 'hardness' and for this reason has not found extensive use in the design process. Provided that all of the material's properties were known and included within the wear coefficient, it would become valuable in design and also help to define the different types of wear, i.e. each type would be reflected by a different value of 'K'.

2.1 2 DELAMINATION THEORY OF WEAR

A more recent theory, called the delamination theory of wear has been advanced by Suh (66). It explains the wear of metals at low sliding speeds. It takes into account the effect of physical metallurgy on deformation processes in metals and offers an alternative to the Archard theory of wear in explaining the mechanism of production of wear debris. It attributes the formation of thin particles to the

initiation and propagation of cracks in the subsurface layer. As these cracks at a critical stage reach the surface, they result in the formation of plate-like sheets of debris. The mechanism of delamination wear is based on the behaviour of dislocations at and below the surface. The stages involved in the delamination theory are:

- 1) When two sliding surfaces come into contact, normal and tangential forces are transmitted through the area of contact. These forces generate new dislocations.
- 2) As wear continues, dislocations move and pile up below the surface. The movement of dislocations is facilitated by the higher number of slip systems. This may explain why the f.c.c materials '12 slip systems' can undergo more strain than the h.c.p with '3 slip systems'. The generation and movement of dislocations result in deformation. When the applied strain exceeds the elastic limit of the material, plastic deformation occurs.
- 3) Loading beyond this stage causes dislocations to interact with other lattice defects, as well as with other dislocations. This interaction generates voids and initiates microcracks.
- 4) On further loading, voids and cracks can link together by three different mechanisms, i.e.
 - a) Growth of voids
 - b) Crack propagation
 - c) Plastic shear deformation of the metal between the voids and cracks.

5) Before the cracks become long enough to produce free particles, considerable additional plastic deformation will have to take place. At certain weak points these cracks shear to the surface, generating thin plate-like debris. The thickness of this debris is largely governed by the physical metallurgy of the material and the magnitude and distribution of stresses below the surface. These parameters determine the location of cracks at the subsurface. For f.c.c materials the location of cracks is deeper than for h.c.p materials under a given applied load. Initiation of voids and cracks at the surface is not favoured because of the following reasons:

- a) The existence of high compressive stresses at the surface just below the rider tends to close voids and cracks.
- b) Dislocations very near and parallel to the surface experience image forces due to this proximity to the surface (60). When there is no continuous coherent oxide layer adhering to the surface, the image force attracts dislocation to the surface. When the image force is greater than the resisting force (drag force), commonly referred to as the dislocation friction force, dislocations attracted to the surface disappear, i.e. there will be no dislocations pile-up. This results in a softer surface layer than the subsurface. This softer layer can undergo larger plastic deformation.

2.13 SOME FACTORS AFFECTING THE WEAR PROCESS

2.13.1 The Role of Hardness

Hardness is significant in the wear process because it is a measure of the elastic strain energy required to cause plastic deformation. Hardness is considered as one of the most influential properties in wear behaviour of materials.

Richardson (67) observed that hardening of a metal by work hardening has no influence on its abrasive resistance. It has also been noted that the surface hardness of an abraded metal may be considerably higher than that of the bulk due to the intense plastic strain induced by abrasion. It was therefore emphasized that wear resistance should be related to the dynamic hardness of the material.

In abrasive wear, the indentation depth, and hence the volume of material swept through a distance, is lower for hard than it is for soft materials. Occasionally, however, an increase in hardness has been observed to cause an increase in the wear rate. This has been attributed to the fact that the reduced real area of contact implies higher local stresses (67).

In adhesive wear, the higher the hardness, the lower is the real area of contact but higher junction growth, as a result of high local stress, occurs. However, Eyre (63) pointed out that no simple relationship between wear resistance and hardness exists and that care is required when making any recommendation about hardness.

2.13.2 The Role of Fracture Toughness

Rosenfield (68) emphasized that since the mechanism of wear involves the formation of debris particles, it is to some extent, a fracture process. Toughness is a measure of the ability of a material to absorb energy and to deform plastically before failure. Therefore, the greater the energy absorbed, the less susceptibility to wear. Honborgen (69) proposed a model in which the relationship between the wear rate and toughness was studied. His model is based on the comparison of the strain (E_d) induced during the wear process with the critical strain (E_c) at which crack growth is initiated (Fig.13). He showed that the wear rate starts to increase if E_c becomes smaller than E_d , i.e. when the applied strain E_d was less than the critical value E_c for crack propagation, the wear rate was low and independent of toughness. When E_d was larger than E_c for the material, there was an increased probability of crack growth and therefore a high rate was expected. The energy required for metal to deform plastically is represented by the area under the stress-strain curve as shown in Fig.14.

Orbel (70) suggested the term 'Modell' which is the ratio of Brinell hardness to elastic modulus (E) multiplied by 10^6 to indicate the depth of penetration that a metal can tolerate without exceeding its elastic limit. He showed that materials of high Modell number behave like a spring, absorbing energy and preventing stresses from building up to a high value.

2.14 SUMMARY

The major features of the literature can be summarised as follows.

There is no shortage of authenticated information on the anodising process, most of which illustrate, in one way or another, an improved method to achieve the production of a high quality coating for a specific application. Many types of anodising have therefore been developed. They all aim at providing a wider choice of coatings to meet the growing industrial demand. The sulphuric acid type is by far the most widely used for many purposes, in particular, friction and wear applications.

The physical, chemical and mechanical properties of anodised aluminium have been investigated in great depth and it has become evident that these properties, as well the performance of anodic films, are dictated by (a) the metallurgical and production history of the base alloys, and (b) anodising parameters. The sealing process after treatment is reported to reduce abrasion resistance of the anodic films by 30% and some reports suggest a reduction of 70%.

There is a potential growth in the use of anodised aluminium alloys in wear applications. It has already been reported that many conventional engineering materials are being replaced by anodised aluminium alloys.

There is no ASTM standard test to evaluate the tribological behaviour of coatings. Therefore, many non standard tests have been developed, most of which are qualitatively comparative based tests aimed at the selection of a specific material. They share an important

disadvantage, namely the sequence of events leading to the failure of a coating during wear cannot be easily followed and therefore a scientific understanding cannot be established.

The other important feature of the literature suggests that many investigators have inherited the idea of referring to hardness to indicate wear resistance, whilst experimental evidence illustrates a much more complicated picture. A harder coating is not necessarily better wear resistant than a softer one. The oxide film itself is very hard but is generally too thin and porous to protect the base alloy from high pressure often encountered in many engineering situations, although it will resist scratches and therefore protect the appearance of a polished surface.

Regarding the wear of electroless nickel coating, there is considerable information about the process technique, structure and properties of the coatings, however, evaluation of its tribological characteristics is far from complete. Different wear tests have been reported in the literature most of which are conducted on this coating plated on mild steel, whilst coatings on aluminium and its alloys have not received much attention.

This work has therefore been initiated to provide further wear data on the abrasion and adhesion, under dry and lubricated conditions, of four anodic films of the sulphuric acid type. The coatings were produced with a similar thickness but with different hardness values. Electroless nickel of three thicknesses produced on one aluminium alloy was also included in this work.

Wear test configurations used in this investigation differ from

those previously reviewed. It allows a more detailed study of the sequence of events during the breakdown of the coatings under both the abrasion and adhesion wear process. This begins from the onset of static loading to the development of loose debris under dynamic loading.

CHAPTER THREE

EXPERIMENTAL DETAILS

3.1 INTRODUCTION

Test methods used in evaluation of the friction and wear properties of materials are many and varied. Their main purpose being to provide a means of analysing the effects of system variables on tribological processes. The final choice of test apparatus is likely to depend on the emphasis placed on the following factors (71).

1. Obtaining a fundamental understanding.
2. Evaluating materials.
3. Lubricant appraisal.
4. The effect of design modifications.
5. Service simulation.

The wear testing of coatings is significantly different to the testing of un-coated materials for two main reasons:

1. Problems of alignment of the two specimens under test, which may result in high contact loads.
2. Difficulty in measuring with sufficient accuracy the wear of relatively thin coatings and deciding when the coating has worn through.

Test methods previously used (10,15,41,44) to evaluate wear of anodic coatings are inadequate because of the following reasons:

1. Most of the published information is related to erosion which only accounts for 8% of the total wear encountered in industry (50).
2. The test methods, which have been reviewed in Chapter 2, do not lend themselves to gaining an understanding of the wear mechanism(s) involved at the surface of the coatings.

From a wide variety of test methods available, it was decided to use a reciprocating wear method. This enabled the following to be investigated:

- a) Friction and wear properties of the anodic and electroless nickel coatings, using both a single point diamond and a steel ball as a rider, under both abrasive and adhesive conditions.
- b) The mechanisms involved in degradation of the coating, where the effects of different kinds of induced stress acting at the surface and beneath the indenter, have been microscopically studied by applying a static and dynamic load, in both single and multi passes.
- c) Generation of wear debris was studied by relating its morphology to the wear surfaces from which it was developed. This was achieved by collecting debris from the worn surfaces.

Having investigated a, b, and c above, the gap between the mechanisms of wear and the performance of these coatings, can be reduced with greater certainty than before.

Selection of a single point diamond in the abrasive wear study was based on:

- a) Minimizing any possible adhesion between the counterbodies.
- b) Keeping the applied pressure at a constant value by using a non wearing indenter, i.e. 'diamond'.
- c) Establishing the abrasive wear properties of the coatings.

Adhesive wear has been investigated by using a steel ball as a rider against flat coated samples. This test configuration permits:

- a) Avoidance of the alignment problem which might otherwise occur if a pin on flat test method is used (Fig.15).
- b) Continuous monitoring of friction and wear throughout the test.
- c) Assessment of the adhesion properties of the coatings to the steel ball.

Arising out of these experiments, it was observed that the fracture characteristics of the coatings played a critical part in the generation of damage outside the immediate wear contact area under both abrasive and adhesive wear conditions.

However, the ball on flat test method is not trouble-free and its main drawbacks are:

- a) The wear data presented here consists of the total wear, i.e. wear of the coating and wear of the steel ball, and there is no easy way to separate either of them while the test is running (Fig.16 Case III).
- b) As the test progresses the surface area of contact increases due to the wear of the ball, subsequently the nominal applied pressure will be reducing throughout the test. This adds another

complication to the interpretation of the wear results.

- c) Debris may be trapped between the counterbodies and therefore less wear may appear to occur.

These drawbacks represent the driving force for further analysis in which wear of the counterbodies was separately measured and the coefficient of wear 'K' was calculated. Having calculated the 'K' factor for both the steel ball and the coatings, an improved understanding of the wear results was then possible.

3.2 MATERIALS INVESTIGATED

The friction and wear characteristics of untreated aluminium alloy, electroless nickel on alloy 6063, and four anodic films produced on aluminium alloys have been evaluated. The four anodised aluminium alloys are sulphuric acid type and designated as:

Natural anodised, code (9N)	produced on 6063 alloy
Hard anodised, code (9H)	produced on 6063 alloy
Hard anodised, code (15H2)	produced on 2014A alloy
Hard anodised, code (30H)	produced on 6082 alloy

The coatings were produced on a number of different alloys, the compositions of which are given in Table 4. All anodic coatings were prepared to a standard thickness of 30-35 micron and subjected to wear

tests in the anodised condition 'unsealed'. Electroless nickel coating of 8% P on 6063 alloy was produced to three different thicknesses, i.e. 10, 20 and 30 micron. All samples were supplied in a standard size, details of which are given below:

Length	75 mm
Width	30 mm
Thickness	6 mm

All relevant properties including the hardness of the coatings are given in Tables 5-7. The anodising process was carried out by Acorn Anodising Company Limited. The electroless nickel plating was produced by using chemical proprietary solutions as follows.

Zincating procedure prior to electroless Nickel Plating

- 1) Remove dirt, etc. from Al surface and wash with clean water.
- 2) Degrease with acetone.
- 3) Soak clean in M & T Alkean A.11 (not-etching soak cleaner for Al)
12.5-50 g/l 60-80°C 10 minutes.
- 4) Cold water rinse thoroughly.
- 5) Acid etch (R.T) 15 seconds. (In FUME CUPBOARD)
10% H₂O₄ + 100 g/l Ammonium bifluoride
(i.e. 100 ml H₂O₄/litre + 10g NH₄FHF) - specimen may froth.
- 6) Cold water rinse thoroughly - specimen may froth.
- 7) Zincate in Alumseal 30 seconds - 2 minutes (R.T.)
- specimen may froth.
- 8) Cold water rinse thoroughly - specimen may froth.
- 9) 8% P electroless nickel plating - specimen will froth for a minute or two.

Note: Regarding the safety in using Alumseal:

This contains small amount of cyanide. Operator must wear protective clothing: gloves, face protection, coat, apron, etc.

Ensure all gloves, etc. do not have holes. Tape up all open cuts, sores, etc. on skin prior to putting gloves on.

A plastic petrol syphon may be used to extract Alumseal from the drum.

Store the Alumseal in a clean dry winchester and label it

'Alumseal Proprietary Zincate Mixture: Toxic and Corrosive: Contains Cyanide' CLEARLY.

Flush out syphon twice with water keeping the used water in a bucket and dispose of water safely, i.e. not into a sink.

Storage and Use of Alumseal. This can be reused over and over but any liquid disposal must be marked 'For Disposal Containing Cyanide - DANGER'.

3.3 SURFACE MORPHOLOGY OF THE COATINGS INVESTIGATED

The anodised and electroless nickel surfaces were characterised by two techniques. First, using a Rank Tayler Hobson Talysurf which shows the dimensional roughness expressed as R_a values (Fig.17). Second, by scanning electron microscopy where the three dimensional texture was observed. The porous structure of the anodic film and the nodular feature of the electroless nickel coating were observed (Fig.18).

The natural and hard anodised coatings have hemispherical pores and pits (Fig.18). These pores play an important role in reducing friction and wear under lubricated adhesive conditions.

3.3.1. Composition of Anodic Films

Analysis of the anodic coatings suggests that about 22-31% of the structure consisted of sulphur in a form believed to be aluminium sulphate (Table 8 and Figs.19,20). This is in agreement with the results shown by other investigators who have observed a high proportion of sulphur. This is attributed to anodising in sulphuric acid.

3.3.2. Coating Thickness Measurement

Thickness measurements were carried out on cross sectioned samples by using an optical microscope. The results obtained are in agreement with those provided by the materials supplier.

3.3.3. Microhardness Measurement

Microhardness measurements were taken on cross sectioned samples. An average of five readings was determined at a load of 50gm.

3.4 WEAR PROCEDURE

3.4.1 Wear Rig

A layout of the reciprocating wear test rig used in this investigation is shown in Fig.21. The test specimens were fastened to a mild steel holder. The specimen holder is fixed to a cast iron platform which

reciprocates on two guides acting as bearing surfaces. A reciprocating movement was achieved by linking one end of the platform to a rotating spindle with a connecting rod. The rod is fixed by screws clamped through the centre of the bolt recess housed at either end of the rod. The output speed of the motor is controlled to vary through a range of 0-200r.p.m..

The specimens were subjected to the action of a diamond rider for abrasion, and also a ball rider in the case of adhesive wear. The rider was screwed in a supporting bar. The load was suspended from the free end of the bar, whereas the other end is pivoted between two ball bearings. This allows free vertical movement of the bar holding the rider and load. Any horizontal movement of the load bar was restricted by two vertical bars. Friction and wear depth were monitored continuously by using linear voltage displacement transducers (L.V.D.T.). The friction force measurements were then utilized to calculate the friction coefficient μ :

$$\mu = \frac{\text{Friction force (F)}}{\text{Applied load (L)}}$$

Continuous monitoring of friction and wear was made under both dry and lubricated sliding conditions. The transducers were calibrated to an appropriate sensitivity whereby any change in either the friction or wear was detected and measured.

3.4.2 Abrasive Wear Test

All specimens were cleaned with methanol and dried immediately prior to each test.

The experiments were conducted on each sample by using a conical diamond profile with an incident angle of 60 degrees (Fig.22), the attack angle therefore, being effectively 60 degrees. The specimens were subjected to different loads ranging from 2 to 10N in increments of 1N, with the number of passes varying from one to a hundred. All wear tests were performed at an average speed of 10 cycles per minute and a track length of 25mm. The experiments were carried out at room temperature (20°C) and relative humidity between 65-75%.

Wear track depth and width were measured by using the profilometry technique and the data produced was used to plot wear curves in four forms:

1. Wear depth in microns versus number of passes
2. Wear depth in microns versus applied load
3. Wear volume in mm^3 versus applied load
4. Coefficient of abrasive wear of anodised aluminium alloys 15H2 and 9H.

The mechanism of fracture of hard anodised aluminium 9H was investigated under static and dynamic loading conditions. Indentations were made using the same diamond at the same loads. The total cycle of loading and unloading was one minute, whilst a single unidirectional pass of 25mm length was carried out for each load.

Multipass tracks were then produced in the same manner mentioned previously.

3.4.3 Adhesive Wear Test

All materials investigated were subjected to adhesive wear against a 5mm diameter steel ball (BS970, A.I.S.I.51100, 950Hv) as a rider. The specimens were cleaned with methanol and then dried prior to each test. The steel balls were first degreased with white spirit, then washed with an organic solution (Hexan) and dried before each experiment. Adhesive wear tests were conducted by rubbing the specimen against the steel balls under both dry and lubricated conditions at room temperature and a relative humidity of 65-75%. The tests continued until breakdown of the coating occurred.

Wear data is presented in the form of curves, as a function of applied load ranging from 10 to 30N, in 5N increments under dry conditions. To accelerate the coating breakdown, a load ranging from 20 to 60N was applied under lubricated conditions.

On the reciprocating wear rig, the total wear in terms of depth and tangential forces were continuously monitored through the test by using linear voltage displacement transducers (L.V.D.T.). The movement of the samples was fixed at 43 cycles per minute with a total track length of 5.6cm. The sequence of breakdown of hard anodised alloy 9H was carefully followed by applying loads ranging from 20 to 60N under static and dynamic conditions. The total loading and unloading time under static conditions was 2 minutes. Under dynamic conditions both single unidirectional and multipass tests were

carried out, the latter for 5, 30, 60 and 300 minutes.

3.5 EVALUATION OF THE ROLE OF COATING THICKNESS

Electroless nickel coatings of 10, 20 and 30 microns were produced on 6063 aluminium alloy only whose composition is shown in Table 4. All coatings were tested at loads in the range of 5 to 20N in a reciprocating movement against an A.I.S.I.51100 steel ball. All tests were conducted at ambient temperatures under both dry and lubricated conditions. A fully formulated 20/50 oil was used in the lubricated experiments. The number of cycles, in terms of sliding distance required to break down the coating, was regarded as an indication of the wear life of different coating thicknesses.

3.6 THE MAJOR ANALYTICAL TECHNIQUES USED

A wide range of qualitative and quantitative analytical techniques have been used, aimed at performing the following tasks:

- 1) Characterising the surface in the as received condition.
- 2) Observing the changes occurring on the surface and subsurface as a result of the wear process.
- 3) Identifying the mechanisms involved during the breakdown of the coating.

The wear test methods and the analytical tools used during the investigation are summarised in Fig.23. However a description of the major techniques used is briefly dealt with as follows:

3.6.1 Talysurf

This tool was employed to assess the surface finish of the coatings investigated, and was also valuable in quantifying the wear track, i.e. measuring the track dimensions in terms of depth and width, from which the amount of wear was determined. An average of four measurements is considered. These were taken at 5mm intervals over a 25mm abrasive wear track.

3.6.2 Scanning Electron Microscopy

This instrument was the major tool used in characterising the surface morphology of the materials investigated. It enables a high depth of field to be resolved, thus revealing the three-dimensional texture of the materials. Invaluable information was obtainable from studying the worn surface, in that it was possible to characterise the different failure mechanisms by which the coatings were disintegrating.

The use of an energy dispersive X-ray analyser in conjunction with the S.E.M. permits direct elemental analysis, both qualitatively as well as quantitatively.

3.6.3 Electron Spectroscopy for Chemical Analysis 'ESCA'

This tool was also available to analyse the wear debris recovered. The particles were mounted on a special holder and exposed to a beam of monochromatic X-rays in a vacuum chamber, causing electrons with

kinetic energies of the parent atoms to be ejected from the debris. A spectrum containing the characteristic of the elements present was obtained.

Some of the debris generated under lubricated conditions was separated from the lubricant by using a Rotary Particle Depositor and Centrifugal technique, then examined in a Scanning Electron Microscopy.

3.6.4 Taper Sectioning

Taper sectioning at 11.5 degrees enlarged the damage in the subsurface of the coating by 5 times. This technique gave invaluable information about the extent of damage induced during the wear process. The procedure used is shown in Fig. 24.

CHAPTER FOUR

RESULTS

The results of this investigation are presented in the following sections.

1. Presentation of wear curves with both a single point diamond and a steel ball on flat configurations, and the construction of surface failure models of coatings under different test conditions.
2. Examination of the worn surfaces, including steel balls, using techniques, which include scanning electron microscopy, was carried out to understand the failure of the coatings.
3. Examination of the debris generated during the tests by scanning electron microscopy, X-Ray and electron spectroscopy for chemical analysis (ESCA) techniques.

4.1 WEAR RESULTS

4.1.1 Abrasive Wear Results

Initially abrasive wear track measurements were obtained by using an optical microscope at a 100x magnification. Data produced from track width measurements were utilized to calculate track depth by using a simple formula.

$$d = \left(\frac{W}{2} \right) \cdot \cot \theta$$

where d = track depth

w = track width

θ = indenter half angle

However, there were some difficulties involved during the measurement of track width, i.e.

1. In the case of untreated aluminium, the edges of the wear track were usually raised due to material deformation. The height of these edges increases as a function of load and number of passes. Edge definition was therefore rather obscure and track width difficult to measure.
2. In the case of coatings, some difficulties were encountered, particularly due to the irregular nature of the cracking, extending from the edges of the wear track into the non-contact areas. In general, the wear track width measurements do not represent the material removed from the non-contact zones and the only way to measure this would be by weight loss. However, weight loss of a thin coating on a relatively large flat wear specimen was itself so small that the weight loss method was not appropriate.

In order to overcome these difficulties, it was decided to adopt the talysurf method in which track depth and width were precisely measured. The other advantage of this method is that the data is produced as a hard copy, hence further reference is possible. An

example of this is shown in Figure 25.

The abrasive wear data generated from the talysurf method illustrate an important point, namely that track depth does not correspond linearly to the track width. This may explain why a variation in either depth or width may result in a noticeable change in wear volume.

Abrasive wear results have been presented as three types of curve. The first type shows the relationship between wear in terms of depth and the number of passes, varying from a single pass to 100 passes, for a given load. The second type illustrates wear ranging from 1 to 5N for a fixed number of passes. The third type shows wear in terms of volume versus number of passes for a given applied load.

In general, the bulk of the wear curves presented in this work demonstrates that abrasive wear of untreated aluminium, anodised aluminium alloys, and the electroless nickel plated on aluminium alloy, is proportional to applied load and sliding distance. Thus the following statements can be made:

1. The untreated aluminium alloy exhibited a linear proportionality between wear depth, wear volume and applied load, for all test conditions except in a few cases where a slight deviation from such a relationship was noted (Figs. 26-41).
2. For a single pass and at loads ranging from 1 to 5N, no significant wear was noted for the coated alloys except natural anodised (9N) and hard anodised (15H2) which showed superficial wear (Fig.26).
3. At 1.5N and 10 passes, natural anodised (9N) exhibited rapid wear and the anodic layer began to break down at an early stage of the

wear test. The remainder of the coatings, i.e. hard anodised '9H', '30H' and the electroless nickel of a 30 μm on 6063 alloy, produced similar results (Fig.31).

4. As the applied load and/or the number of passes increased, the resistance to wear diminished and indicated that hard anodised '9H' had undergone complete destruction at 3N and 100 passes (Fig.29).
5. Figures 28,29,34,35,36 show that hard anodised 15H2, 30H and electroless nickel alloys started to disintegrate at loads ranging from 4 to 5N and 50 to 100 passes. At this stage the coating was worn through to the substrate.

Since a linear relationship between a wear track depth and width does not exist, wear volume versus the number of passes, indicated a slight shift in wear results from those presented earlier, thus:

- a) At 1N, hard anodised 15H2 and 30H alloys showed a greater wear volume than the remainder of the coatings (Fig.37).
- b) At 2N, two distinct bands of wear behaviour were recorded. The upper band comprised the natural anodised '9N' in addition to the untreated aluminium alloy, whilst the rest of the hard anodised alloys, '9H', '15H2', '30H' and the electroless nickel on 6063, have shown less material removed (Fig.38).
- c) At loads greater than 2N the breakdown of the coatings was faster and this appeared to be facilitated by the deformation of the underlying substrate alloy.

The above results produced a specific coefficient of wear for each material. An example of this is shown in Figure 42 in which anodised alloy 15H2 '303Hv' initially exhibited a higher coefficient of wear than hard anodised alloy 9H '403Hv'. This suggests a higher wear rate for 15H2 which can be attributed to its relatively low penetration resistance. Thus, more material has been swept in front of the indenter. Owing to its scratch resistance, 9H alloy shows better resistance to abrasive wear for the first few passes. The damage is elastic and the probability of producing loose particles, i.e. its 'K factor' is very low. As the wear test progresses, the accumulation of residual stresses in the 9H alloy becomes higher because of its relatively limited ability to absorb these stresses. The main manifestation of these stresses is the development of a lateral crack system which is responsible for the material removal in a brittle solid by a chipping process. Thus more material breaks away from areas well beyond the wear track boundary. This signifies a higher coefficient of wear. Being more flexible, 15H2 alloy shows a lower coefficient of wear. The residual stress in this alloy is consumed by plastic deformation, and therefore the amount of loose particles is low.

4.2 ADHESIVE WEAR RESULTS

4.2.1. Under Dry Conditions

These results are for those experiments with a steel ball sliding on all the materials investigated under both dry and lubricated conditions.

Figure 43 shows results obtained for hard anodised alloy 9H over

the range 10 to 30N. It can be observed that a relatively smooth curve of wear depth against sliding distance is obtained prior to breakdown when a very much greater wear rate then occurs. The wear curve showed a high initial wear changing to a lower value preceeding the breakdown of the coating. Therefore, wear graphs can be divided into three regions.

- 1) Running-in
- 2) Steady state
- 3) Breakdown

At these stages wear is proportional to applied load and sliding distance but the wear coefficient 'K' will be different indicating a change in the wear mechanism. K factor was calculated from Figure 44 using equation 4.2 (72)

$$K = \left(\frac{D2 - D1}{T2 - T1} \right) \frac{H}{PV} \quad (4.2)$$

Where K = Coefficient of Wear

D1 = Depth at Stage I

D2 = Depth at Stage II

T1 = Time at Stage I

T2 = Time at Stage II

H = Hardness

P = Pressure

V = Velocity

A K value of 2.5×10^{-5} was obtained. This suggests that only two or three events out of 100,000 events cause damage and produce loose particles. Figure 44 shows that the wear depth ($82 \mu\text{m}$) is greater than the coating thickness '30-35 μm '. This would imply that the difference is accountable by wear of the steel ball and a K value of 2.5×10^{-5} will be incorrect with respect to the wear of the coating. There is another consideration with respect to the wear of the steel ball. Because of the changing geometry, wear depth is not directly proportional to wear volume. It was therefore decided to approach the problem from a different angle in which the K factor of both counterbodies was evaluated. In order to achieve this, a series of separate tests were conducted under dry conditions at 10N for 15 minutes, one hour, four hours, six hours, twelve hours, and twenty-four hours.

The apparent area of contact was measured macroscopically for each test. The data obtained was utilized to calculate the material worn from the ball in terms of depth by using equation 4.3:

$$h = r - \sqrt{r^2 - \frac{d^2}{4}} \quad \text{--- (4.3)}$$

Where h = wear track depth

r = indenter radius

d = wear track width

Wear volume was then calculated by using equation 4.4:

$$W_{(v)} = \frac{1}{3} \pi h^2 (3r-h) \quad \text{--- (4.4)}$$

Equation 4.5 was then used to evaluate the coefficient of wear for the steel ball.

$$K = \frac{W(v)H}{Ld} \quad - - - \quad (4.5)$$

Where

K	=	Coefficient of Wear
W(v)	=	Wear volume
H	=	Hardness
L	=	Applied load
d	=	Sliding distance

The results are summarised in Figure 45 and Table 9.

On the anodic coating 9H, wear track depth and width were measured for each test by using a profilometry technique. The data obtained was utilized to evaluate wear volume by using equation 4.6.

$$V = \frac{1}{3} \int h^2 (3r-h) \times L \quad - - - \quad (4.6)$$

Where

V	=	Wear volume
h	=	wear track depth
r	=	indenter radius
L	=	wear track length

The coefficient of wear was then calculated by using equation 4.5 and the results tabulated in Table 9 and Figure 45 show that:

1. During running in the coefficient of wear was higher for the ball than for the anodic film, most of the material loss was due to the wear of the steel ball.
2. In the steady state region, wear of the ball was reduced due to a flat scar being produced. This diminished the pressure exerted on the system. Wear of the anodic film increased, probably due to the presence of trapped debris between the counterbodies acting as an abrasive.
3. Breakdown occurs as a sudden failure of the coating. This produces a high coefficient of wear.

It would have been very interesting if there was no sharp transition in wear due to the sudden coating failure because it would then be possible to extrapolate the results of Figure 46 'broken line' and this would facilitate the calculation of the 'K factor' of the counterbodies separately, directly from wear curves and the material selection for a specific wear application would be easier.

Once again from Figure 44

$$Dt = Dr + Dc$$

Where Dt = Total depth

Dr = Material removed from the rider (steel ball)

Dc = Material removed from the coating.

When considering the longest test, i.e. 24 hours, the depth calculated from the ball and the anodic coating does not agree with that plotted in Figure 44.

$$Dt = 130. + 2$$

$$Dt = 132 \mu\text{m}$$

Whereas a total depth of $82 \mu\text{m}$ is seen in Figure 44. Such results were not surprising because some of the loose particles were trapped between the counterbodies, and the wear transducer (L.V.D.T.) has measured the total depth minus the height of debris.

One can argue that wear coefficient calculation for the wear curve would not be accurate due to the presence of these trapped particles between the surfaces. However, in any engineering system there is no absolute method to prevent debris from being trapped between the rubbing components. Therefore, one has to accept this assumption. From a fundamental point of view, a technique whereby the loose particles are being removed while the test is in progress should be adopted, such as brushing the worn surfaces, bearing in mind that this may affect the nature of the wear mechanisms which may otherwise occur.

Information of the type shown in Figure 43 was obtained for all materials investigated (Figs.47-51). It can be clearly seen that the breakdown condition given by the sliding distance varies considerably from one material to another and the following observations can be made:

1. The untreated alloy does not show three regions of wear and exhibits very poor wear resistance.
2. 9N alloy which is the natural anodic coating provides a significant improvement in wear, but this is further improved when the hard anodised alloy 9II is tested.

3. In comparing the hard anodised coatings on different alloys it will be observed that there are considerable improvements in the adhesive characteristics as the alloy is changed from 15H2 to 9H and finally to the best material, 30H alloy.
4. Friction was measured for all the experiments reported in this investigations and in all cases was high for the dry experiments and low for the lubricated experiments. The individual results are not reported here but are represented by the values in Figure 52.

4.2.2 Results of Lubricated Tests

Figures 53-56 show results of all lubricated tests at different applied loads. It will be observed that there is a considerable improvement for all materials investigated. The results of both dry and lubricated wear for 15H2 are shown in Figure 56. They show a considerable reduction of wear and an increase of life, expressed as sliding distance, i.e. from 5×10^4 cm. to 34×10^4 cm.

The coefficient of friction in all cases is substantially reduced from values greater than 0.4 down to 0.1 which is indicative of boundary lubrication (Fig 52). The minimum load in relation to the number of cycles or 'sliding distance' required to cause fracture has been established (Fig.57). This relationship suggests that surface fatigue was also operative in addition to the other mechanisms like brittle fracture and adhesion. The failure of the coating was a markedly load dependent phenomenon. Similar observations have been made by Rabinowicz (57), in which time (t) to failure as a function of load was expressed as:

$$t = \frac{\text{constant}}{L^3}$$

where t is the time to failure and L is the load.

4.2.3 Adhesive Wear of Electroless Nickel

Electroless nickel coating of all thicknesses offered no protection to the underlying aluminium alloy 6063. Under dry sliding conditions the coating failed catastrophically mainly by adhesion. There is an approximate linear relationship between the thickness and life of the coating (Figs.58,59) but a few more points on the graph are required before a precise relationship can be established. The wear rate and the wear mechanisms for all three thicknesses are similar which would tend to show a linear relationship.

The presence of lubricant significantly prolonged the wear life of this coating. The as-plated nodular morphology of the electroless nickel coating was of a great benefit in oil retention to the contact zone (Fig.60). These results are shown in Figure 61.

The tribological characteristics of these coatings appeared to be sensitive to:

- a) Surface topography
- b) Environment

Smoothing of the surface diminishes the potential protection of

the lubricant. As a result of which, an early breakdown of the polished surface of the electroless nickel coating was noted and the number of cycles required for the rider to breakthrough the coating was significantly reduced.

The coefficient of friction (0.14) of the as-plated coating appeared to be unaffected by the polishing process.

4.3 MICROSCOPIC EXAMINATION OF WORN SURFACES

4.3.1 Under Abrasive Wear

Examination of the worn surfaces suggests a number of different mechanisms by which the untreated, anodised and electroless nickel plated aluminium alloys have worn.

During the initial stage of the abrasive wear process, wear particles could be seen building up on the leading edges of the diamond. The process of debris build-up continued until the diamond started to penetrate through the coating.

Scanning electron microscopy of the untreated aluminium showed typical signs of abrasive wear of a ductile material. The worn surface is characterised by a smooth appearance with the material deformed in the wear direction. The general morphology within the track suggests a ploughing mechanism (Fig.62), with sporadic cracks developing perpendicular to the sliding direction as a direct result of the shear stresses. Delamination was also noticed (Fig.62). Profile examination of wear by using the Talysurf showed that the edges of the wear were

raised by a deformation process (Fig.25).

With regard to the anodised alloys, the initial contact appeared to induce elastic stresses near the contact zone. As a result of this contact, no lateral cracks were noted outside the wear track at low loads and a small number of passes. The worn surfaces are characterised by a smooth appearance and abrasion marks in the direction of wear with the exception of the natural anodised coating '9N' which showed intergranular fracture at an early stage in the wear process, since at loads less than 2N brittle fracture was the predominant mechanism, with evidence of fracture confined to the wear track (Fig.63a). As the load increased, the damage begins to include areas beyond the wear track boundaries (Fig.63b). At 3N the rider broke through the coating and a complete disintegration of the coating occurred (Fig.63c).

The resistance to abrasive wear was further improved when hard anodised aluminium alloy '9H' was tested, and the following observations can be made:

1. At loads less than 2N and 50 passes, the original surface morphology was observed to consist of materials deformed in the wear direction (Fig.64). This indicates that some plastic deformation occurred, which resulted in the production of sheet-like debris. Some of these were detached from the surface leaving small impressions in the plastically deformed surface (Fig.64).
2. At loads greater than 2N, cracks perpendicular to the sliding direction were apparent. These developed in response to the frictional stresses, fractures occurring at or below the surface.

This was caused by the repeated strain inflicted upon the surface by the reciprocating motion. As lateral cracks spread towards the outside of the wear track more material was removed, eventually by a chipping mechanism (Figs.62,63,64).

This process is an essential feature of abrasive wear of hard anodised aluminium alloys. The lateral cracks appeared to have intersected the anodic coating and electroless nickel at different test conditions of loads and number of passes. For natural anodised '9N', lateral cracks developed at an earlier stage than that at which hard anodised '9H', '15H2', '30H' and electroless nickel begin to break down. For the latter three coatings, plastic deformation was the predominant mechanism acting on their surfaces. Judging by the appearance of the worn surfaces, different mechanisms were operating, either individually or collectively, resulting in surface degradation of the coatings (Figs.63-69). Figure 69 shows the latest stages of crack initiation and propagation in the electroless nickel coating as it is subjected to abrasive wear. Figure 69 illustrates an optical observation of lateral cracks appearing at the surface and intersecting the wear track. Under a reciprocating motion for 50-100 passes, material outside the wear track is removed, and this signifies a chipping mechanism.

Static tests on a hard anodised alloy 9H produced damage normally encountered in brittle materials such as glass and ceramic. Figure 70 shows that the plastic contact zone is surrounded by lateral cracks in a spiral path. This spiral crack path may be due to the use of a conical profile diamond indenter. Median cracks, emanated from the

edge of the contact zone, grow to a greater distance away from the area of contact. In dynamic tests as a result of combined normal load, together with an applied tangential force, the median cracks travel ahead of the diamond and the fully developed lateral cracks travelled sideways from the wear track (Fig.71). As a result of the reciprocating motion, the wear tracks became deeper, and denser cracks emerged from beneath the surface, leading to the removal of the coating from areas well away from the immediate zone of contact with the indenter (Fig.72,73). These results of static and dynamic tests appear to be in agreement with the model of fracture mechanics of brittle solids suggested by Marshall (73).

The damage was not confined to the surface only but extended into the subsurface. An examination was made using taper sectioning of the wear track. The anodic coating appeared to have been pushed into the softer substrate. The bottom of the coating layer had a proliferation of cracks growing in various directions. These seemed to generate from an area deep inside the coating (Fig.74). An illustration of the major mechanism involved during abrasive wear of anodised aluminium is shown in Figure 75. It will be observed that brittle fracture is represented by a higher proportion than that of fatigue and plastic deformation.

4.3.2 Under Adhesive Wear

Scanning electron microscopy reveals the nature of damage imposed on both coatings as well as the steel balls.

Figures 76-81 illustrate different mechanisms by which the coatings have been worn. For the first few cycles, steps normal to the sliding direction appeared over the whole conformal area (Figs.76,77). These steps seemed to travel ahead of the steel ball leaving an accumulation of flowed layers at the end of the wear track (Fig.76). Close examination of Figures 76,78 shows well developed cracks emanating from the wear track and extending a relatively long distance. At critical loads, depending on the material, the surface of the wear track has superimposed upon it a series of folds or ridges. The ridges following the displacement of the underlying substrate, leading to the breakdown of the anodic coating. At low magnification the surface, at the conformal contact, showed grooving (Fig.80). Grain pull-out was also observed from some areas. The shallow side of the wear track looked quite different with a relatively rougher appearance. Figure 81 illustrates a mixture of fine and deep cracks developed perpendicular to the sliding direction. They form a network at the shallow side of the wear track.

This demonstrates the way in which quite different wear mechanisms can co-exist across and within a narrow band.

The sliding process has been closely observed by comparison with normal (static), as well as combined normal and horizontal (dynamic) loads on the hard anodic film. Figure 82 illustrates a schematic representation and an S.E.M. of the possible types of stress which may generate when a flat surface is statically loaded by

a blunt indenter or sphere. The S.E.M. shows two types of cracking systems, ring-like and radial cracks. Interestingly enough, there was no pronounced evidence of damage in the area of direct contact with the ball.

When a tangential load is applied, due to friction between the anodic film and the steel ball, the geometry of the ring crack system may well be changed. The concentration of stresses for different engineering contacts is demonstrated in Figure 83. For pure sliding the stresses become closer to the surface due to the frictional forces for a single unidirectional pass, the developed cracks intercepting each other at regular spaces, spreading beyond the contact zone. Figure 84 shows a clear definition of the wear track resulting from the reciprocating movement and regularly spaced cracks extended outside the wear track. It appeared however, that brittle fracture was the predominant mechanism. Under lubricated conditions, metal transfer diminishes and brittle fracture was the predominant mechanism by which hard anodised aluminium alloys had worn, an example of which is shown in Figure 85.

Poor wear performance of electroless nickel coating under dry conditions has been detected by scanning electron microscopy in conjunction with microprobe analysis. Figure 86a shows evidence of shearing of junctions which led to the exposure of the underlying aluminium alloy (Fig.86b).

The role of surface topography on the wear performance of

electroless nickel coating under lubricated conditions is illustrated in Figure 87. Polishing of the surface diminishes the potential protection of the lubricant. However, the presence of lubricant reduces the metal transfer mechanism between the electroless nickel coating and the steel ball. Brittle fracture becomes the predominant mechanism (Fig.88) with evidence of mechanical polishing (Fig.89).

4.3.3 Microscopic Examination of the Worn Balls

Examination of the steel balls indicates that they too have suffered a great deal of wear despite their hardness (950Hv) which is about two to three times the hardness of the coating. Figures 90,91,92,93 qualitatively illustrate how much material has been removed from the steel balls. Figure 92 shows a build up of aluminium on the steel balls. Transfer from the anodic layers occurs at an early stage within the first few cycles of the sliding tests. Material transfer is therefore observed on the steel ball.

Microprobe analysis was used to detect whether or not the major elements have transferred from the ball to the coating layers. Figure 94 shows iron and chromium have transferred from the steel ball to the coating.

The predominant wear mechanism of all coating layers, under lubricated the condition, appears to be brittle fracture (Fig.85) with very little damage to the steel ball. Most of the wear therefore, is confined to the coating. The metal transfer mechanism was

markedly diminished. A number of elements were deposited on both the coating and the steel ball, namely silicon, chlorine, potassium and calcium with very little chromium and iron being deposited (Fig.95,96).

4.4 EXAMINATION OF WEAR DEBRIS

4.4.1 Abrasive Wear Debris

Wear debris analysis was developed as an additional source of information concerning the wear process beyond that provided by wear surface analysis.

Scanning electron microscopy of debris recovered during the course of the abrasive process indicated the different mechanisms by which materials have been worn (Fig.97-99).

Plastic deformation was the predominant mechanism which acted on the uncoated aluminium alloy (Fig.97). A ploughing mechanism was evident with materials being compressed perpendicularly in the wear track direction. Whereas, the major feature of abrasive wear debris generated from the anodised aluminium alloy 9H was brittle fracture. The presence of sharp edges, as well as striated particles, was evident (Fig.98). These characteristics supported the suggestion of the involvement of a brittle fracture mechanism by which these particles were generated. Striation marks observed, offer evidence to indicate fatigue

fracture is operating in conjunction with the abrasive wear process. The sequence of events by which debris is generated from the hard anodic film 9H is demonstrated in Figure 66. Plate-like debris with abrasion marks was associated with the abrasive wear of electroless nickel. Debris collected from the wear process also shows evidence of shearing steps which suggest a plastic deformation mechanism (Fig.99).

4.4.2 Adhesive Wear Debris

Many techniques were used in order to establish a better understanding of the mechanisms acting on the coating during the sliding process. The S.E.M. was a major tool in characterizing sliding wear debris. Figure 100 shows a plate-like debris produced from anodic film 9N. It shows ridges covering the total surface of debris resembling the appearance of coating surfaces developed during the early stage of the sliding process.

Figure 101 illustrates another example of the plate-like debris which contains a network of cracks. Shearing marks and grooving were also noted. Figure 102 indicates evidence of brittle fracture. Some of the debris were also subjected to Electron Spectroscopy for Chemical Analysis (ESCA). It will be observed that debris generated from the sliding of anodised aluminium alloys against the steel ball consist of a number of elements in a chemical compound form of aluminium oxide, aluminium sulphide, with some silicon and iron (Figs.103,104).

Under lubricated conditions, rubbing the steel ball against uncoated aluminium alloy 6063 produces platelike debris deformed in the sliding direction (Fig.105a,b). The morphology of this debris suggests that the particles may have been rolled between the counterbodies. The mechanism by which they are generated appeared to occur in two stages:

1. Coating of the steel ball by aluminium due to adhesion.
2. Adhesion then occurs between the aluminium coated on the steel ball and the aluminium sample, i.e. like on like sliding. This enhances the growth of the welded junctions, and as sliding commences, these junctions fracture and wear debris is produced.

Debris generated from the as-plated and polished electroless nickel coating also suggests evidence of brittle fracture (Fig.106).

CHAPTER FIVE

DISCUSSION

The wear process is widely accepted as a multifaceted phenomena that depends on materials and environments, as well as the type and magnitude of the loading. A wear test for coatings must be carefully selected, with particular attention given to:

1. Coating thickness.
2. Mechanical and physical properties of the coating.
3. Coating integrity, i.e. adhesion of the coating to the substrate.
4. System alignment: It is important to have an alignment between the counterbodies. Lack of it may generate non-uniform stresses beneath and around the area of contact, and a premature breakdown of the coating will occur (Fig.15).
5. Performance of the coating must be monitored continuously by a strain gauge or transducer. This enables both the friction and wear to be measured. The transducer should be calibrated to a sensitivity range, enabling any change of friction or wear due to breakdown of the coating to be detected instantaneously.
6. Attention must also be given to whether a simulative or fundamental test method should be adopted.

From the discussion of wear test methods 'Chapter 2', it appeared that understanding of the wear mechanisms of coatings has been immensely handicapped by the co-existence of test limitations. Efforts have therefore been concentrated on establishing a more

understanding approach in order to control the fragmentation and crushing processes to minimize surface degradation of the coatings and eventually to enhance materials performance in a tribological application.

A test method using a single point diamond, and steel ball on flat configuration has been discussed in Chapter 3. The results of which are discussed here under the following headings:

1. Abrasive wear.
2. Evaluation of adhesive wear data.
3. The role of substrate.
4. The effect of coating thickness.
5. Friction properties.

5.1 ABRASIVE WEAR

Anodic and electroless nickel films continue to offer good potential protection to the otherwise poor wear properties of a relatively soft substrate until breakdown of the coating occurs, after which the protection is lost and the substrate exposed to direct contact with the rider.

The abrasive wear results of the untreated alloy show a linear proportionality between wear and applied load, and the number of passes, whereas anodic and electroless nickel films exhibit a non linear relationship, thus:

1. For a single pass and loads of less than 2N, no wear was measurable and almost all coatings afford good protection to the substrate. This can be attributed to the fact that the contact under these conditions has predominantly been elastic, and the bulk of the work applied by the diamond has been consumed at the surface with no measurable damage.
2. At intermediate loads in the range of 2N to 3N, the anodic films start to show some yield. This suggests a transition from purely elastic to plastic contact.
3. At higher loads in the range of 3N to 5N, all coatings appeared vulnerable to intense strain, under which they were unable to provide enough protection. The generated stresses have manifested themselves in different types of damage.

This suggests that different mechanisms were involved in the disintegration of the coatings. This can be attributed to the fact that the potential protection of the coating is intimately tied up with the physical and mechanical nature of both the coating and substrate. For example, if the hardness of the coating is similar or less than that of the substrate, then both will deform together and gross disintegration of the film will be restricted. In contrast, the greater the difference in hardness, the more susceptible the coating is to cracking and fracturing. The cracks run at right angles to the tensional stress. Hard anodised alloy 15H2 exhibited a superior abrasive wear resistance to natural and hard anodised 9N and 9H alloys respectively, despite its hardness being the lowest amongst the coatings investigated. Calculation of coefficient of abrasive

wear of 15H2 and 9H alloys showed two different trends, i.e. for the former, a high K was initially obtained which then reduced as the test continued to run, whereas a low K value was obtained with the latter which increased as the test proceeded. The high initial K value for 15H2 alloy can be attributed to its low penetration resistance. However, as the test continued the energy was consumed in deforming the coating. Unlike 9H alloy in which the energy was mostly consumed in breaking the coating down in a brittle manner which resulted in high wear (Fig.4.2). This suggests that a direct relationship between hardness and abrasive wear cannot be established. Hardness, however, is significant in the wear process because it is a measure of the elastic strain energy required to cause plastic deformation. Fracture toughness may be another important parameter to be considered in addition to hardness. The early breakdown of the natural anodised film 9N alloy can then be attributed to its poor ability to absorb the energy generated during abrasion. In contrast, the superiority of hard anodised 15H2 and 30H alloys in resisting abrasive wear resides in their ability to accommodate the different kinds of induced stresses.

It appears that wear performance of these coatings is largely governed by:

1. Hardness of the coating.
2. Hardness of the substrate.
3. Fracture toughness of the coating.

It is almost impossible to draw a demarcation line between these parameters because they are inter-related. The harder the

coating the more resistant it is to penetration by the rider, and if a hard coating is supported by a soft substrate, the coating collapses. An increase in hardness is accompanied by a reduction in fracture toughness and the coating fails by brittle fracture. A compromise between hardness and fracture toughness should be reached.

Scanning electron microscopy reveals three major mechanisms acting at the surface of the coatings, they are:

1. Plastic deformation.
2. Brittle fracture.
3. Fatigue failure.

Plastic deformation occurs as a consequence of the nature and magnitude of the local stress under the diamond at low loads. The worn surface appeared to be fully plastic with little evidence of cracking (Fig.64a). On loading, lateral cracks became visible around the wear tracks with a smooth worn surface and abrasion marks running in the direction of the movement (Fig.64b,c). At loads of 3N or greater, the stresses can not be relieved by plastic deformation and cracks of different types develop in order to release the stored energy. The coating will then fail by a brittle fracture mechanism (Fig.65).

Generally speaking, brittle fracture becomes imminent when:

1. A sharp indenter is used.
2. The depth of indentation or groove is high.
3. The ratio of fracture toughness to hardness is low.

A brittle fracture mechanism is reported to cause about ten times material removal as that due to plastic deformation (74). Its

main feature being the development of median and lateral cracks. Material removal of the anodic coating due to an abrasion process can be attributed to the frequent intersection of the surface by the propagating lateral cracks. Development of this type of crack is largely governed by the amount of residual stresses acquired by the coating due to the following:

1. The anodising process, in which internal stresses are developed as a response to the change in volume taking place as a result of the oxidation of aluminium into aluminium oxide, and also the volume change due to the dissolution reaction of aluminium oxide into aluminium in the ionic state, Al_2O_3 to Al^{3+} . The anodic coating first shows compressive stresses. This is subsequently converted to tensile stress when the limiting coating thickness is reached (75). A primary manifestation of these residual stresses is the development of crazing.
2. The inability of the coating to recover completely elastically in the presence of localised plastic flow.

The development of lateral cracks in the anodic coatings corresponds to a 'chipping mode' of fracture (Fig.65). Close examination of Figures 64,65, suggests that a delamination mechanism may also be involved in abrasive wear of anodic films. It is caused by pile-ups at dislocations at grain boundaries close to the surface which are unlikely to be relieved by slip in the adjacent areas (76).

In a reciprocating wear test, stress reversals are taking place

which will ultimately lead to a cycle dependent type of failure, i.e. fatigue. A schematic representation of the influence of fatigue in wear acting at the surface of anodised aluminium is shown in Figure 75.

5.1.1 Fracture of Hard Anodised Alloy 9H under Abrasive Wear Conditions

The fracture pattern generated by small-scale contact events is related to the general mechanical properties of materials. When a sharp indenter is used, the elastic/plastic stress field governs the development of cracks prior to fracture. On a full cycle of loading and unloading, under both static and dynamic conditions, different types of cracks initiate and propagate and ultimately lead to disintegration of the coatings. In this section the development of brittle fracture of hard anodised aluminium alloy, under both static and dynamic loading, is discussed.

During Loading

Under static loading a stress field is set up beneath the surface of the coating, and its size is dependent on the shape of the indenter, the applied load and the material tested. The intensity of stresses at the subsurface increases as the sharp indenter is used (77). As the load increases, a transition from purely plastic deformation to fracture by the formation of disc shaped cracks beneath the surface occurs, where the greatest concentration of tensile stress reaches its maximum. Prior formed cracks continue to grow and are

completely contained beneath the indenter in the median plane which contains the normal load axis. At a critical load the median cracks extend and intersect the surface (Fig.70).

During Unloading

The complex elastic/plastic field beneath the contact zone is resolved into two components as follows:

1. Elastic component.
2. Residual stresses.

The residual stresses provide the primary driving force for the configuration in the later stages of the development of fracture. They also play a significant role in the enhancement of surface radial extension during indenter withdrawal. Whereas the elastic component being reversible, generally assumes a secondary role in the fracture process of a brittle solid.

There are additional residual stresses generated in response to incompatibility between the plastic zone and the surrounding elastic zone. Such mechanical mismatch appears to induce a reverse field prior to complete withdrawal of the load. Thus, the stresses which on loading act to generate median cracks, now tend to enhance closure of these cracks by virtue of their compressive nature.

The residual stresses appear to initiate lateral cracks which emanate from the deformed zone and grow in a saucer-like shape enveloping the entire plastic zone. At a critical stage depending on the amount of loading, these cracks propagate to the surface corresponding to a chipping mode of fracture (Fig.70).

The application of a tangential force reduces the contact mean pressure because the rear half of the contact area will be partially released from the load. The principal features of the stress field are that the σ^{11} and σ^{33} components are almost entirely tensile behind the indenter and compressive in front of it respectively.

Damage around the wear track

For a single pass track, in the absence of plastic deformation, the already formed median cracks tend to travel ahead of the conical diamond (Figs.71,72). These appear to have an insignificant role in the material removal from the anodic film, whereas the lateral cracks tend to progress sideways out of the wear track (Figs.71,72).

These results are in reasonable agreement with those suggested by Conway and Kirchnel (78). They showed a similar crack pattern occurs during the scratching of glass with sharp diamond points.

The extent of lateral cracks is intimately associated with the amount of residual stresses generated inside the coating as a result of the loading and unloading cycle. However, residual stresses appear to be significantly related to the hardness of the materials. According to Swain (79) the harder the coating, the greater the residual stress and the extent of lateral cracks will subsequently be larger. This may explain why the anodic film '15H2', with a hardness value of around 300Hv, exhibits better resistance to abrasive wear than that offered by the hard anodic coating 9H which has a hardness of around 400Hv. In other words, the 15H2 coating shows a better capability to accommodate the energy in the form of residual

stresses. A schematic representation of the elastic/plastic stress field and an S.E.M. micrograph of an indentation feature, produced by a 60 degrees diamond, are shown in Figure 70. For a single pass, median and lateral cracks are observed to extend well beyond the contact zone boundaries. They contribute to material removal on a larger scale and judging by the width and depth of the damage (Figs.73,74), in some places brittle fracture appeared to cause significantly more damage than that caused by direct contact with the abrasive.

Under the reciprocating movement, the principal feature of stress trajectories are subjected to an alternate state of tensile and compressive stress. This may lead to failure of the coatings by fatigue. Fracture striations in close proximity to the contact are observed in Figure 66.

The appearance of an abrasive wear track of an anodic film resembles the fracture mechanism of a glass when scratched by a diamond. Examination of wear debris recovered from the abrasive wear process also suggests the mechanisms by which these particles generate. Figure 98 illustrates that relatively large particles of the coating have been lifted off the surface by the intersection of the surface by lateral cracks. Striations at the side of the debris indicate that this fracture process is typical of fatigue failure.

5.2 EVALUATION OF ADHESIVE WEAR DATA

A number of difficulties are involved with the method of wear measurement where a ball-on-flat configuration is used. Due to the nature of contact, a number of processes may be acting on the surface simultaneously, i.e.

1. Indentation of the coating due to the normal loading.
2. Development of different types of cracks outside the contact zone, i.e. Hertzian Cone cracks, median, and lateral cracks.
3. Displacement of the material by means of a shear component due to tangential force.
4. Generation of alternate stresses, i.e. compression in front of the rider and tensile stresses behind it which leads to the production of loose particles by:
 - a) Plastic deformation
 - b) Adhesion
 - c) Fracture
5. Abrasion due to the possible existence of hard loose debris between the mating surfaces.

To establish a quantitative meaning of wear is therefore complicated. It is essential to identify which of the above indicate wear, and whether wear should be evaluated in terms of the depth, width, or weight loss. However, each of these methods has its own limitations, some of which are discussed below.

Weight Loss Method

This method is only applicable for a comparative purpose because:

1. The amount of material detached from the wearing surface may only represent 10% of the total displaced material whilst 90% of it adheres to the surface in contact.
2. The inaccuracies in the weight loss method are due to:

- a) The weight of the anodic film represents a small portion of the total weight of the anodised samples. Calculations based on the density of the aluminium and the dimensional data of the samples show that the weight of the anodic film is about 4% of the total weight. The total wear represented only a small percentage of this 4% of the total weight. Simple calculations were made as follows:

Sample dimensions:

Length: 75 mm

Width: 30 mm

Thickness: 6 mm

Coating thickness: 35 μ m

Density of aluminium: 2.7 gm/cm³

Total volume of the substrate: 13.298 mm³

Weight of the substrate: 35.9071 gm

Total weight of the sample: 37.5100 gm

Weight of the anodic film: 1.6029 gm

Weight loss of the anodic film: 0.066 gm

- b) Absorbtion of the atmospheric moisture occurs at the surface of a porous structure.

Track Wear Measurement

Track dimensions can be measured by a number of methods, i.e.

1. Macroscopically
2. Microscopically
3. Profilometry

The data obtained can then be utilized to calculate wear volume. However, there are some difficulties involved during the measurements, i.e.

1. In the case of a ductile material, the edges of the wear track are usually raised due to material deformation. The height of these edges increases as a function of load and number of cycles. Edge definition is therefore rather obscure and difficult to locate. However, profiles can be used to estimate the amount of deformation related to the amount of debris produced.
2. In the case of the coated alloy, the fracture of the wear track edges and the extent of damage outside the wear tracks once again makes the exact location of the wear track difficult to define.

More information about wear mechanism can be obtained and related to S.E.M. observations of wear tracks and the debris generated.

Furthermore, with all the above techniques, measurements can only be conducted at the end of the wear test. It was therefore decided to use a linear voltage displacement transducer (L.V.D.T.). This device permits continuous measurement of wear in terms of

contact displacement throughout the wear test. Data can be obtained at any stage of the test.

Although evaluation of wear by L.V.D.T. is now widely practised and has many advantages, its main limitation is that, in the tests described in this investigation, wear of the two counterbodies cannot be separated, i.e. wear data presented in Figure 44 is in fact resolved into two components:

1. Wear of the rider steel ball.
2. Wear of the coating.

Having said that, it becomes necessary to analyse the results on the basis of quantitative measurements of the amount of material removed from the counterfaces separately. A specific example is taken in which hard anodic film 9H is rubbed against a steel ball under dry conditions at 10N and the wear curve will be analysed on the basis of calculation of the coefficient of wear of both counterbodies.

The wear curves show three distinct features:

1. A running-in stage where proportionality between wear depth and sliding distance and applied load exists and the wear rate is high.
2. A steady-state regime in which the wear rate is diminished. The change in wear rate in this regime can be attributed to one or more of the following:

- a) Decrease in porosity as the rider penetrates towards the oxide/metal interface.
 - b) The pores may have become filled with debris developed at the earlier stage.
 - c) Changing of the pressure caused by flattening of the ball and the load will eventually be supported by a larger area of contact.
3. A sharp transition stage which results from the complete breakdown of the coating.

In all these regions, wear is proportional to applied load and sliding distance but the 'K' factor will be different, indicating that the wear mechanism is changed. There is no significant correlation, however, with hardness, and this suggests that other properties of the coating contribute in controlling wear.

The effect of applied load

As the load increases wear depth increases until a stage is reached in which a breakdown of the coating occurs.

The effect of sliding distance

The sliding wear law is applied here, since as the number of passes increases wear depth increases. The high wear rate at the run-in stage starts to diminish gradually until a drastic change occurs

which signifies a breakdown of the coating.

Adhesive wear of these coatings occurs by compaction and smoothing of the wear track followed by brittle fracture to produce different types of wear debris. However, at loads of less than 10N, surface and sub-surface cracking was not visible, hence the wear track was plastically deformed. The accumulation of plastically controlled events may result in a mechanical polishing which is characterised by low material removal. Clear evidence of this was observed with the electroless nickel plated coating (Fig.89).

Plastic deformation occurs as a consequence of the nature and magnitude of the local stress. It is probable that the shear stresses generate dislocations and initiate deformation by slip or twinning.

Fracture occurs when the stresses can not be relieved by plastic deformation, since the layer, in which deformation takes place, is of limited depth and the amount of stress, necessary to cause fracture, extends beyond that depth. This theory can be put forward to explain the observation that at loads greater than 10N, evidence of plastic deformation, associated with the wear track, is reduced and the mechanism changes to brittle fracture. The amount of material removed by brittle fracture is governed by the development of mainly three types of cracks, i.e.

1. Median cracks.
2. Hertzian cone cracks.
3. Lateral cracks.

In theory, the median cracks are always associated with a sharp

indenter, whereas Hertzian cone cracks are intimately related to a blunt indenter, such as ball on flat configuration. In this case the load is distributed over an area of contact relatively larger than that accounted for by a single point diamond and the stresses are concentrated at a shallow depth.

The symmetrical shape of the deformed field immediately below the indenter causes the material to exert a uniform hydrostatic pressure on its surrounding. It is this plastic region within which flaws occur. The onset of plastic deformation is associated with the maximum shear stress reaching a critical yield value of the material. The maximum shear stress is said to occur below the surface at a distance of $0.5a$ where 'a' is the radius of the area of contact' (80).

In the absence of plastic deformation, cracks nucleate outside the elastic contact zone where the stresses are high at the pre-existing flaw. As the stress intensity builds up with the load, one or more of the flaws nucleate cracks. The dominant flow runs around the contact circle to form ring cracks. Subsurface propagation of ring cracks is shown in Figure 82.

In addition to the development of ring and Hertzian cone cracks, the inelastic deformation zone expands and from this zone, in which shear and hydrostatic compression are maximum, radial cracks are also evident. This suggests that as the ball effectively penetrates the specimen surface at a high pressure, it begins to produce similar results as those obtained with a pointed indenter. Radial cracks as well as Hertzian cone cracks tend to close during

unloading. However, the mechanical mismatch between the plastic zone and the surrounding elastic field generates residual stress which significantly contributes to generate a reversal field of stress. This type of stress is generated as a direct result of the inability of the material to recover completely elastically in the presence of the localised plastic flow. The prime manifestation of the residual stresses is the initiation of a lateral crack system. Figure 82 shows both a schematic representation of elastic/plastic stress field and an S.E.M. micrograph of the static loaded anodised alloy 9H.

The application of a tangential force adds a new complication to the system due to the generation of different types of stresses, i.e.

1. Frictional stresses.
2. Compression stresses travelling in front of the indenter.
3. Tensile stresses behind the indenter.

The combined effect of these stresses produces the formation of parabolic shaped cracks which extend well beyond the wear track boundary. Examination of the single pass track shows little damage at the centre of the track, with some fine cracks intersecting at the edge with their free ends travelling well away from the contact zone into the non-contact area (Fig.83). Figure 84 shows lateral cracks more clearly in a more well developed wear track and it can be seen therefore, that this type of fracture occurs outside the contact zone.

Metal transfer was also evident, transfer of aluminium from the anodic layer to the ball was observed (Fig.92). In a similar study of the flat surface, transfer of major elements such as iron and

chromium from the steel ball to the flat was observed (Fig.94). The nature of element transfer is not clear, since the formation of welded junction on a molecular scale is highly unlikely because of the physical and chemical nature of the mating surfaces which make it difficult to develop such junctions, i.e. the high melting point of aluminium oxide and the low reactivity of the oxide towards steel. However, the temperature gradient and stresses may be sufficient to cause migration of lattice vacancies which facilitates diffusion of the major elements like iron, chromium and aluminium on an atomic scale (53).

Electroless nickel plated aluminium appears to exhibit a disastrous behaviour under dry sliding conditions, i.e. breakdown at early stages of sliding. This behaviour can be attributed to a *strong chemical* tendency between this coating and the steel ball promotes adhesion. This phenomena has been observed by scanning electron microscopy in conjunction with microprobe analysis which revealed nickel transfer from the flat sample to the steel ball after the first few cycles (Fig.93).

Figure 89 shows a polishing mechanism at the early stages of wear in which the nodules have been plastically smeared out along the wear direction. Further wear initiates cracks which propagate under highly localised stresses causing crushing under the steel ball. Brittle fracture was also evident. Figure 88 shows development of lateral cracks.

5.3 THE ROLE OF THE SUBSTRATE

The tribological performance of anodised aluminium alloys is closely connected with the whole metallurgical history of alloy production which determines whether the presence of impurities are in homogenous solid solutions, intermetallic compounds, or precipitates. Pure aluminium anodises better than its alloys and wrought alloys produce a superior anodic film to the cast alloys because of their greater homogeneity. However, it is usually important to couple the hard surface of the anodic film with a strong base metal. This can be achieved by the addition of alloying elements. Alloys with high silicon and copper are strong but difficult to anodise because they require a high forming voltage in order to maintain sufficient current flow. This deteriorates the coating integrity and thus impairs the potential protection of the anodic film. 15H2 alloy with up to 5% Cu produces a relatively soft and more flexible anodic film. This flexibility enables the coating to accommodate more stresses than the harder anodised alloy 9H.

The good abrasive resistance exhibited by 15H2 alloy can be attributed to two points:

1. Strong substrate due to the presence of alloying elements, mainly Si, Cu, thus more support is given to the coating.
2. High flexibility of the anodic film, thus protecting the coating from brittle failure.

Unlike 15H2, hard anodised alloy 9H has failed by brittle fracture. This behaviour is due to two main factors:

1. Being harder than 15H2, the amount of residual stresses is higher. These stresses play an important role in fracture phenomenon in brittle solids.
2. The smaller amount of Si, Cu in the 9H alloy '6063' produced a softer substrate than 15H2 alloy '2014A'. The weaker substrate provides less support to the anodic film.

Alloys based on AlMgSi systems '9H,30H' are being used in industry. A high percentage of Mg tends to soften the coating because of the formation of an oxide.

5.4 THE EFFECT OF COATING THICKNESS

Generally speaking, when a hard coating is applied on a softer substrate, a thicker coating is recommended for wear applications. However, a thinner coating may also be adequate to protect a hard substrate.

Electroless nickel plating on aluminium alloy exhibits a rather poor performance under dry adhesive wear conditions regardless of the coating thickness. The major failure mechanism is by adhesive and metal transfer from the coating to the steel ball. Failure by the brittle manner was also involved and is facilitated by two factors:

1. Work hardening of the electroless nickel layer just below the surface.

2. Soft aluminium alloy as a substrate offered inadequate support to the harder coating. As the applied force is transmitted through the coating to the substrate, the latter tends to deform and at some weak points, the coating disintegrates in a brittle manner.

Under lubricated conditions, adhesive and metal transfer is diminished. A brittle fracture mechanism appears to be the major failure mode for all coating thicknesses.

5.5 FRICTION PROPERTIES

The high friction values of all coatings investigated under dry conditions can be attributed to:

1. Adhesion between the coating and the steel ball. Microprobe analysis of the worn surfaces shows evidence of metal transfer in both directions.
2. Material deformation and displacement to accommodate the stresses generated due to sliding.

Plastic deformation will always be accompanied by a loss of energy and it is this energy loss which accounts for the major part of the friction of materials under most practical circumstances.

Generally speaking, if the mechanical properties of both the metal and coating are similar, the coating will deform with the underlying metal and break through will not easily occur. Thus

friction as well as surface damage will be relatively small. However, if the coating is very much harder than the substrate, break through will readily occur even with light loading, and high friction can be anticipated.

The introduction of a film of lubricant between components with relative motion provides a solution to a vast number of tribological problems in engineering systems (80). The existence of a lubricant in the system prolongs the life of all coatings by reducing the real area of contact and by inhibiting junction contact diminishes the growth of junctions. As a result, the frictional force required to maintain motion will be reduced and the degree of metal transfer is markedly lowered. The lubricant appears to have two fundamental roles:

Physical Roles

Depending on the surface topography of the coating, the molecules of the lubricant are physically absorbed and orient themselves at each of the solid surfaces to form a monomolecular film. Under an applied load, plastic flow occurs until the area of contact is large enough to accommodate the applied load, consequently a film of lubricant will be trapped between the two surfaces and subjected to high pressure. This pressure will not be uniform over the area of contact and at some weak points breakdown of the lubricant occurs, resulting in metallic adhesion. The extent of this breakdown is governed by the physical nature of the lubricant and the morphological characteristics of the coatings, since the porous and

nodular features of the anodic film and electroless nickel respectively, appeared to play an important role in oil retention.

It has been demonstrated (Fig.61,87) that smooth surfaces produced on the electroless nickel coatings, diminish the potential protection of the lubricant and the number of cycles required to break through the coating was significantly reduced.

Chemical Role

When the contact surfaces are separated by a monomolecular film the physical properties of the lubricant, such as viscosity, play very little part in protecting the surfaces from wear. The chemical constitution of the lubricant and the nature of the *underlying* surfaces however, are of considerable potential to maintain partial protection. This is termed boundary lubrication in which it is assumed that the resistance to motion is due to intermolecular forces at the point of contact.

Electron microprobe analysis of the worn surface under lubricated conditions shows a deposition of a number of elements such as potassium, sulphur, silicon and chlorine. The source of these appears to be the lubricant between the contacting surfaces. Organic chlorine or sulphur reacts with the metal at the hot spots forming metal chloride or sulphide films which inhibit the welding of asperities and reduce friction and wear to an acceptable level.

In summary, it is apparent from the literature that the bulk of the work carried out on anodised aluminium seems to place a considerable emphasis on the methods of improving the anodising process in a way that makes it efficient in attracting a wider range of engineering applications. Owing to its thickness and hardness, anodising in sulphuric acid is the most attractive type for many purposes. The surface appearance, as well as the mechanical properties are largely dependent on the alloy's structure and the anodising process parameters.

Despite the growing interest in using anodised aluminium in wear applications, friction and wear studies have received little attention. Furthermore, most of the reported work in this area tends to underestimate the importance of:

1. The selection of the appropriate test method in order to evaluate a specific wear mechanism.
2. An understanding of the wear mechanism(s) by which the coatings fail.
3. Interpretation of the wear results.

This is due to the misunderstanding of the complexity of wear processes which can then lead to over-emphasizing the use of the hardness concept in determining the wear behaviour of the coatings. Ways are being sought to improve the wear performance of the coatings by increasing their thickness and hardness. A direct relationship between the wear characteristics and these parameters has apparently been substantiated. The results of this investigation however, paint a different picture, in which the

tribological behaviour of the coatings investigated appears not to be dictated by hardness alone. It is shown that anodised alloy 15H2 exhibited a superior abrasive wear resistance to natural and hard anodised alloys 9N and 9H respectively, despite its hardness being the lowest among the coatings investigated. Electroless nickel, however, showed excellent resistance to abrasive wear, its hardness being the highest among these coatings. This suggests that no direct relationship can be made between hardness and abrasive wear. The tribological performance of anodised aluminium alloys appears to be intimately tied up with the metallurgical history and composition of the base alloys. The harder the coating, the greater the penetration resistance. However, it may collapse if it is not supported by a strong base alloy. An increase in the hardness of the anodic film is usually accompanied by a reduction in fracture toughness and the likelihood of the coating to fail in a brittle manner increases. The early breakdown of the natural anodised alloy 9N, can be attributed to its limited ability to absorb the energy induced under abrasive conditions. Owing to their high plasticity, anodised alloys, 15H2, 30H, and the electroless nickel, showed satisfactory behaviour irrespective of the difference in their hardness value.

Adhesive wear of these coatings, which has rarely been reported in the literature, shows that the behaviour of electroless nickel aluminium alloy (500Hv), and also the anodised alloy 15H2 (300Hv) was unsatisfactory. Both failed during the early stages of sliding by adhesive transfer which dominates all other factors including hardness. Attention must therefore be paid to selection of a

counterbody surface which will not adhere to the nickel or anodic coatings. The introduction of a lubricant to the system prolongs the wear life of all the coatings investigated. This improvement was brought about due to:

1. The nature of the lubricant.
2. The nature of the counterbodies.

The morphology of surfaces in contact is of considerable importance in adhesive wear under lubricated conditions. The nodular and porous morphology of electroless nickel and anodised aluminium were beneficial for oil retention to the contact zone. This phenomena is important in two ways:

1. It minimizes the surface contact between the counterbodies.
2. The lubricant supports the load, thereby reducing the pressure at the asperities.

The results of this work also show that a number of mechanisms were acting at the surface of these coatings. These mechanisms operate individually or collectively causing a breakdown of the coatings and material removed. Evidence of brittle fracture, fatigue failure, adhesion and plastic deformation within a small band of the worn surfaces, represents the driving force for further work aimed at separating as many mechanisms as possible, and also to assess and identify the major reasons contributing to the disintegration of anodised and electroless nickel coated aluminium alloys. Microscopic examinations of abrasive wear show brittle

fracture is the major cause of breakdown of the coating and material removal, viz. the early development of median, and lateral cracks. Plastic deformation, and fatigue failure begin to operate as the coating is subjected to repeated tangential force in the opposite direction.

Brittle fracture was also operative during adhesive wear. Due to the geometry of the contact mechanics, brittle fracture is believed to develop due to Hertzian stresses. Radial and ring cracks were also evident under static loading. Microprobe examinations of the worn coatings and steel balls, reveal transfer of the major elements in both directions. This indicates the involvement of adhesion.

The test procedure allows not only the identification and understanding of the wear mechanisms involved, but also the calculation of the wear coefficient.

Another interesting feature of these results is that wear of the ball (950Hv) occurred even though the hardness of the anodic film, as measured, was of the range of 350-400Hv.

Having investigated the wear mechanisms acting at the coatings surface, and the wear coefficient calculated under both abrasive and adhesive wear conditions, designers will benefit by:

1. Assessing the type of damage inflicted on the coatings for given contact mechanics.
2. Estimating the wear life of the counterbodies for a given tribosystem condition.
3. Selection of materials for a specific tribological application would be easier.

CHAPTER SIX

CONCLUSIONS

1. Tribological properties of the coatings investigated are a function of the tribosystem, i.e. test method, materials, and environment.
2. A single point diamond and a steel ball on a flat configuration are satisfactory test methods for the fundamental study of abrasive and adhesive wear processes, respectively.
3. Abrasive and adhesive wear of the materials investigated is proportional to the applied load and sliding distance.
4. No direct relationship between hardness and tribological characteristics of the coatings has been established.
5. Anodised alloys, 15H2, 30H and electroless nickel were superior to natural and hard anodised alloys 9N and 9H respectively, under abrasive wear conditions.
6. Under dry adhesive wear, anodised alloy 15H2 and electroless nickel aluminium alloys were poor. The 9H alloy exhibited satisfactory behaviour. Wear resistance is further improved when anodised alloy 30H is used.
7. The wear life of all coatings investigated has been substantially prolonged under lubricated sliding conditions. The porous and nodular morphology of anodic films and electroless nickel respectively, have been beneficial in oil retention in the contact zone. Under such circumstances, anodised alloy 15H2 exhibited a superior behaviour to the rest of the alloys investigated.

8. A frictional value of about 0.5 obtained under dry sliding conditions is reduced to 0.1 when lubricant is introduced to the system.
9. There were a number of mechanisms acting at the surface of these coatings, such as:
 - a) Plastic deformation was favoured by the uncoated alloy, hard anodised (15H2), (30H), and the electroless nickel aluminium alloys.
 - b) Adhesion is only prominent with sliding of a steel ball against the coatings investigated. Metal transfer in both directions is facilitated by (a) the nature of the counterbodies, and (b) the environment.
 - c) Brittle fracture was predominant under both abrasive and adhesive wear in the natural, and hard anodised alloy 9N, 9H respectively. This is due to the development of different crack systems such as median, lateral, and Hertzian cracks.
 - d) Fatigue failure occurs in response to a repeated stresses due to the reciprocating movement of the samples against the rider.
10. As brittle fracture contributes to excessive wear, particularly beyond the wear track boundaries, it is important therefore, to develop coatings which do not fail in a brittle manner. It will become necessary to take into consideration the alloy to be coated, as well as the processing details, in order to optimise the wear performance of coatings.

REFERENCES

1. **Wilson, R.W.**, A.S.L.E., (1970), 30, 5, 263-269.
2. **Czichos, H.**, Tribology, (1978), Elsevier, Amsterdam.
3. **Eyre, T.S., Abdul-Mahdi, F.S.**, Aluminium Technology '86, Int. Conf., 11-13th March, (1986), London.
4. **Halling, J.**, Seminar organised by I.MECH, 10th October, 1985.
5. **Wernick, S., Pinner, R.**, The Surface Finishing of Aluminium and its Alloys, Robert Draper Ltd., (1972), Vol.1.
6. Year Book of Industrial Statistics Commodity Production Data, Vol.11, (1975), United Nations.
7. Year Book of Industrial Statistics Commodity Production Data, Vol.11, (1978), United Nations.
8. **Perfect, M.**, Proc. Conf. on Anodising Aluminium, Nottingham, (1961).
9. **Jack, L.W.**, Plating and Surface Finishing, February (1984), 71, (2), 33-36.
10. **Wernick, S., Pinner, R.**, The Surface Finishing of Aluminium and its Alloys, Robert Draper Ltd., (1972), Vol.2.
11. **Brace, A.**, Technology of Anodising, Robert Draper Ltd., (1966).
12. **Jenny, A.**, Anodic Oxidation of Aluminium and its Alloys, (1940), Griffin & Co., London.
13. **Kape, J.M., et al**, Trans. of IMF, (1984), 62, (2), 41-45.
14. **Kneeshaw, J.A., Gabe, D.R.**, Trans. of IMF, (1984), 62, (2), 59-63.
15. **Campbell, J.C.**, Proc. Conf. Anodising Aluminium, Nottingham, (1961) 137-149.
16. **Henely, V.F.**, Anodic Oxidation of Aluminium and its Alloys, Pergaman Press Ltd. (1982).
17. **Setoh, S., Miyata, A.**, Science Paper Inst. Physics, Chemistry, Research, Tokyo, (1932), 17, 189-236.
18. **Baumann, W.Z.**, Physik, (1936), 102, 59-66.
19. **Gunterschulze, B.Z.**, Physik, (1934), 91, 70.
20. **Scherk, M., et al**, Seine Anodische Oxidations, A. Franke, A.G. Berne, (1948).
21. **Fischer, H., Kurz, F.**, Korrosion and Metallschutz, (1942), 18, 42-50.

22. **Lewis, J.E., Plumb, R.C.**, Journal on Electrochemical Society, (1958), 105, (9), 496-498.
23. **Barkman, E.F.**, Symposium Proc. on Anodising Aluminium, April (1967), Birmingham.
24. **Gabe, D.R.**, Principle of Metal Treatment, Surface Treatment and Protections, (1972), Pergamon Press.
25. **Franklin, R.W.**, Proc. Conf. on Anodising Aluminium, Nottingham, (1961).
26. **Tylor, C.S., et al**, Trans.Electrochem Society, (1945), 88, 325-335.
27. **Erick, F., Barkman, E.**, Symposium Proc. on Anodising Aluminium, April, (1967).
28. **Johnson, D.R.**, Plating (1962), 49, (10), 1079-1086.
29. **Machlin, I., Whitney, N.J.**, Metal Finishing, (1961), 59, (2), 55-57.
30. **Spooner, R.C.**, Proc. American Electroplater Society, (1957), 44, 132-142.
31. **Deal, B.E.**, Plating, (1954), 46, 7, 823-827.
32. **Gawrilou, G.G.**, Chemical Electroless Nickel Plating, (1979) Portculus Press Limited.
33. **Mallory, G.O.**, Plating and Surface Finish, June, (1985), 72, 6.
34. **Ma, U., Gawne, D.T.**, Trans. IMF, August, (1985), 63, 64-69.
35. **Gould, A.J., et al**, Trans. IMF, (1983), 61, 97.
36. **Justice, B.**, Product Finishing, January, (1984), p.56.
37. **Ruff, A.W., Lashmore, D.S.**, Selection and Use of Wear Tests for Coatings, A symposium sponsored by ASTM, (1981).
38. **Groshart, E.A.**, Metal Finishing, November, (1983), 81, (11), 19-21).
39. **Tulsi, S.S.**, Welding Institute, 1st International Conference on Surface Engineering, (1985), Proc. Pater No.57, 1-9.
40. **Dennis, J.K., et al**, Trans. IMF, (1981), 59, P118.
41. **Bayer, R.G.**, Selection and Use of Wear Tests for Coatings, A symposium sponsored by ASTM, (1981).
42. **Lee, T.J.**, Proc. Conference on Anodised Aluminium, Nottingham (1961), Paper No.10.
43. **Smith, A.T.**, Product Treatment and Finishing, Macmillan Press Limited (1972).

44. Roberts, A.G., et al, ASTM Bulletin, (1955), 208, 36-41.
45. Weinmann, K., et al, Farbe U. Lack, (1959), 65, 647.
46. Schweiz, V.S.M., Normen Bull, (1961), 12, 134-36.
47. Thomas, R.W., Trans. of IMF, (1981) 59, 97-104.
48. Hurrick, P.L., Wear, (1973), 26, 285-304.
49. Scott, D., Proc. of the Int. Conf. on the Fundamentals of Tribology, (1978), MIT.
50. Eyre, T.S., Powder Metallurgy, (1981), 2, 57.
51. Eyre, T.S., Brunel University Workshop, 1982.
52. Eyre, T.S., Treatise on Materials, Science and Technology, Vol.13, Academic Press, New York, (1980).
53. Kragelskii, I.V., Friction and Wear, Butterworths, (1985).
54. Peterson, M.B., Boundary Lubrication, An Appraisal of World Literature, ASME., (1969).
55. Vingsbo, O., Proc. Conf. on Wear of Materials, ASME (1979), 621-635, New York.
56. Peters, J.A., M.Sc. Dissertation, University of the Witwatersrand, South Africa, 1983.
57. Rabinowicz, E., Friction and Wear of Materials, John Wiley & Sons, New York, (1965).
58. Abdul-Mahdi, F.S., Eyre, T.S., Welding Institute, 1st Int. Conf. on Surface Engineering, (1985), Proc. Paper No.38, 1-20.
59. Abdul-Mahdi, F.S., M.Phil Thesis, Brunel University, (1981).
60. Suh, N.P., Turner, A.L., Element of the Mechanical Behaviour of Solids, Script Book Company, Washington D.C., (1975).
61. Bitter, J.A.A., Wear, (1963), 6, 169.
62. Alphonse, S., Automobile Engine Lubrication, Vol.II, Scientific Publications (G.B.) Ltd., (1972).
63. Eyre, T.S., Ph.D. Thesis, Brunel University, (1971).
64. Archard, J.F., J. Appl. Phys. (1953), Vol.24, p.981-988.
65. Archard, J.F., Wear Handbook, ASME, (1980).
66. Suh, N.P., Wear, (1973) Vol.25, p.111-124.
67. Richardson, R.C.D., Wear, (1967), 10, 291-309.

68. Rosenfield, A.R., *Wear*, (1980), 61, 125.
69. Honborgen, E., *Wear*, (1975), 33, 251.
70. Orbel, T.L., *Journal of Metals*, (1951), 3, 438.
71. Crowley, B., Ph.D. Thesis, Brunel University, (1984).
72. Peterson, M.B., *Wear Handbook*, ASME, (1980).
73. Marshall, D.B. et al, *J. Amer. Cer. Soc.*, (1982), 65, 11, p.561-566.
74. Moore, M.A., King, F.S., *Wear of Materials, Proc. Int. Conf.*, (1979), 275-285.
75. Csokan, P., *Trans. IMF* (1974), 52, 92-94.
76. Head, A.K., *Phil.Mag.*, (1953) 44, 92-94.
77. Swain, M.V., Hagan, J.T., *Journal on Phys.D: Appl.Phys* (1976), Vol. 9, 2201-2214.
78. Conway, J.C., Kirchner, H.P., *Journal of Material Science* (1980), 15, 2879-2883.
79. Swain, M.V., *Journal of the American Ceramic Society*, (1979), 62, 5, 318-319.
80. Halling, J., *Principles of Tribology*, MacMillan Press Ltd., (1975).

Table (1) Aluminium and its alloys for wear resistance

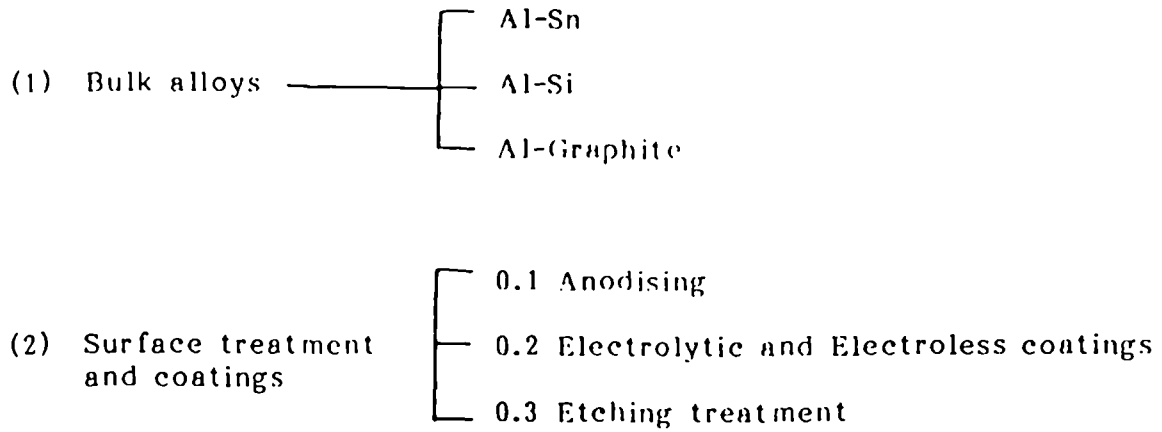


**Table (2) Total World Production of Aluminium
Units - thousand metric tons.**

1970	1971	1972	1973	1974
11228.4	11976.5	13166.4	14321	15326.3

1975	1976	1977	1978
14116.1	14877.6	16454.3	16938.9

Table 3 Mechanical properties of hard anodic coatings

Basis metal	Coating thickness		U.T.S.		Elongation on 2 in (per cent)
	(mil)	(μm)	(lb per sq in)	(MN/m ²)	
61S T6 (0.32 in thick) (Al-Mg-Si)	—	—	47,700	329	12.0
	0.5	13	49,100	339	12.5
	1.0	25	48,800	336	11.5
	3.0	75	45,400	313	8.0
	5.0	125	45,100	311	5.5
24S-T3 (0.32 in thick) (Al-Cu-Mg-Mn)	—	—	67,700	467	18.0
	0.5	13	66,500	459	17.5
	1.0	25	67,200	463	15.0
	3.0	75	62,700	432	11.0
	5.0	125	58,600	404	—
24S-T4 Alclad (0.32 in thick)	—	—	64,200	443	17.5
	0.5	13	65,400	451	16.0
	1.0	25	67,000	462	14.0
	3.0	75	64,000	441	11.5
	5.0	125	58,200	401	—
75ST (0.32 in thick) (Al-Zn-Mg-Cu)	—	—	80,000	552	8.5
	0.5	13	80,600	556	7.5
	1.0	25	79,800	550	7.5
	3.0	75	78,000	538	7.0
	5.0	125	72,900	503	6.5*
356-T6 (0.150 in thick) (Al-Si, cast)	0.5	13	24,750	170	3.0
	1.0	25	29,700	205	6.5
	3.0	75	26,350	181	4.0
	5.0	125	31,200	215	5.5

* Coating flaked off partially.

Elongation is, of course, reduced by hard anodizing and the endurance strength is also markedly reduced

Table 4 Chemical composition of the alloys investigated

Materials Designated	Chemical Composition (%)													
	Si	Fe Max	Cu Max	Mn Max	Mg	Cr Max	Ni Max	Zn Max		Ti Max	Others		Al	
											Each	Total		
6063 (9H) (9N)	0.20- 0.60	0.35	0.10 max	0.10	0.45- 0.90	0.10	-	0.10	-	0.10	0.05	0.15	Rem	
2014A (15H)	0.50- 0.90	0.50	3.9- 5.0	0.40- 1.20	0.20- 0.80	0.10	0.10	0.25	Zr+Ti 0.20 Max	0.15	0.05	0.15	Rem	
6082 (30H)	0.70- 1.30	0.50	0.10	0.40- 1.00	0.60- 1.20	0.25	-	0.20	-	0.10	0.05	0.15	Rem	
Steel Ball EN31	0.1 0.35	Rem		0.30- 0.75		1.00- 1.60	C			P		S		0.05 Max
							0.90- 1.2	0.05 Max	0.05 Max	0.05 Max				

Table 5 Mechanical properties of alloys

Material Designated	0.2% proof stress MPa	Tensile Strength		Elongation On 50mm min
		Min MPa	Max MPa	
6063 (9H) (9N)	-	-	MPa 140	% 13
2014A (15H)	230	370	-	10
6082 (30H)	-	-	170	14

Table 6 Microhardness of Materials Investigated, average of five readings

Material Designated	A1	9N	9H	15H2	30H	Electroless Ni on 6063 alloy
Hv (50 gm)	91	391	403	303	388	507
Hardness of substrate	-	89	89	130	90	89

Table 7 Thickness and C.L.A. Measurement of the materials investigated

Material Designated	9N	9H	15H2	30H	Electroless Ni on 6063 alloy
Coating thickness μm	30	38	37	38	10,20,30
Ra (μm)	0.7	0.65	1.0	0.8	0.9

Table 9 Coefficient of Wear (K) Values

Test No.	K value of the ball	K Value of the Anodic Film 9H
1 (15 mins)	2.1×10^{-4}	2.5×10^{-7}
2 (1 Hour)	1.1×10^{-4}	2.9×10^{-7}
3 (4 Hours)	7×10^{-5}	5.4×10^{-7}
4 (6 Hours)	3.3×10^{-5}	2.2×10^{-7}
5 (12 Hours)	4.1×10^{-5}	3.1×10^{-7}
6 (24 Hours)	3×10^{-5}	8.1×10^{-6}

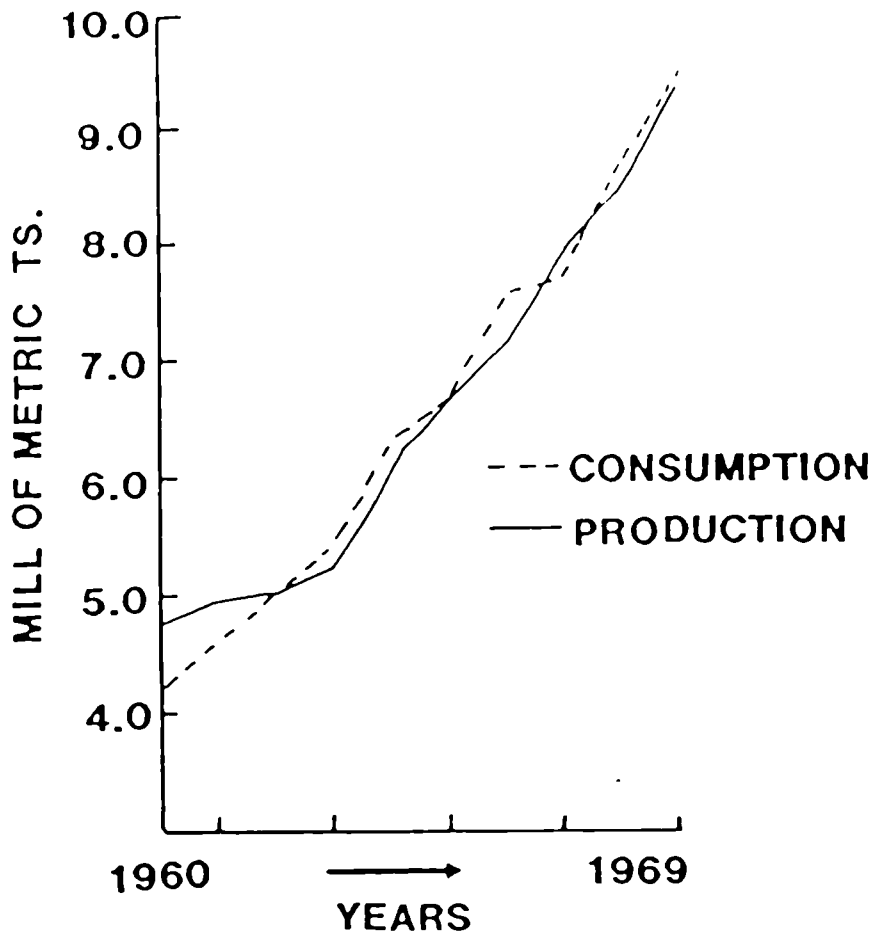


Fig.1 World production and consumption of aluminium (5).

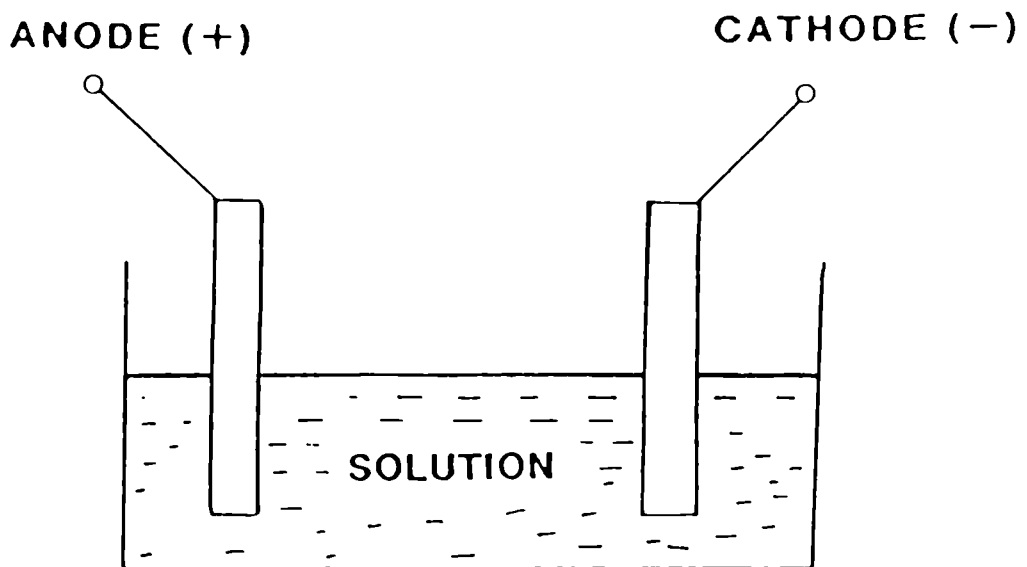


Fig.2 Current entering and leaving solution in anodising.

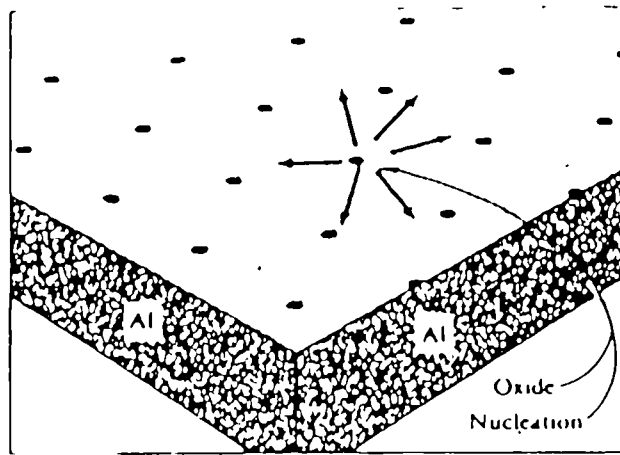


Fig.3 Schematic illustration to indicate the formation of nucleation sites on the surface of aluminium at the early stages of anodic oxidation.

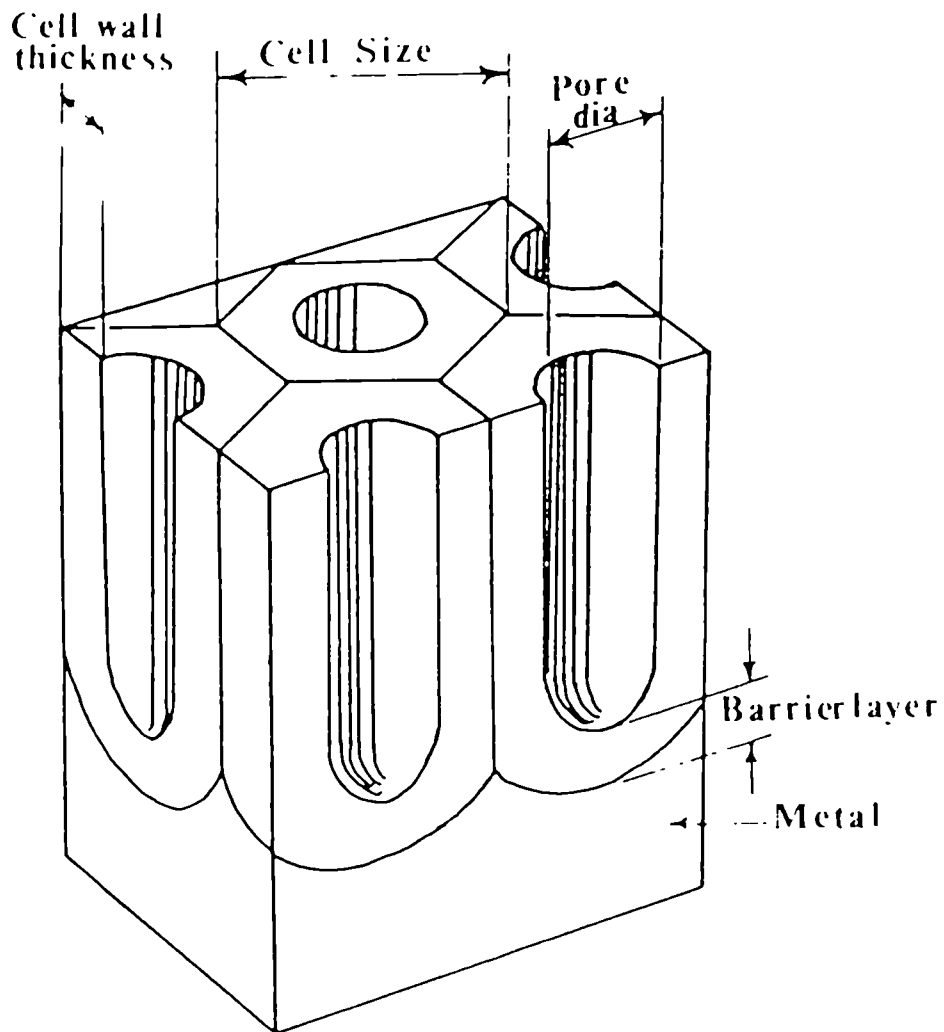


Fig.4 Microstructure of anodic film.

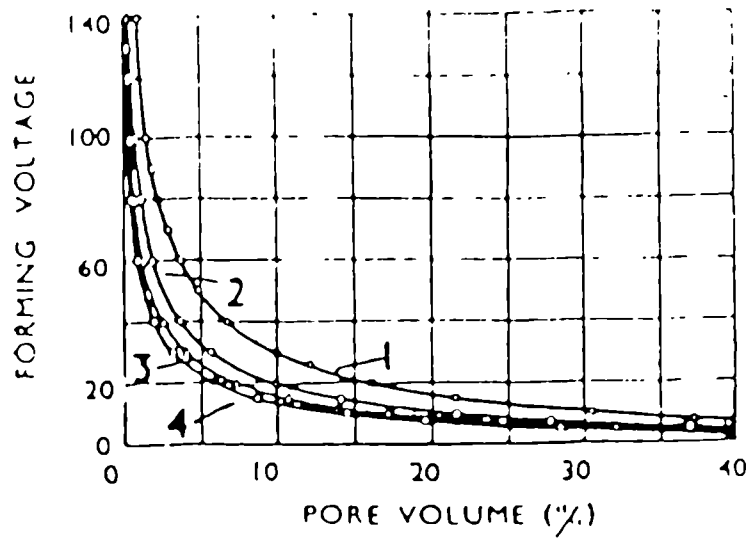


Fig.5 Relationship between pore volume and forming voltage in anodic coating electrolytes (10):

1. 4% Phosphoric acid 25°C
2. 3% Chromic acid 50°C
3. 2% Oxalic acid 25°C
4. 15% Sulphuric acid 10°C

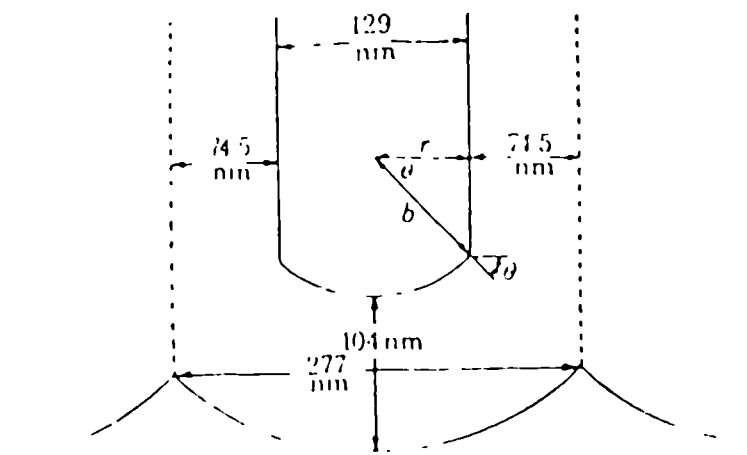


Fig.6 Schematic diagram of the barrier layer, pore and oxide cell dimension of anodic film (10).

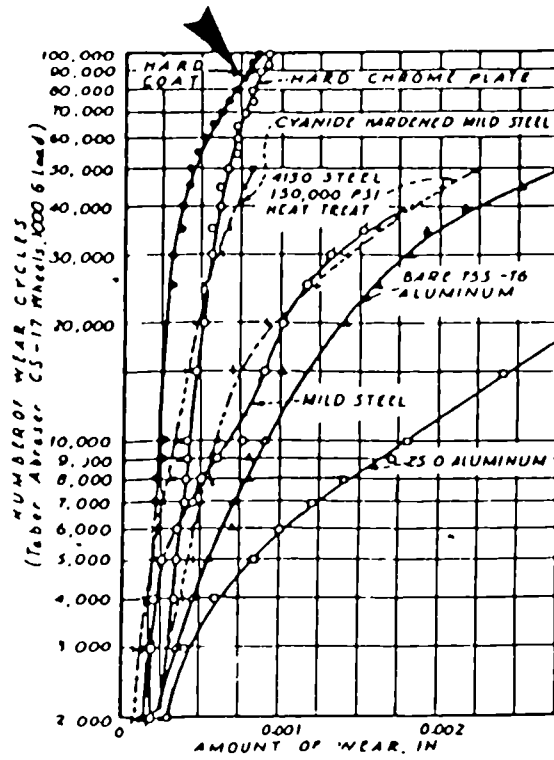


Fig.7 Comparison of the wear-resistance of hard anodised aluminium alloy with that of other materials and coatings (10).

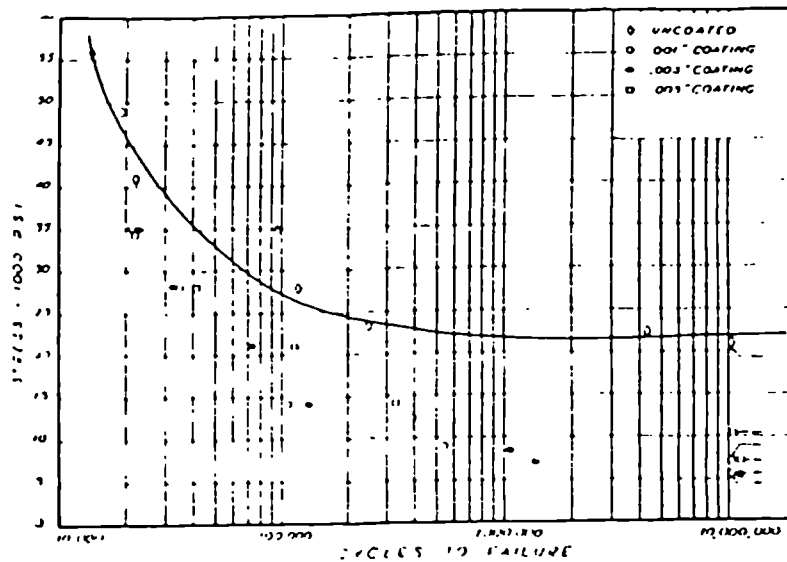


Fig.8 Effect of hard coating on fatigue strength of Al.Zn.MgCu alloy for different coating thicknesses (10).

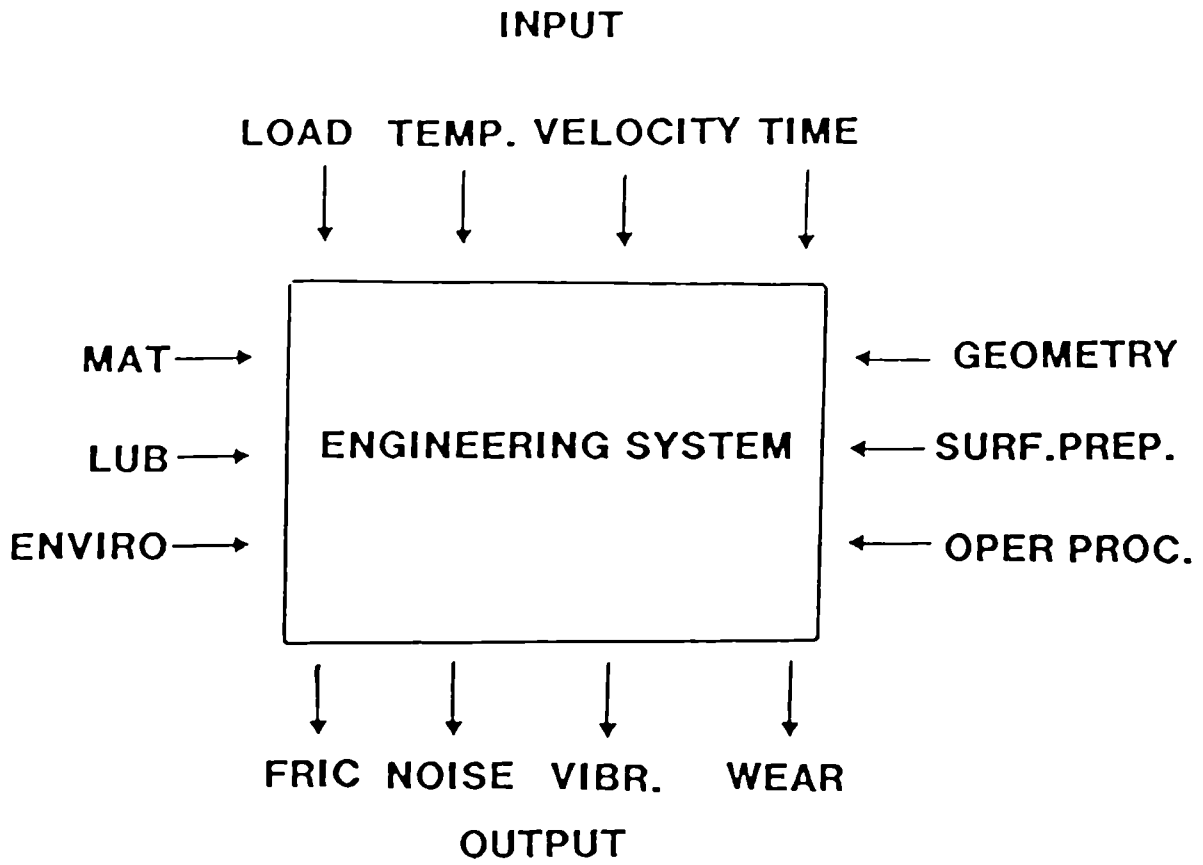
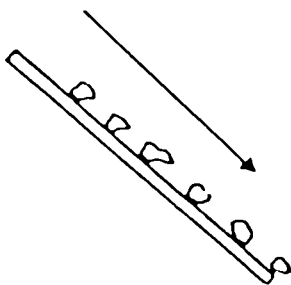


Fig.9 System Approach in Tribology (51).

TWO BODY WEAR

A)



THREE BODY WEAR

B)

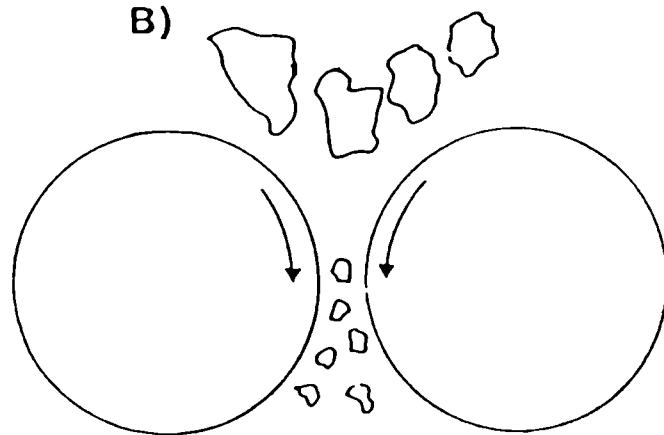


Fig.10 Abrasive Wear Conditions (51).

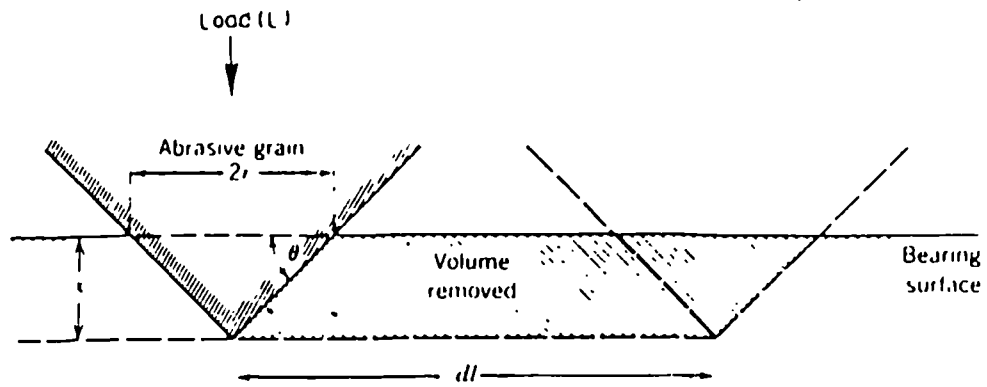


Fig.11 A simple model of abrasive wear (57).

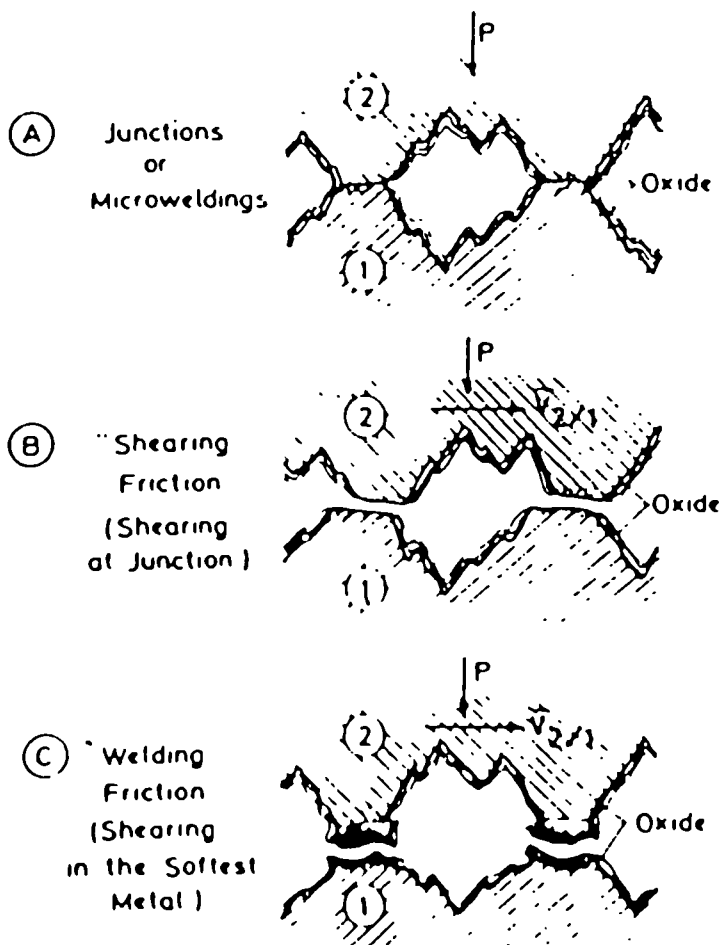


Fig.12 Illustrates different types of metallic friction (62).

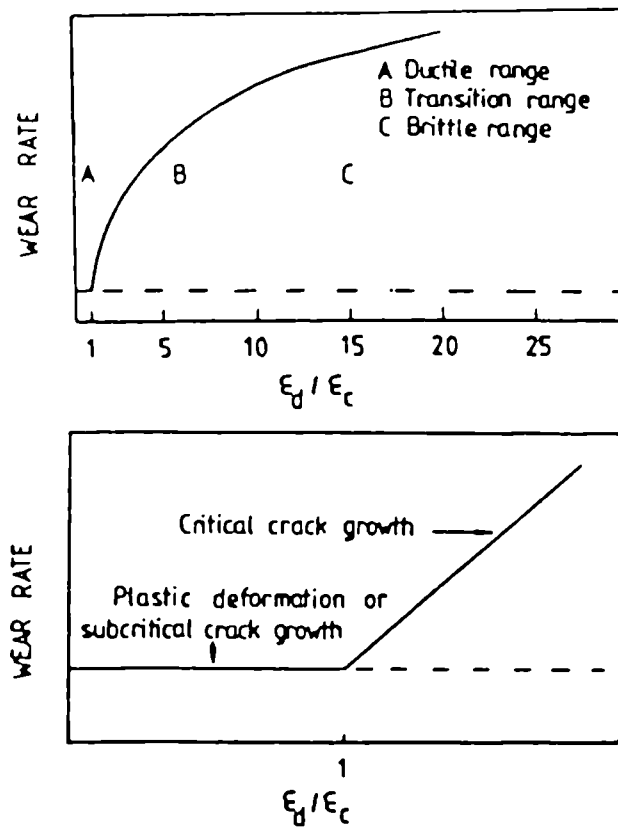


Fig.13 A model to explain the increase in wear rates with decreasing material toughness. (69)

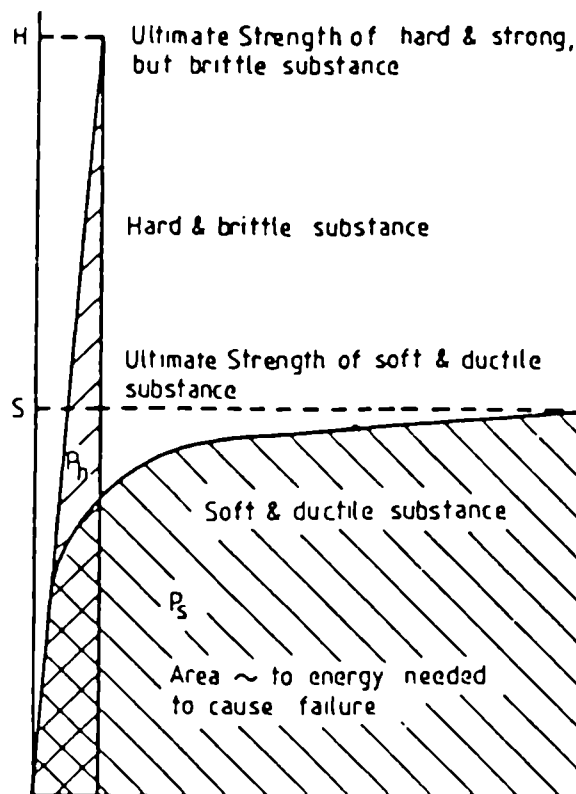


Fig.14 Energy required to deform a metal plastically.

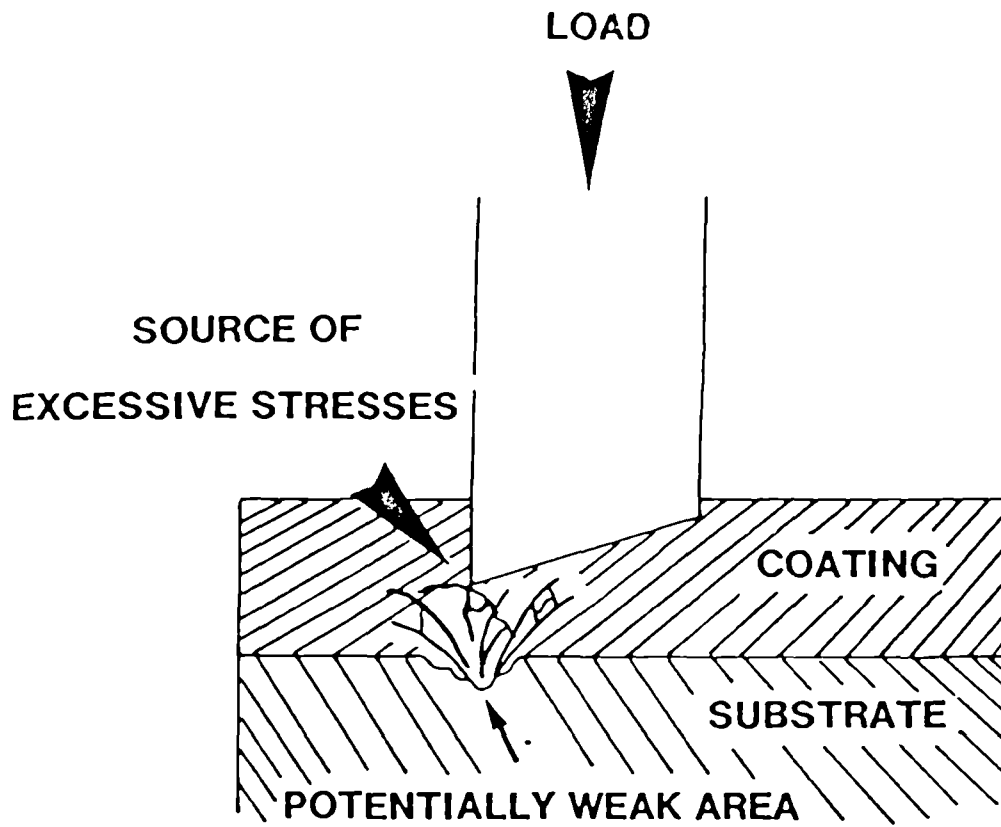
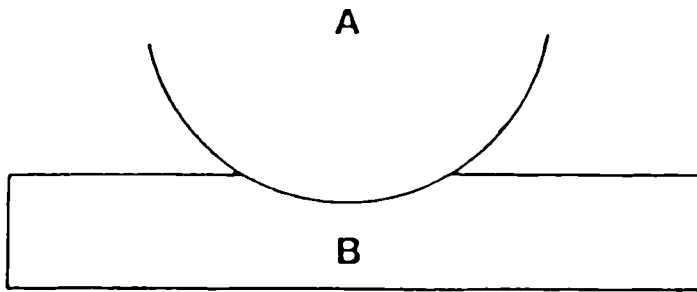
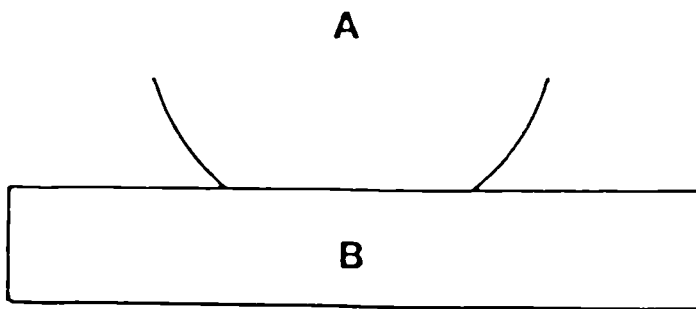


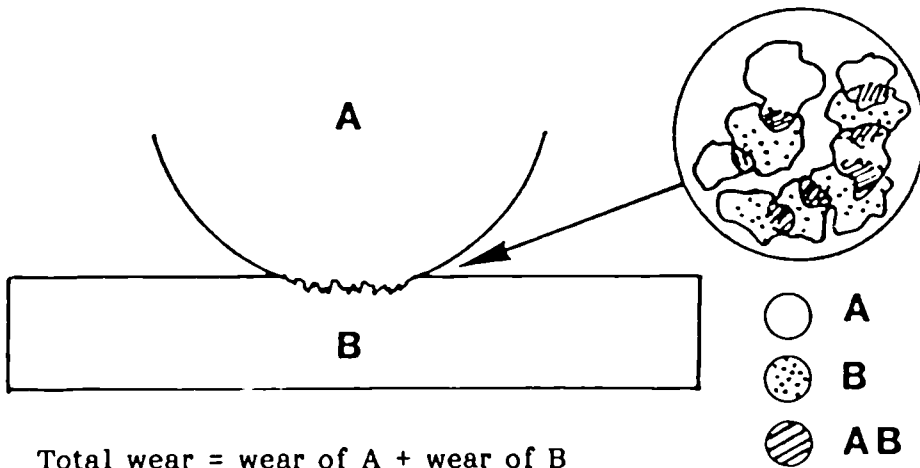
Fig.15 Breakdown of the coating due to misalignment.



CASE I Total wear = wear of A + wear of B
 when wear of A is zero
 then total wear = wear of B



CASE II Total wear = wear of A + wear of B
 when wear of B is zero
 then total wear = wear of A



CASE III Total wear = wear of A + wear of B
 This occurs when A and B are wearing bodies

Fig.16 Possible cases of wearing counterbodies.

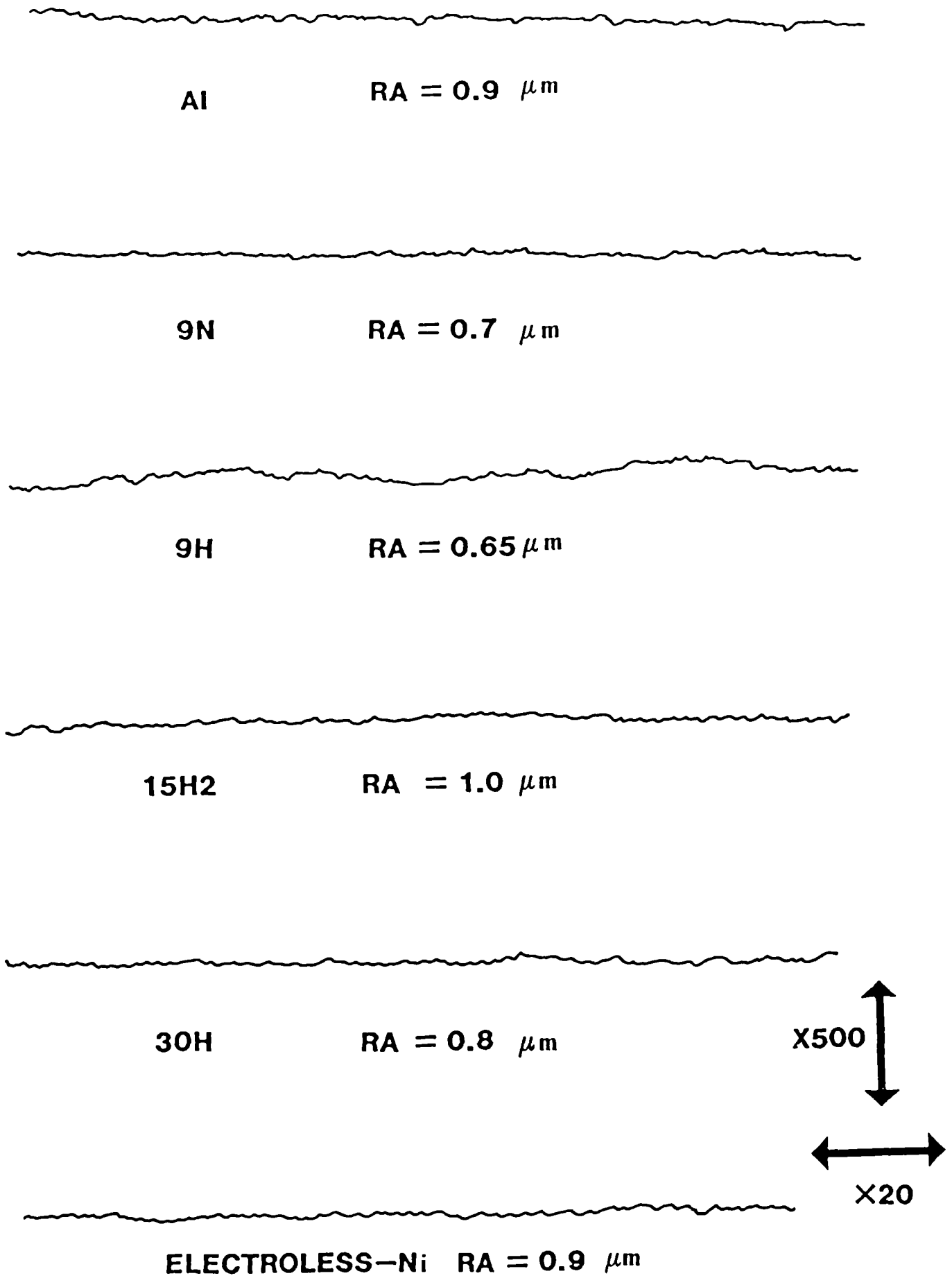
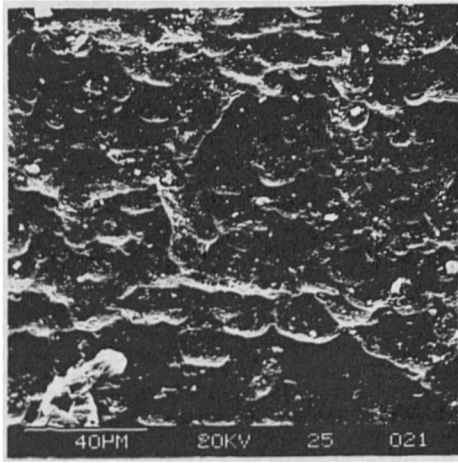
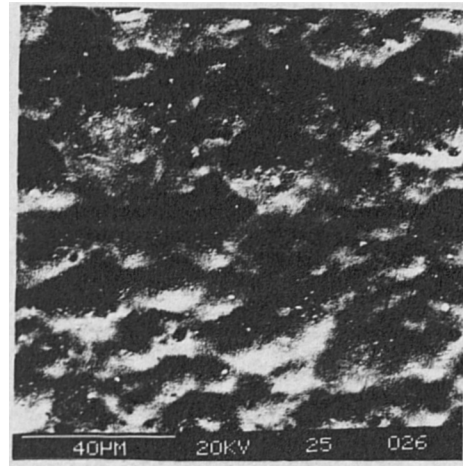


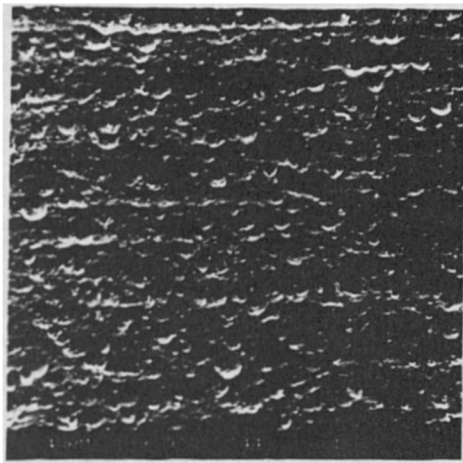
Fig.17 Surface roughness (Ra) values of all materials investigated.



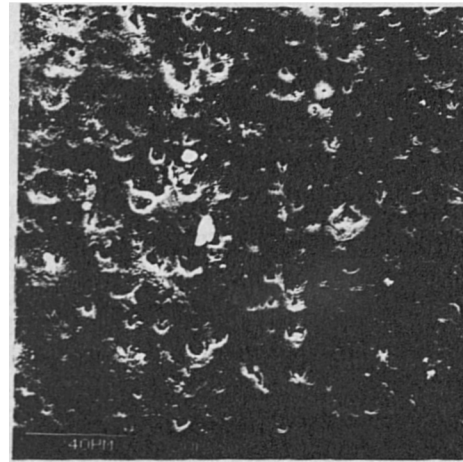
A



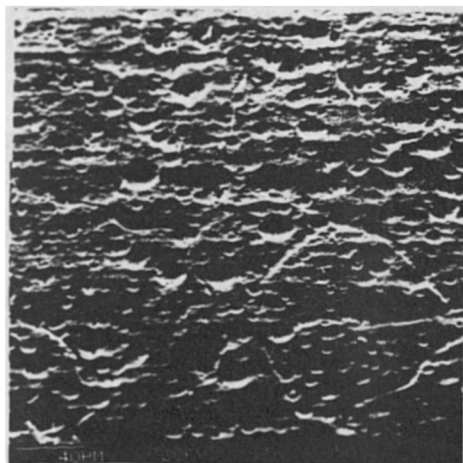
B



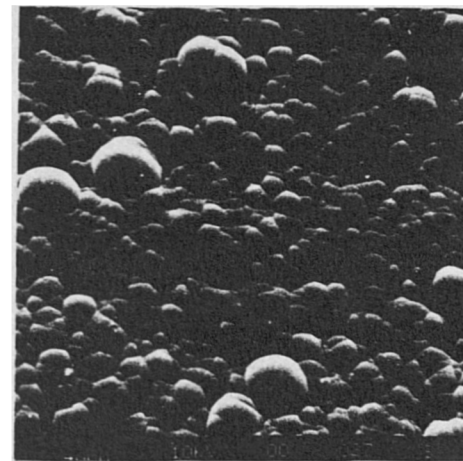
C



D



E



F

Fig. 18 Surface appearance of
A) Uncoated aluminium
B) Natural anodised 9N
C) Hard anodised 9H
D) Hard anodised 15H2
E) Hard anodised 30H
F) Electroless Ni

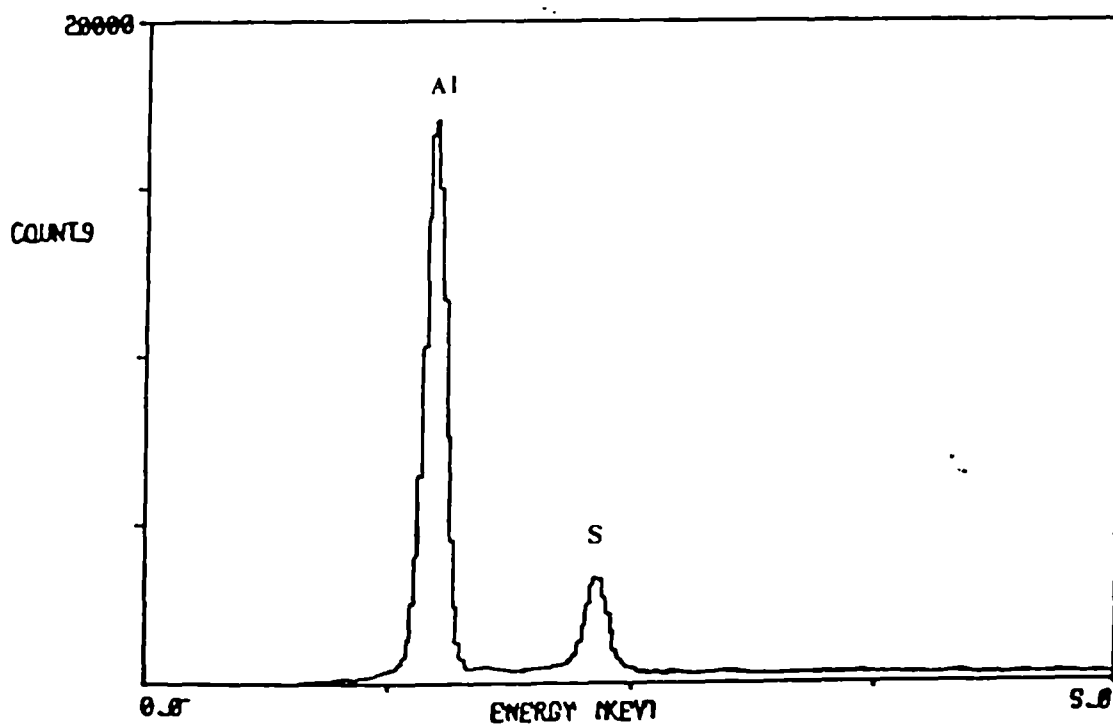


Fig.19 Composition of anodised aluminium 9N.

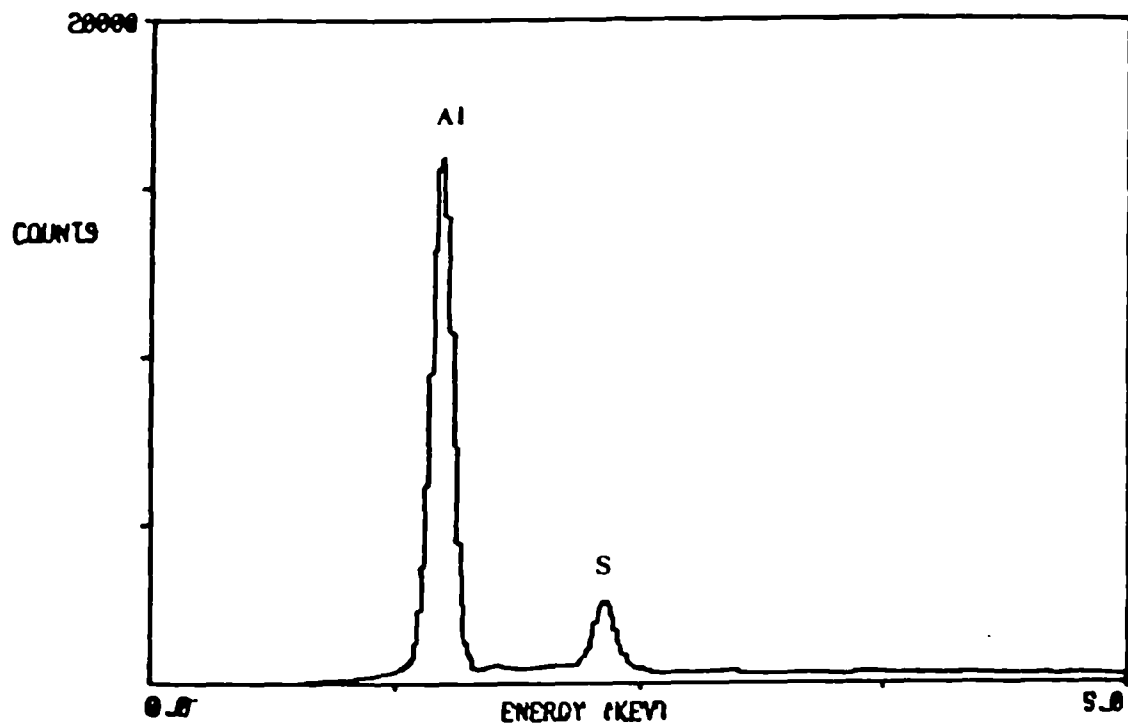


Fig.20 Composition of hard anodised aluminium 9H.

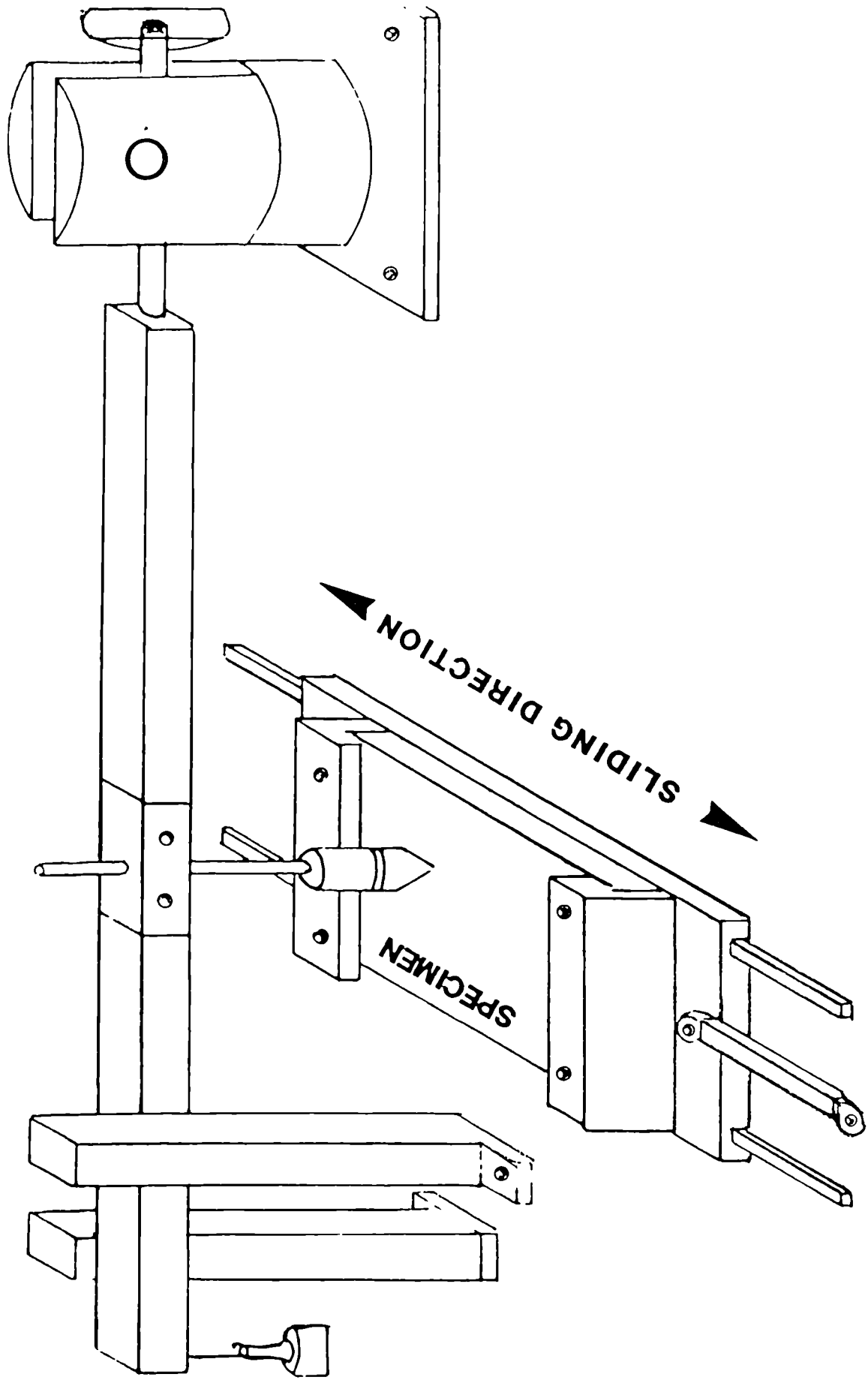
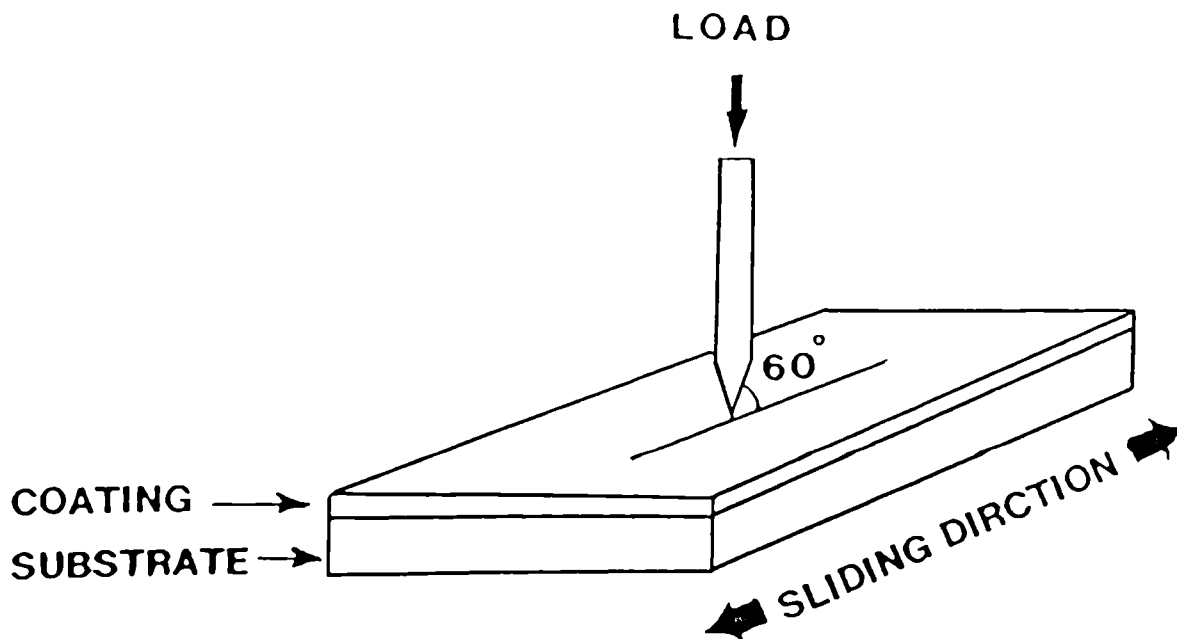


Fig. 21 Schematic representation of a reciprocating wear rig.

DIAMOND ON FLAT (ABRASIVE WEAR)



WEAR TRACK LENGTH = 5 CM

AT SPEED OF 10 C.P.M

Fig.22 Layout of abrasive wear testing machine.

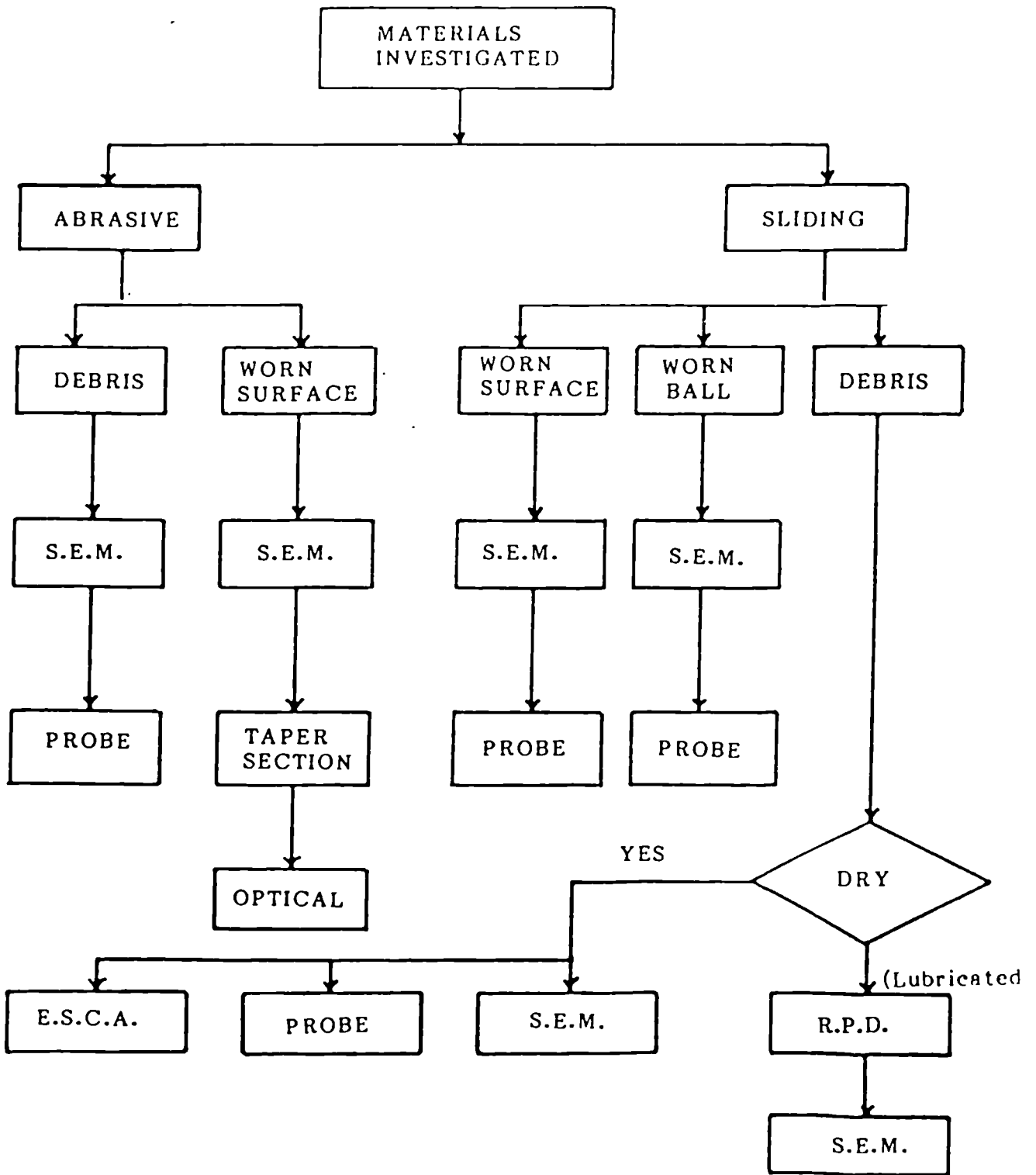


Fig.23 Flow chart represents the analytical techniques used during the investigation.

S.E.M. is Scanning Electron Microscope
 PROBE is Microprobe Analyser
 R.P.D. is Rotary Particle Depositor

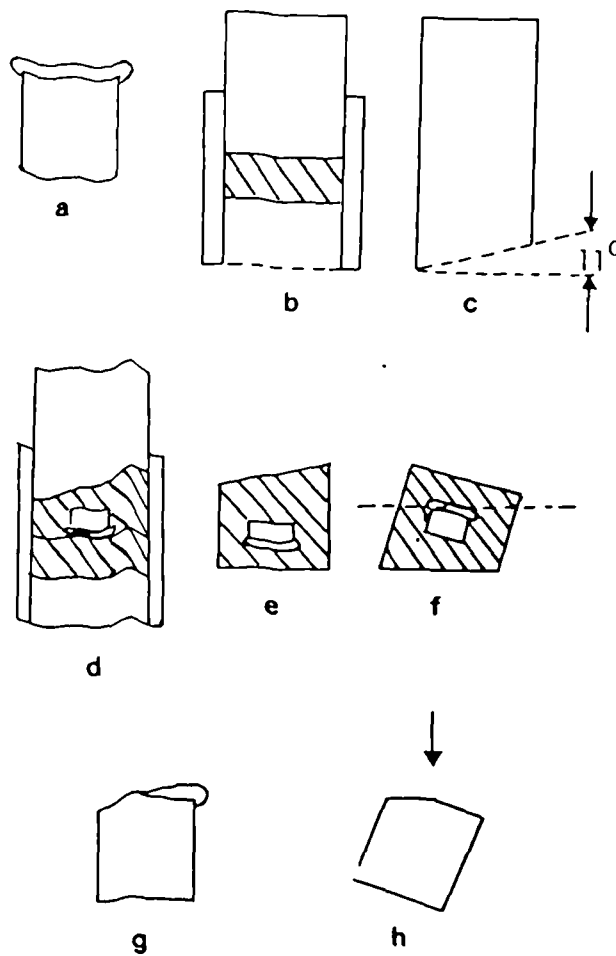


Fig.24 Preparation of a taper section through a wear surface for both optical microscopy and SEM examination.

- a) Epoxy resin applied to the wear surface.
- b) Preparation of a block of uncured bakelite.
- c) Eleven degree angle ram.
- d) Final mounting of the wear specimen.
- e) Mounted specimen removed from the pressure cylinder.
- f) Specimen inverted through 180° , top surface grund, polished and etched. At this stage an optical metallographic examination is carried out.
- g) Wear specimen removed from the bakelite and epoxy coating is then removed.
- h) Wear surface topography and metallurgical substrate ready for simultaneous viewing in the SEM.

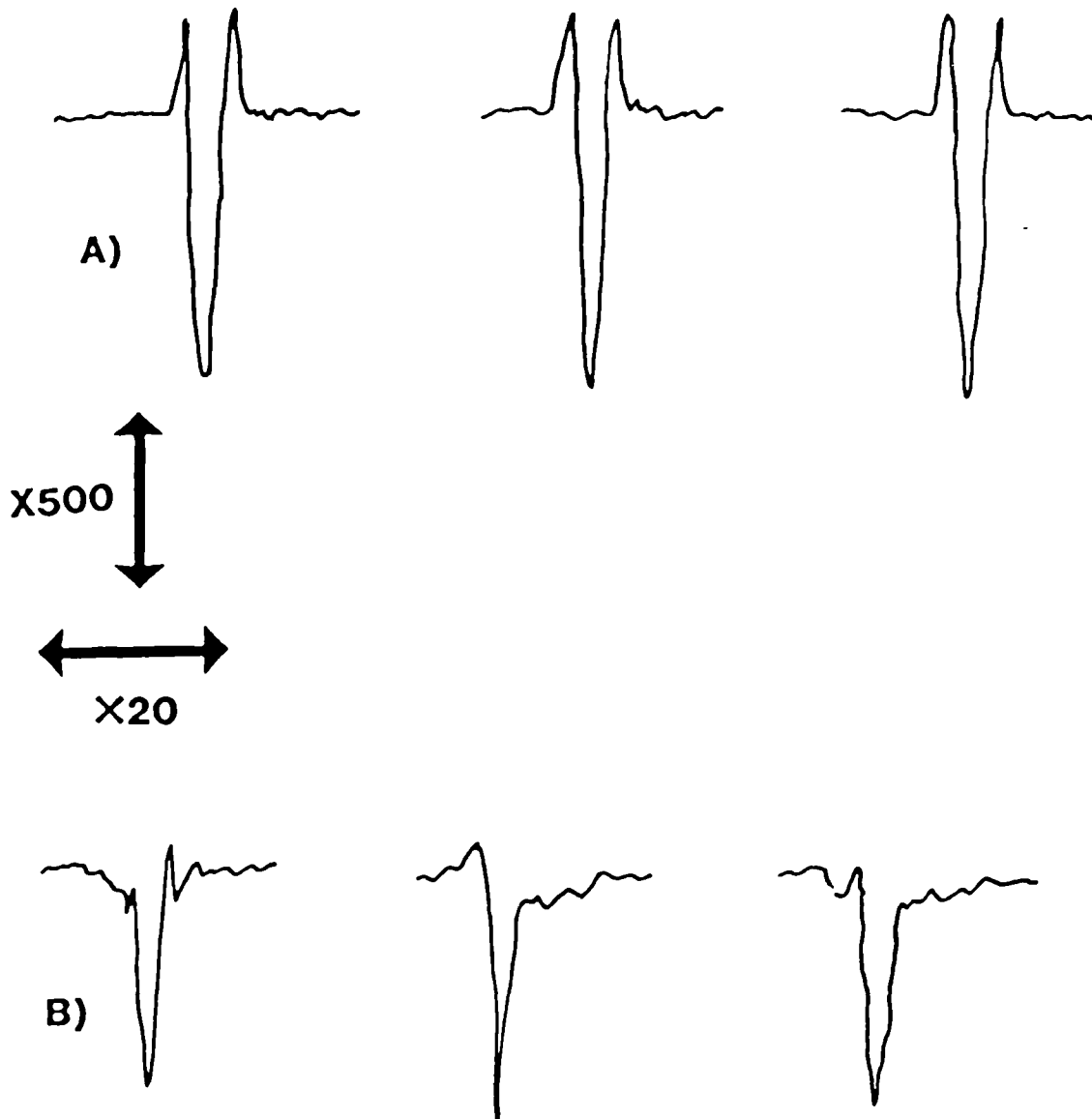


Fig.25 Profilometric traces illustrates

- A) Deformed edges of the uncoated aluminium alloy
- B) Fractured edges of a hard anodised aluminium alloy 9H.

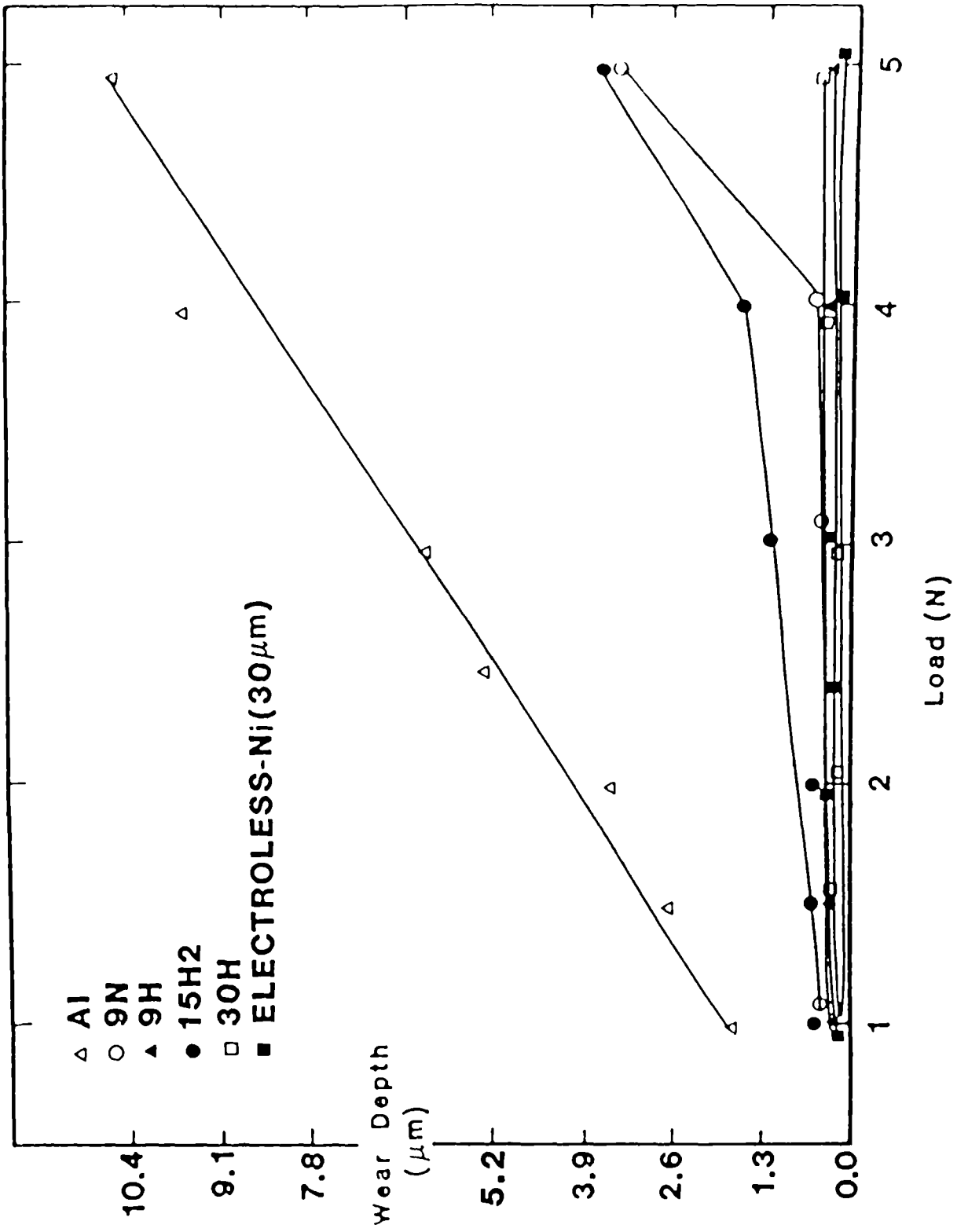


Fig.26 Abrasive wear at a single pass and different applied loads.

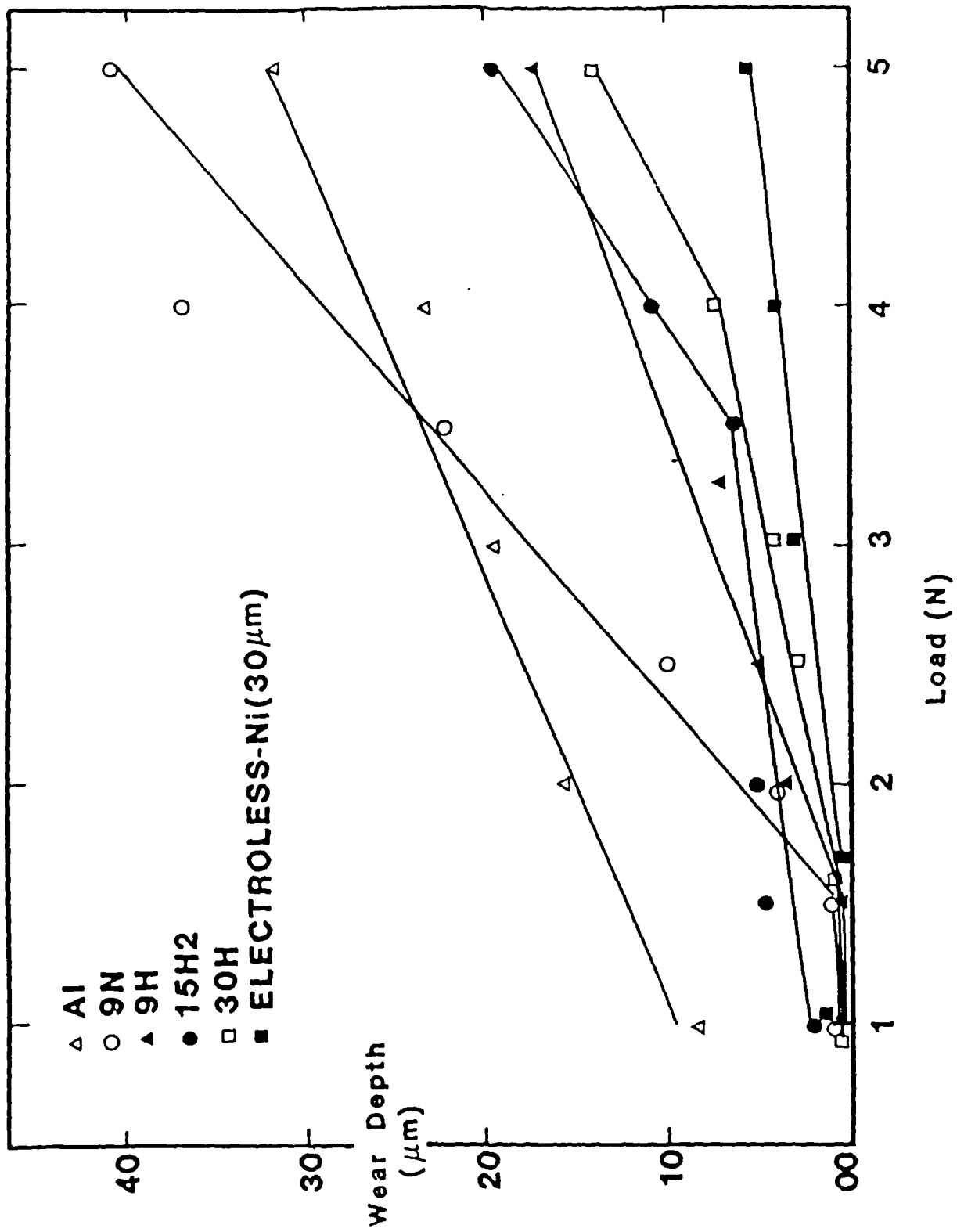


Fig.27 Abrasive wear at 10 passes and different applied loads.

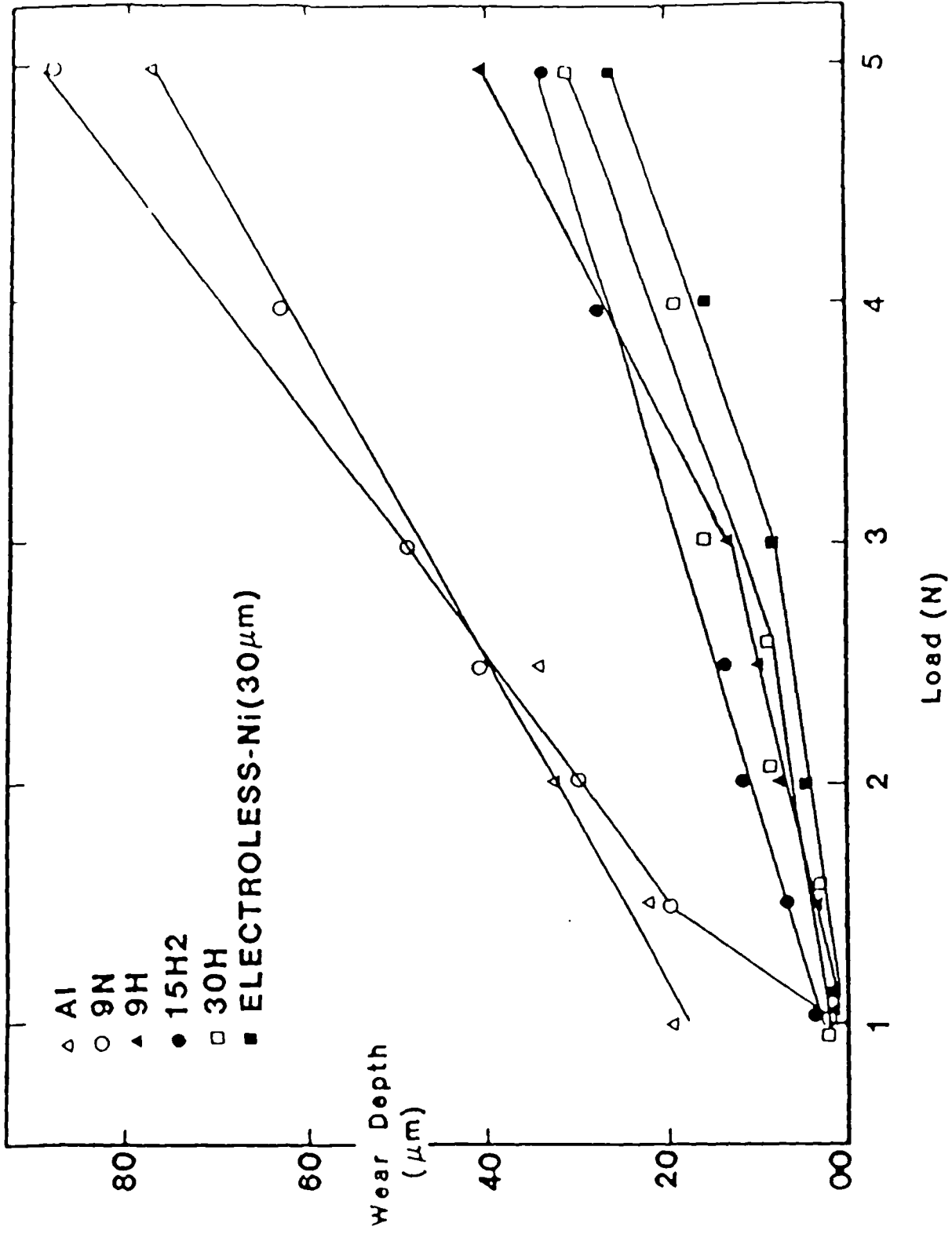


Fig.28 Abrasive wear at 50 passes and different applied loads.

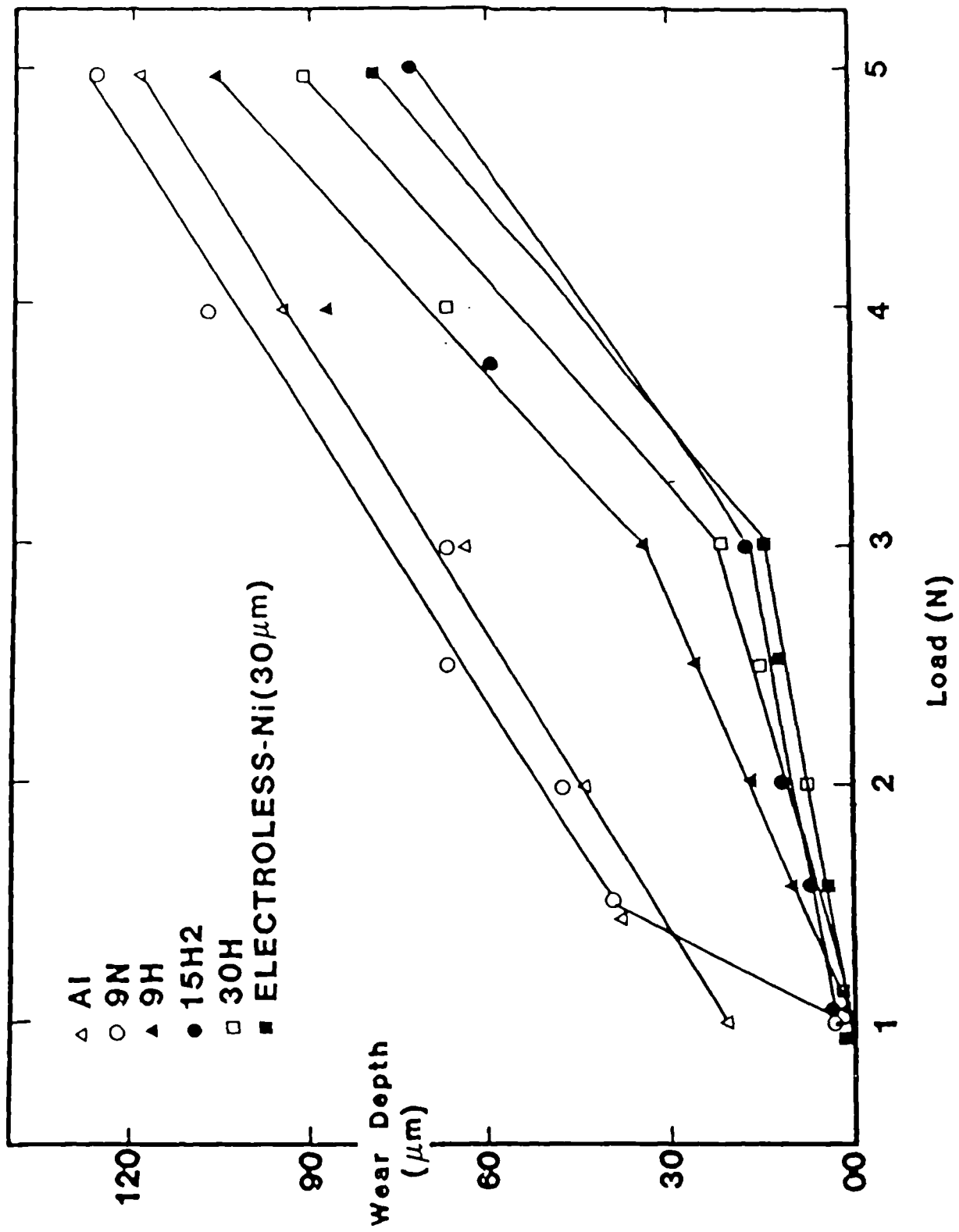


Fig.29 Abrasive wear at 100 passes and different applied loads.

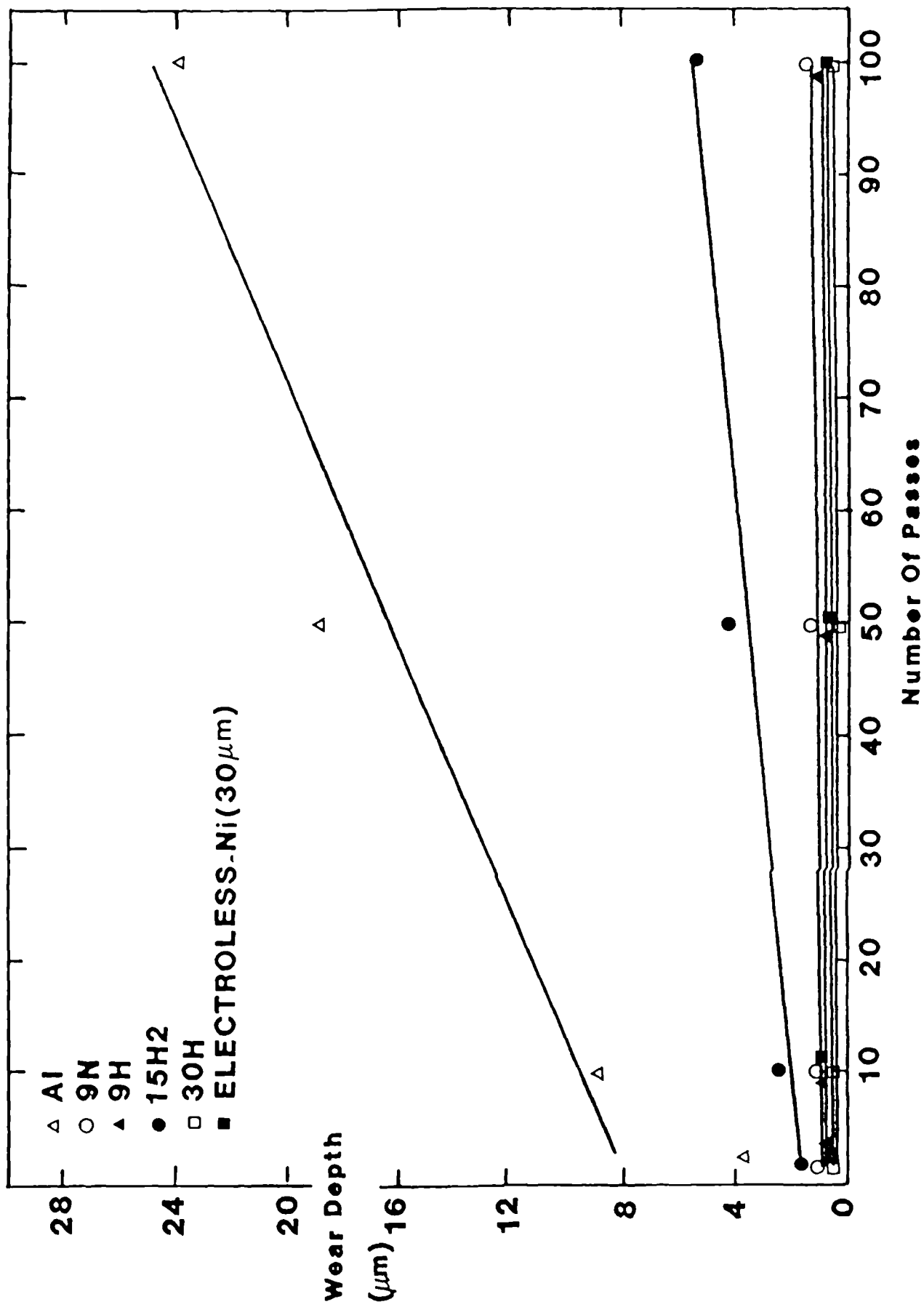


Fig.30 Abrasive wear at 1N and different number of passes.

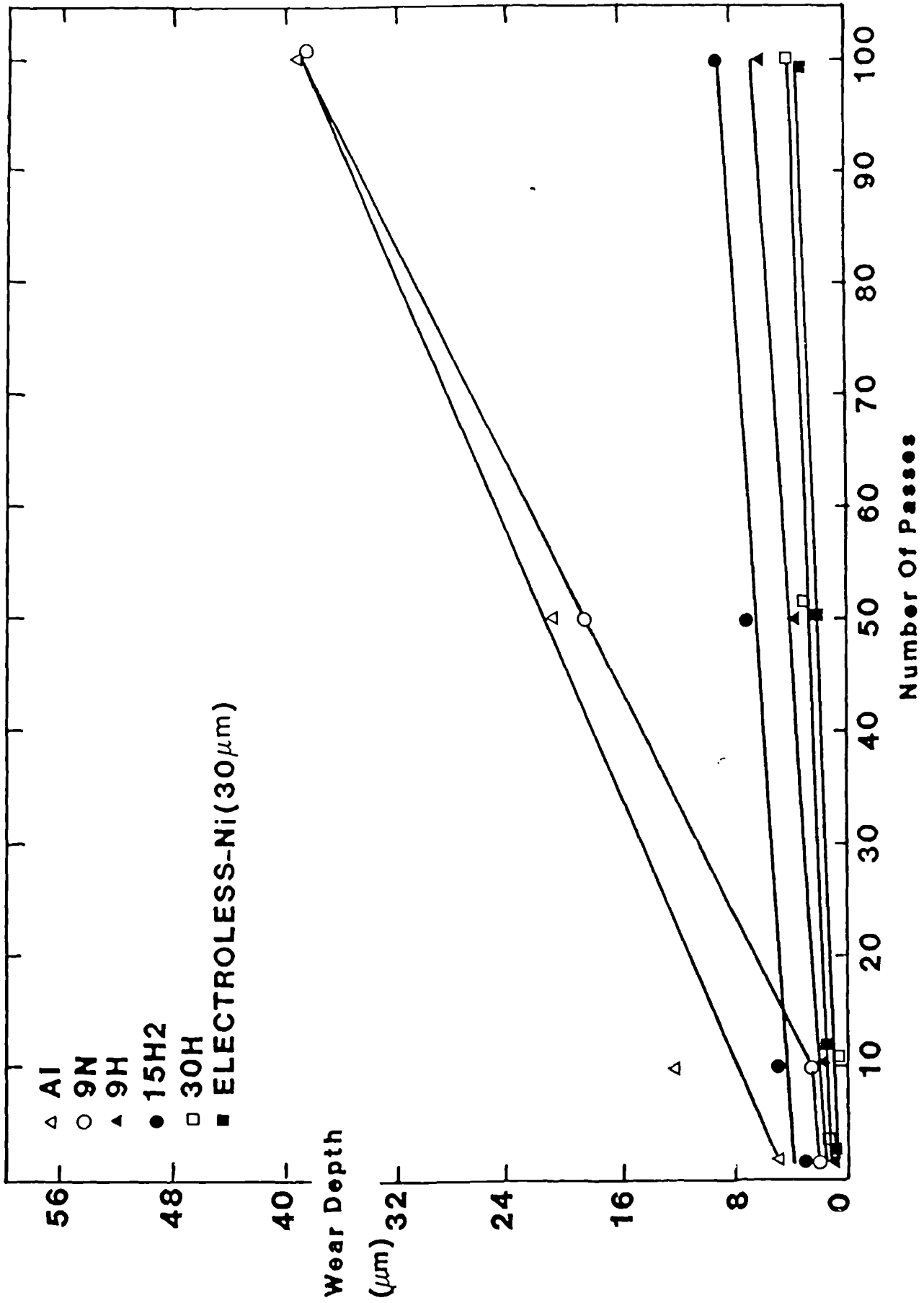


Fig.31 Abrasive wear at 1.5N and different number of passes.

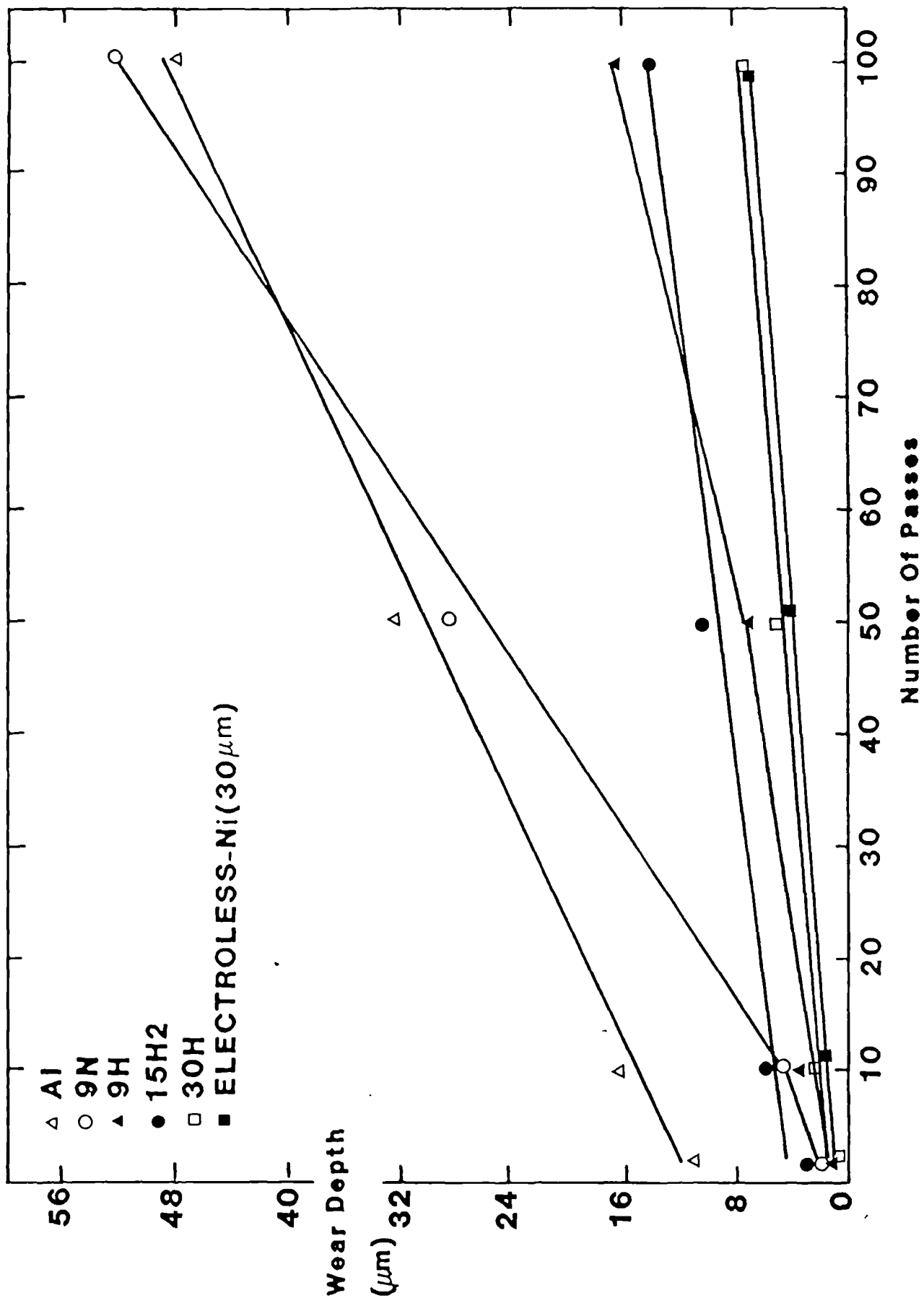


Fig.32 Abrasive wear at 2N and different number of passes.

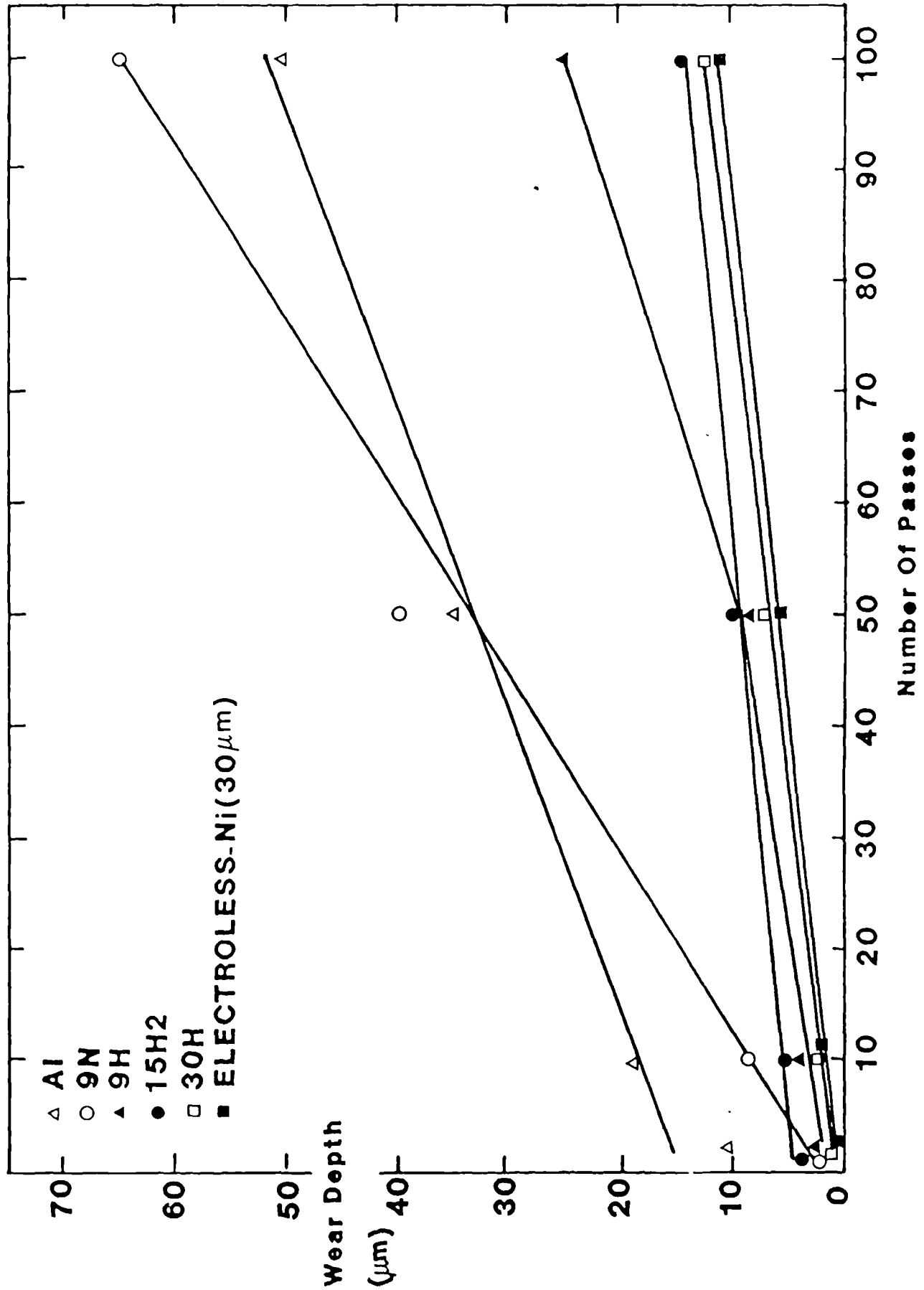


Fig.33 Abrasive wear at 2.5N and different number of passes.

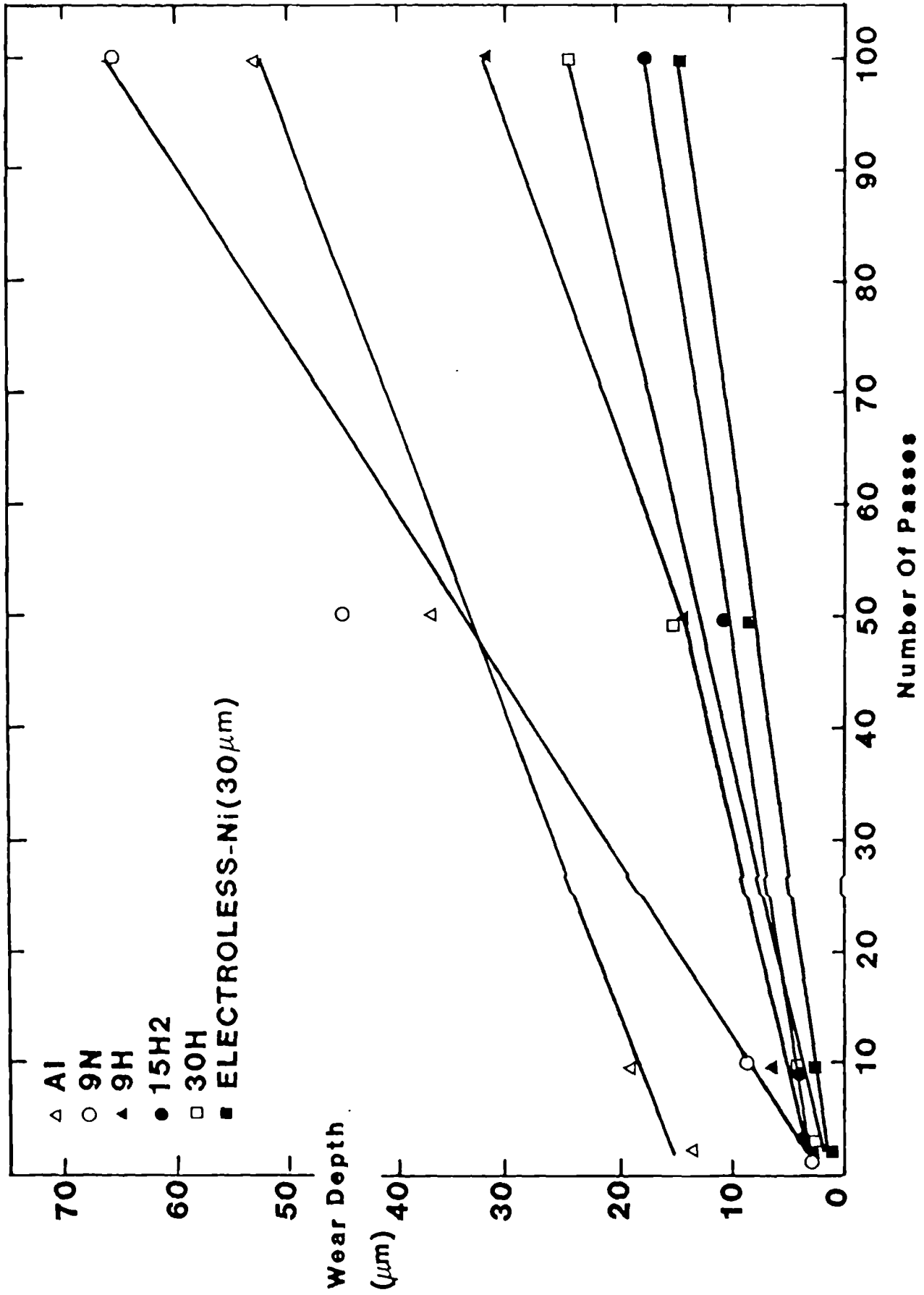


Fig.34 Abrasive wear at 3N and different number of passes.

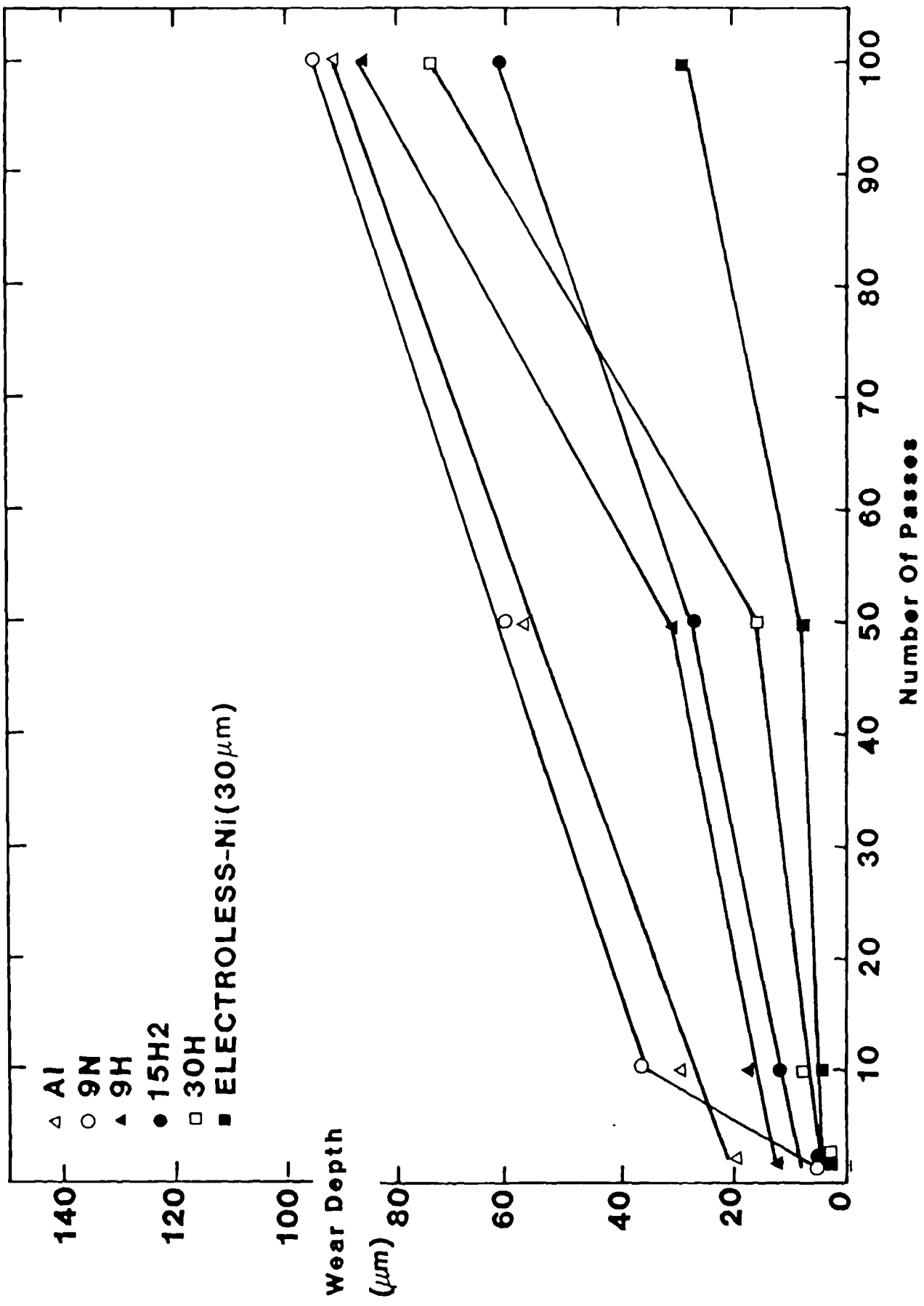


Fig.35 Abrasive wear at 4N and different number of passes.

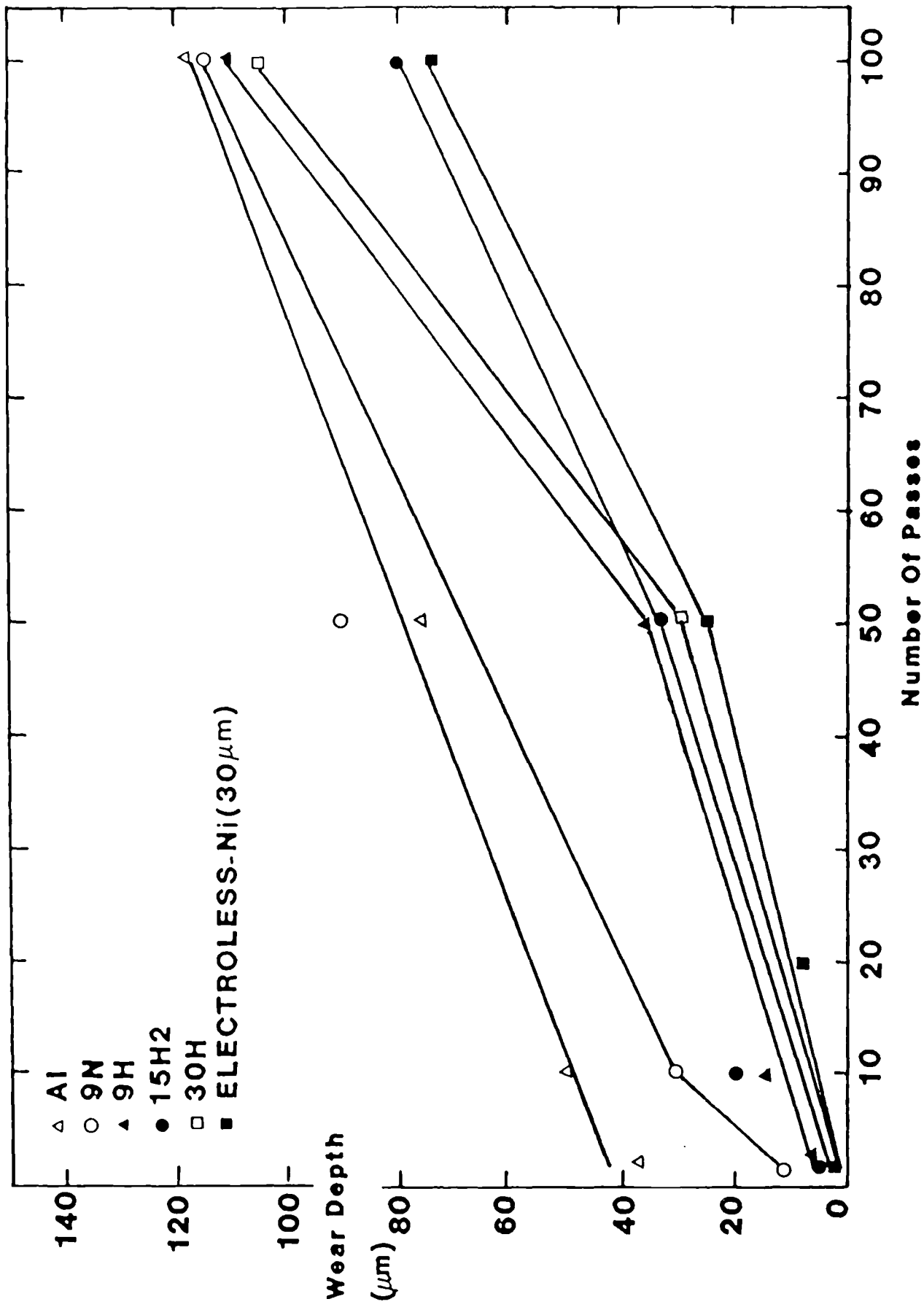


Fig.36 Abrasive wear at 5N and different number of passes.

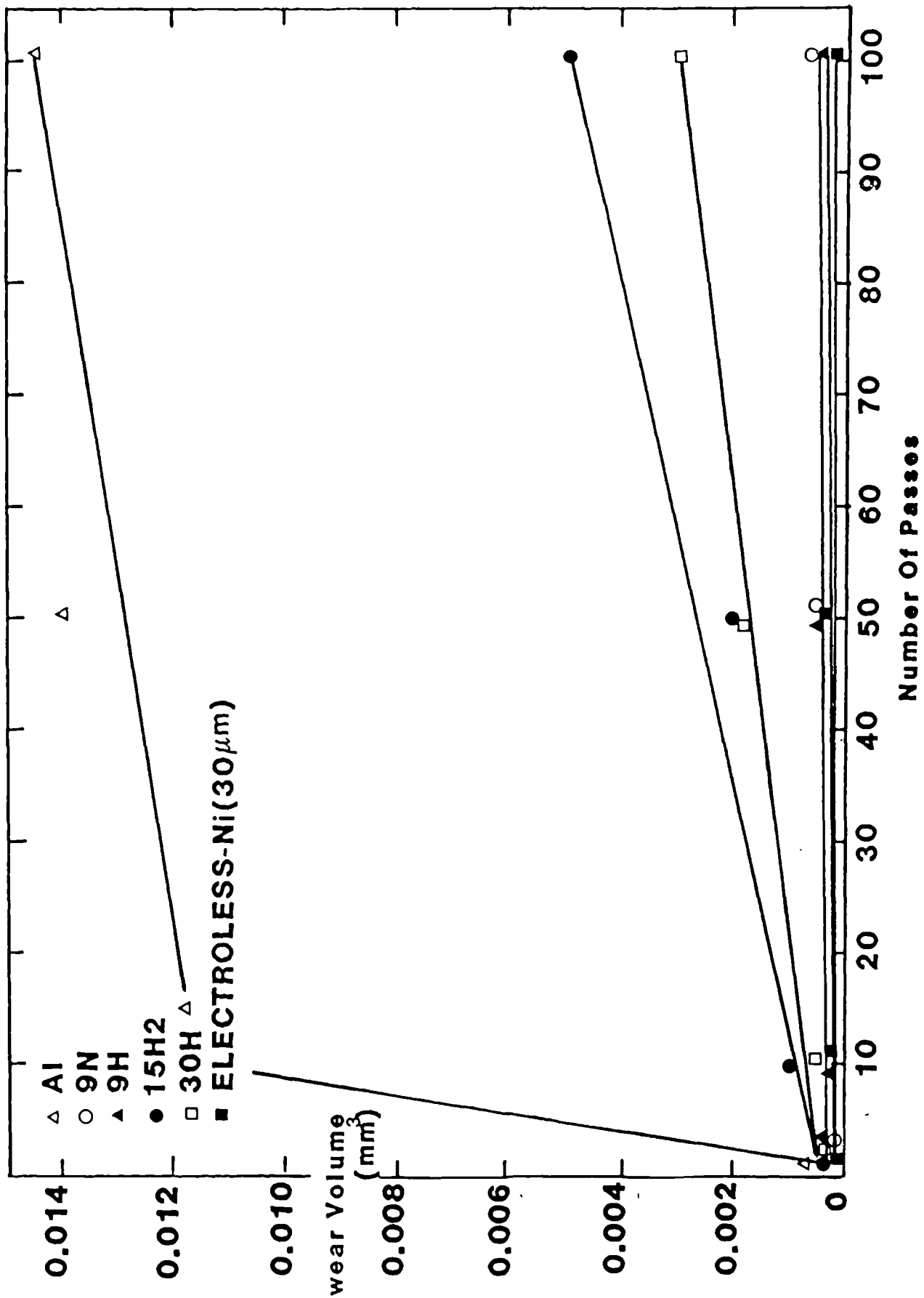


Fig.37 Abrasive wear at 1N and different number of passes.

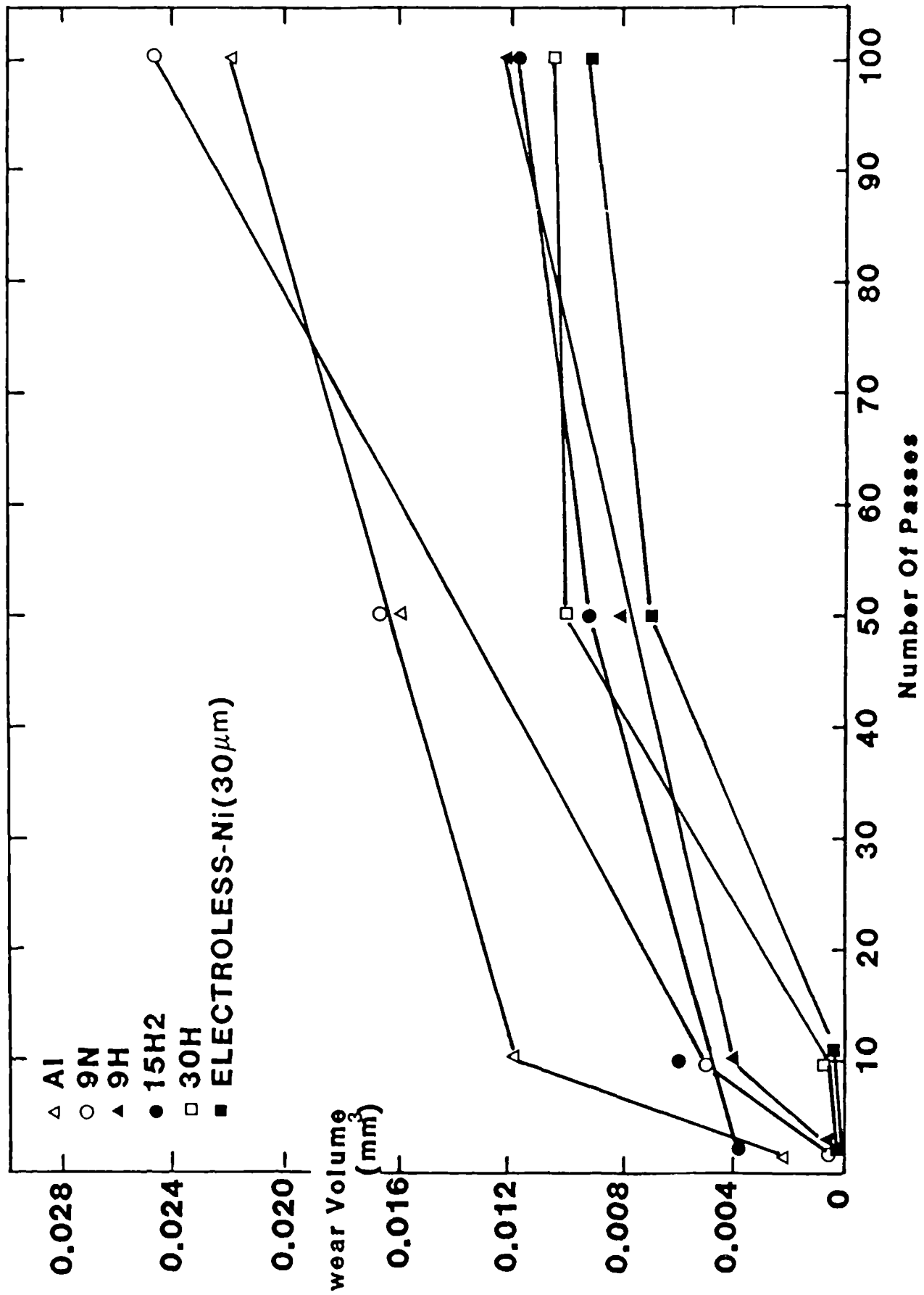


Fig.38 Abrasive wear at 2N and different number of passes.

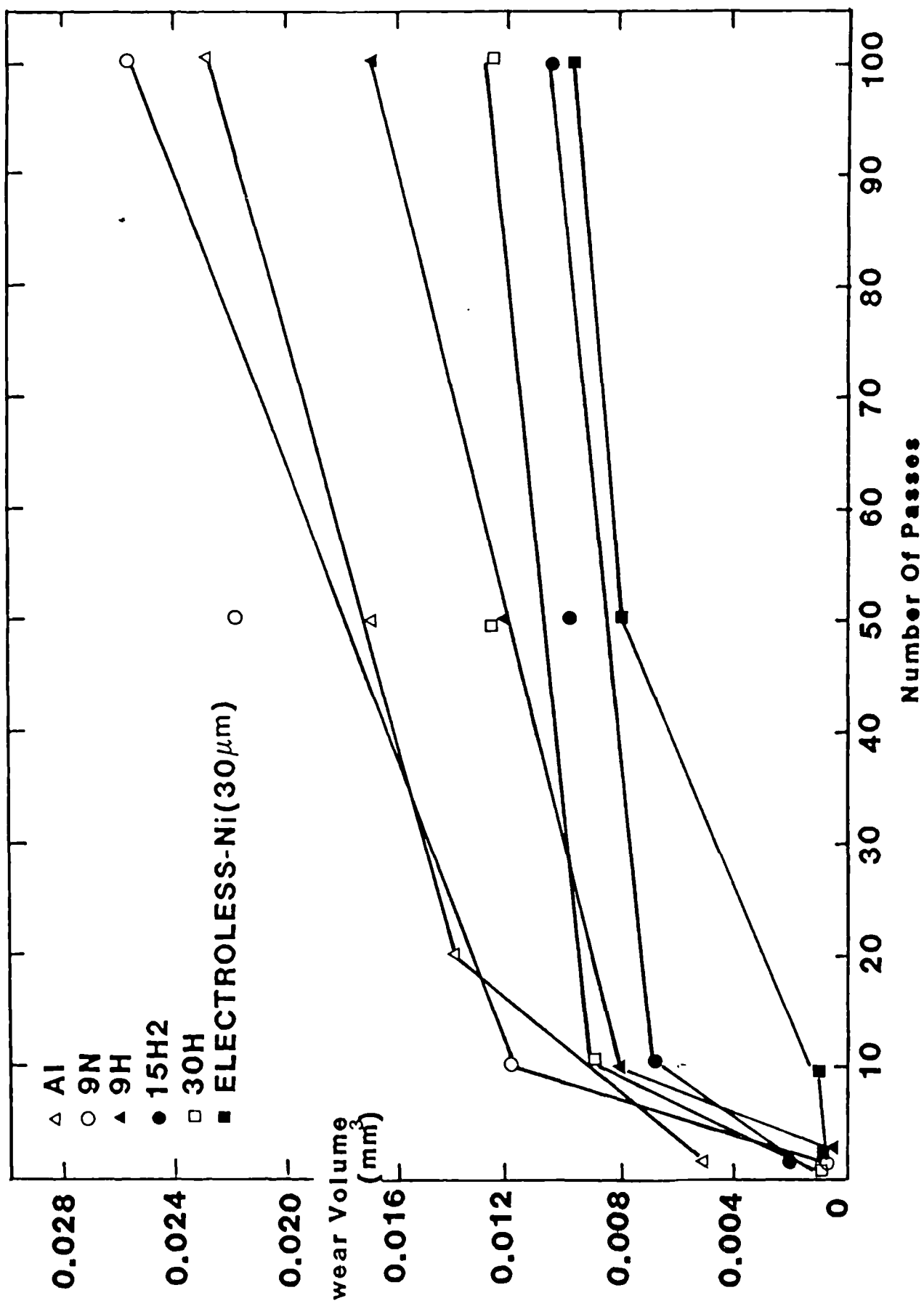


Fig.39 Abrasive wear at 3N and different number of passes.

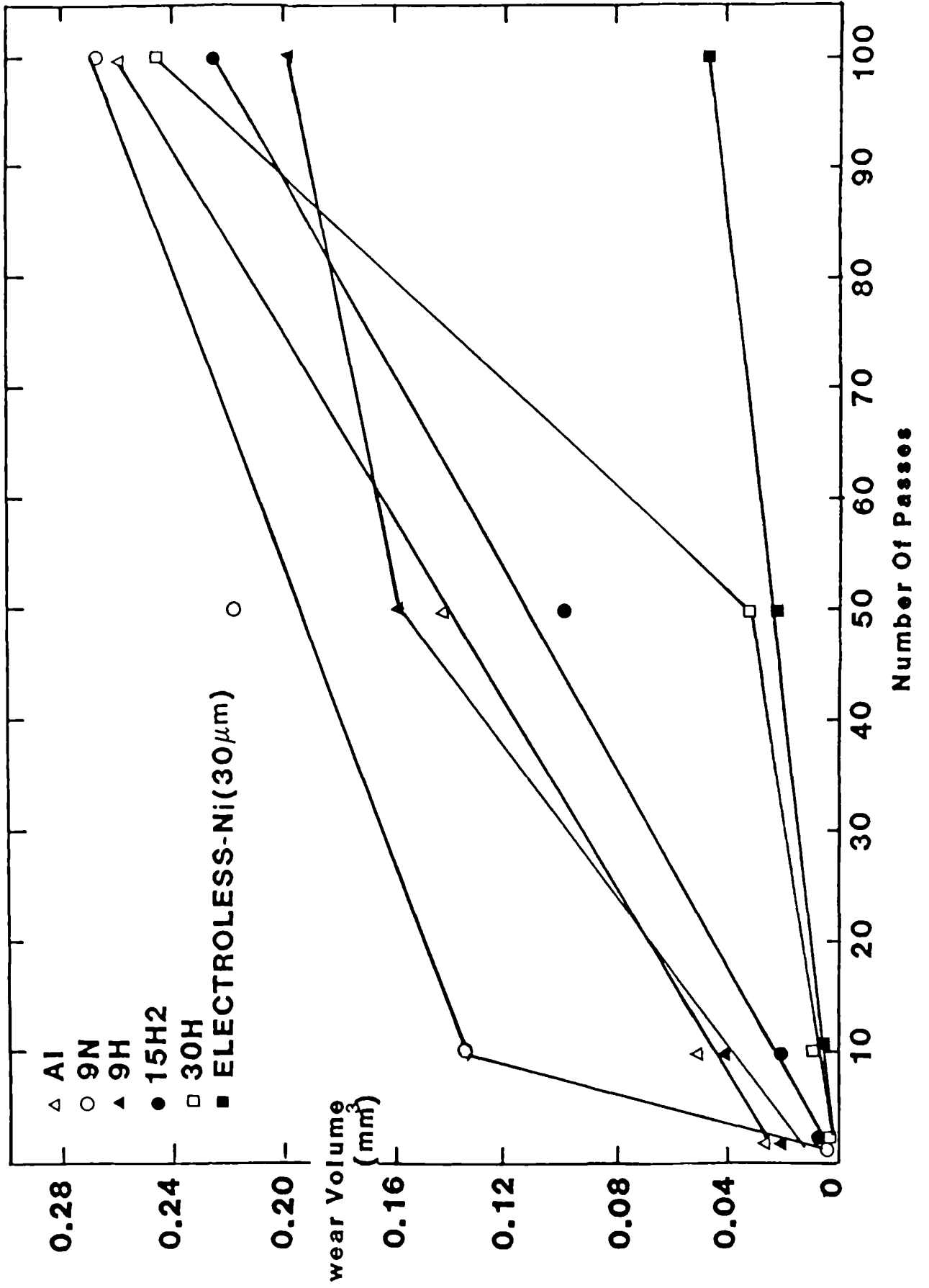


Fig.40 Abrasive wear at 4N and different number of passes.

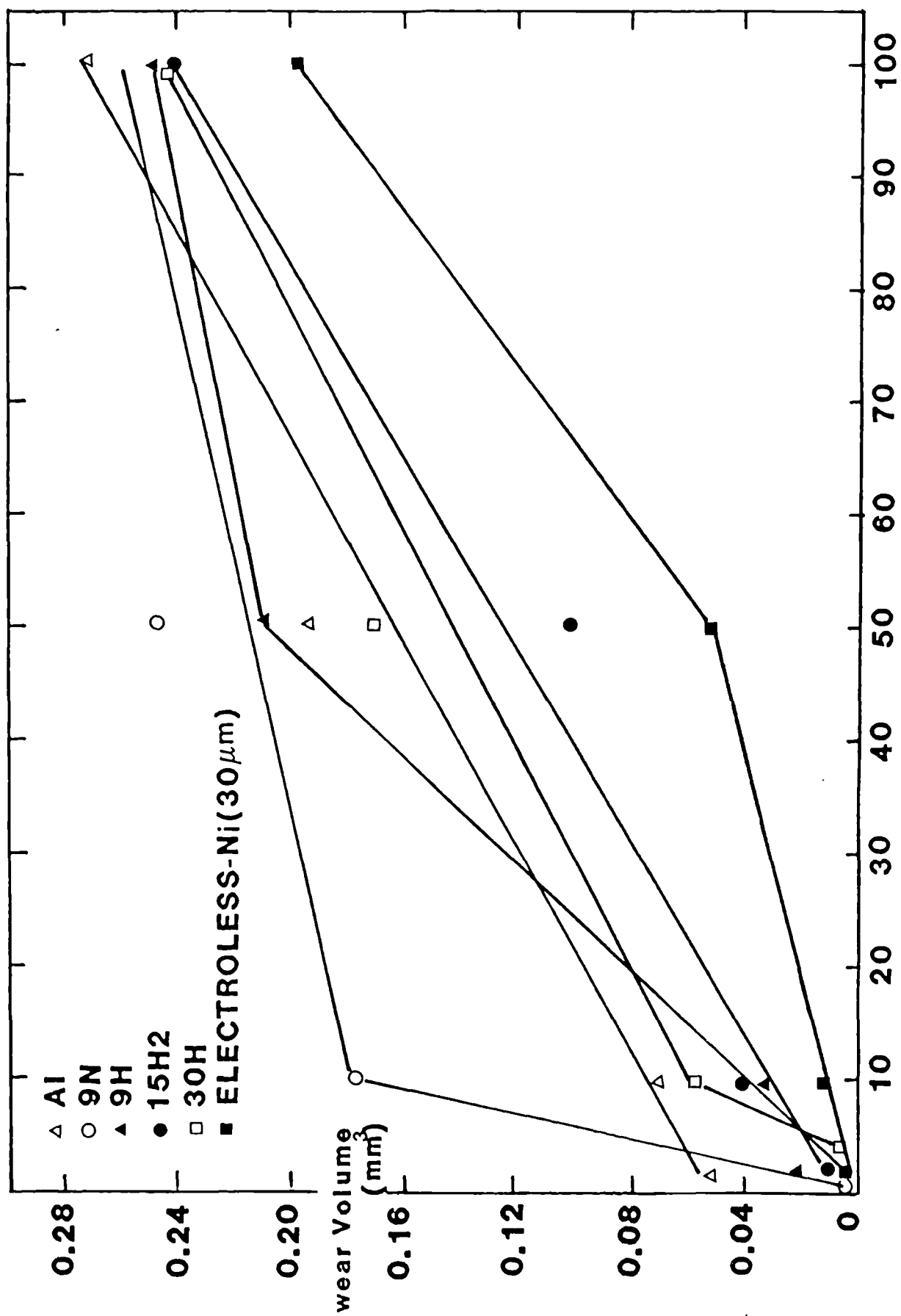


Fig.41 Abrasive wear at 5N and different number of passes.

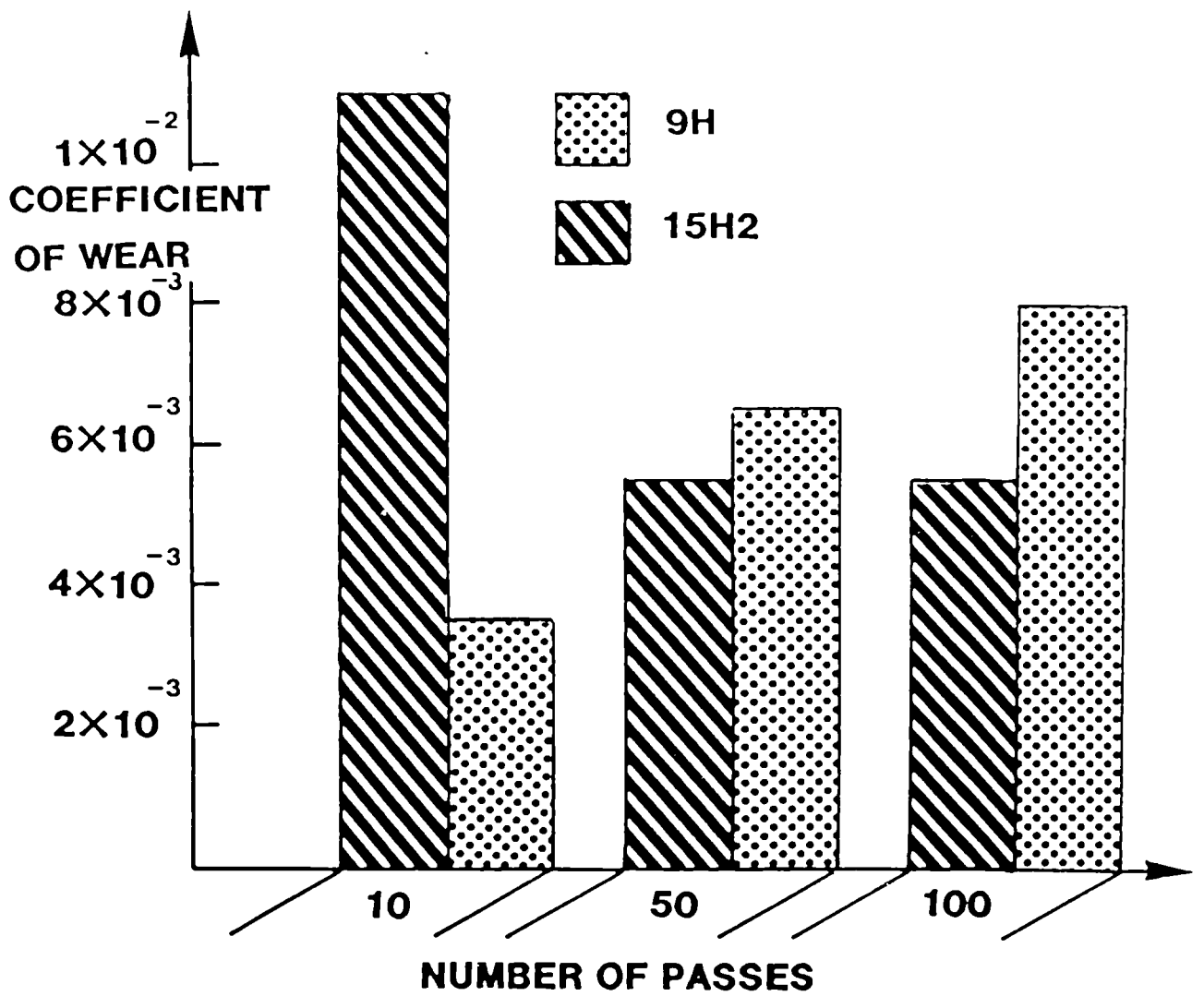


Fig.42 Coefficient of abrasive wear (K) of anodised alloys, 9H, 15H2.

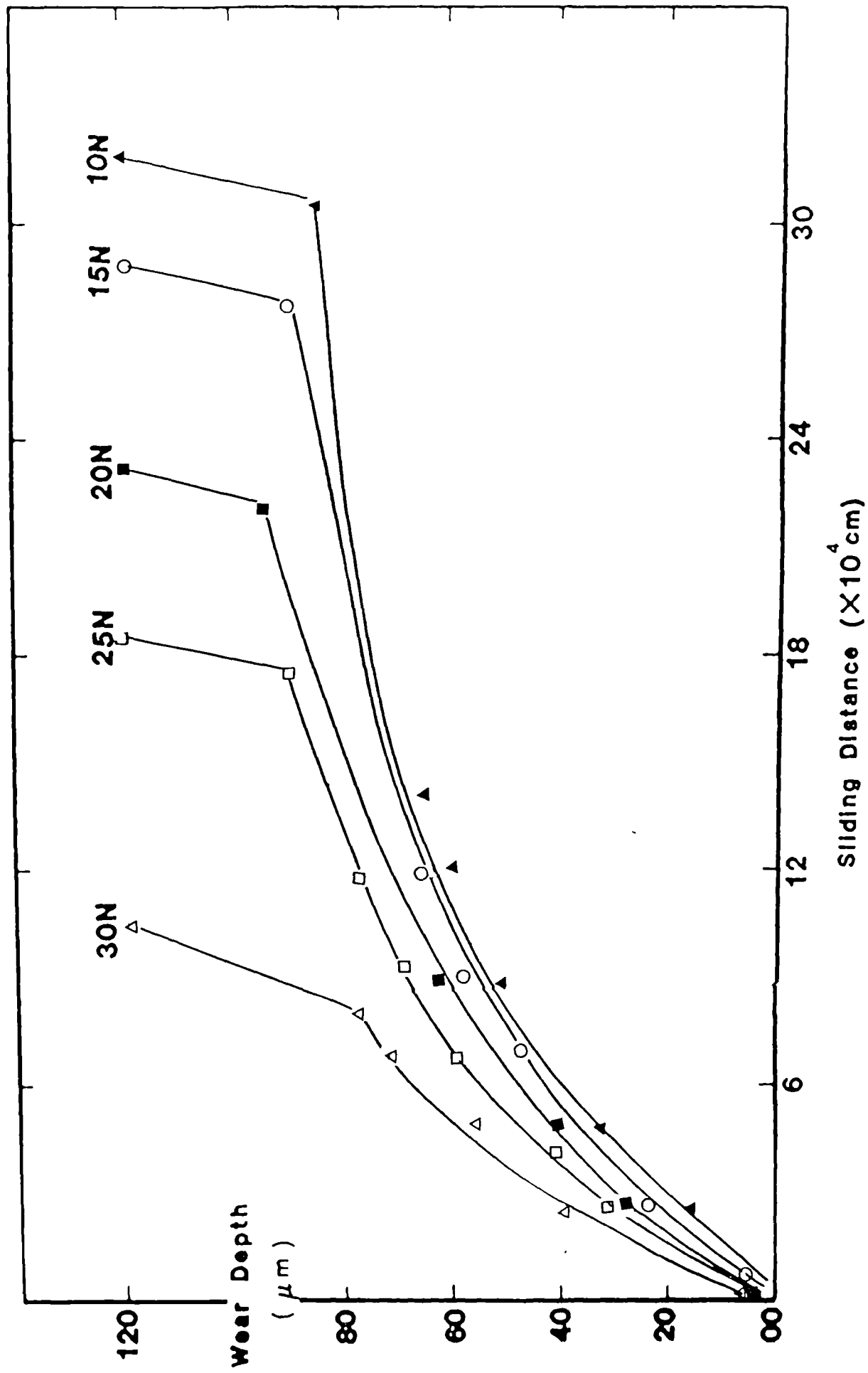


Fig.43 Dry adhesive wear curves obtained for hard anodised alloy 9H at different applied loads against steel ball.

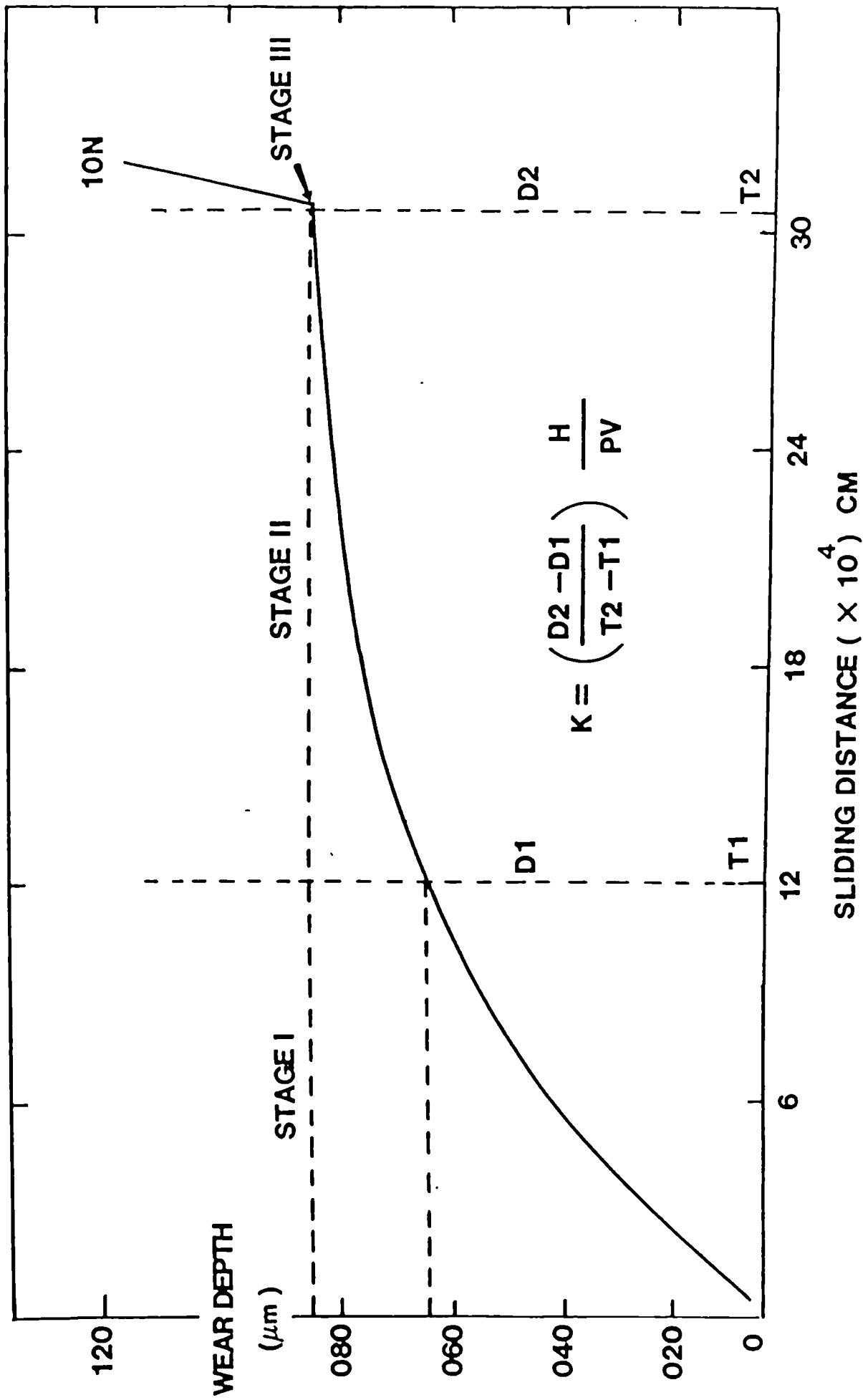


Fig.44 Typical adhesive wear results obtained for the anodised alloy 9H against steel ball.

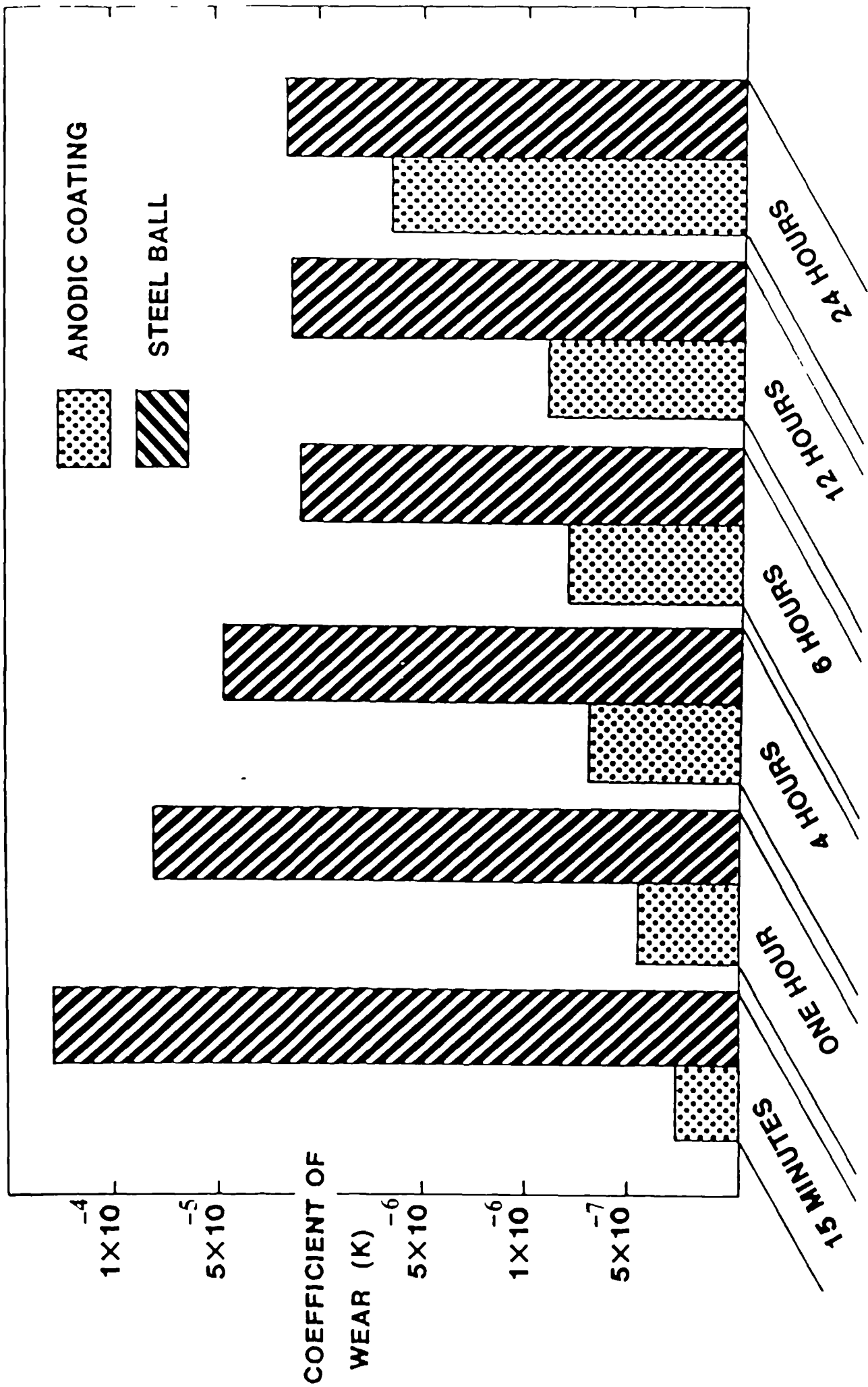


Fig.45 A graphic representation of the coefficient of wear (K) of the anodised aluminium alloy 9H and the steel ball

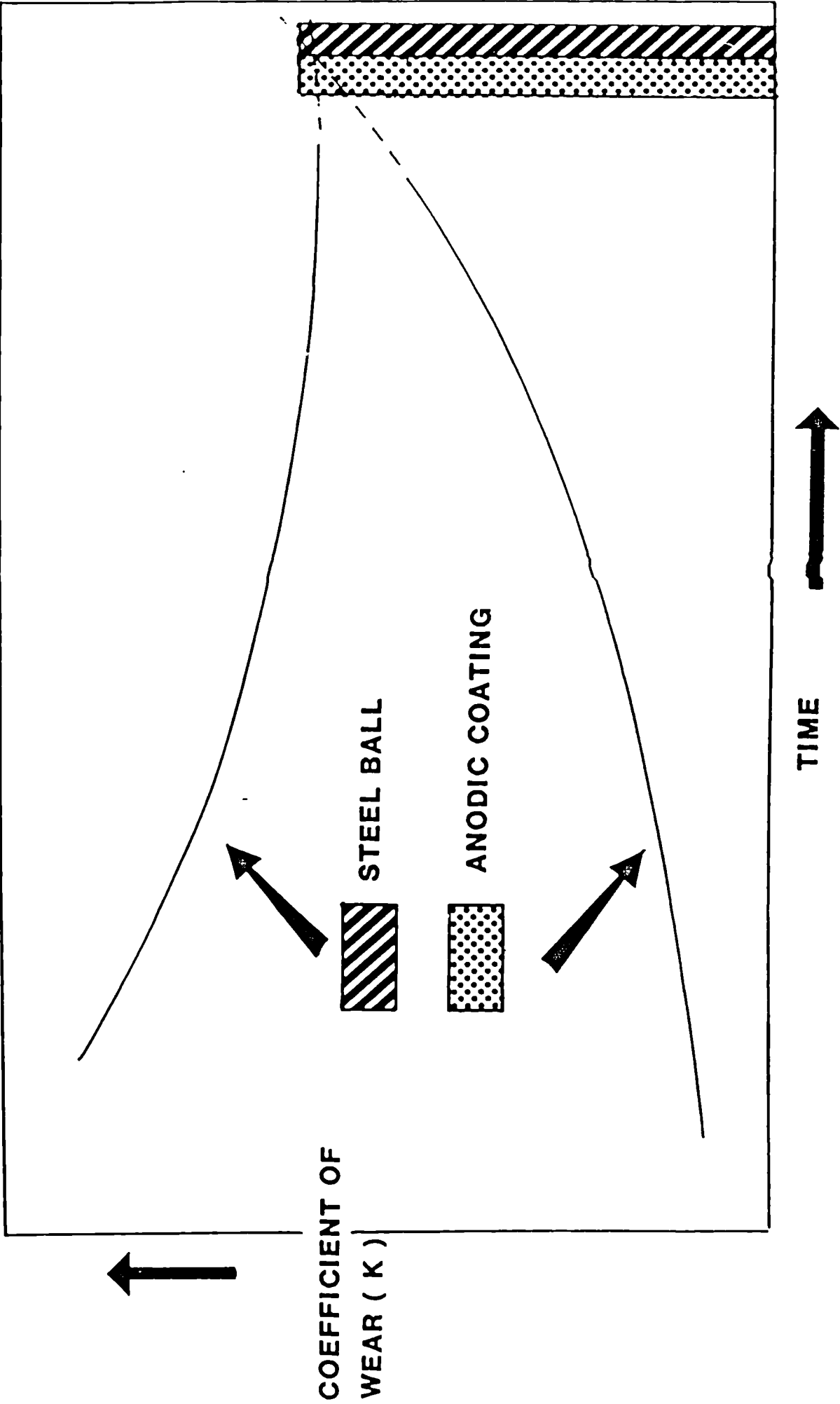


Fig.46 The trend in the coefficient of wear of the anodised aluminium alloy 9H and the steel ball.

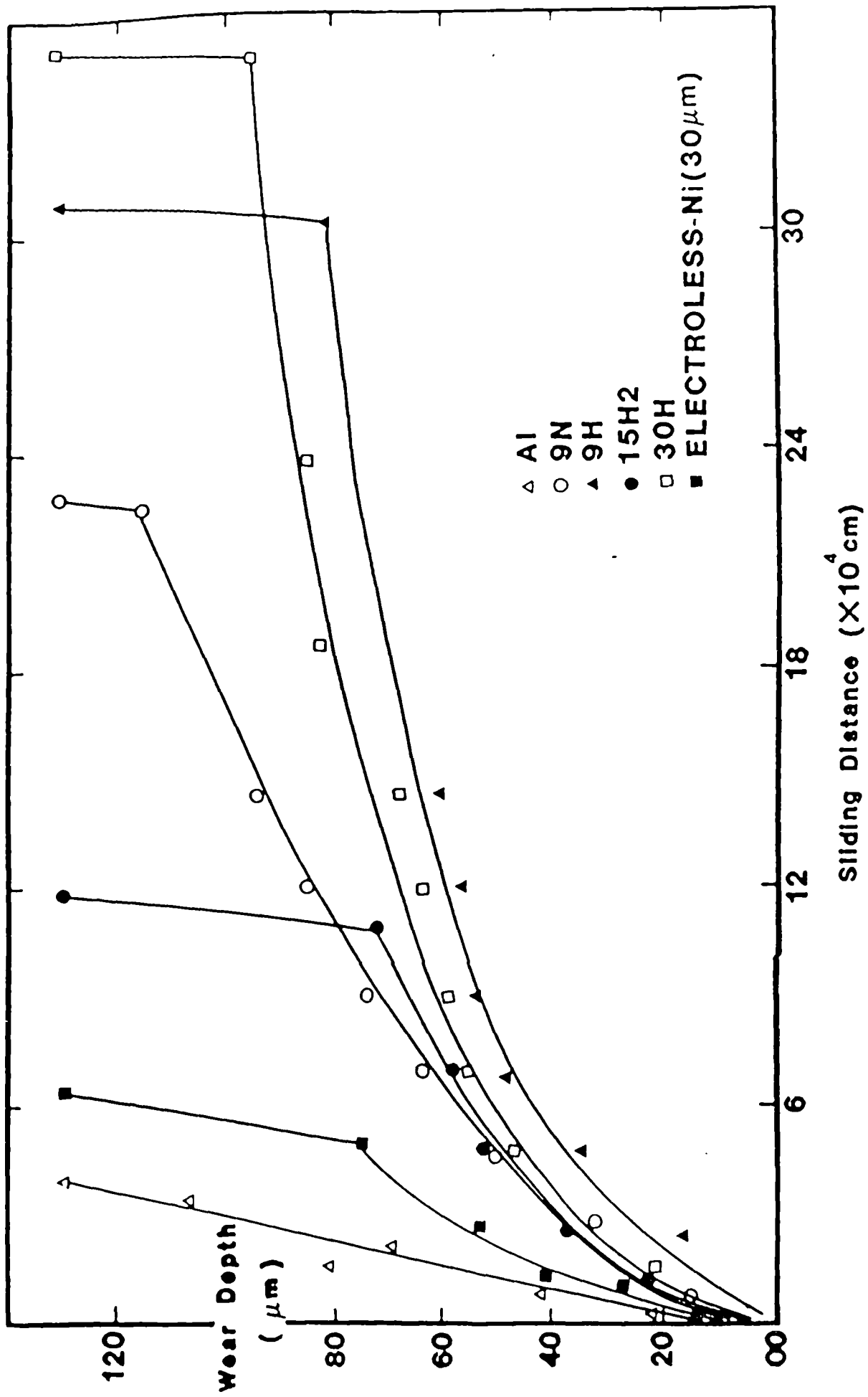


Fig.47 Dry adhesive wear of materials investigated at 10N against steel ball.

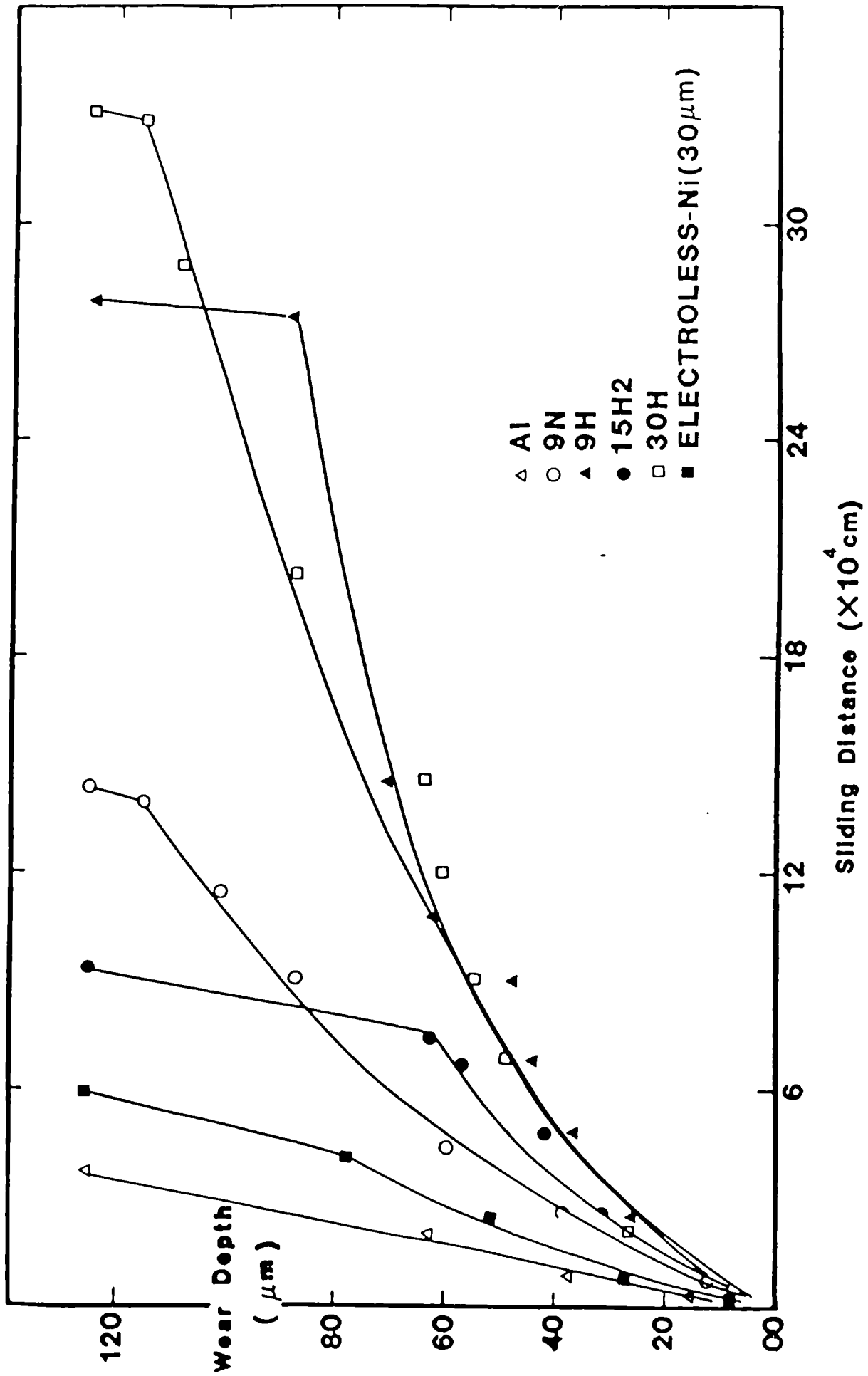


Fig.48 Dry adhesive wear of materials investigated at 15N against steel ball.

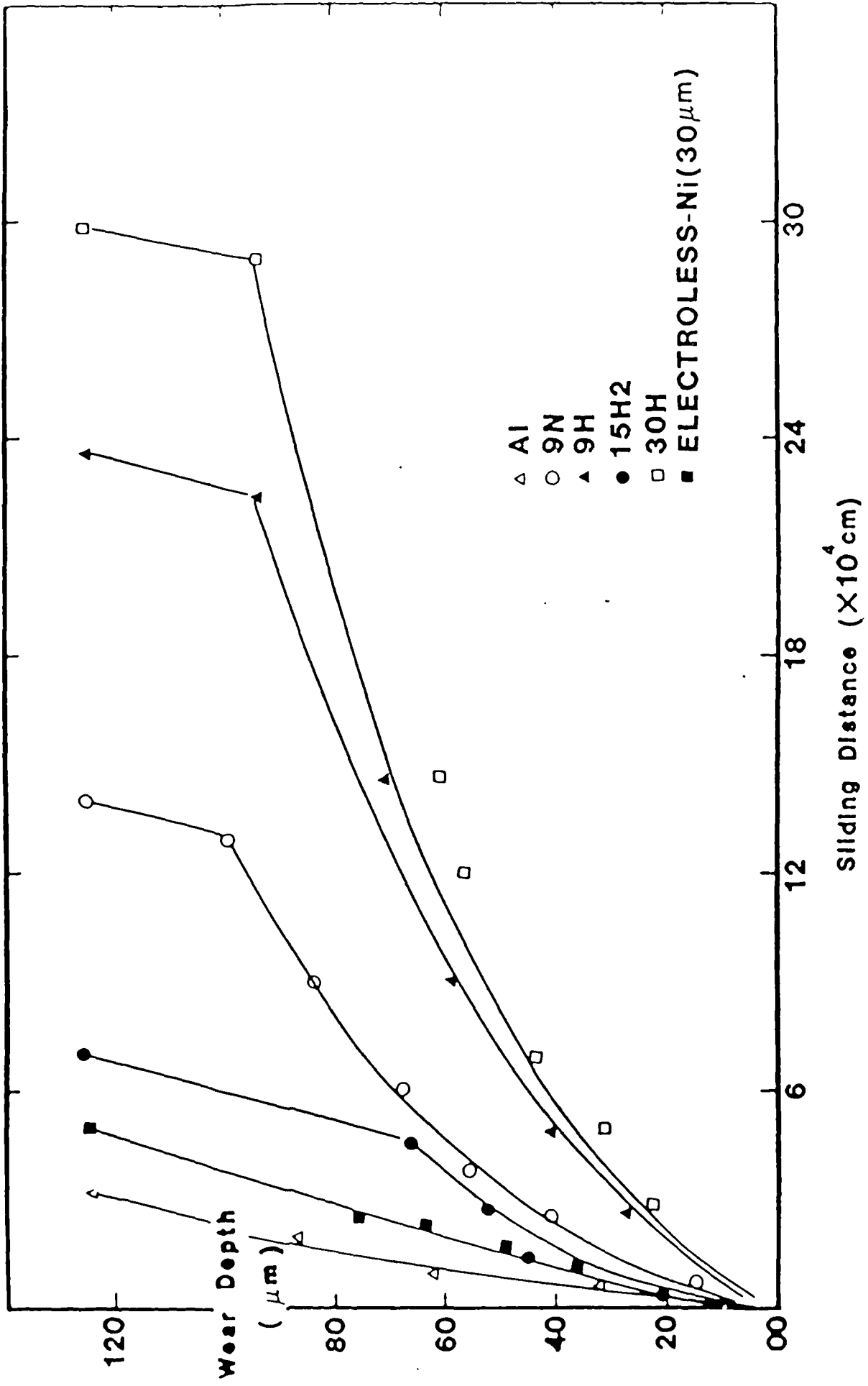


Fig.49 Dry adhesive wear of materials investigated at 20N against steel ball.

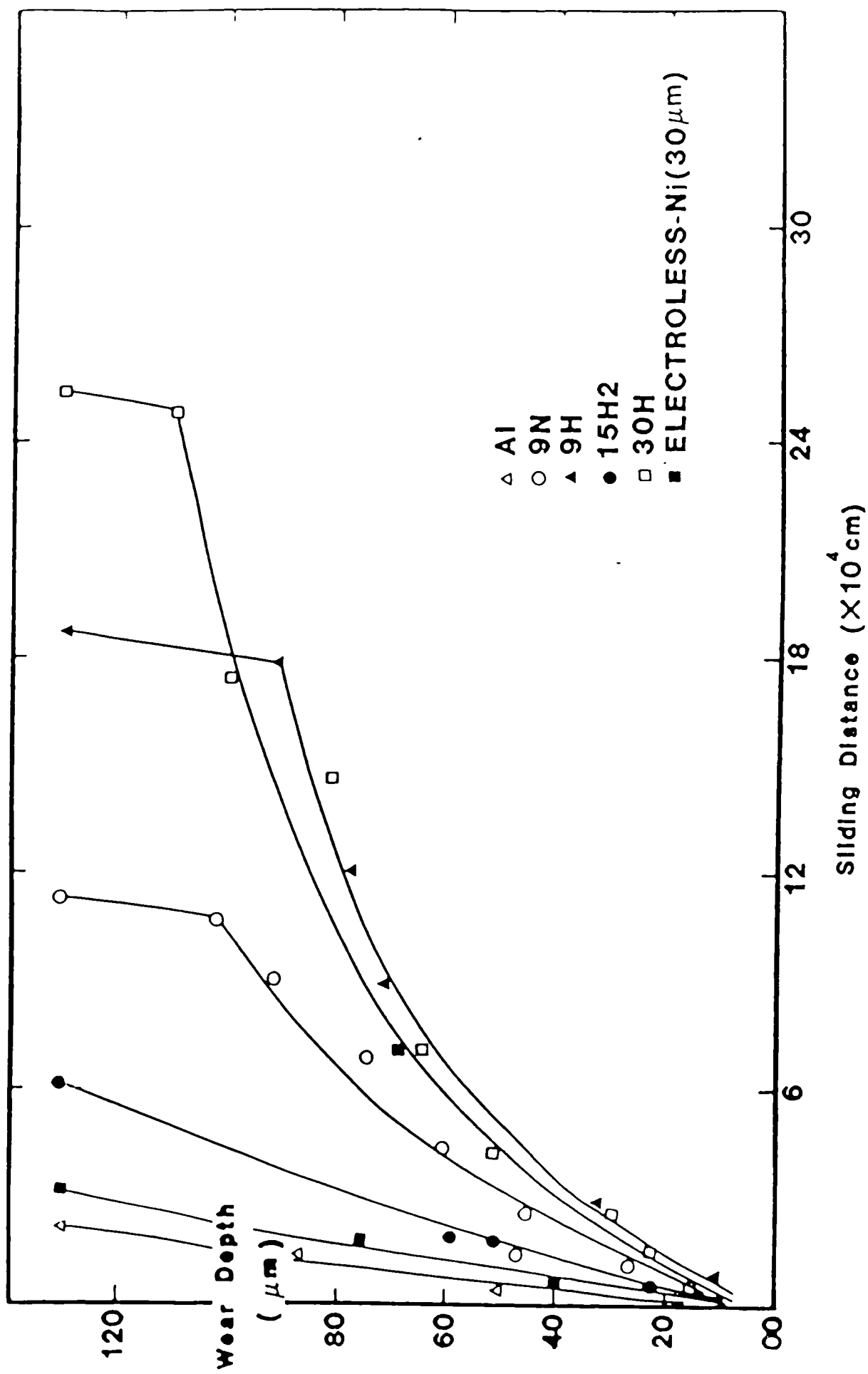


Fig.50 Dry adhesive wear of materials investigated at 25N against steel ball.

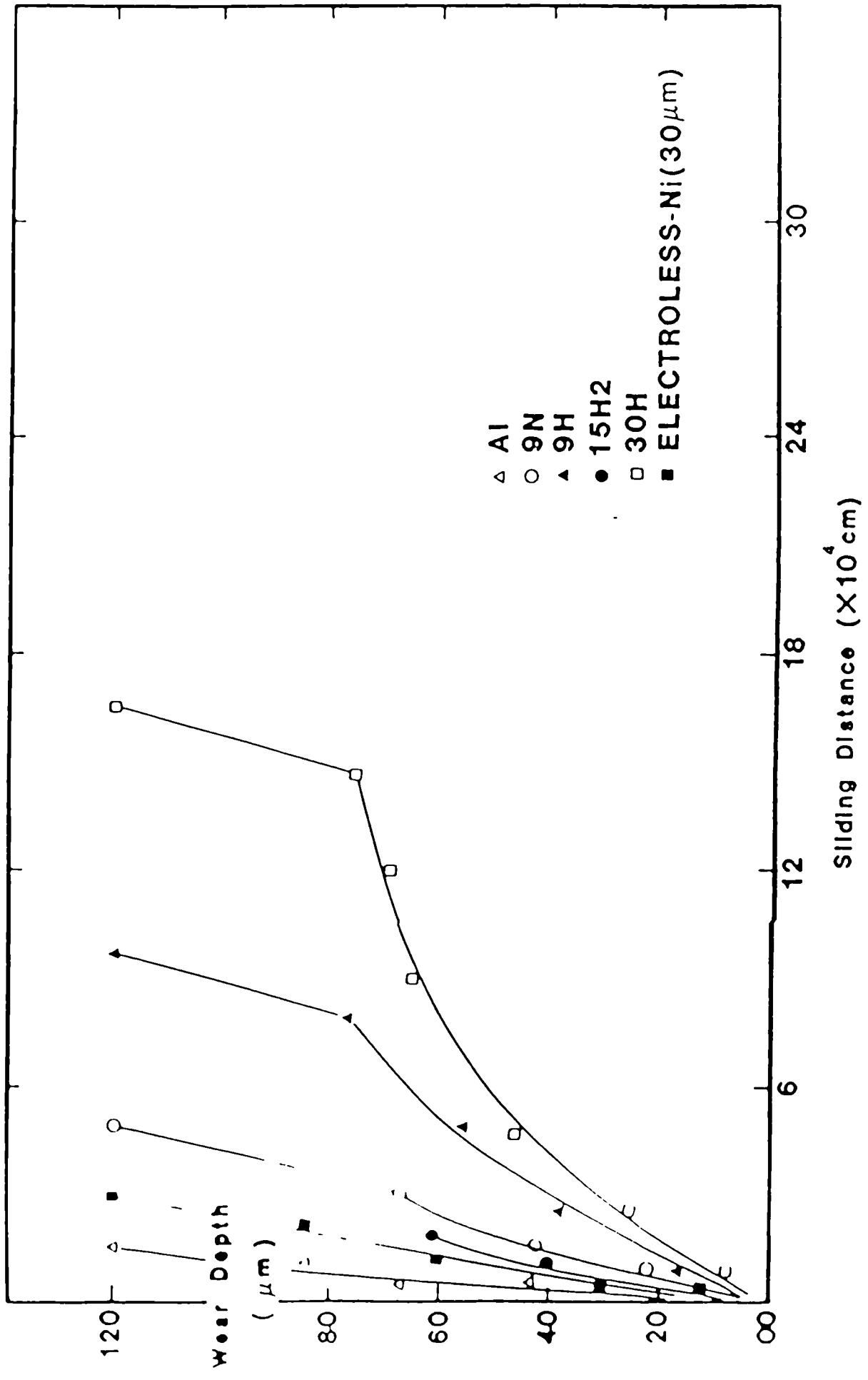


Fig.51 Dry adhesive wear of materials investigated at 30N against steel ball.

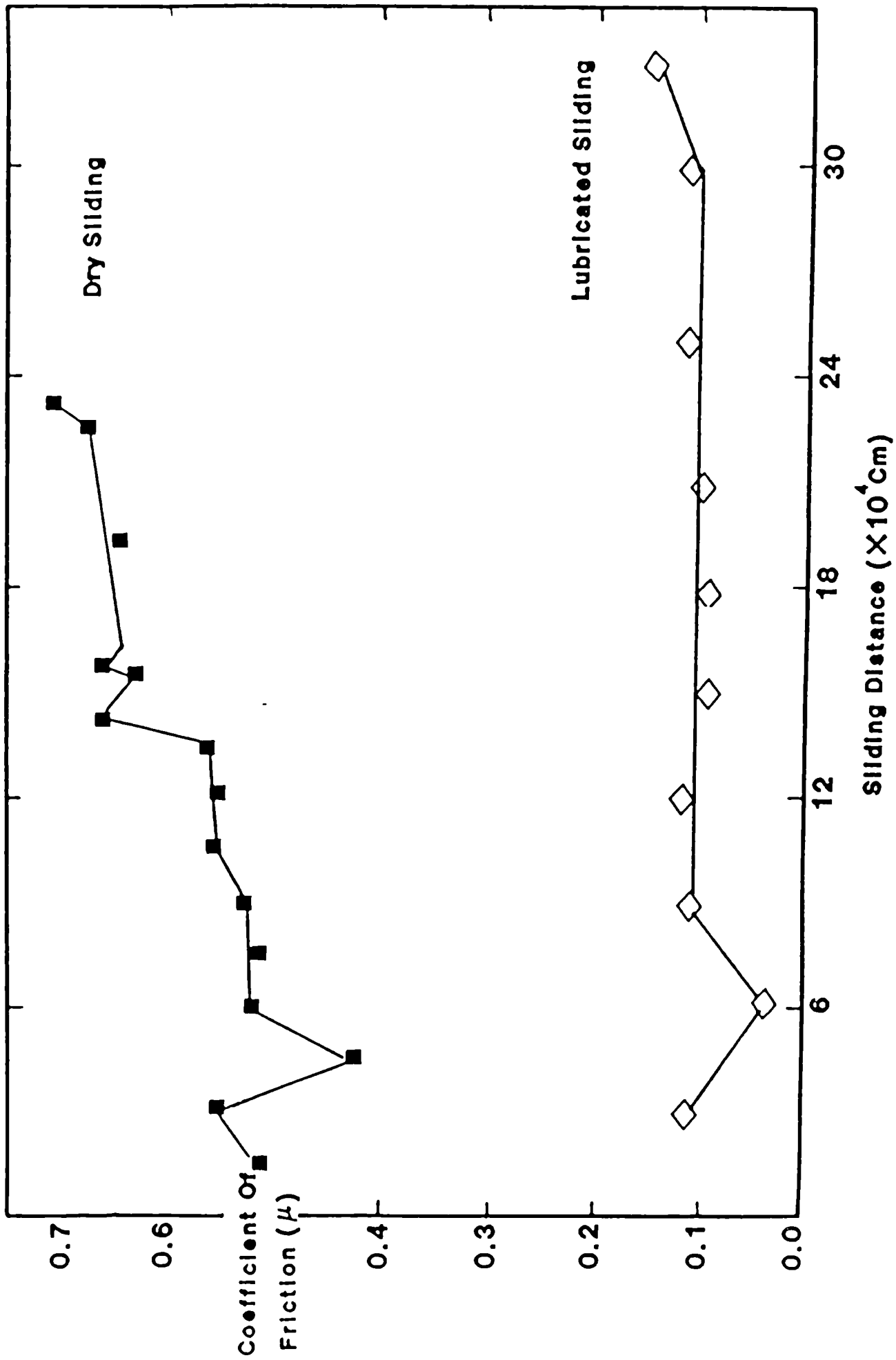


Fig.5.2 Coefficient of friction values of hard anodised alloy 9H against steel ball.

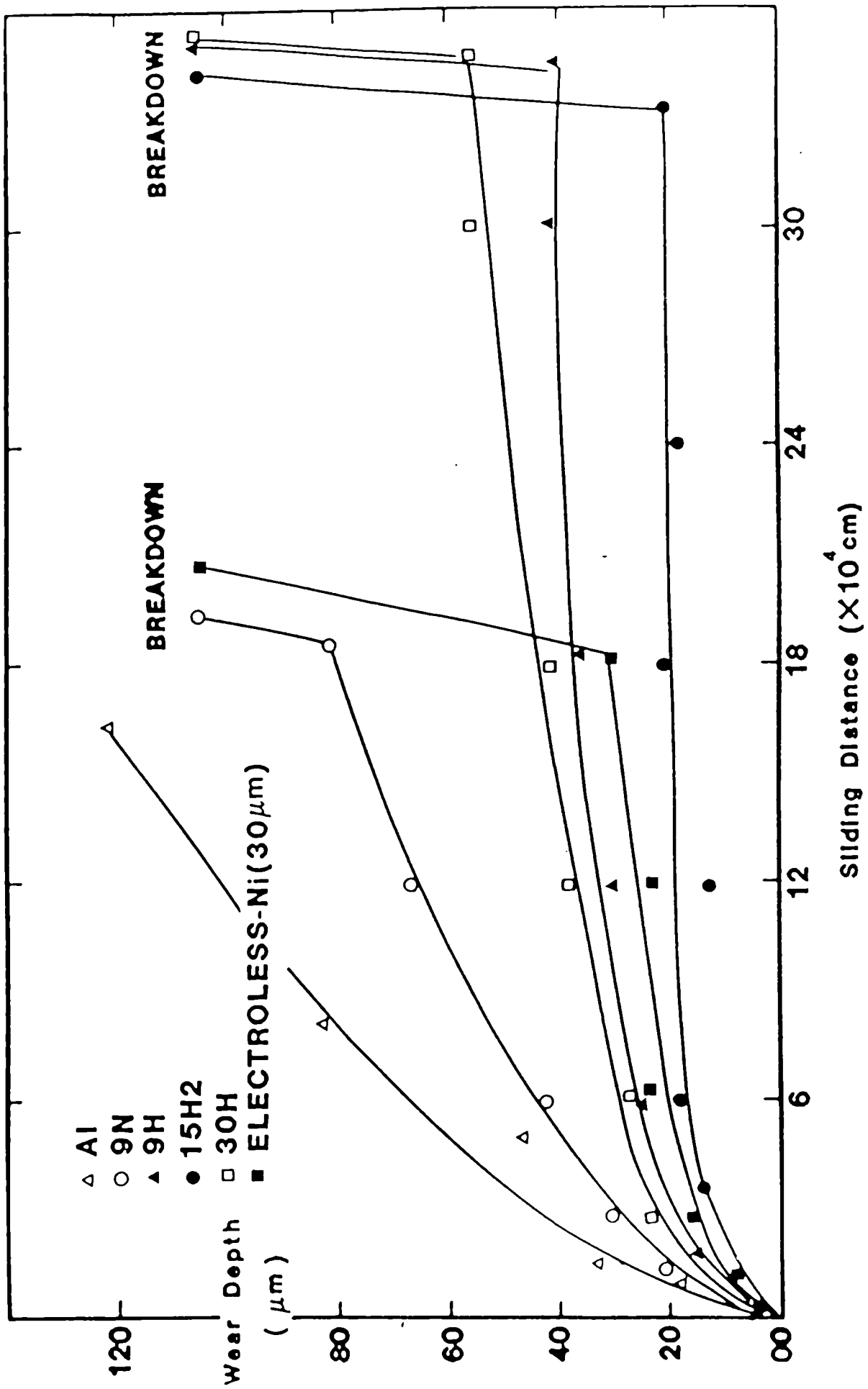


Fig.5.3 Lubricated adhesive wear of materials investigated at 20N against steel ball.

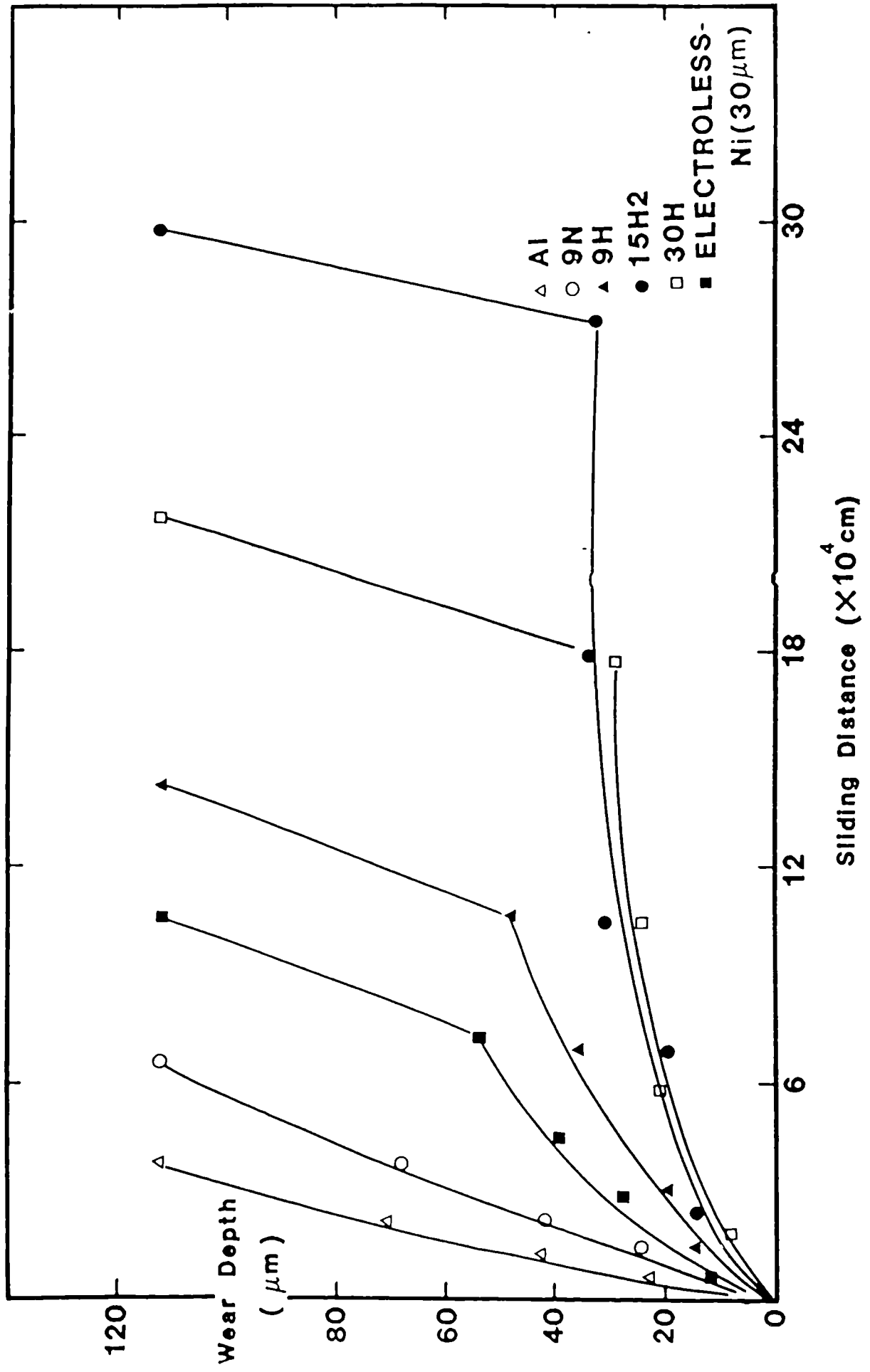


Fig.54 Lubricated adhesive wear of materials investigated at 40N against steel ball.

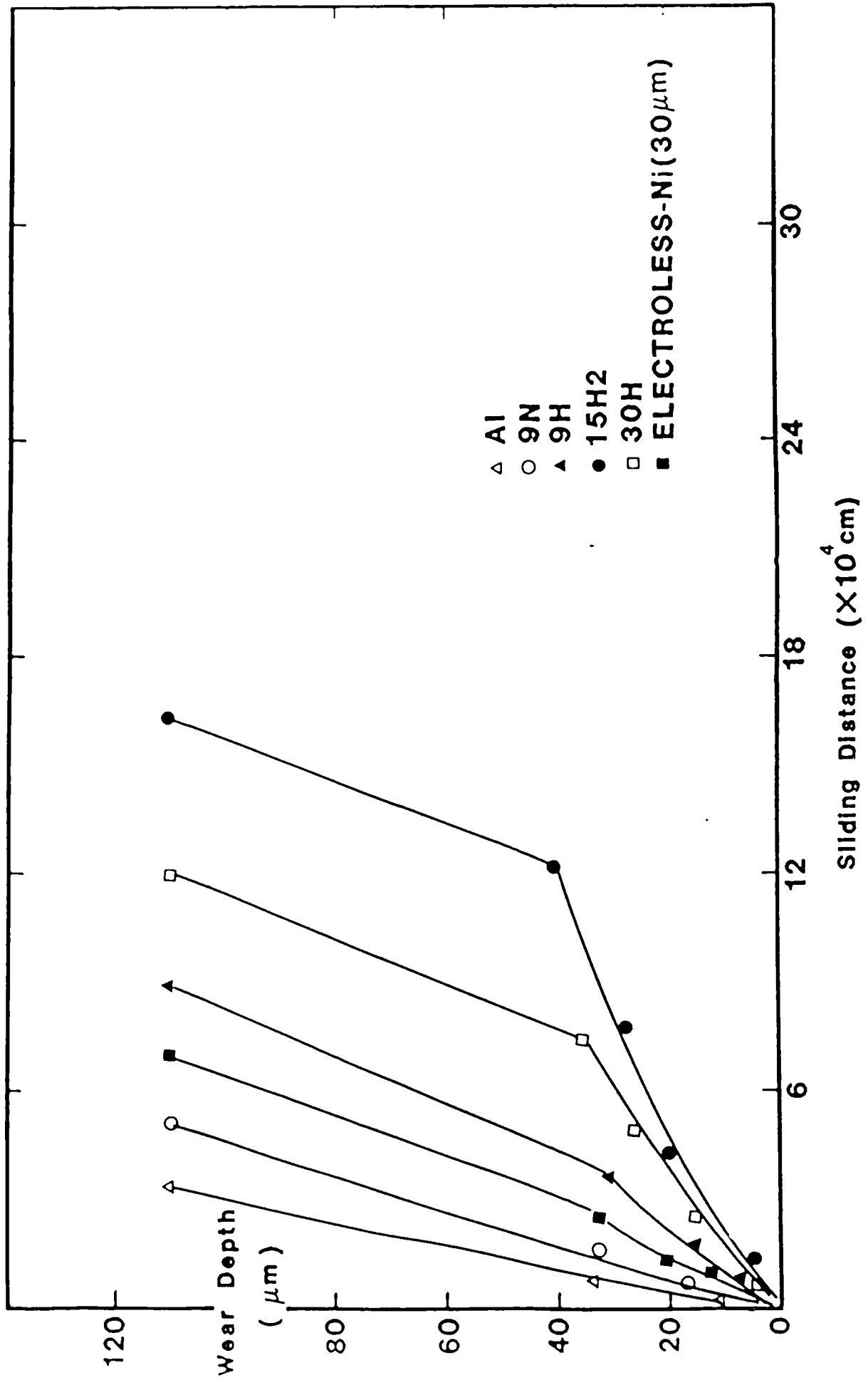


Fig.55 Lubricated adhesive wear of materials investigated at 60N against steel ball.

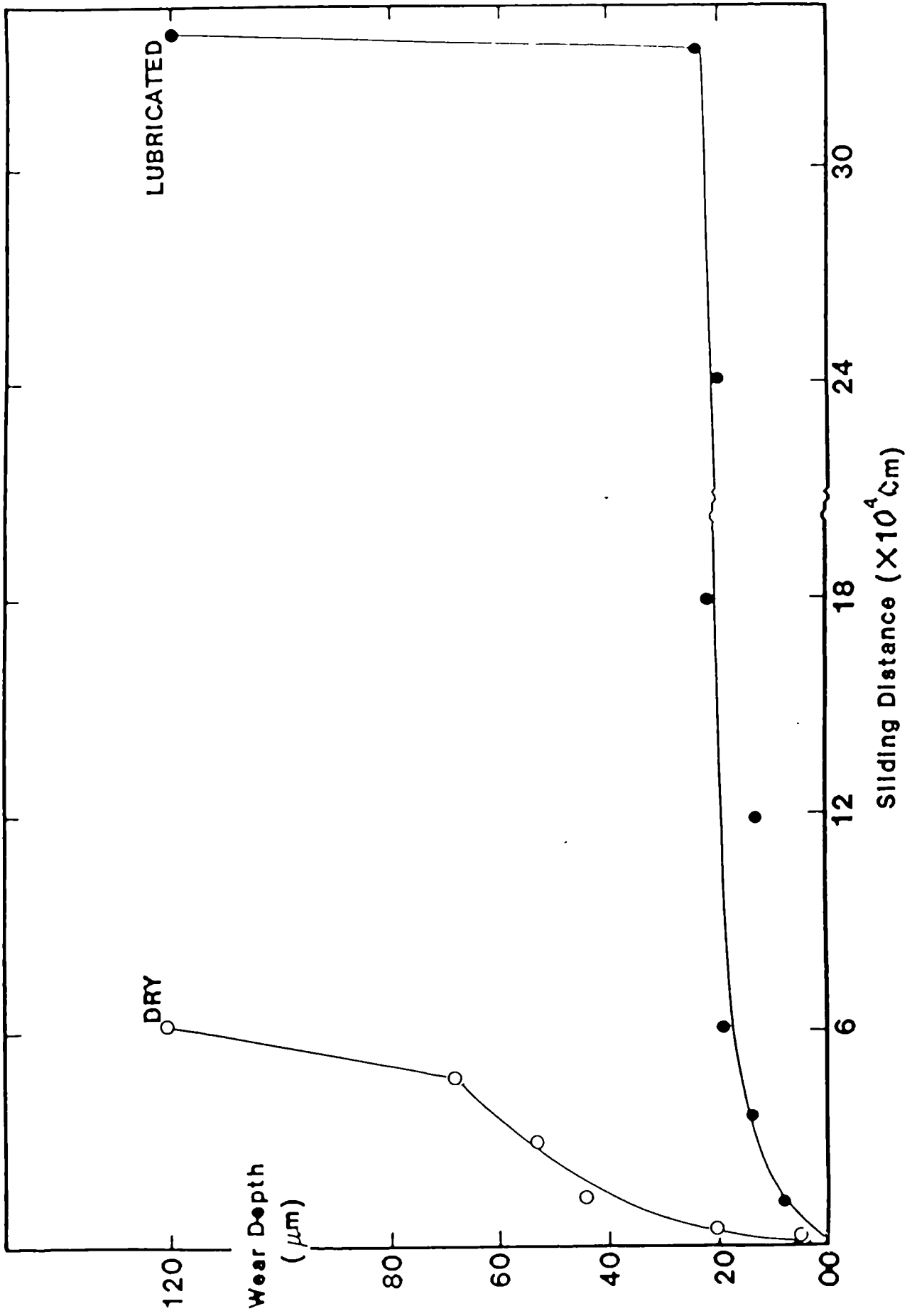


Fig.56 Adhesive wear of hard anodised 15H2, under dry and lubricated conditions, at 20N against steel ball

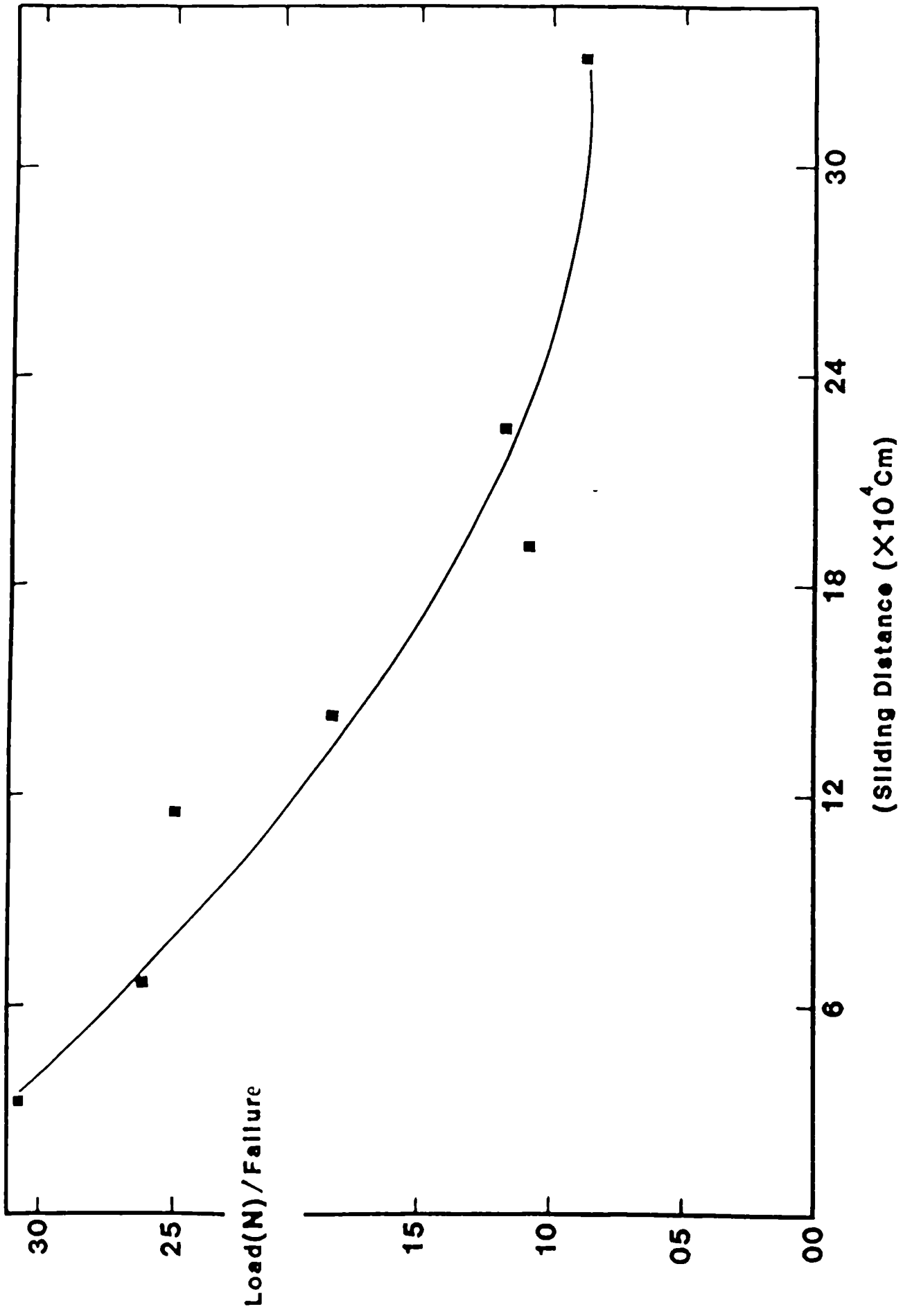


Fig.57 Relationship between load required to failure and sliding distance of anodised alloy 9H against steel ball.

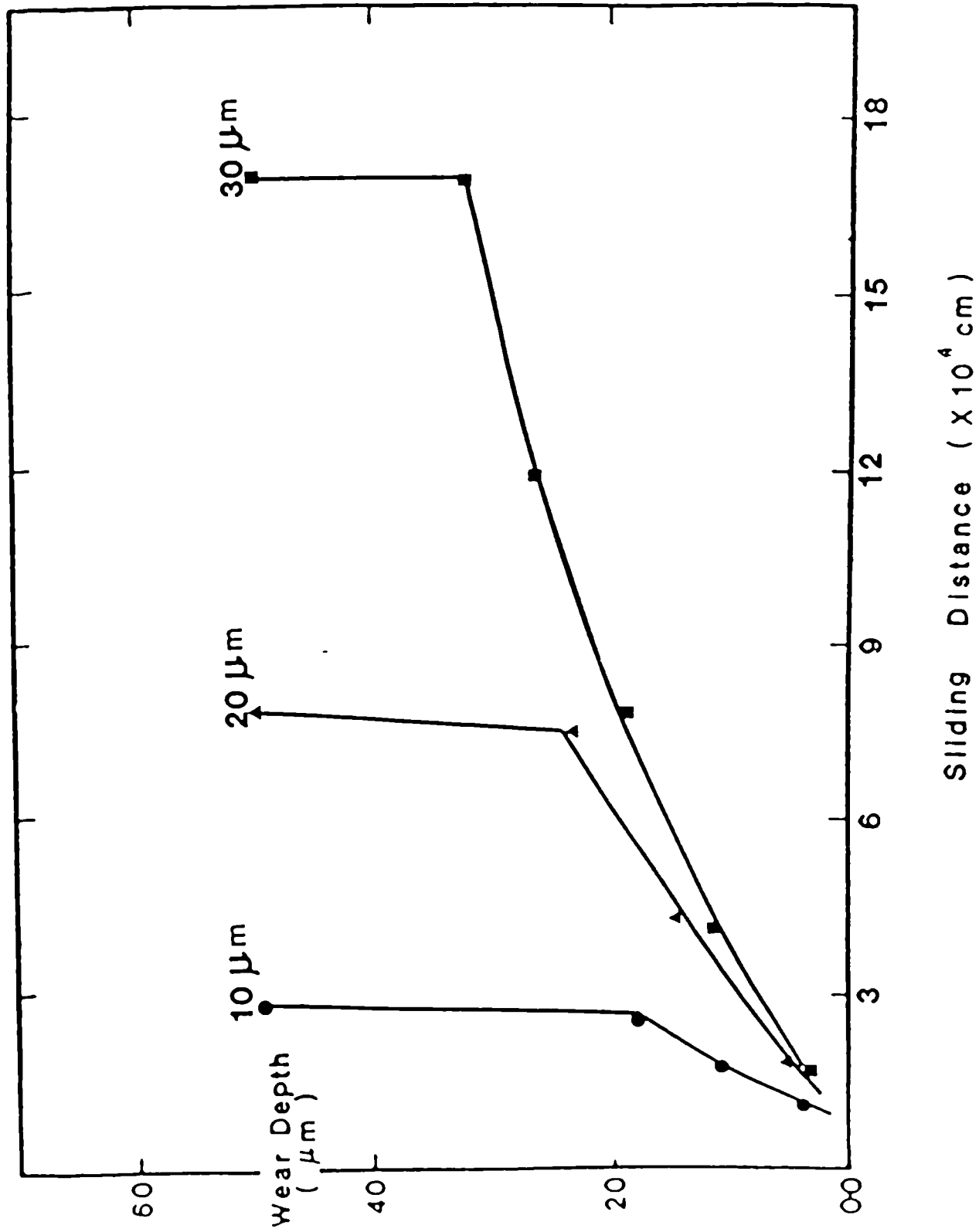
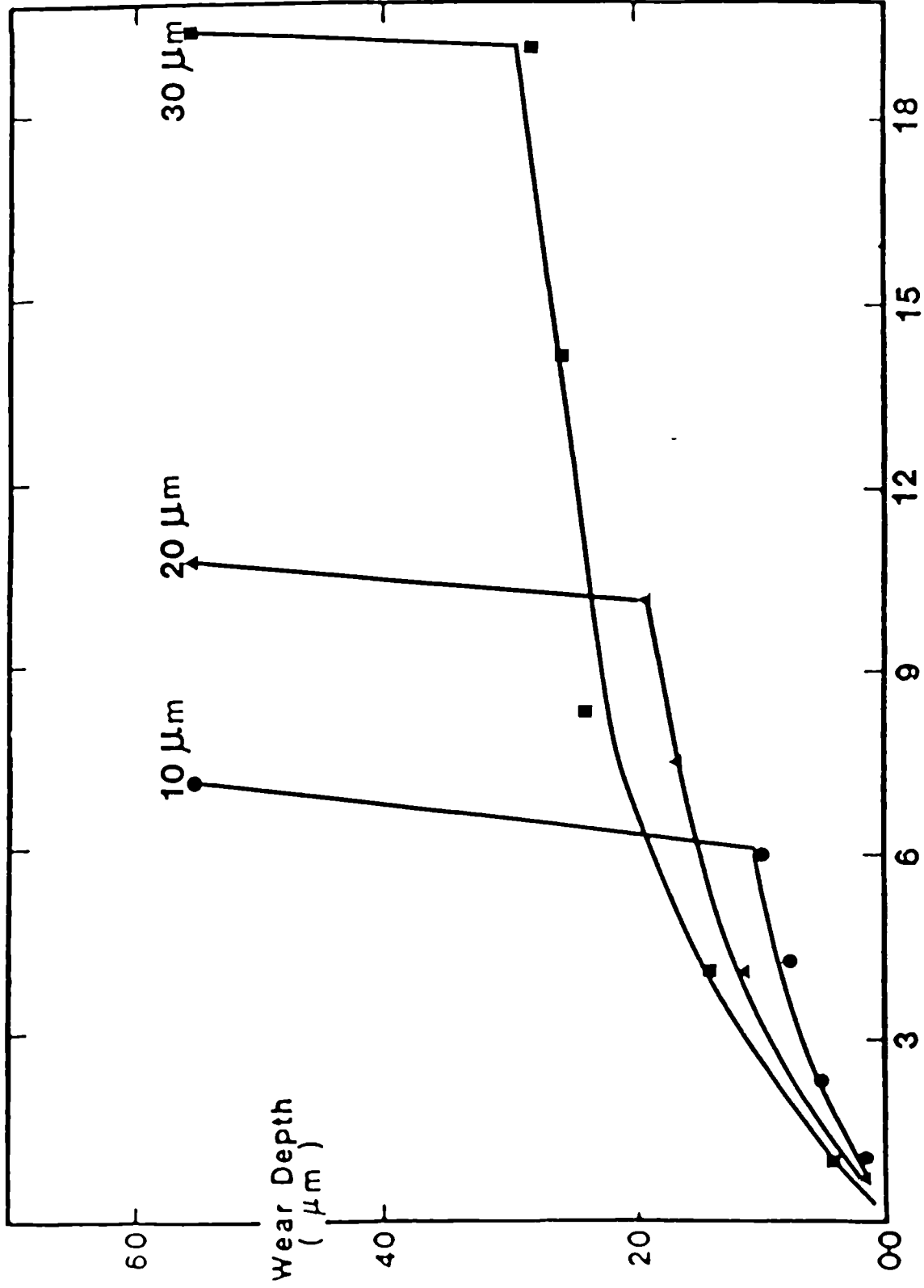


Fig.58 Dry adhesive wear of electroless nickel of different thicknesses at 5N against steel ball.



Sliding Distance (X 10⁴ cm)

Fig.59 Lubricated adhesive wear of electroless nickel of different thicknesses at 20N against steel ball.

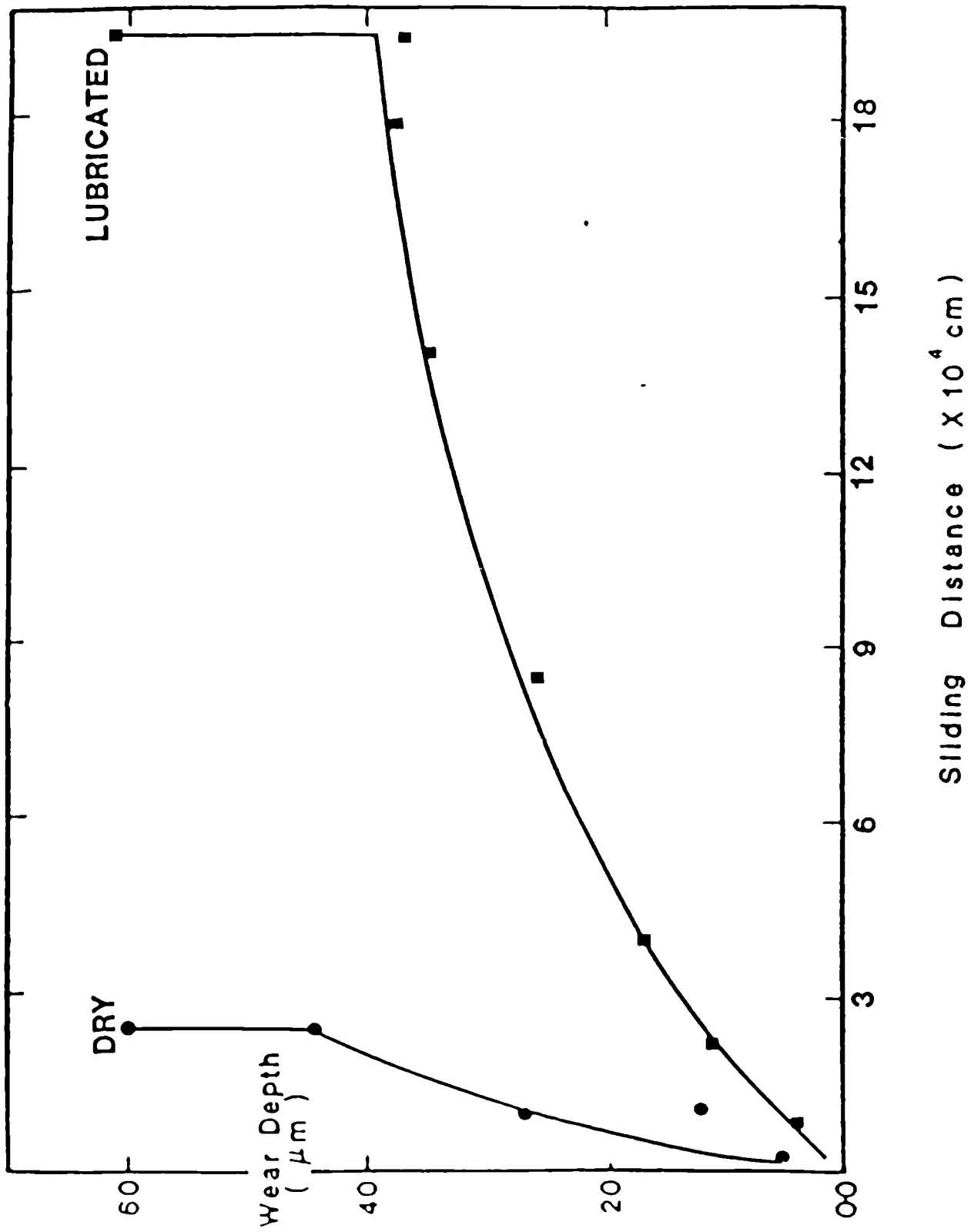


Fig.60 Dry and lubricated adhesive wear of electroless nickel coating of a 30 micron thickness at 20N against steel ball.

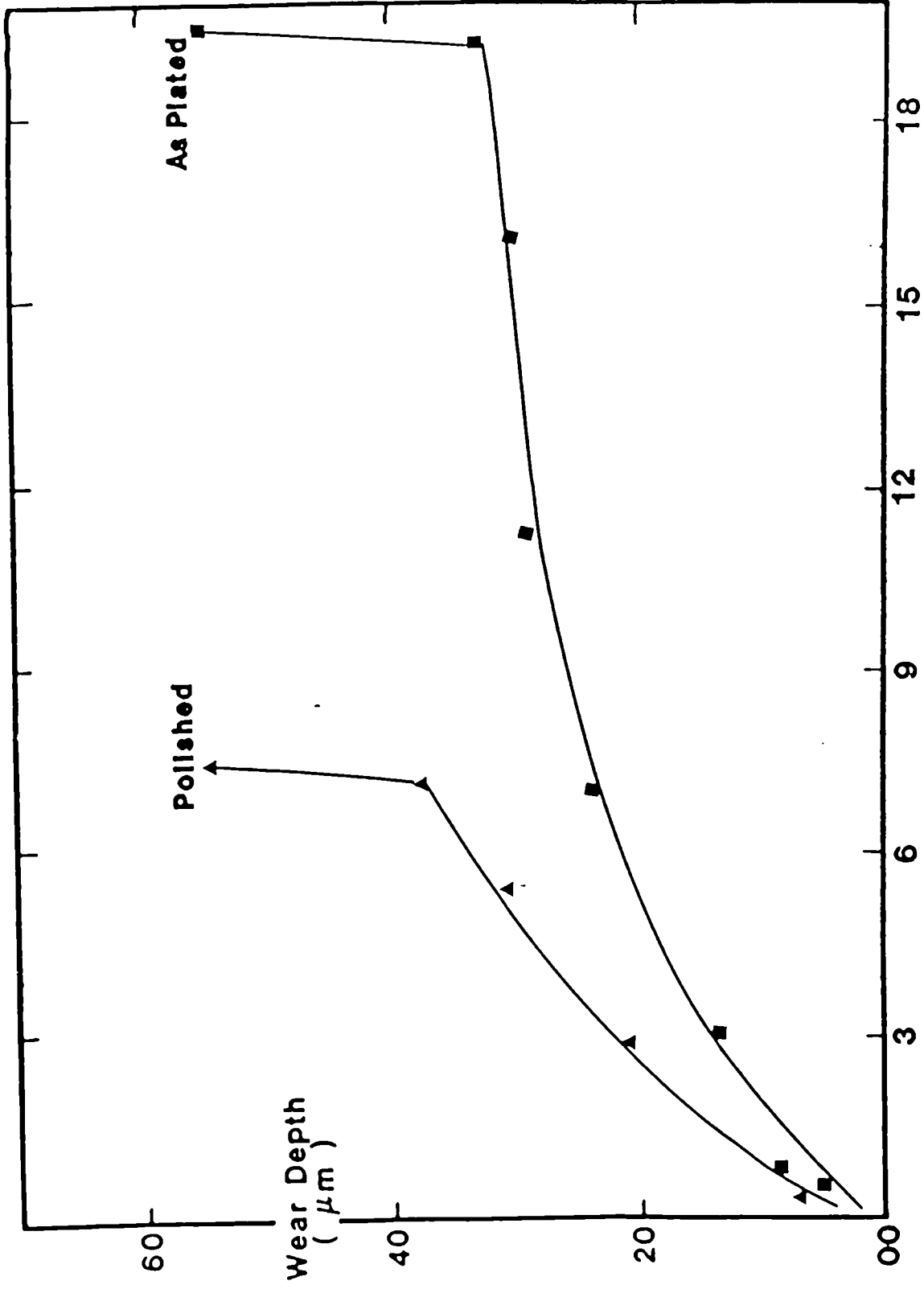


Fig.61 Lubricated adhesive wear of 30 micron thickness of electroless nickel at 20N in the as-plated and polished conditions against steel ball.

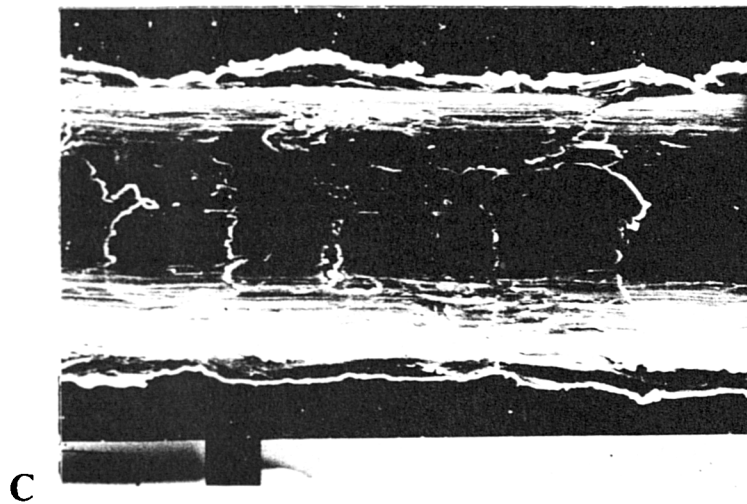
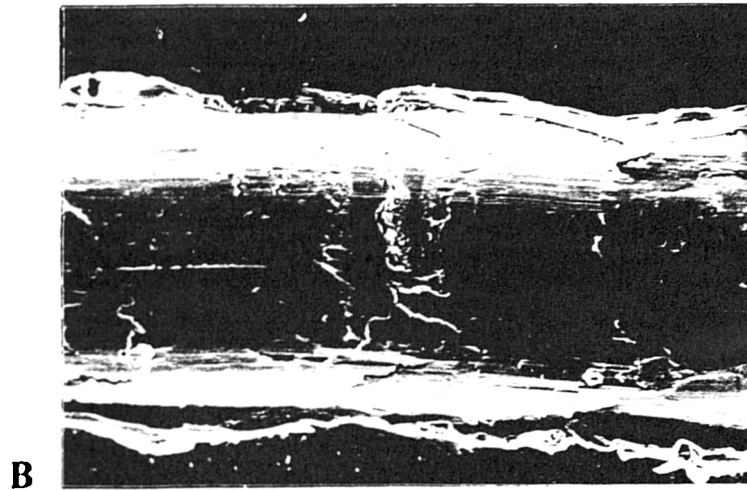
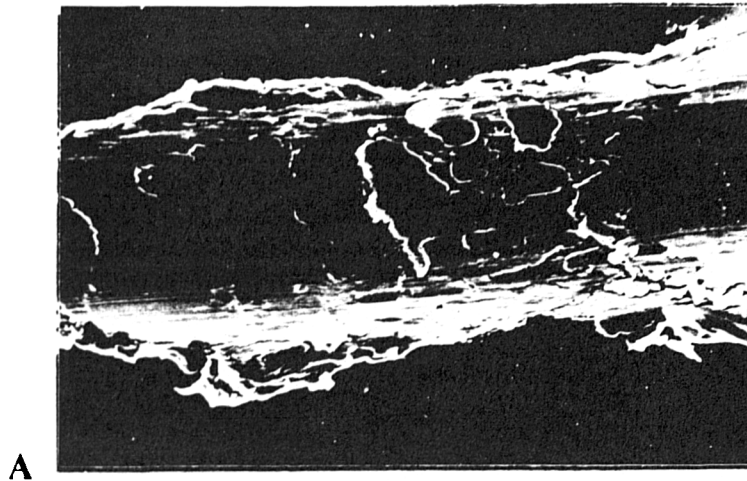
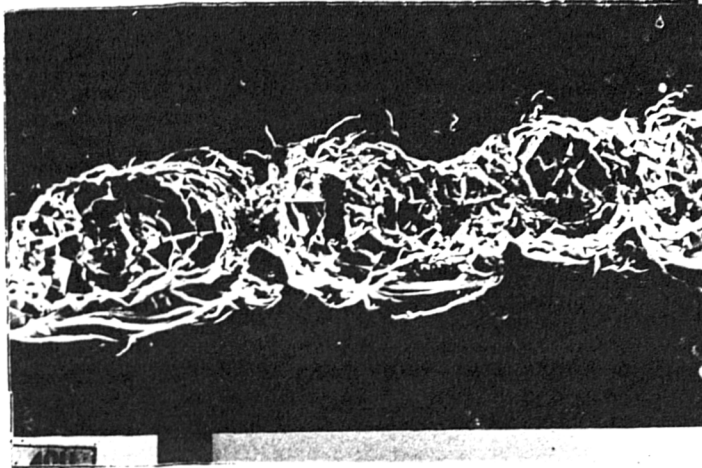
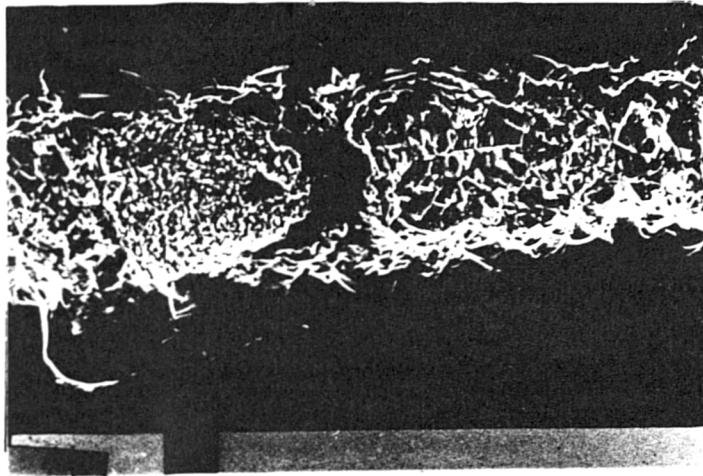


Fig.62 Surface appearance of abrasive wear of uncoated aluminium alloy 6030 at

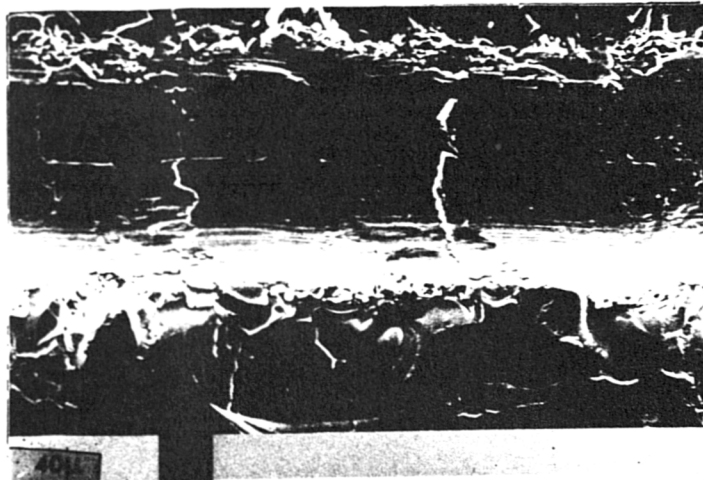
- A)** 1N, 50 passes
- B)** 1N, 100 passes
- C)** 2N, 100 passes



A



B



C

Fig.63 S.E.M. micrograph illustrates

- A) an early breakdown of the natural anodised aluminium alloy 9N
- B) development of damage outside the wear track
- C) complete removal of the coating

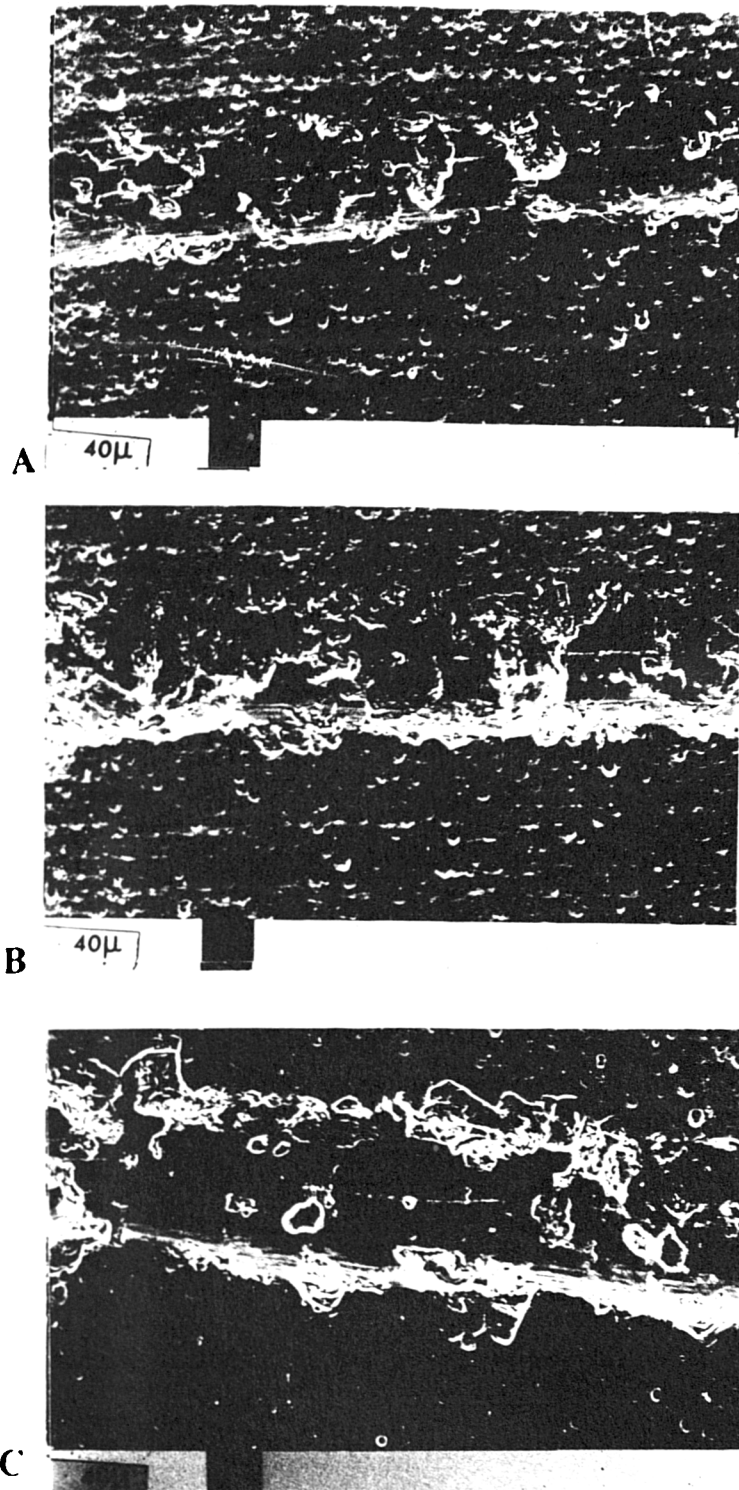
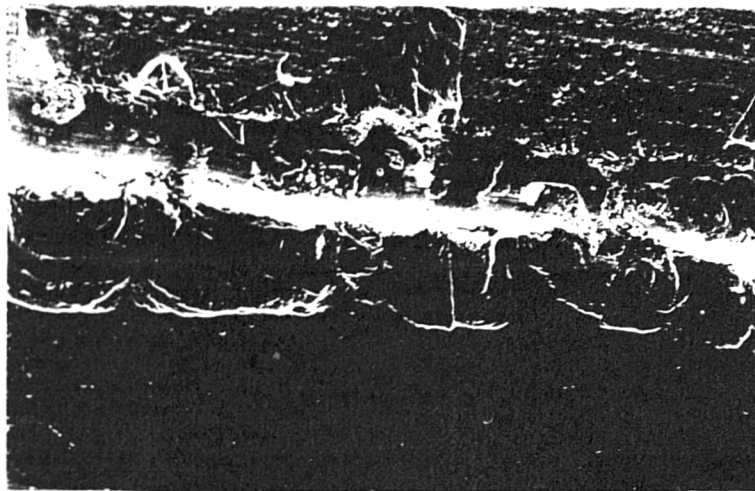


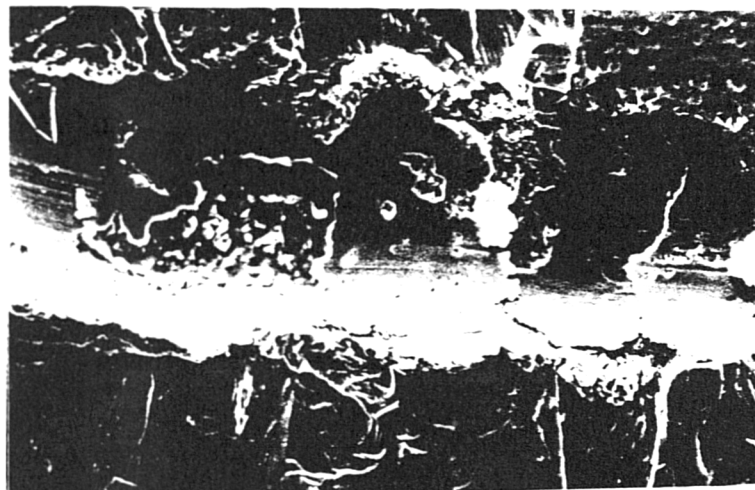
Fig.64 Surface appearance of the hard anodised 9H alloy illustrates

- A)** Plastic deformation
- B,C)** Initiation and propagation of damage outside the wear track.



100μ

A



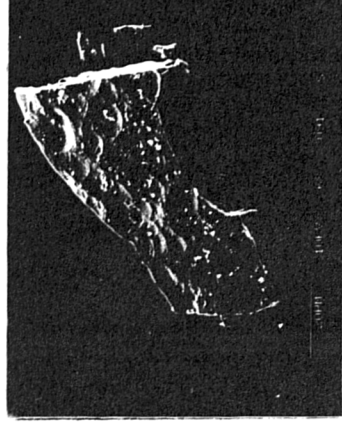
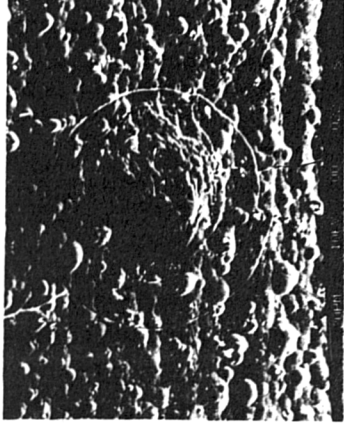
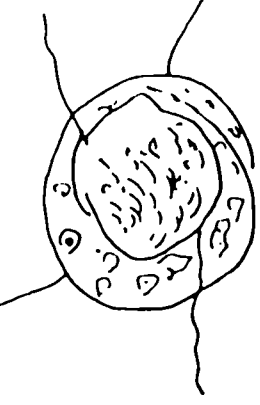
40μ

B

Fig.65

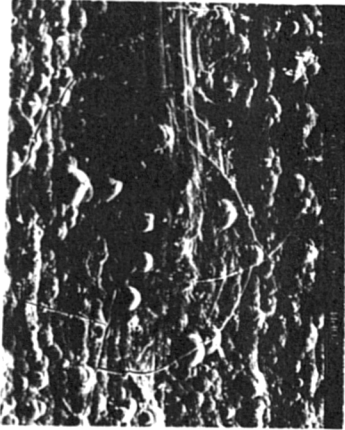
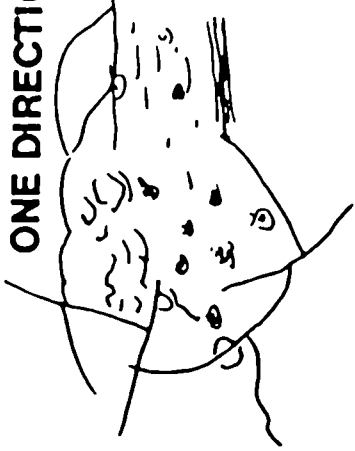
- A) Abrasive wear of hard anodised 9H at 3N, 100 passes showing failure of the wear track edges.
- B) Inside the wear track at high magnification.

STATIC LOADING



RECOVERED DEBRIS

SINGLE PASS, ONE DIRECTION



MULTIPASSES

WEAR DIRECTION

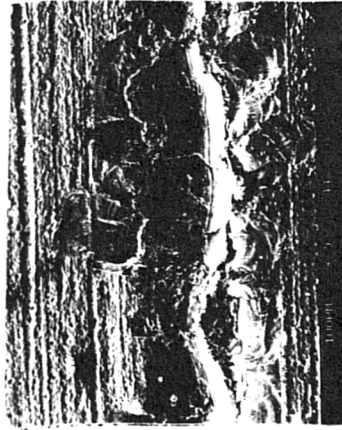


Fig.66 Illustrates the sequence of events in abrasive wear of hard anodised alloy 9H.

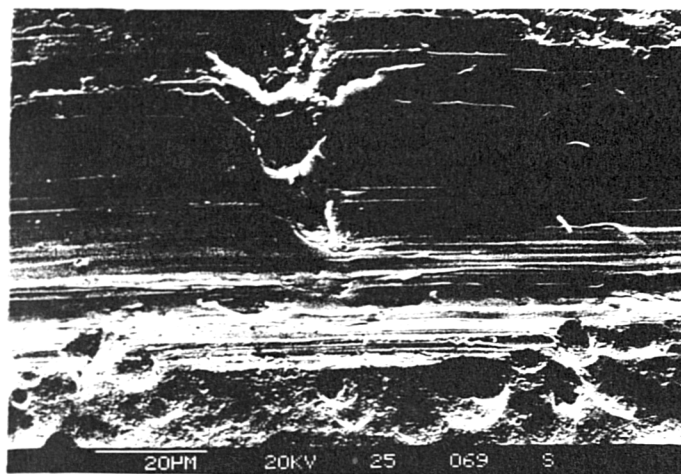
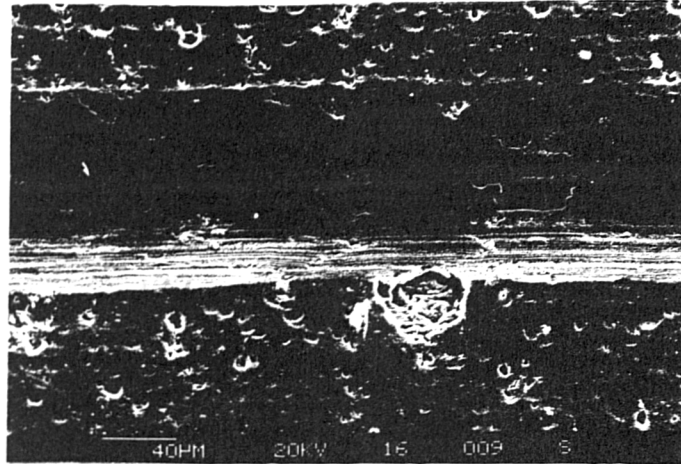


Fig.67 Abrasive wear of anodised alloy 15H2 illustrates the domination of plastic deformation.

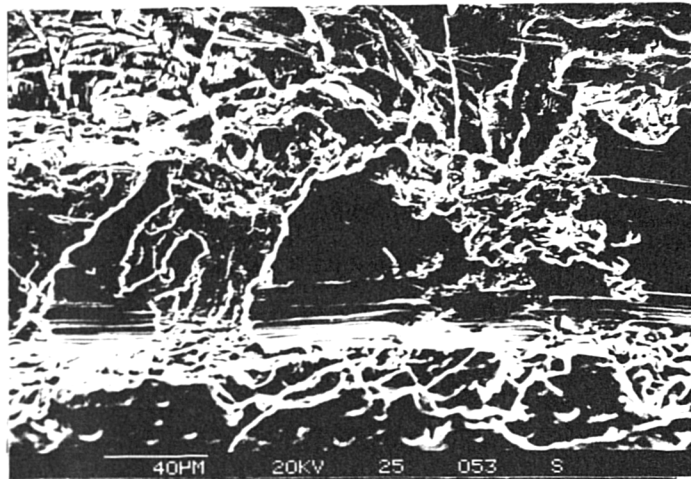
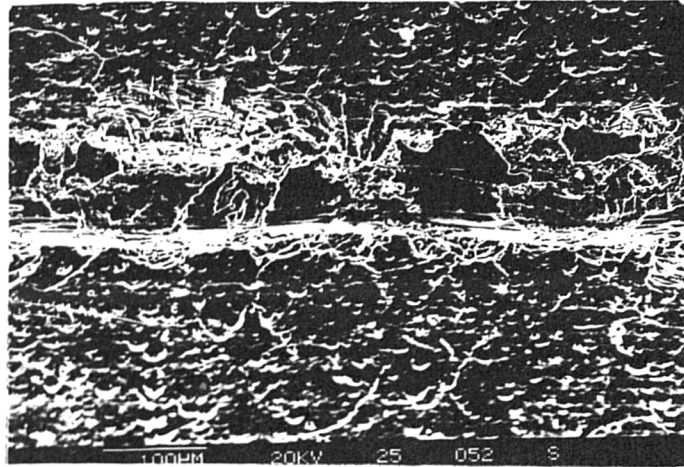
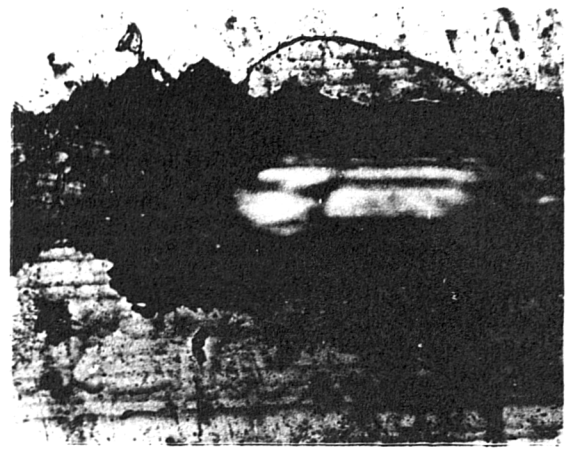


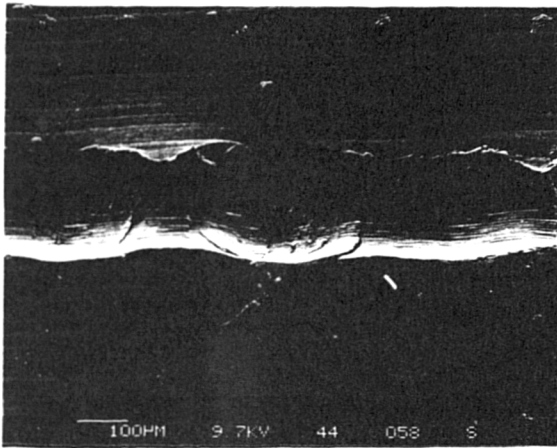
Fig.68 Abrasive wear of hard anodised alloy 30H illustrates the domination of plastic deformation.



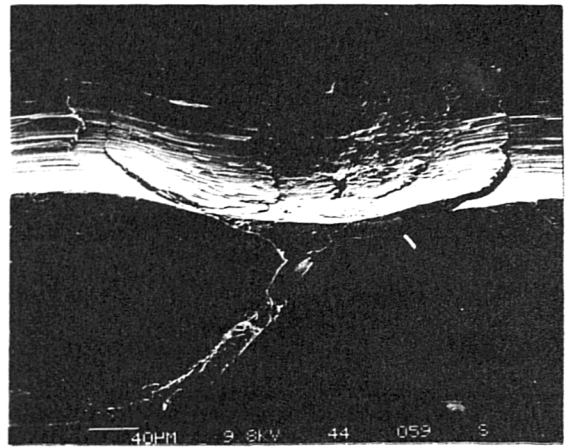
200 μ



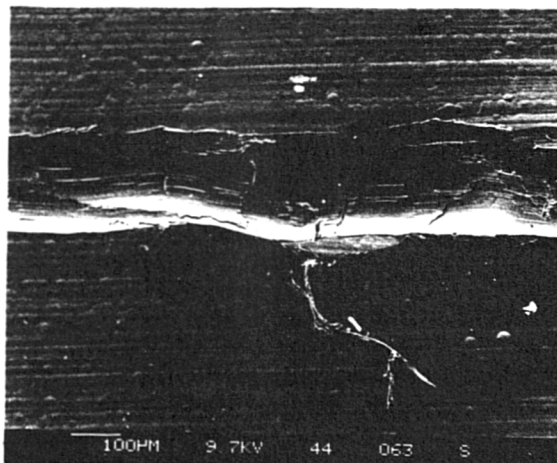
40 μ



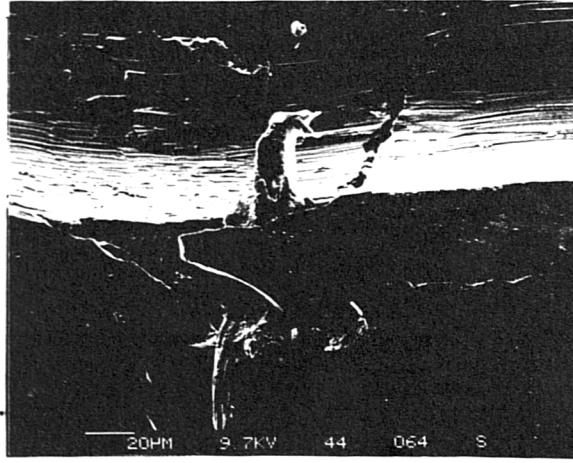
100PM 9.7KV 44 058 S



40PM 9.8KV 44 059 S



100PM 9.7KV 44 063 S



20PM 9.7KV 44 064 S

Fig.69 Abrasive wear of electroless nickel of a 30 micron thickness shows the initiation and propagation of lateral cracks and material lifts off the surface outside the wear track.

L.C : LATERAL CRACK

M.C : MEDIAN CRACK

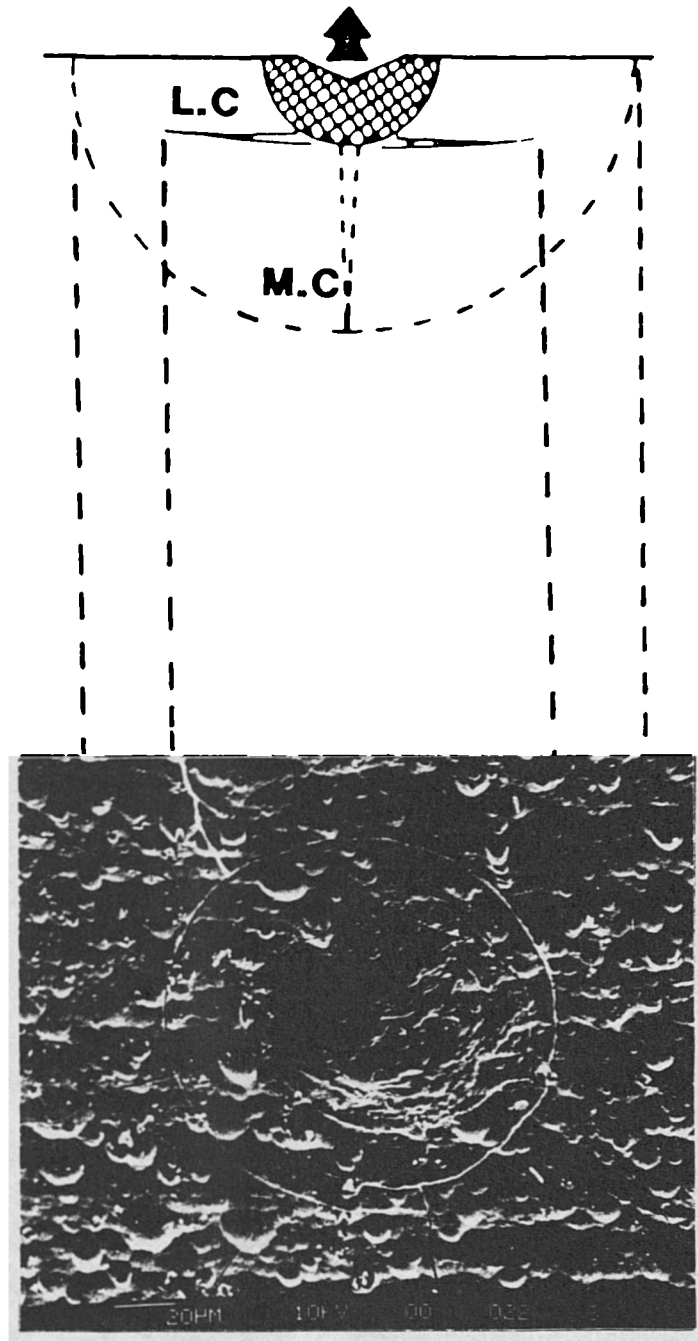


Fig.70 Schematic and S.E.M. representation of the development of lateral, and median cracks, under static loading of anodised alloy 9H.

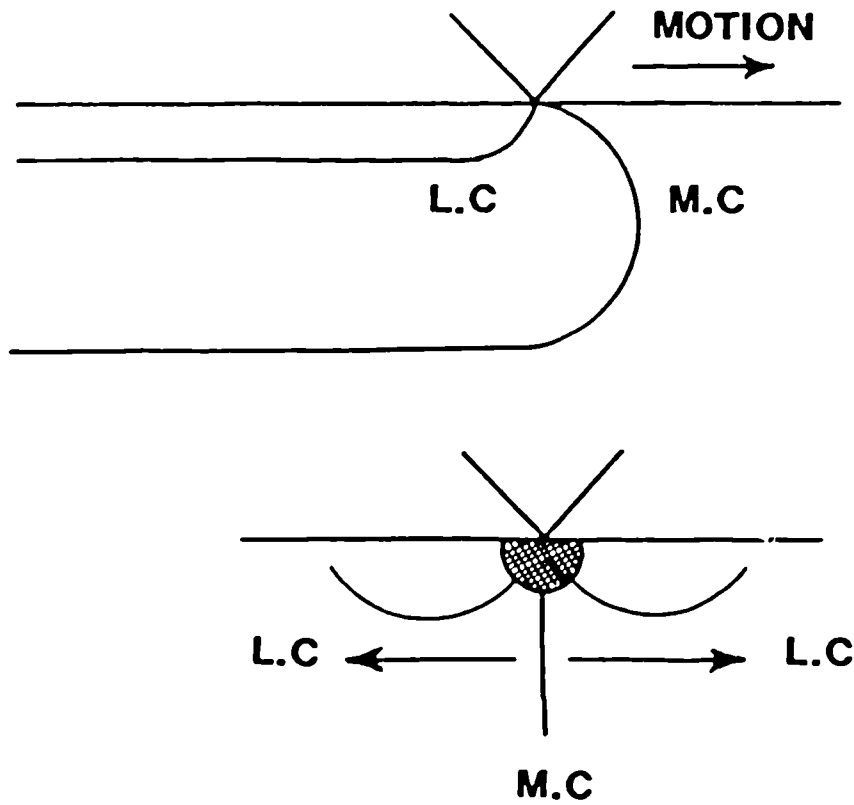


Fig.71 Schematic representation of the crack path under abrasive wear.

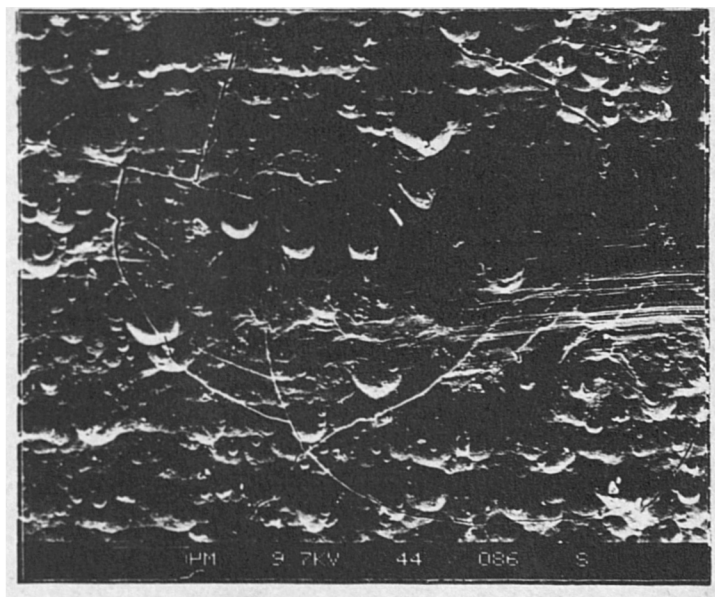
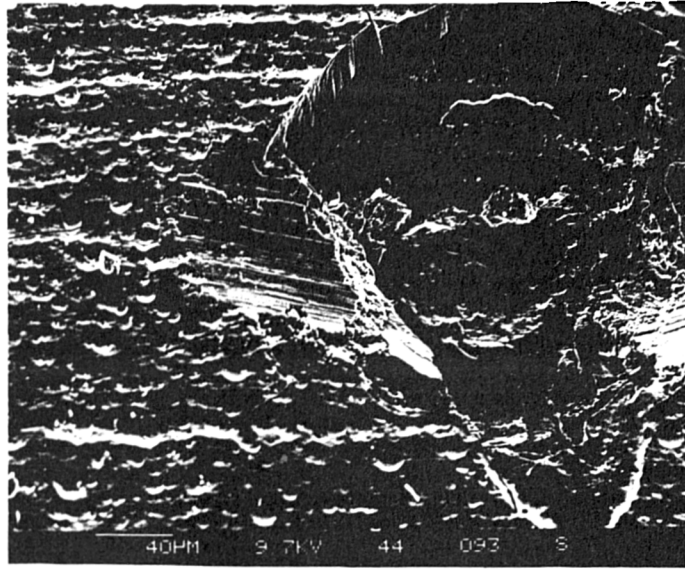
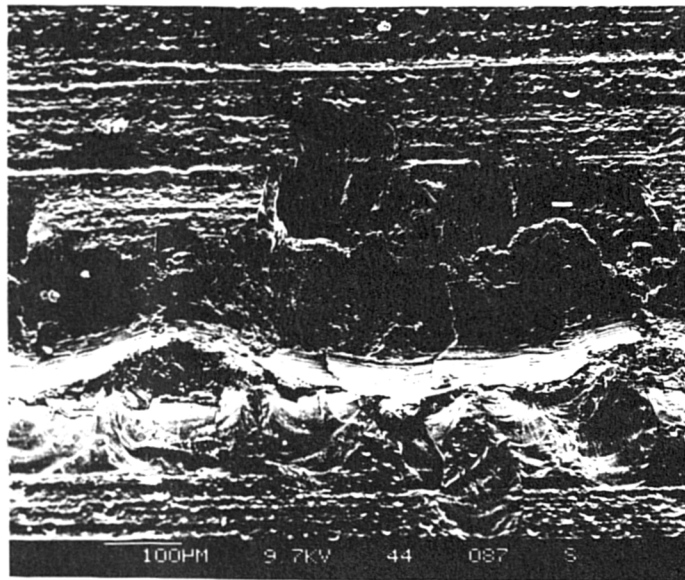


Fig.72 An S.E.M. micrograph illustrates the lateral and median cracks for a single unidirectional abrasive wear pass of anodised alloy 9H.



A



B

Fig.73 Material has been removed from the surface outside the wear track of anodised alloy 9H under a reciprocating movement

- A)** the end of the wear track.
- B)** the middle of the wear track.

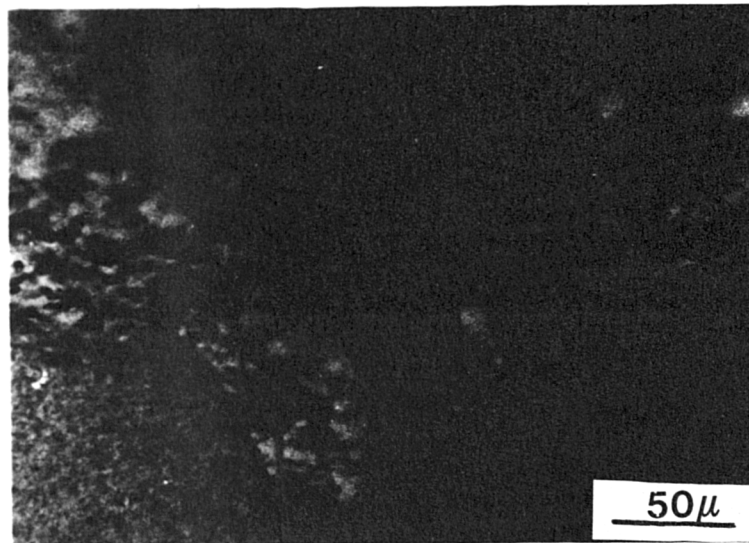
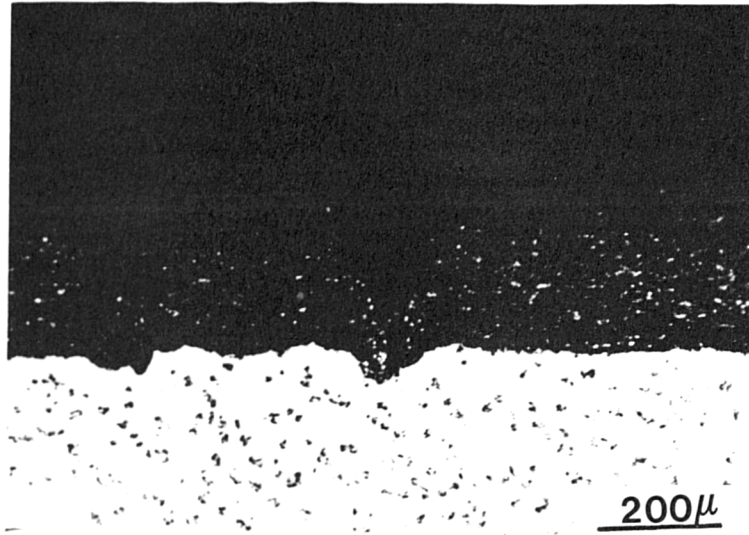
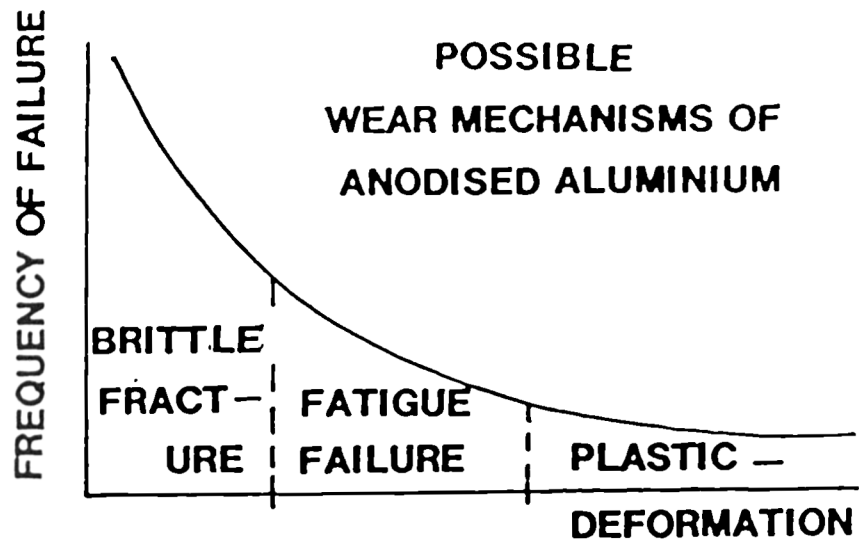


Fig.74 Taper section illustrates the extent of damage at the subsurface of anodised alloy 9H under abrasive wear.



SOURCE OF STRESSES

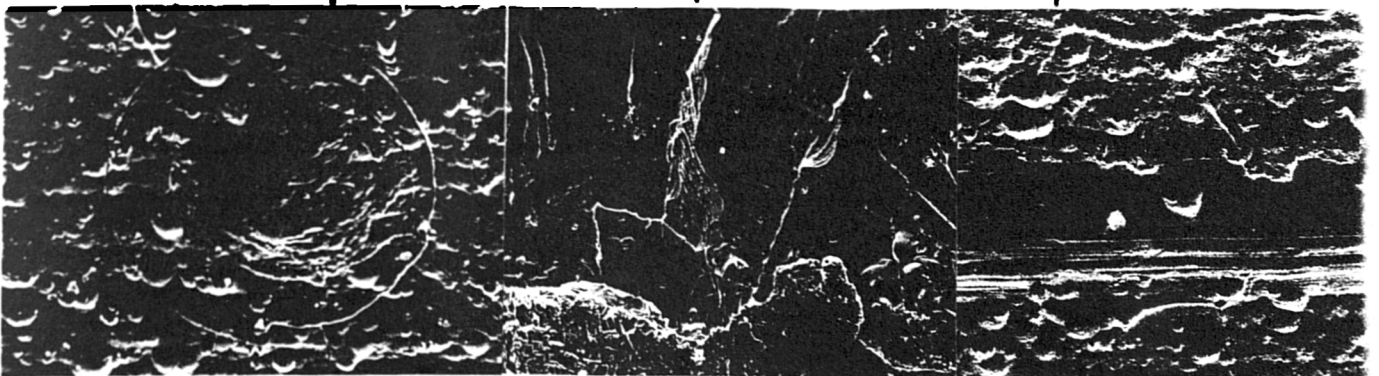
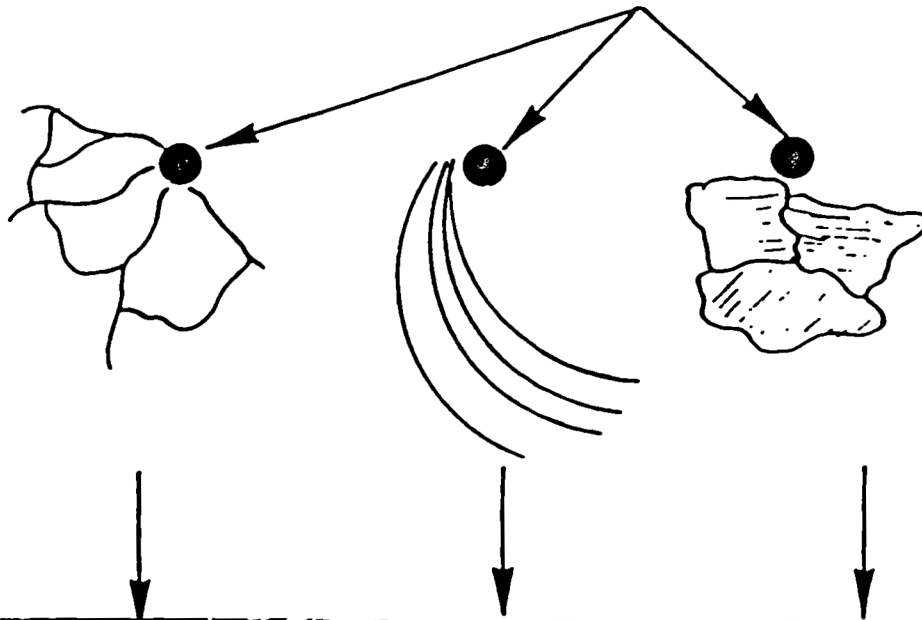


Fig.75 Illustrates the major mechanisms of abrasive wear encountered by anodised aluminium alloys.

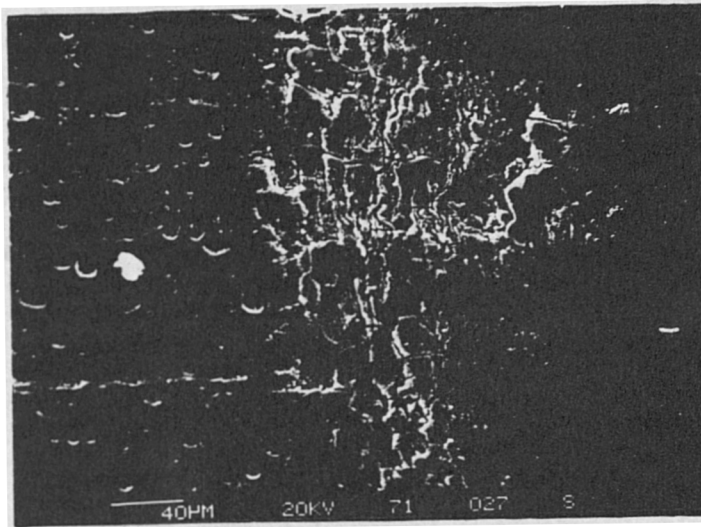
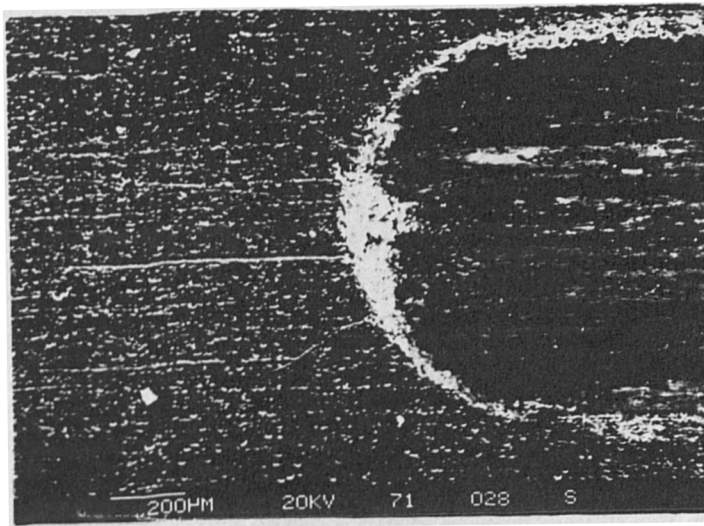


Fig.76 Surface appearance of hard anodised alloy 9H at the early stage of dry adhesive wear process against a steel ball.

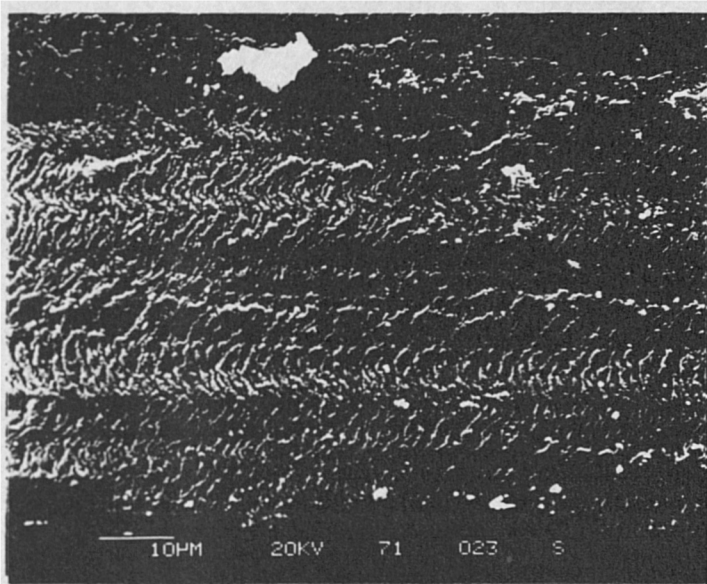
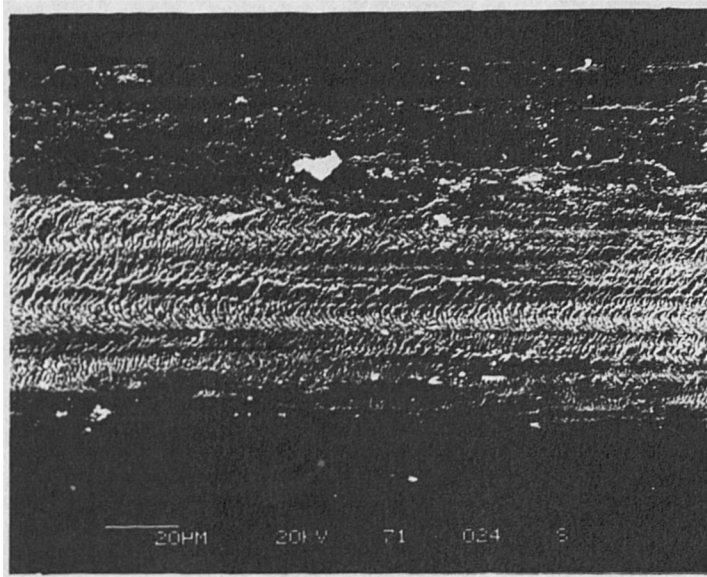


Fig.77 Development of fine cracks before complete breakdown of anodised alloy 9H under dry sliding against steel ball.

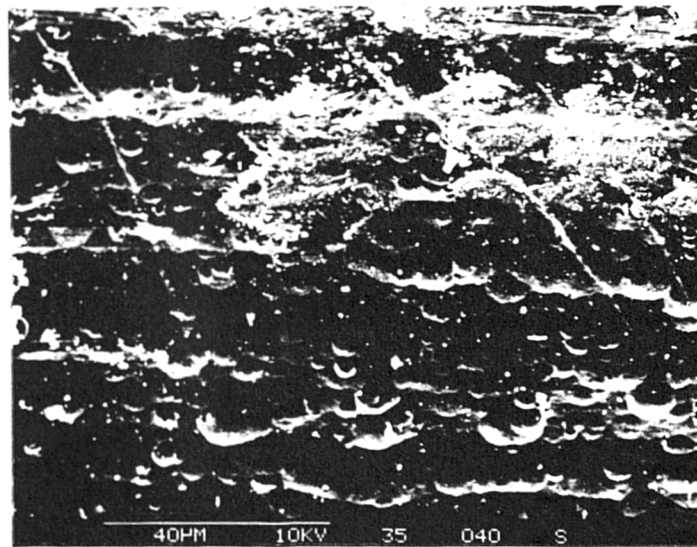
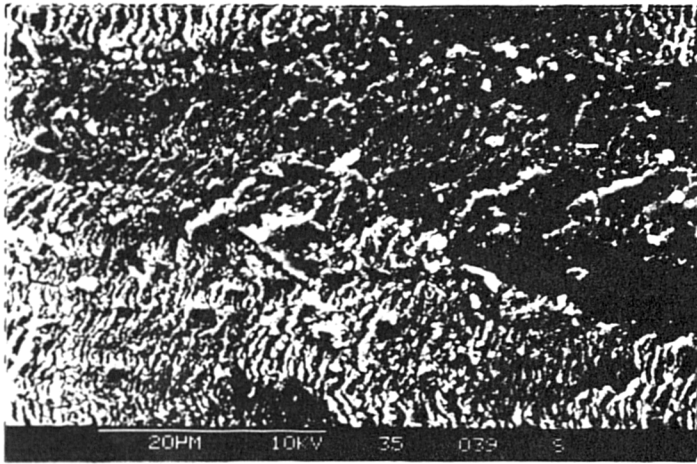
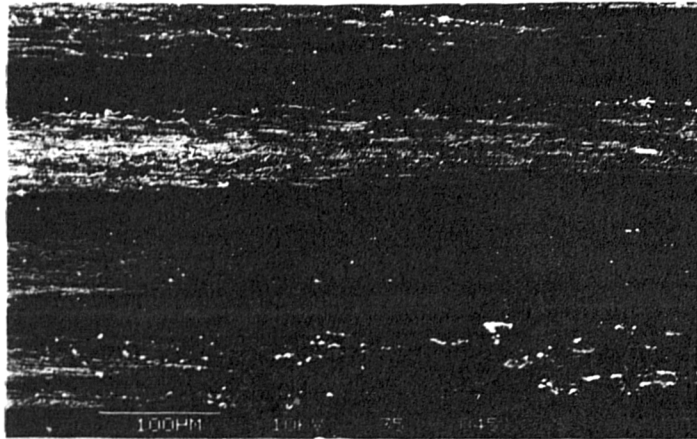


Fig.78 Showing the extent of cracks outside the wear track of anodised alloy 9H under dry adhesive wear.

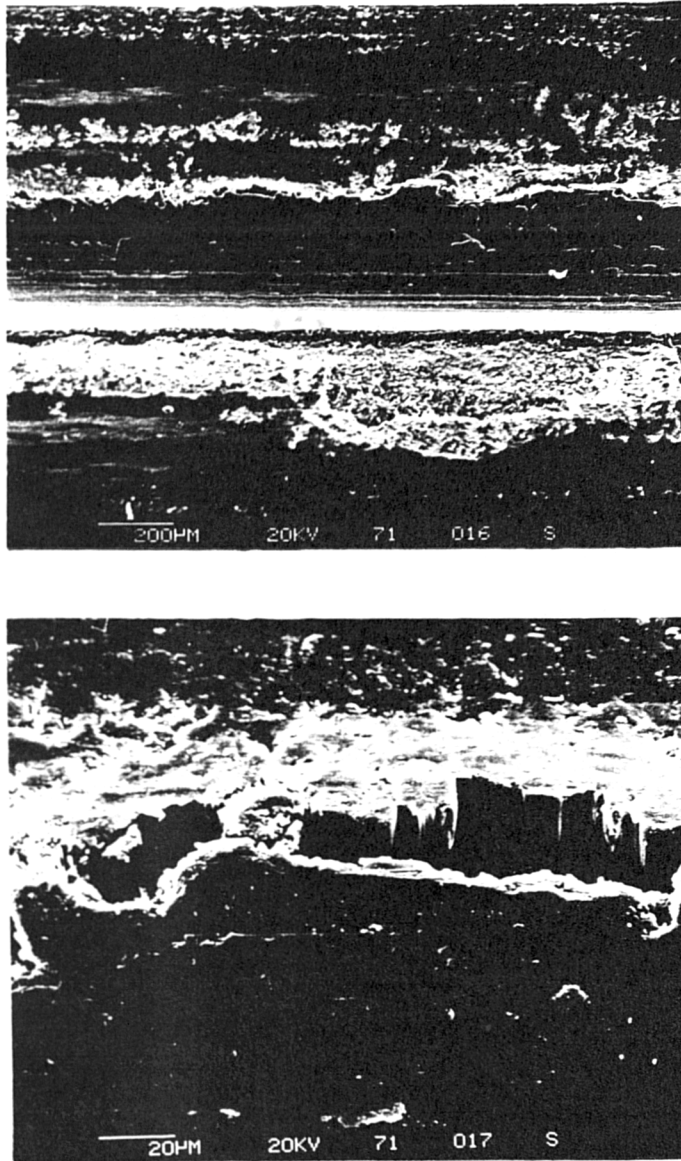


Fig.79 Showing a total destruction of anodised alloy 9H under dry adhesive wear.

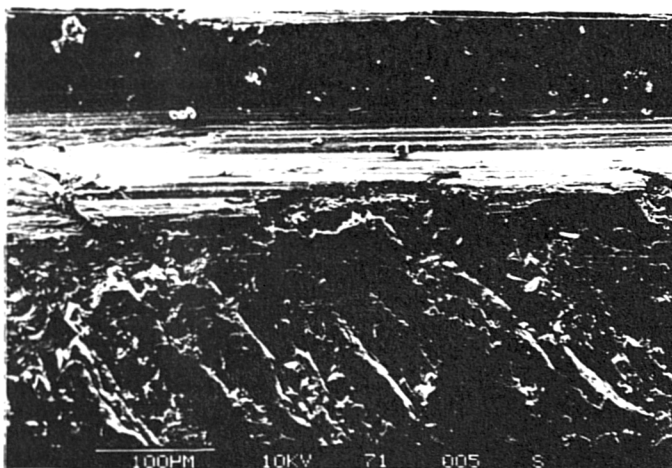
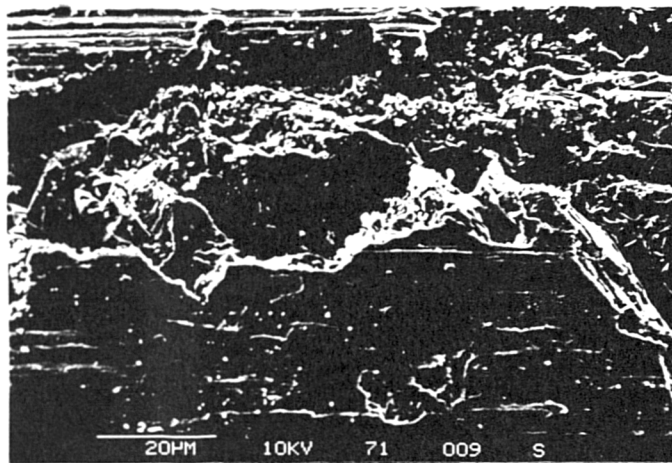
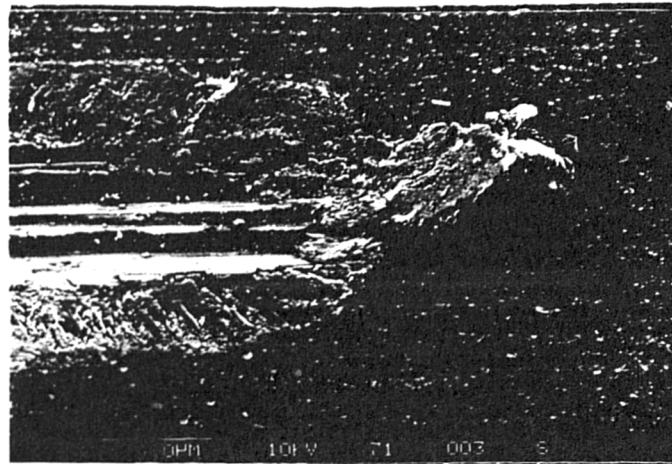


Fig.80 Build up of material at the end of the wear track of anodised alloy 9H suggests evidence of ploughing under dry adhesive wear.

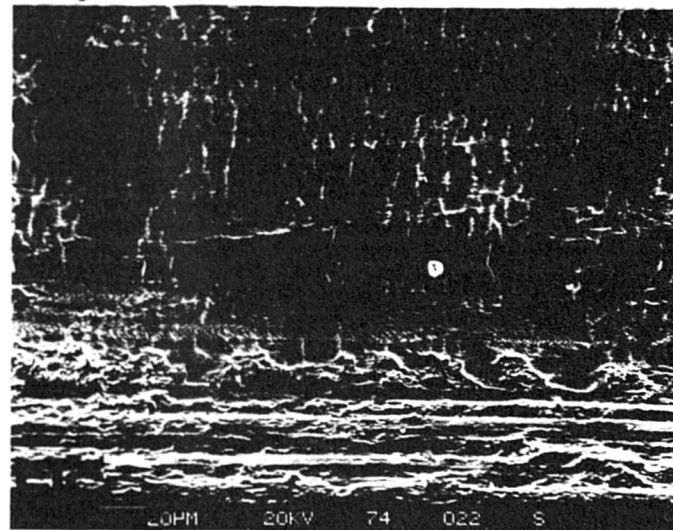
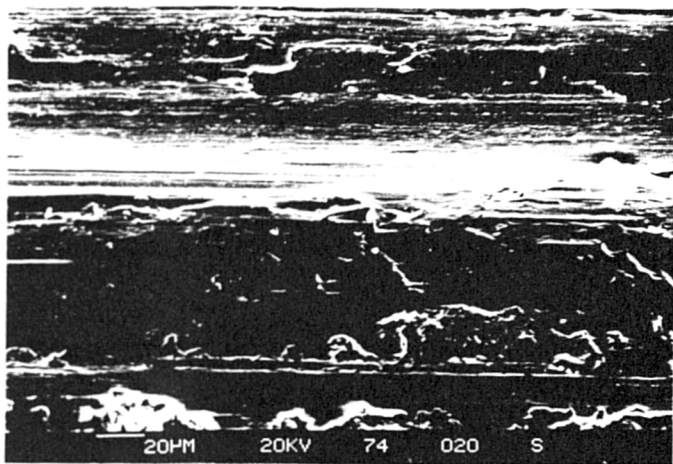
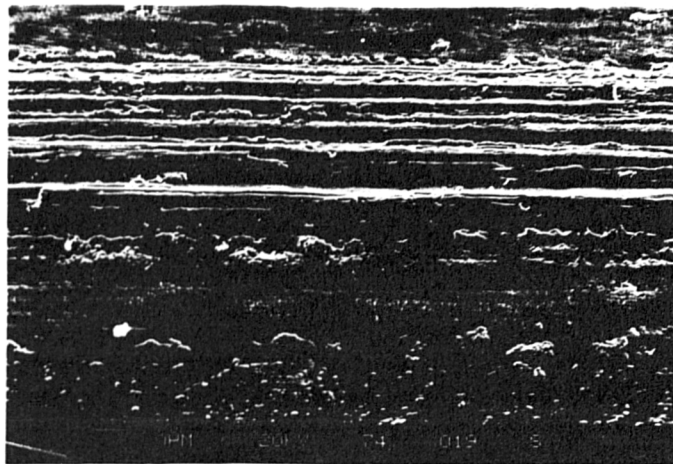
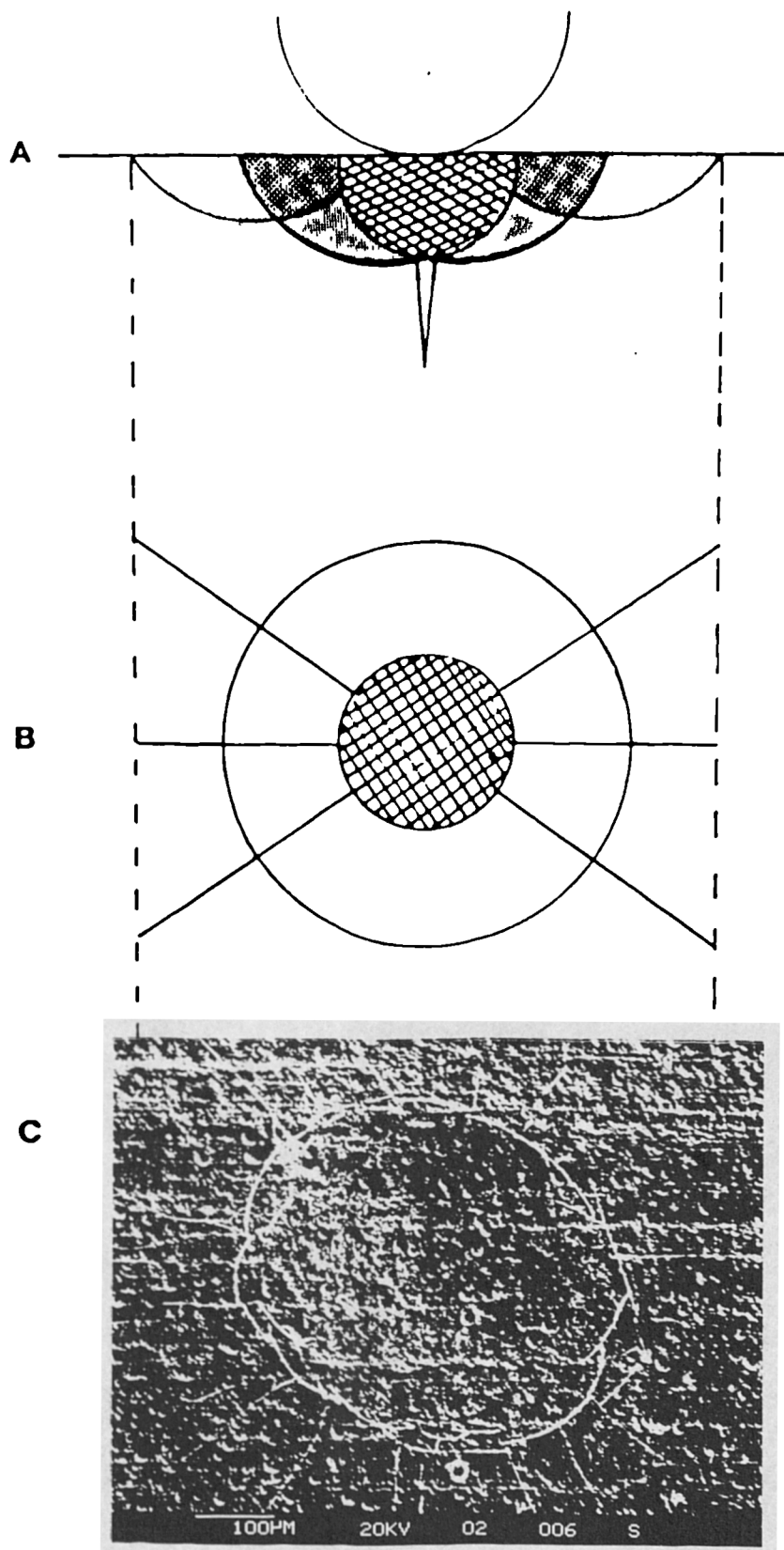


Fig.81 Dry adhesive wear of hard anodised 15H2 illustrates the development of a network of cracks outside the wear track.



STATIC LOADING

Fig.82 Modelling of sliding wear

- A,B) Schematic representations of the development of different types of cracks.
- C) S.E.M. illustration of ring and radial cracks.

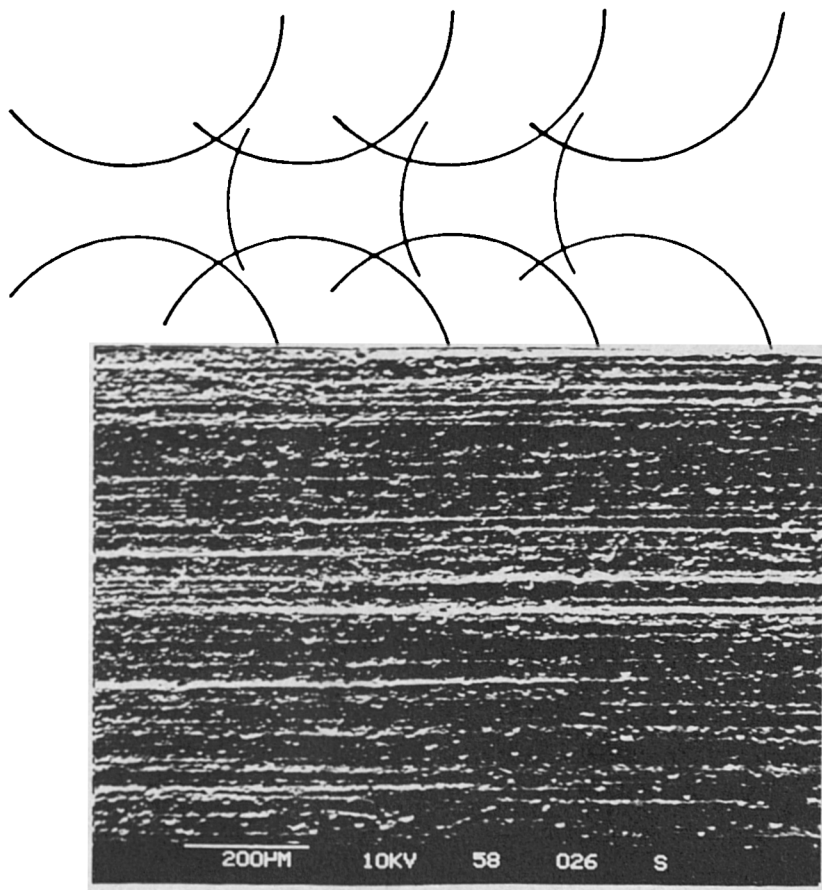
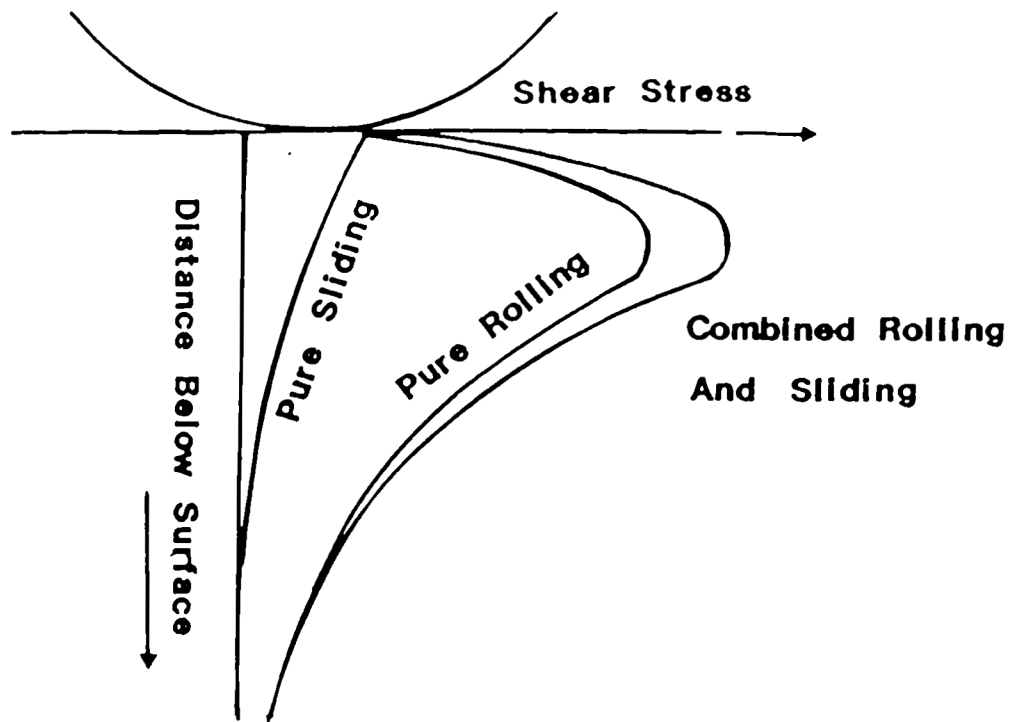
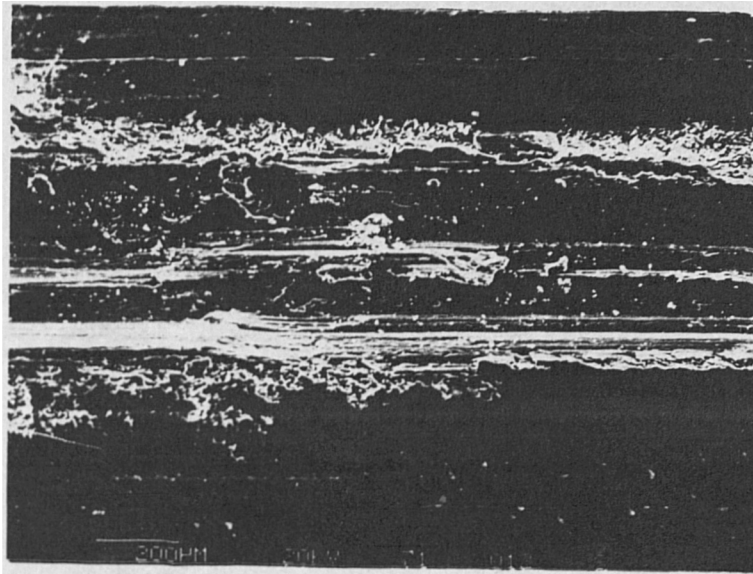
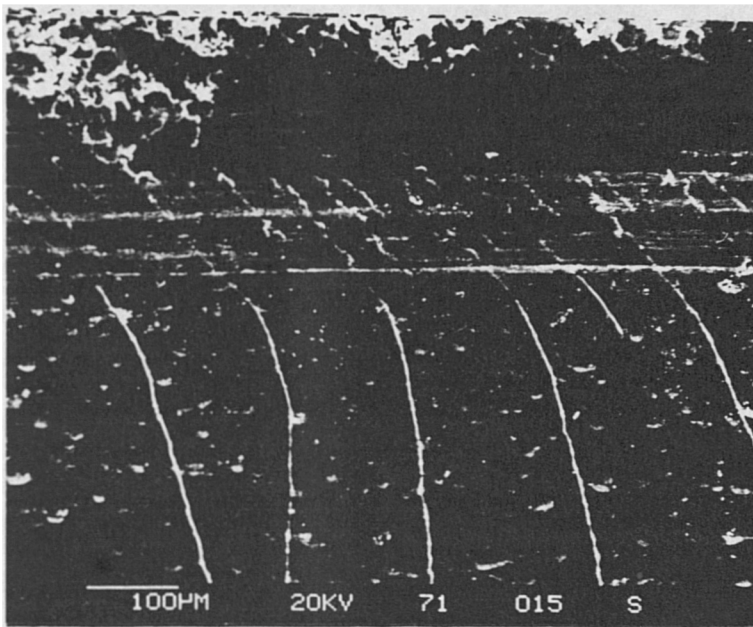


Fig.83 Development of cracks under dynamic loading of anodised alloy 9H. One direction, single pass.



A



B

Fig.84 Wear track of anodised alloy 9H under dry reciprocating motion showing

- A)** the middle of the track
- B)** cracks extended beyond the wear track boundaries.

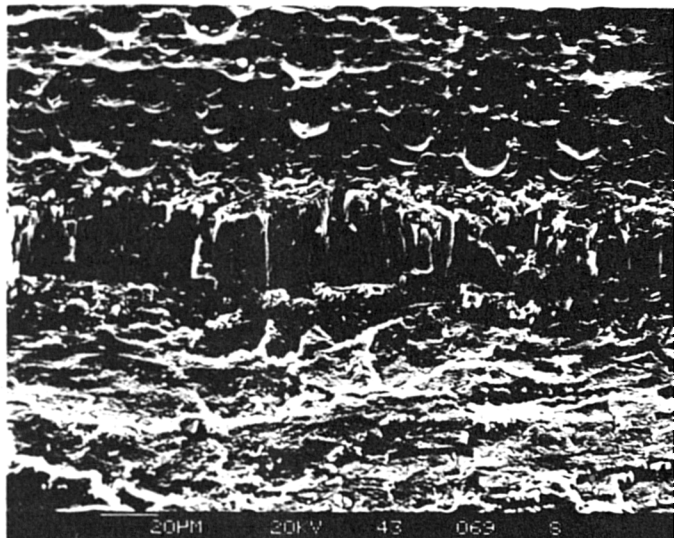
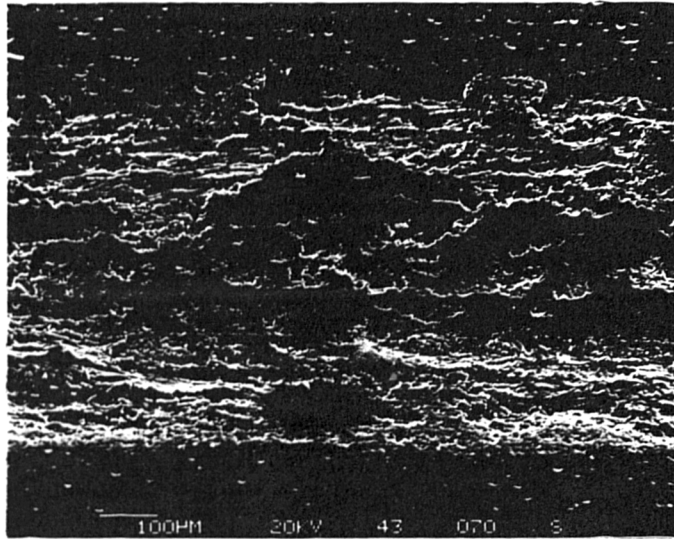
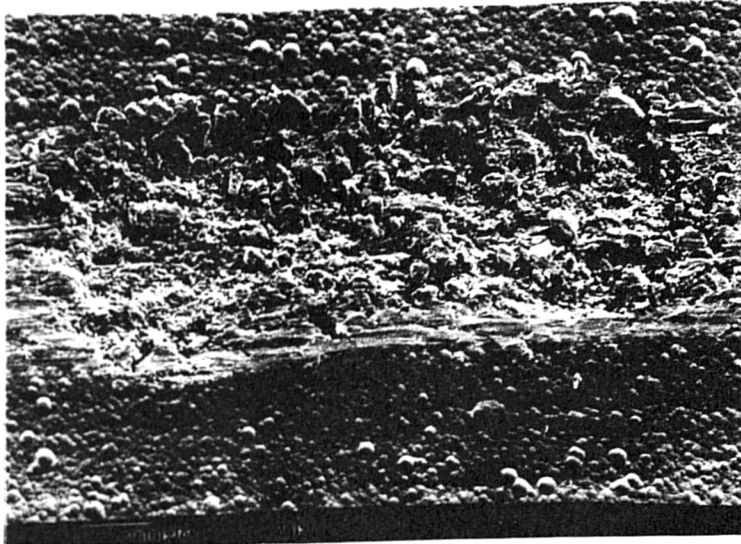
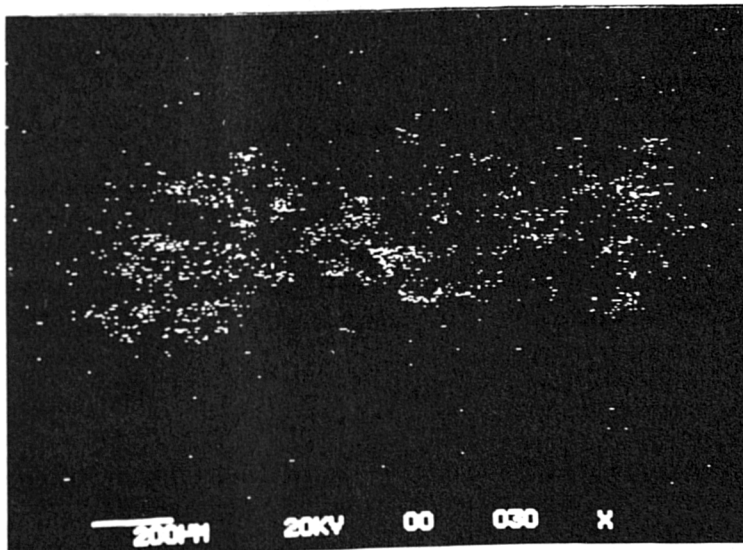


Fig.85 Brittle fracture of anodised alloy 9H under lubricated adhesive wear.

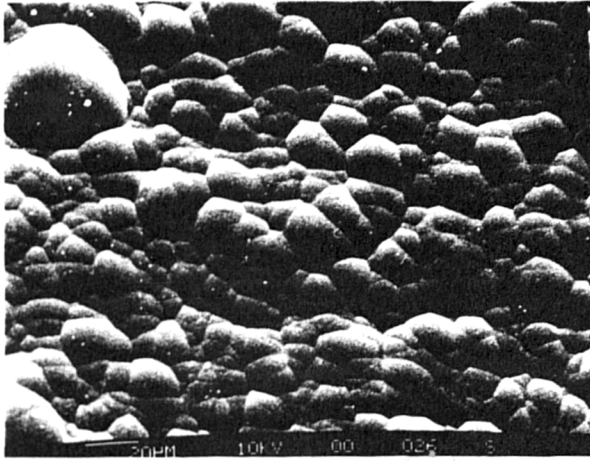


A

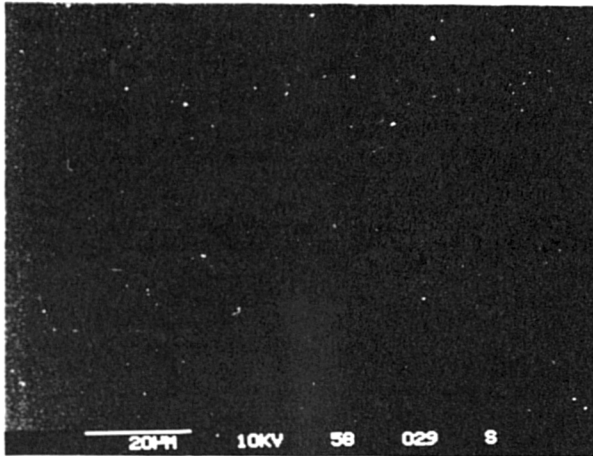
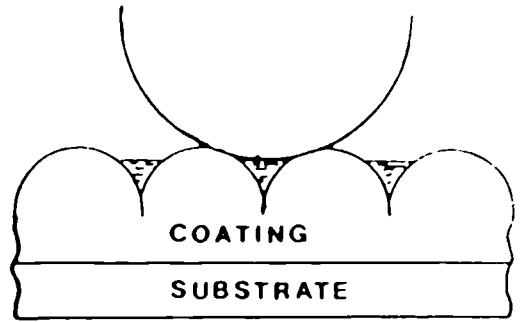


B

Fig.86 A) Early breakdown of electroless nickel of a 30 micron thickness under dry adhesive wear.
B) Al X-ray



A



B

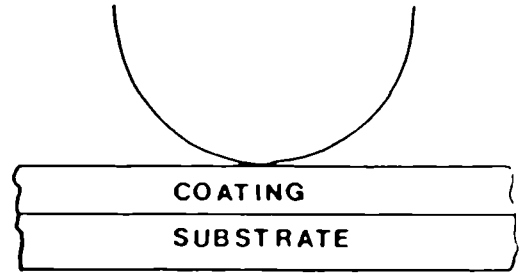


Fig.87 Schematic modelling and S.E.M. representation of the role of nodular texture of a 30 micron electroless nickel coating under lubricated adhesive wear.

- A) as-plated
- B) polished surface

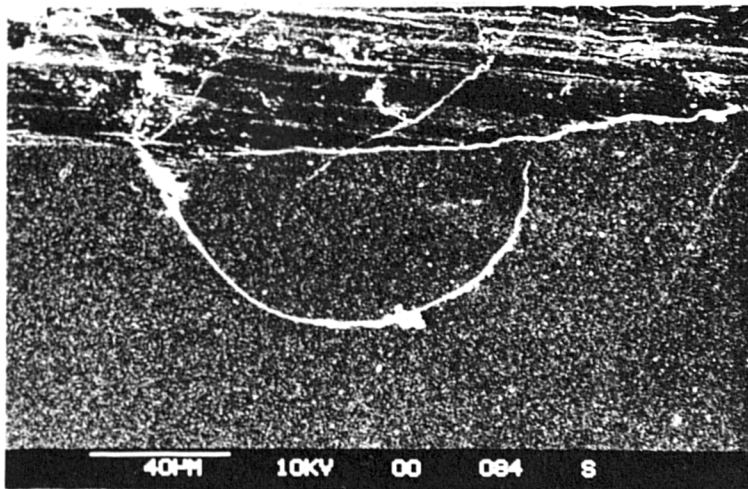
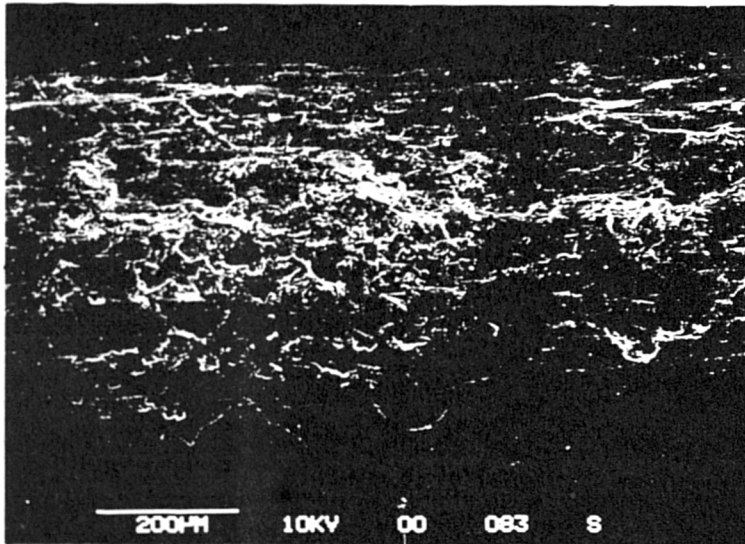
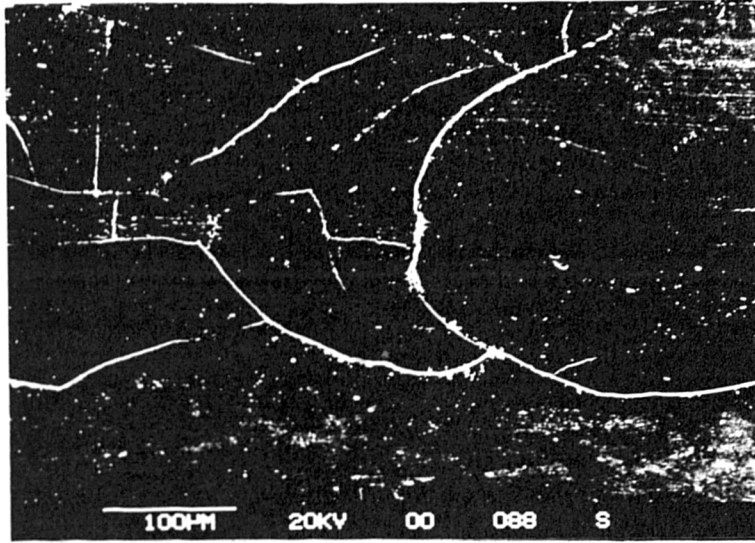


Fig.88 Initiation and propagation of lateral cracks in the as-polished electroless nickel coating of 30 micron under lubricated adhesive wear against a steel ball.

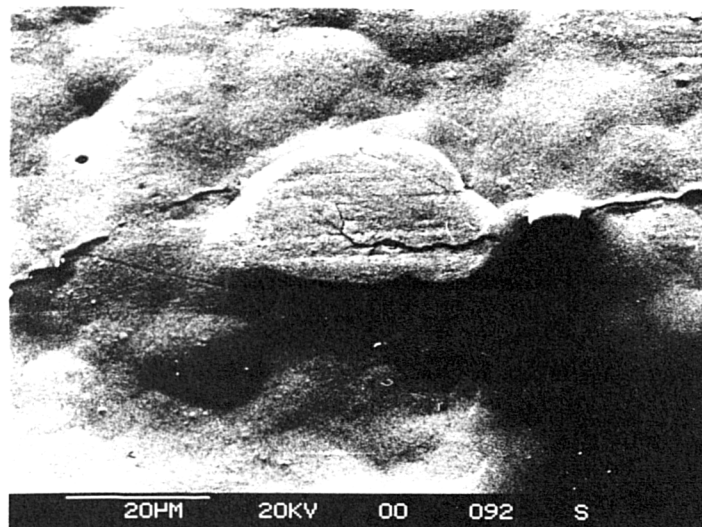
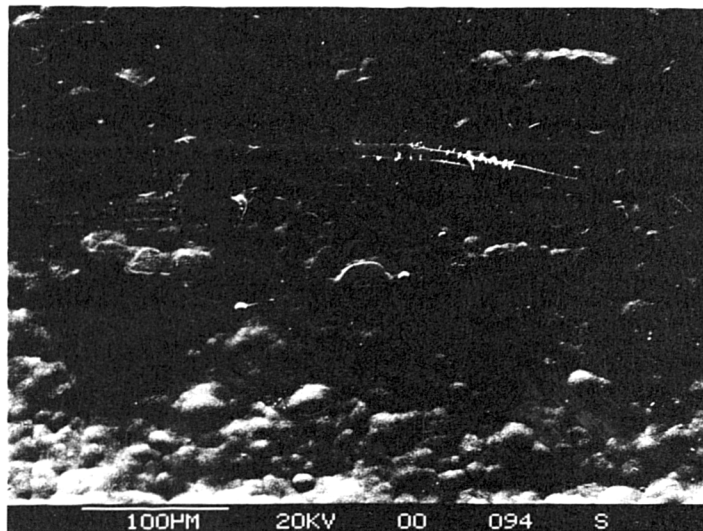


Fig.89 Mechanical polishing at the early stage of sliding of electroless nickel of a 30 micron thickness.

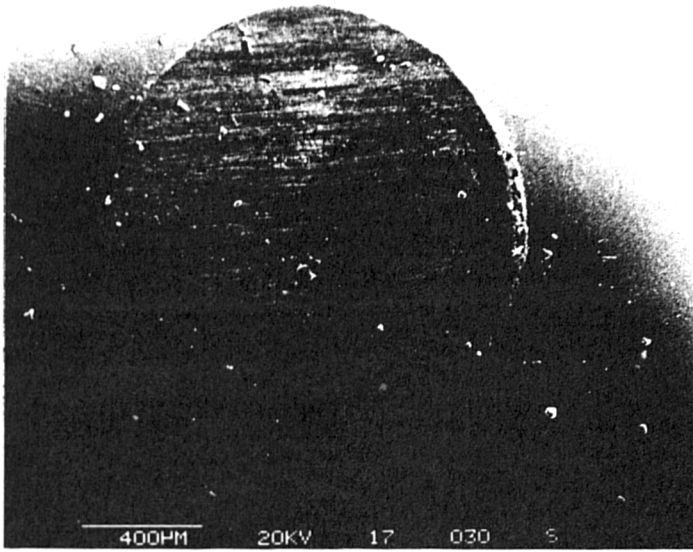
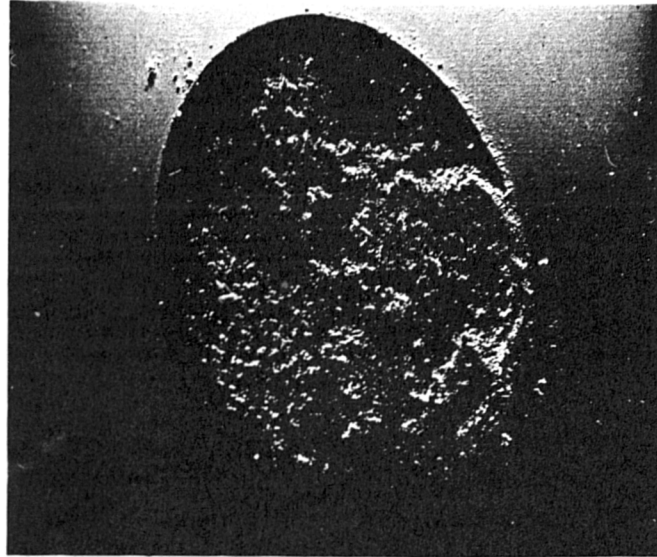
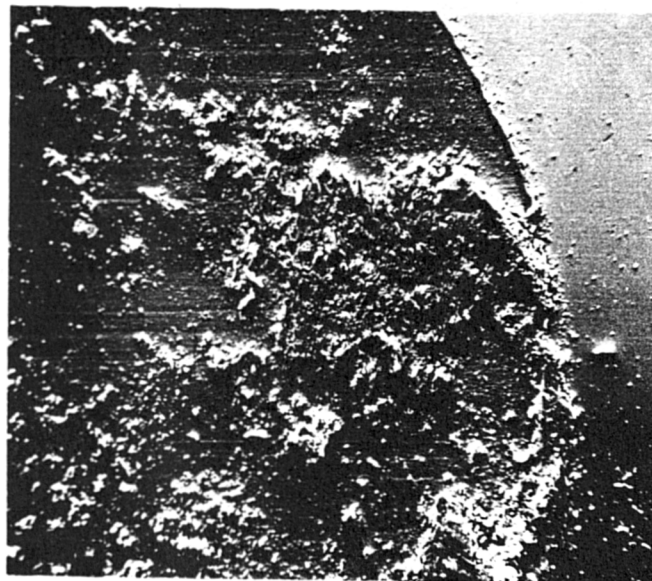


Fig.90 Trapped debris between the counterbodies.



400 μ



20 μ

Fig.91 Wear of the steel ball showing trapped debris.

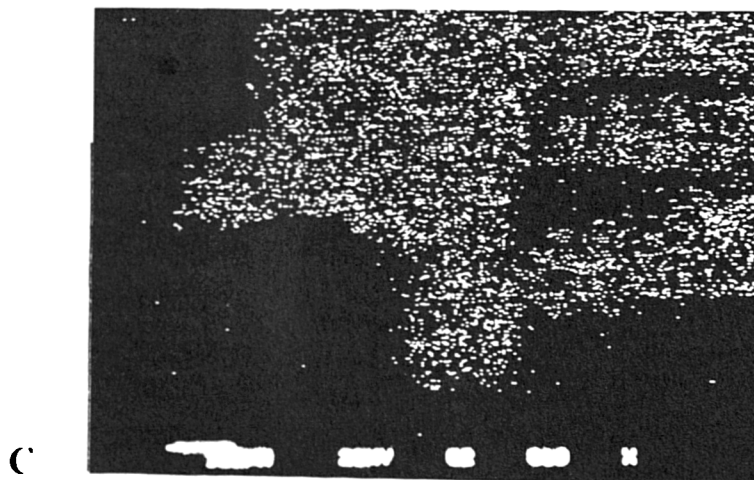
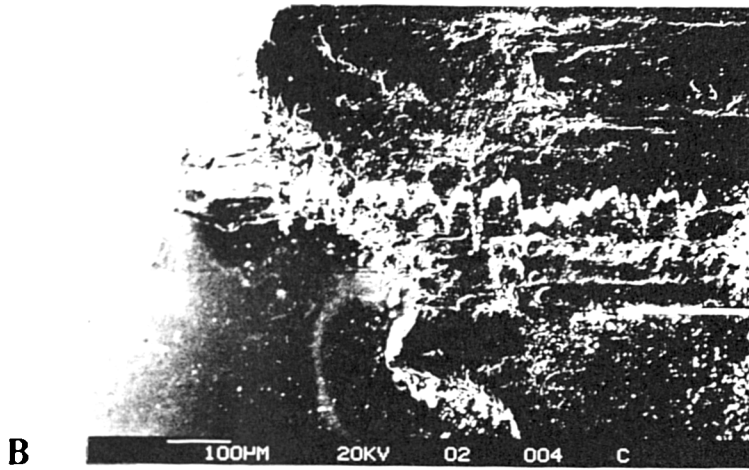
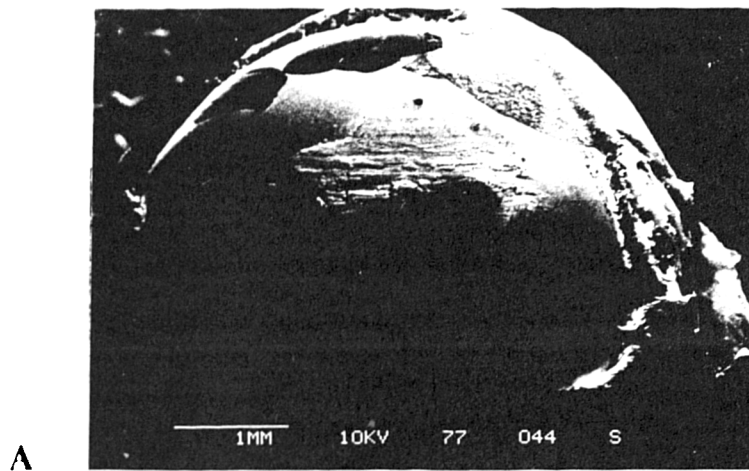


Fig.92 A) wear of the steel ball against the anodised aluminium alloy 911.
B,C) aluminium transfer from the anodic film.

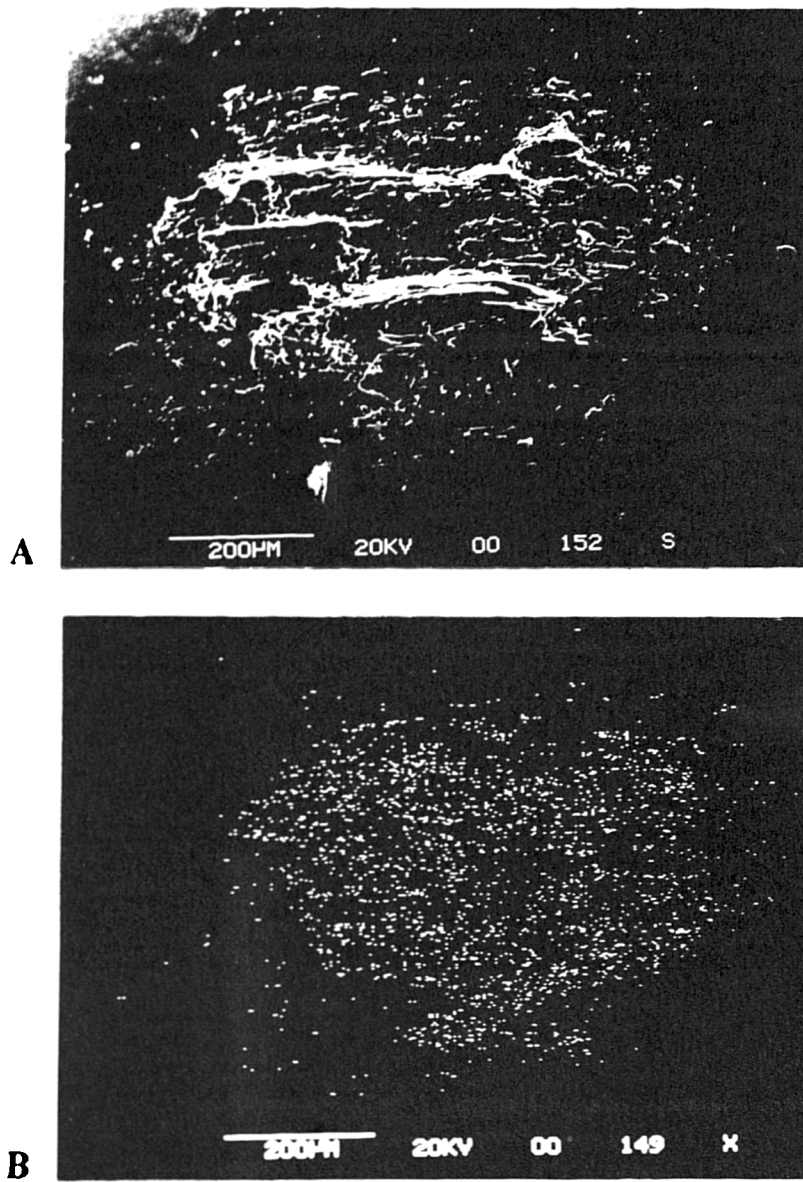


Fig.93

- A) Worn steel ball against electroless nickel of 30 micron thickness under dry adhesive wear.**
- B) Ni transfer to the steel ball.**

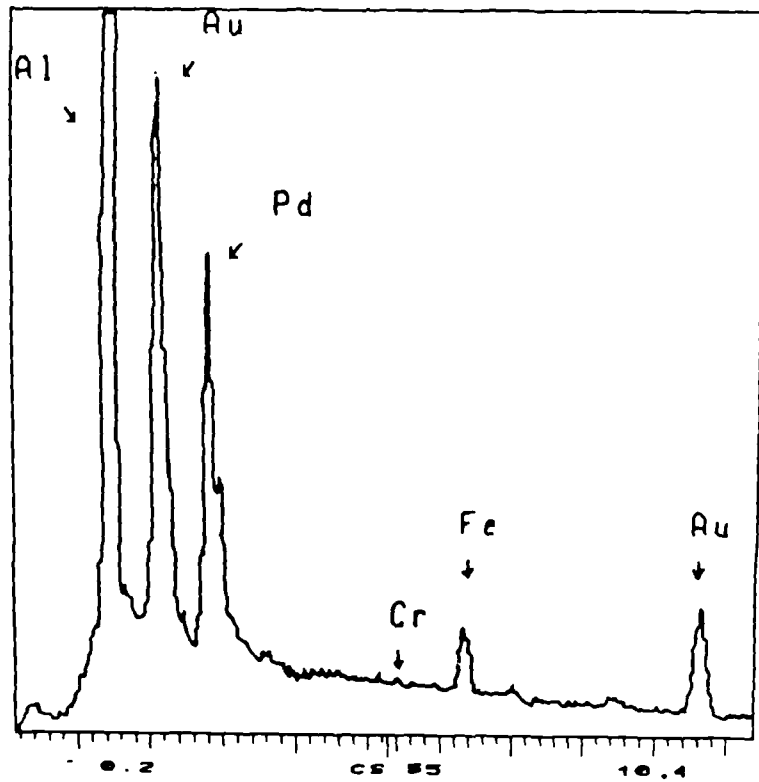


Fig.94 Transfer of iron and chromium from the steel ball to the anodised alloy 9H under dry conditions.

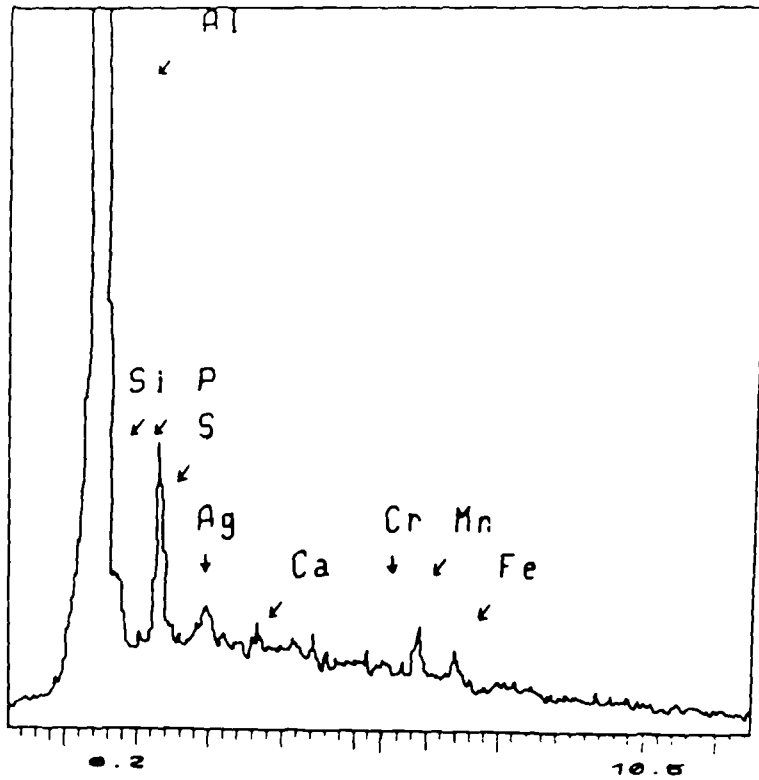


Fig.95 Transfer of iron and chromium from the steel ball to the anodised alloy 9H under lubricated conditions.

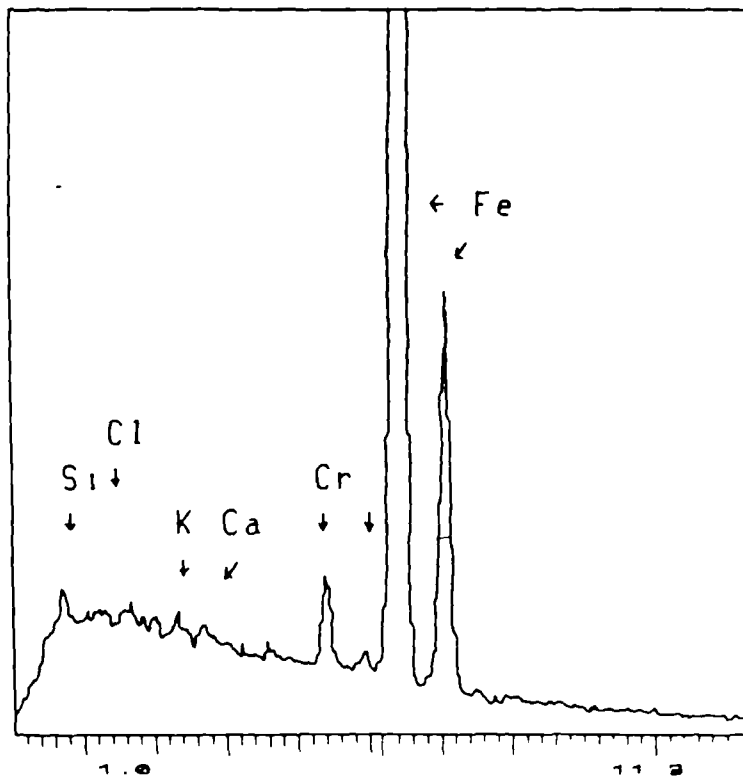


Fig.96 Deposition of organic elements between the counterbodies under lubricated conditions.

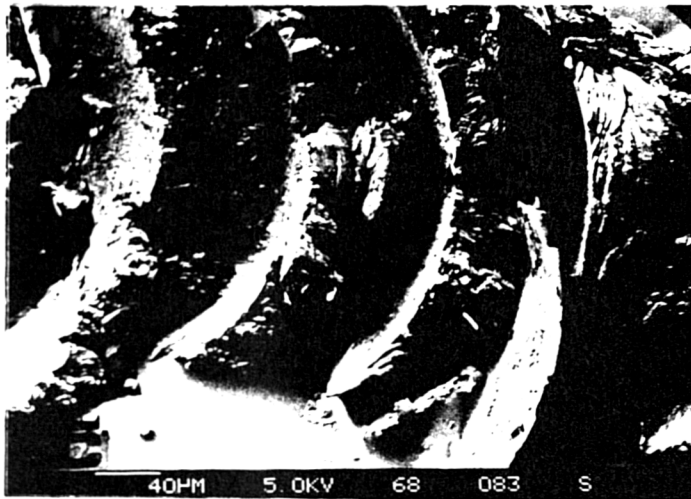
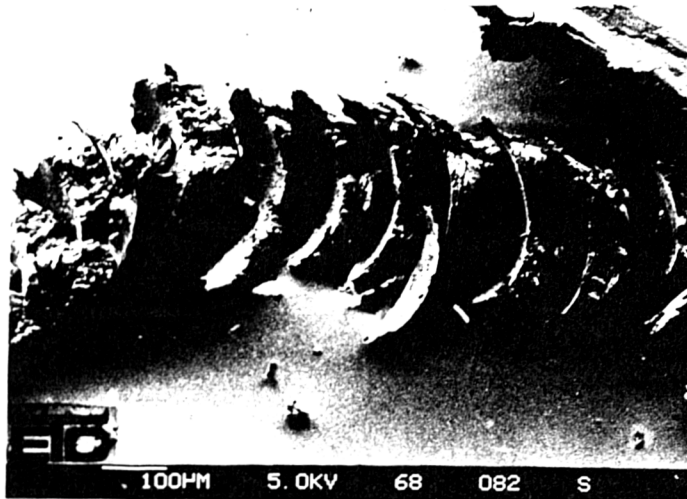


Fig.97 Ploughed debris generated from abrasive wear of uncoated aluminium alloy 6030.

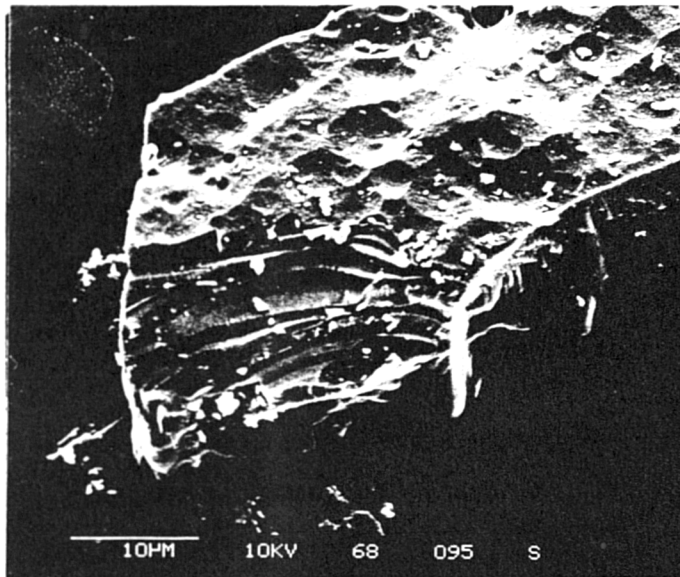
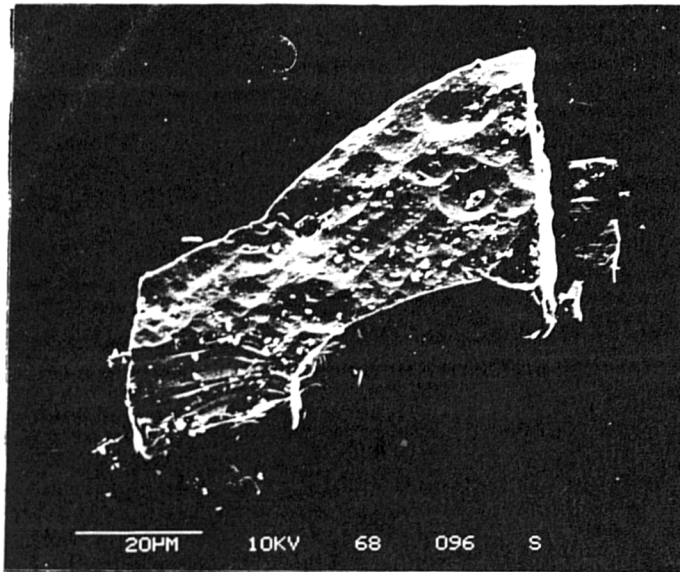
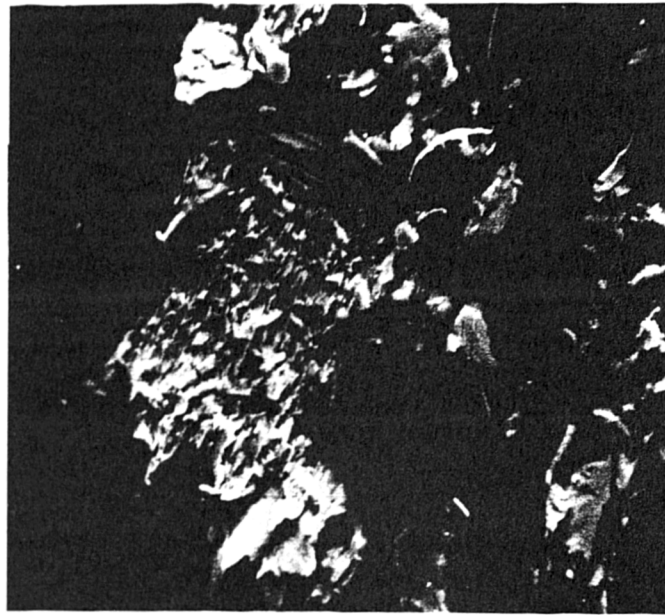
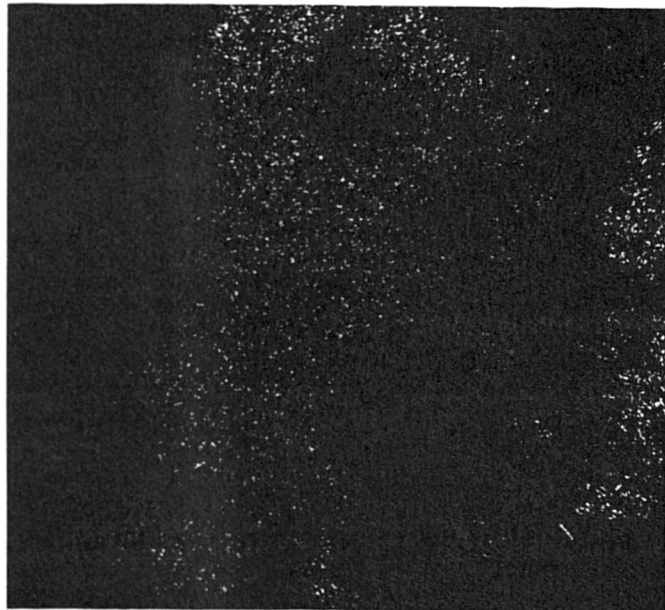


Fig.98 The nature of deris recovered from abrasive wear of hard anodised alloy 9H.



A



B

40 μ

Fig.99 A) Deformed debris generated from abrasive wear of electroless nickel plated alloy of a 30 micron thickness.
B) X-ray Ni distribution.

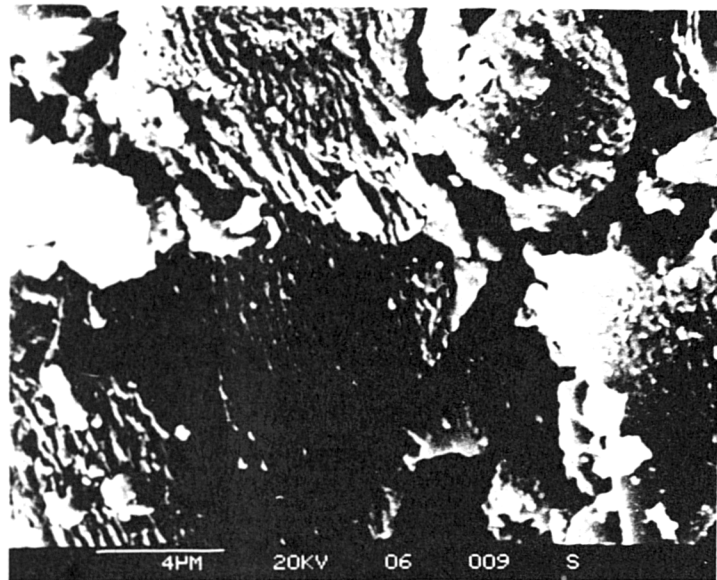
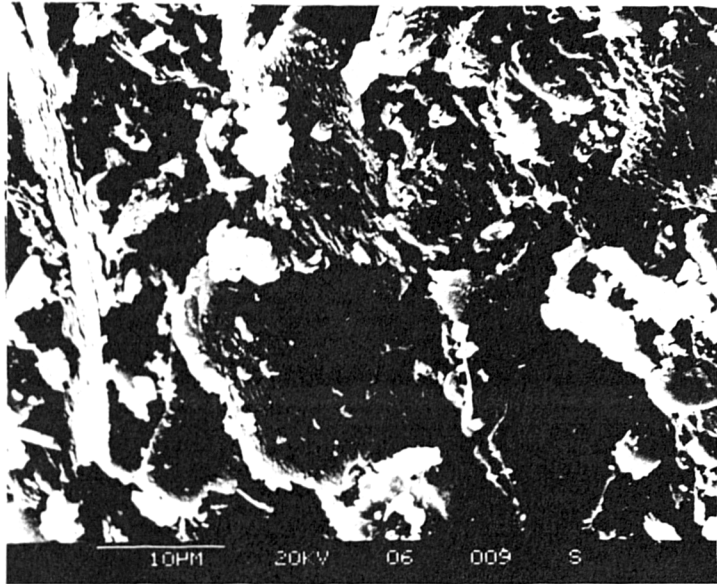


Fig.100 Wear debris produced under dry adhesive wear of anodised alloy 9N.

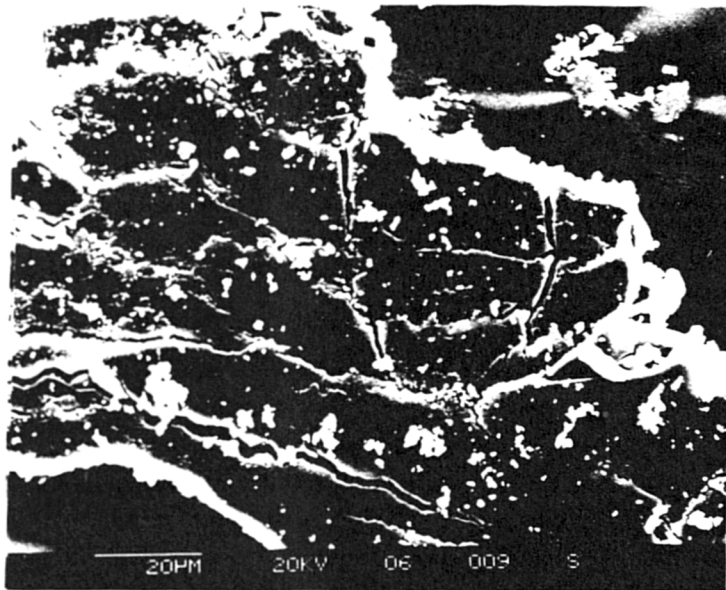
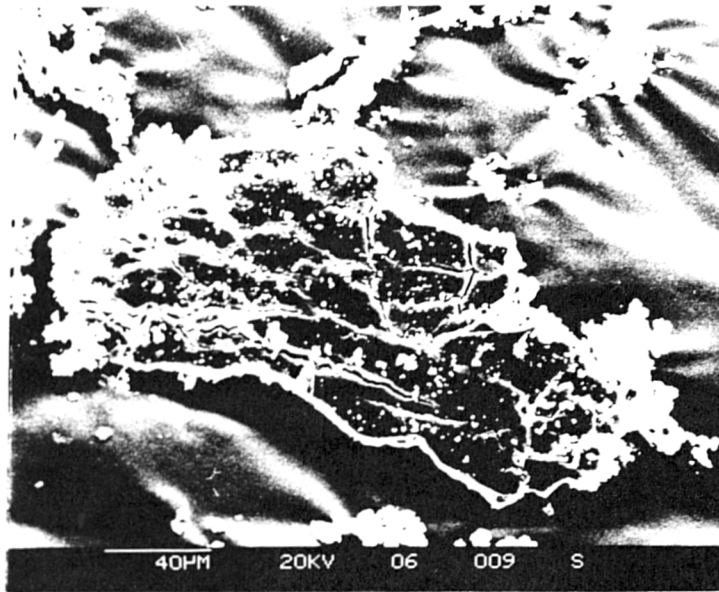


Fig.101 A network of cracks developed on a platelike debris produced under dry adhesive wear of hard anodised aluminium 30H against a steel ball.

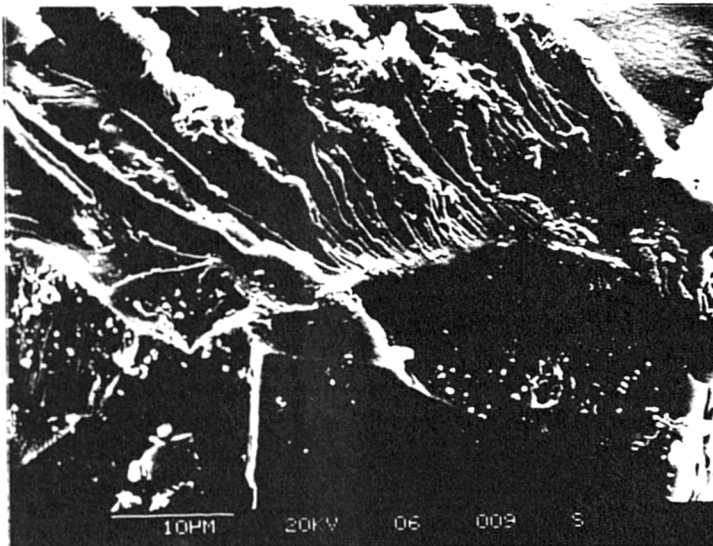
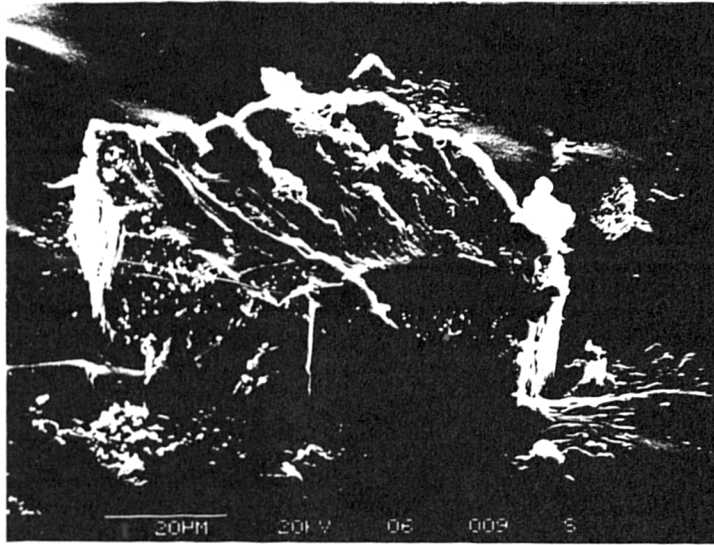


Fig.102 Nature of debris generated from dry adhesive wear of anodic film 9H.

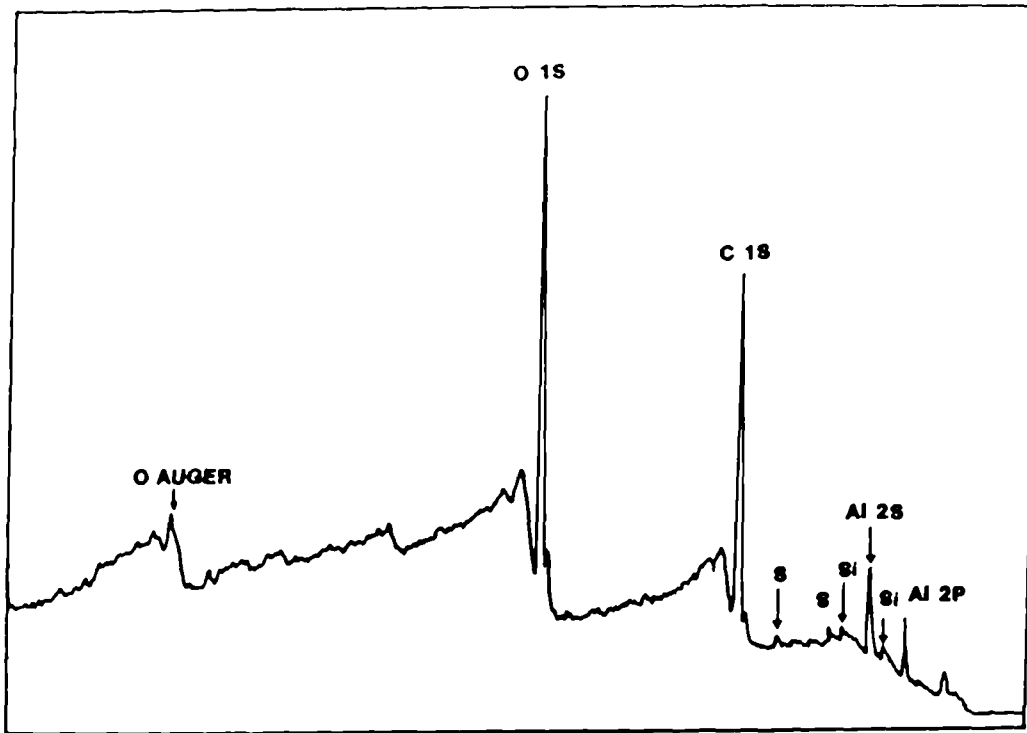


Fig.103 ESCA of debris produced under dry sliding wear of anodised alloy 9H.

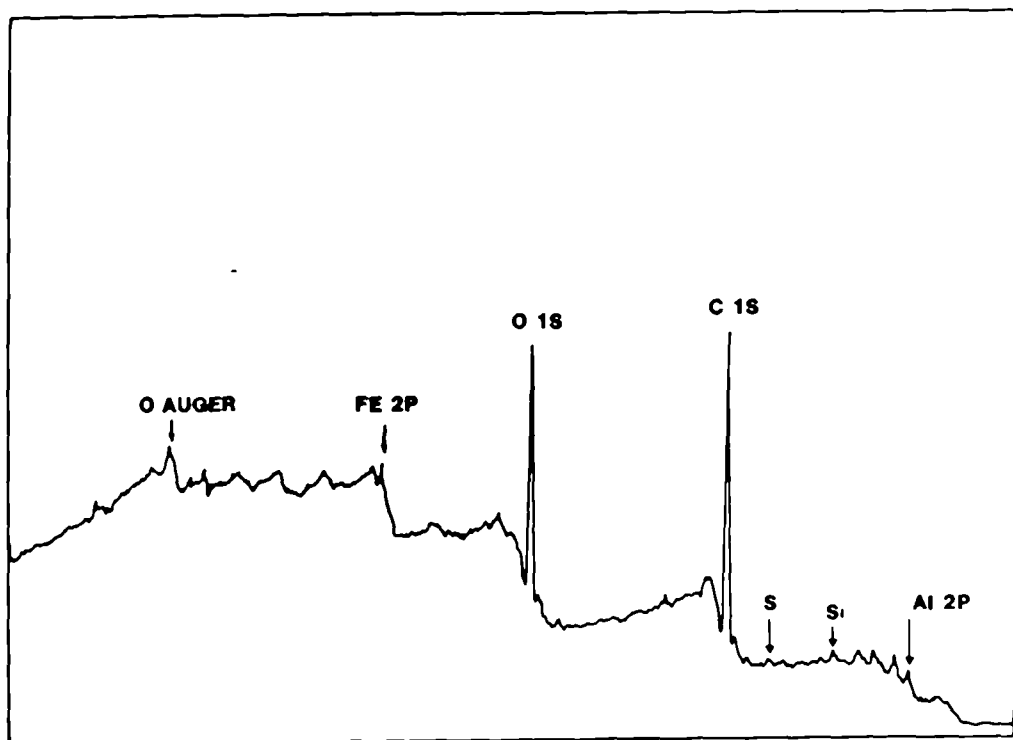


Fig.104 ESCA of debris produced under dry sliding wear of anodised alloy 30H.

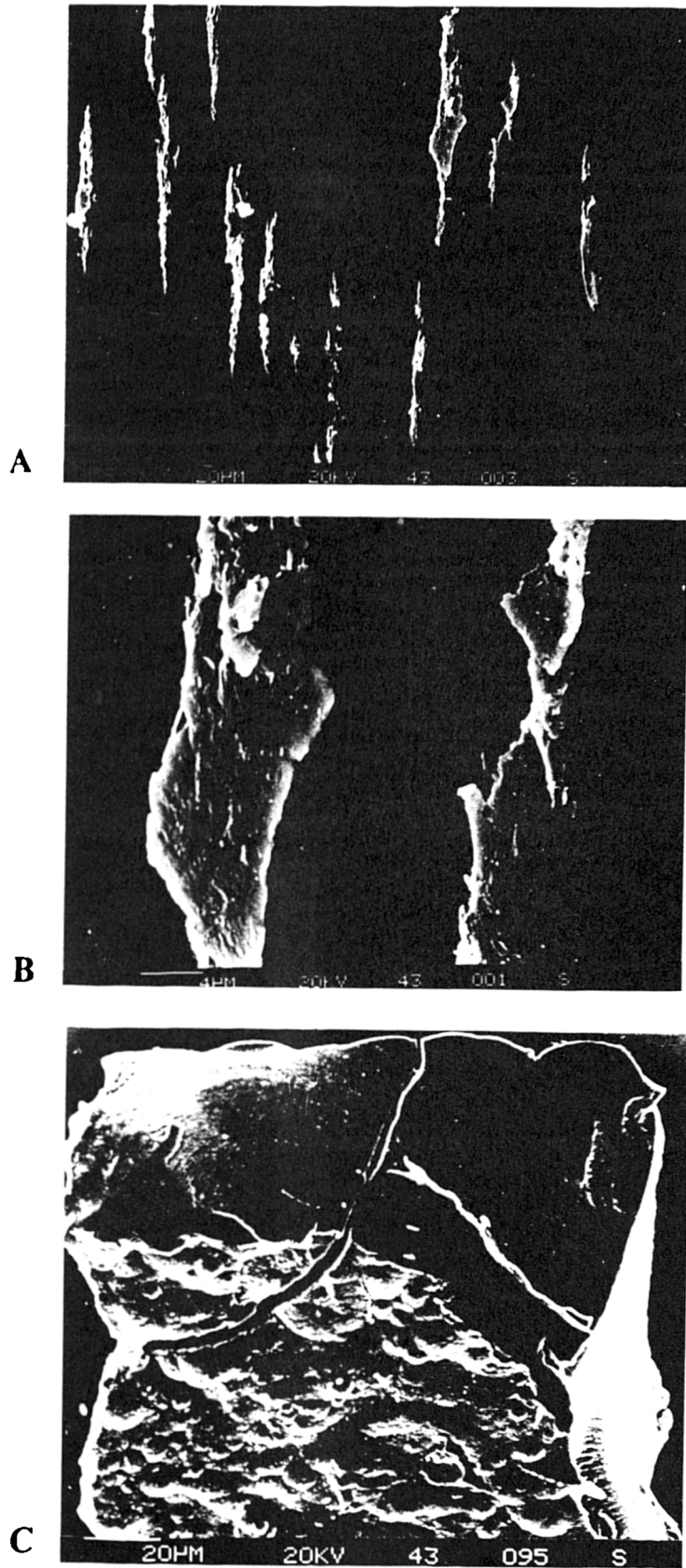
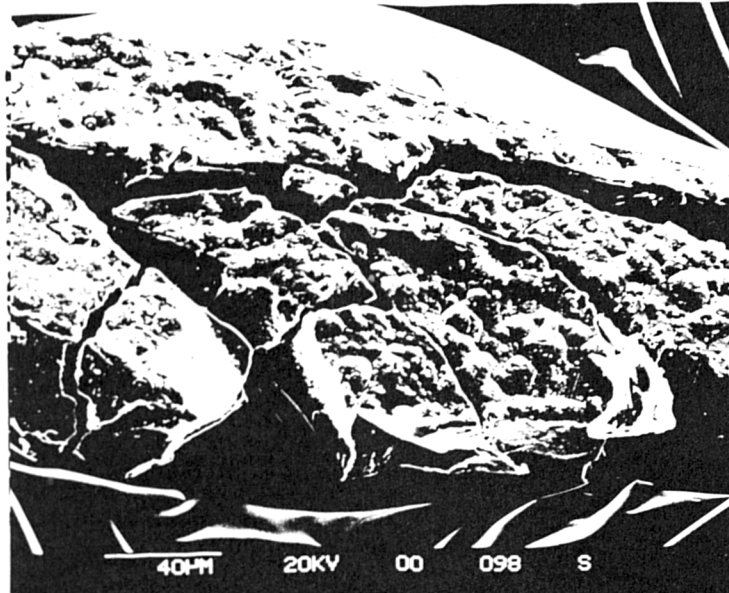
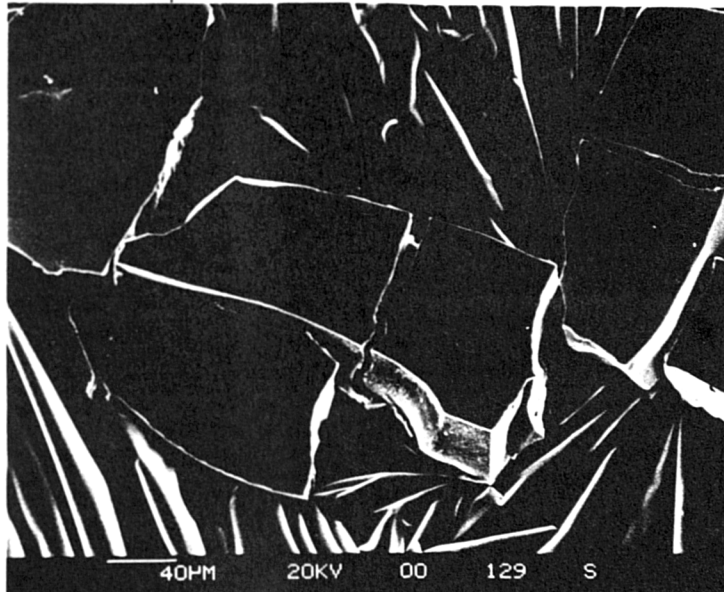


Fig.105 Nature of debris generated under lubricated adhesive conditions of A), B) uncoated aluminium, C) anodised aluminium alloy 911.



A



B

Fig.106 Fractured debris of the
A) as plated
B) polished electroless nickel coating of 30 micron thickness
under lubricated adhesive wear against a steel ball.